OPTIMIZATION AND CONTROL OF SOLAR-POWERED TELECOMMUNICATION NETWORK BASE STATIONS IN NIGERIA USING STANDALONE BIFACIAL PHOTOVOLTAIC SYSTEM

BY

OSUJI, CHRISTOPHER UCHE [ND (MECH), HND (MECH) B.Eng. (Elect). MSc (Elect)]

REGISTRATION NUMBER: 20224399658

PRESENTED TO

THE DEPARTMENT OF ELECTRICAL ENGINEERING, SCHOOL OF POSTGRADUTE STUDIES, FEDERAL UNIVERSITY OF TECHNOLOGY, OWERRI, IN PARTIAL FULFILMENT FOR THE AWARD OF Ph.D. IN ELECTRICAL ENGINEERING, [POWER SYSTEM OPTION]

OCTOBER[2025

CERTIFICATION

This is to certify that this research thesis titled: "Optimization and Control of Solar-Powered Telecommunication Network Base Stations in Nigeria using Standalone Bifacial System" is the original thesis of the research conducted by **OSUJI, CHRISTOPHER UCHE (20224399658)**, and has not been submitted elsewhere for the award of any degree whatsoever.

Signature.....
ENGR. PROF. E. N. C. OKAFOR
Supervisor
Date...21/10/25

Signature.....
ENGR. PROF. O. J. ONOJO
Supervisor
Date...21/10/25

Signature.....
ENGR.DR I.O. AKWUKWAEGBU
Supervisor
Date...21/10/25

Signature.....
ENGR. PROF. N. CHUKWUCHEKWA
Head of Department
Date...21/10/25

Signature.....
ENGR. PROF. D. O. DIKE
Dean of School of Electrical Systems Engineering Technology
Date.....

Signature.....
PROF MRS. J.N NWOSU
Dean of Postgraduate School
Date.....

Signature.....
External Supervisor
Engr. Prof. B. O. Anyaka
Date...21/10/25

DEDICATION

To God Almighty whose grace and protection has been my source of survival.

and

My parents, Ezinna Nze Titus Uwaoma Osuji (1922-1994) and Ezinne Mrs Susan Ihuoma Osuji (1927-2014) of blessed memories, they did everything they could in moulding my academic destiny. To my mother-in-law, late Mrs Ngozi Ezeobele; may God grant their souls eternal rest. Amen.

To My Brother's Wife; Mrs Peace Chidimma Osuji who was with me till my Internal Defence and unfortunately departed this World on the 3rd of May, 2025. My Peaceful PEACE, may the God Almighty grant your soul eternal rest. Goodnight this morning.

ACKNOWLEDGEMENTS

Immense gratitude to my supervisors, Engr. Prof. E.N.C Okafor (my Supervisor during my undergraduate days) for his guidance and endless supply of fascinating information as it concerns my research. His unassuming approach to research and science is a source of inspiration. This approach is reflected by his simple but clear explanations, which was something that I followed throughout my thesis writing. He did not spare anytime in proof reading my thesis at every chapter. His directives and series of meetings contributed immensely to the actualization of the result of this research. An accolade of gratefulness to Engr. Prof. O.J Onojo and Engr. Dr I.O Akwukwaegbu , my second and third supervisors for guiding my Simulation during this thesis.

I cannot write further without a kind appreciation to my Head of department, Engr. Dr N. Chukwuchekwa, for encouraging me to take up this challenge irrespective of my late admission. Above all, he is instrumental to my expected timely completion of this program. To him, I doff my cap. With heart full of gratitude, I wish to show my appreciation to the lecturers in my department, who irrespective of their tight schedules and the harsh economic condition spared their time for the respective presentations I made in the process of this research; Engr. Prof. D. O. Dike (Dean School of Electrical System Engineering Technology), Engr. Prof. Mrs. G.N Ezeh, Engr. Prof. F.K Okpara, Engr. Prof. M.C Ndinechi, Engr. Dr .M. Olubiwe, Engr. Dr .C.K Joe-Uzuegbu, and Engr. Dr S.O. Okozi. Their critics and corrections made me proud. To them, I am most grateful.

I wish to appreciate those who supported me financially and otherwise during my academic endeavour. Pertinent to mention are; Mr Nicholas Asham, Chief Timothy Ogude, Mr Jude Osuji, all of blessed Memories. To My elder brother's wife, Mrs Martha Osuji, her motherly role was wonderful. Special thanks to my one and only friend, Mr Okechukwu Asham who was financially supportive during my undergraduate days. I cannot forget my friend and brother; Mr Ethelbert Anyanwu who was instrumental to my first appointment in the then Oceanic Bank PLC. My dear, I am forever grateful to you.

With gratitude, I am highly indebted to my Father-in-law, Engr. Emmanuel Ezeobele who has always been supportive in every situation both financially and otherwise. Special thanks to Rev

Fr. (Barr.) Augustine Obiora, Rev Fr. Anthony Mmuo, Rev Fr. Dr Augustine Ebebe and Rev Fr. Dr Paul Dimude; they are my wonderful and good spiritual mentors and friends.
My Rector Dr Mrs. Chioma Irene Awauzi deserves endless gratitude for appointing me as the Director of Affiliation and Linkages (Local and International) in her Cabinet recently. My colleagues at Federal Polytechnic, Oko; Dr Onyeka Obi, Mr. Francis Anyaora, Mr Chikem Nwolum, Engr Iheanyi Anosike, Mr Achuama Anthony, Aristotle, Solomon, the Deputy Rector Academics; Dr Mrs. Nkeiruka Akabuike, Director Students Industrial work Experience; Dr Patrick Ezeigwe, Mr Peter Atodo, Mr. Obeche, Udeke, and Nzewi. These guys are my close allies, I salute them all. In my Department at Federal Polytechnic, Oko, I salute my friend Engr. Dr John Ananti, and the entire staff of Electrical Engineering.

Special thanks to my lecturers at Coventry University, United Kingdom during my MSc program in the persons of; Dr Navid, Salman (my MSc project supervisor), Prof. Daa Asleem (the man who moulded me in control System and Simulation), Dr Andrew Ticler (he made me in Robotics and AI), Dr. Chittah Saha (My mentor in Renewable Energy and Smart grid) and my electrical machine giant; Prof. Quiin Ji Pin; I gladly say; Thank you guys immensely.
My colleagues at DHL Prologis Park UK; Mike, Sammy, Kelly, Rash, Carlin and Mathew; they were more than friends during my stay in the UK. My pals at Klippers and Daventry and those that worked with me at TEXCO glossaries Daventry; I did not forget. Honestly, I miss you guys, thumbs up.
To my brother; Reverend Dr .E.A Osuji and his wife Pastor Mrs Peace Osuji (of blessed memory), I am thankful with gratitude. My humble family sacrificed everything for me, particularly my Wife; Lolo Lady Treasure Ifunanya Osuji (LSM) (Ochomma gide Aku I of Obollo), her support was immensurable. She is one in a million. My dear and wonderful children; Clinton and Chelsea I remain grateful for their prayers and timely endurance of my absence each time I travelled. May God guide and protect them all the days of their life. To my step-brother and wife Mr. and Mrs Odinakachukwu Osuji I am grateful. Their solar energy system kept my laptop live all the time
With gratitude, I want to appreciate our capacity and indefatigable Dean School of Post Graduate Studies, Prof. Mrs J.N. Nwosu for her motherly role and timely attendance at every presentation. To the associate Dean School of Post Graduate Studies, Prof Celestine Egwuonwu for being meticulous in going through my thesis at every presentation. Warm regards to the schedule Mr.

Njemanze Ikechukwu for being of help all the time. I am indebted to Mrs. C.E Sani, Nwoga, K.K, Nkechi Okeke, Patricia Chinwoke, and promise Nwosu in PGS. They are staff to reckon with.

Finally to Mr David (Galaxy Business centre FUTO) who printed my works from Seminar I to External Defence with dedications. Thanks a lot for your tireless efforts all these periods.

TABLE OF CONTENTS

CHAPTER THREE: MATERIALS AND METHODS

CHAPTER FOUR: RESULTS AND DISCUSSION

CHAPTER FIVE: CONCLUSION AND RECOMMENDATIONS

LIST OF TABLES

LIST OF FIGURES

LIST OF PLATES

ABSTRACT

This thesis compared the potentials of using two different configurations of photovoltaic systems; Monofacial Photovoltaic (MFPV) Panel, and Standalone Bifacial Photovoltaic (BFPV) panel to generate electricity that will meets energy requirement of a mobile telecommunication base based on theoretical mathematical modelling, simulation, and optimization using PVsyst version 7.4.8 and Hybrid Optimization Model for Electric Renewables (HOMER) software. In achieving this, six off-grid telecommunication base station sites at different geographical site were selected which include; Imo (Umuagwo, 4.33 kWh/m^2/day), Kwara (Oje, 5.97 kWh/m^2/day), Sokoto (Kiso, 5.81 kWh/m^2/day), Rivers (Chokocho, 4.76 kWh/m^2/day), Lagos (Kwame, 4.50 kWh/m^2/day), and Borno (Baje, 5.51kWh/m^2/day). Research gaps covered are: space constrains, poor power output, and CO_2 emission etc. associated with MFPV, generator, and battery system. Therefore, different configurations of standalone systems of MFPV panel with generator and battery backup and the proposed BFPV module with battery backup were studied and compared for energy optimization to determine the most economically feasible system that conforms to less Carbon IV Oxide (CO_2) emission and cost minimisation. The Net Present Cost (NPC) and total CO_2 generated were used as indices for measuring the optimization level of each energy configuration, and the option with the highest optimal value was considered to be the best energy solution for telecom base station. Results obtained shows that the installation cost of the MFPV panel, Battery, and the generator is ₦1, 288,000.00/Wp and the total yearly cost is ₦483, 200.00/Wp/Yr. The used energy cost is ₦4, 597,964,800.00/kWh which is the Levelized cost of energy (LCOE). The net present value of the project is –₦7, 731,200.00 and the return on investment is -750.3%. On the other hand, the LCOE for installing BFPV panel system is N95,184.64.00/kWh. The net present value of the project is ₦266, 895,136 and the return on investment is 55191.3%. This shows that the adoption of BFPV panel installation at TBs is profitable. This result is a validation of the objective of this research. Environmentally, CO_2 emission in using BFPV systemen is 0.25tons/W while that of installing MFPV system is 102tons/W. Consequently, there is a reduction of CO_2 emission (101. 75) by adopting the BFPV system.

Keywords: bifacial module, CO_2 emission, monofacial module, Net Present Cost, optimization.

CHAPTER ONE

INTRODUCTION

1.1 BACKGROUND OF THE STUDY

Nigeria with its growing population and a range of socio-economic challenges requires a reliable energy sources to meet the growing needs for all the sectors of its economy and achieve universal access to modern energy services. Provision of energy services for cooking and power are key objectives of national energy policies, in addition to priorities of energy affordability, energy security, and reduced air pollution and carbon dioxide (CO_2) emissions to conform the clean energy solution of United Nation (UN) 2030 agenda. Renewable energy sources can be a driving force in achieving all these goals because they are some of the lowest-cost energy sources today and are domestically abundant and less polluting than fossil fuel. One of the key areas that require affordable and reliable energy access is the telecommunication industries which are increasingly developing due to the recent transformations in the technology.

Telecommunication services have faced several challenges with the increasing spread of wireless voice and data signals into remote areas (Infinite Focus, 2020). Power supply is one of the critical challenges the telecommunication operators confront in deploying their networks. This challenge is readily overcome in the developed countries as a result of well-developed power infrastructure. In the developing world, where grid electricity grid is insufficient, it is always the energy solution of choice for powering Base Transceiver Stations (BTSs). Unfortunately, it is not always reliable and has limited coverage. This situation becomes complicated in developing countries like Nigeria as mobile telecommunication extends more and more into rural areas outside the reach of national grid. The electrification by grid extension or secondary power station can only reach a small minority of the population in rural areas. In view of the dispersion of localities, the cost of production, transmission and especially distribution of electricity, would be expensive. In Nigeria, Airtel Nigeria (Mobile Operator) has embarked on upgrading 250 diesel-powered stations on–sites. The company regretted that non-availability of regular grid power supply to sites across the country is responsible for over 70% of downtime, resulting in poor Quality of Service (QoS) (Vanguard News, 2019). MTN Nigeria, one of the four mobile telecommunications operators in Nigeria with over 4,798 base stations spends a whopping $82.8 million on generator acquisition almost every three years and $3.5 million monthly on diesel oil and generator

maintenance (Africa Article, 2024). This puts the operating expenditure (OPEX) of generators and diesel at about $42 million annually.

In most of the remote sites, extension of utility grid lines experiences a number of problems such as high capital investment, high lead time, low load factor, poor voltage regulation and frequent interruptions in power supply. The costs for installing and servicing the distribution lines are considerably high for the remote areas (Supriya & Siddarthan, 2024). Also, there will be substantial increased losses in transmission line plus poor power supply reliability. This poor quality in power supply leads to unsatisfactory quality of services. Decentralized and stand-alone systems could effectively become a viable option in these areas.

To manage this challenge, telecommunication operators in developing countries have to generate their own electricity. At present, the problem of poor electricity supply experienced at the telecommunication installations in Nigeria, is being tackled by using diesel generators. These generators, however, are associated with many problems. These include, among other things, transportation and storage of diesel which is a major problem in rural areas, environmental pollution due to noise and emission of harmful hydrocarbons in the atmosphere during operations. Generators also produce significant waste heat, which is essentially wasted energy. Moreso, their particulate emissions are a short-lived climate pollutant that contains considerable black carbon which causes harmful effects to humans such as health problems (respiratory diseases and eye problems). They produce high proportions of health-harmful particulate matter (PM) and CO_2 emissions per kWh of power generation, contributing to air pollution exposures and its resultant effect of climate change.

The operation and maintenance of diesel generators are relatively costly which typically accounts for 35 percent of the total cost of ownership (TCO) (Tamm, Christian, Allen, and Rush, 2010) of a BTS in some countries, but more than 50 percent in Nigeria. Thus, it has become increasingly evident that diesel generator-powered stations are becoming a much less viable option for network operators looking to expand into rural areas.

Replacing diesel with sustainable alternative energy sources that are cost-effective and clean, such as solar allows telecommunication companies to circumvent rising energy costs and realize an excellent return on investment (ROI). This will make communications more accessible and again reduce the environmental impact. For sustainable telecommunications services that benefit both the operators and the end user, a simple, efficient, and cost-effective wireless

base station that can run on sustainable and reliable alternative energy sources is needed. Base stations powered by alternative energy are good options that will reduce network operators' OPEX and have a positive impact on the environment by reducing their carbon emission. If alternative energy system can be deployed at base stations at rural communities, telecommunication services can be extended to millions of potential new customers.

Several studies have been carried out to evaluate the competitiveness of renewable energy systems as an alternative to the diesel generator (Schmid et al., 2024). For sites that are already on the grid, switching to an alternative source of energy can mean substantial cost savings for the network operators, as well as the possibility of actually generating revenue by reselling excess electricity that the sites will produce. Renewable energy technologies create opportunities for economic growth and also reduce greenhouse gas emissions. Use of renewable energy, for example, helps to reduce or eliminate health problems associated with using fossil fuel.

Hence, most mobile telecom operators in a bid to use alternative energy that would lower cost of operation deploy monofacial polycrystalline Solar panel (MFPV) as a sought alternative. The performance of MFPV module is affected by varying environmental conditions like low energy optimization efficiency, low power output, and ambiguities in the required land area. Research carried out show that in most of the monofacial solar-power telecom BSs, generators are still used as backup because of the low power output of the MFPV module (Yahya & Alomari, 2020).

Therefore, replacing the MFPV with Bifacial photovoltaic (BFPV) module will increase the energy output required at the base station and possibly remove the presence of backup generators while using batteries as backup on the specified days of autonomy (DOA). BFPV module harnesses energy from both the front and back sides of the panel thereby presenting an opportunity to optimize energy generation and reduce costs. However, using bifacial PV modules in solar-powered telecommunication networks in Nigeria requires careful optimization and control to ensure efficient and reliable operation of system. Optimizing and controlling solar-powered communication networks with bifacial PV modules is imperative for addressing the energy needs of mobile telecom base stations in the country for sustainable development and reliable network connectivity (Alsharif et al., 2019).

Renewable energy sources are appealing as a result of their availability and environmentally friendly in terms of power generation (Hernández-Callejo et al., 2019) (Rajesh & Mabel, 2015).

Among these renewable energy sources, solar photovoltaic (PV), in particular, is quickly expanding, with the installed capacity of solar photovoltaic systems reaching 800GW in 2021, from 50GW (Yakubu et al., 2024) in 2010, as shown in figure 1.1. Furthermore, within the same period, the contribution of solar photovoltaic power to globally installed renewable energy has increased from 3.29% in 2010 to 28.03% in 2021 as shown in figure 1.2 (a) (IRENA Technologies, 2021).

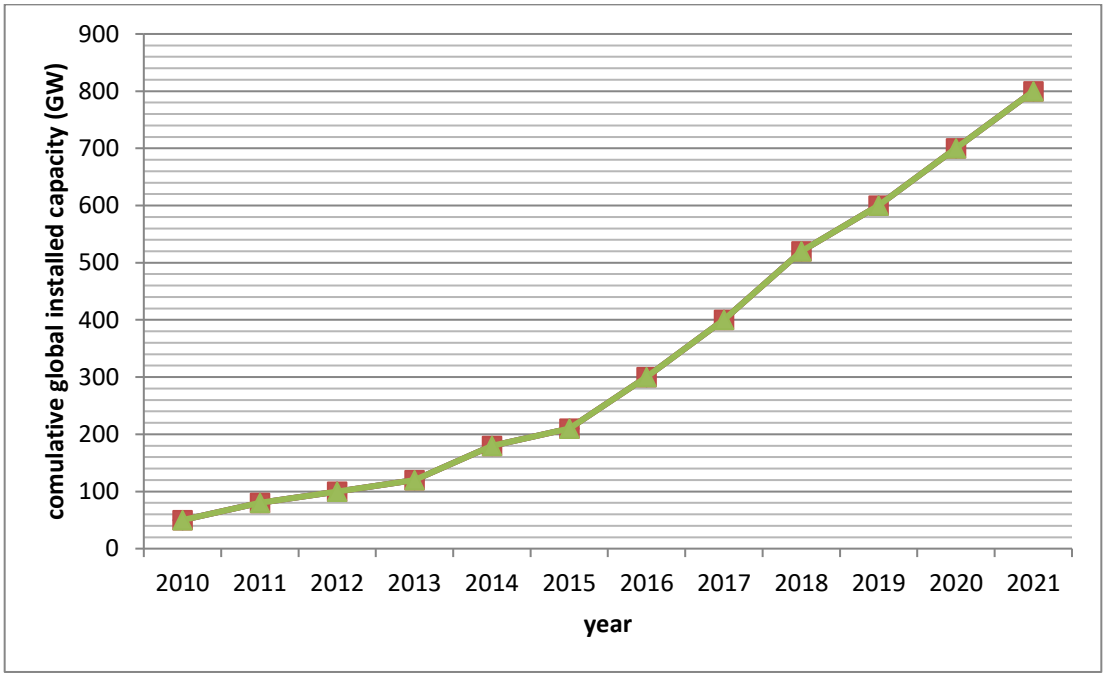

Figure 1.1: Trends in global cumulative installed solar photovoltaic capacity. Source: IRENA technologies, 2021).

In Figure 1.2 (a), there is a clear indication that solar PV has overtaken onshore wind energy as the second-renewable energy. Therefore, many different PV cell technologies are available due to the rising demand for the energy source. The renewable energy of solar PV cells is divided into three generations and is primarily based on the basic material used and their level of commercial production

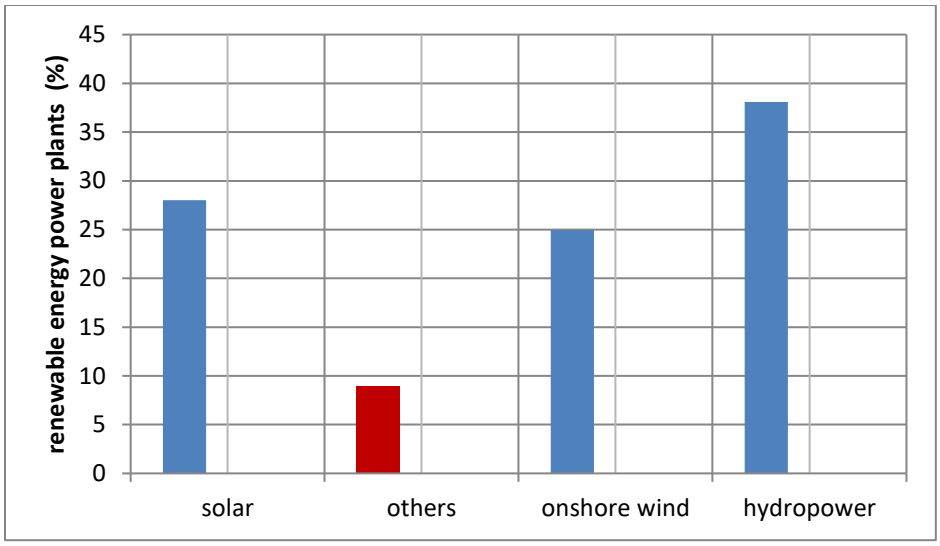

Figure 1.2 (a): Percentage share of renewable energy technologies power plants in 2021. Source: IRENA Technologies, 2021

Monofacial crystalline silicon PV modules in fixed-tilt system configurations dominate contemporary PV installations (IEA, 2024) while BFPV systems are becoming increasingly popular nowadays since they are displacing monofacial PV technologies in market share. Silicon wafers have been used to build more than 90% of photovoltaic solar cells and this dominance is projected to continue in the future (Saga, 2010). For bifacial PV modules, the story is not different, as crystalline silicon is the most commonly utilized material (Guerrero-Lemus et al., 2016).

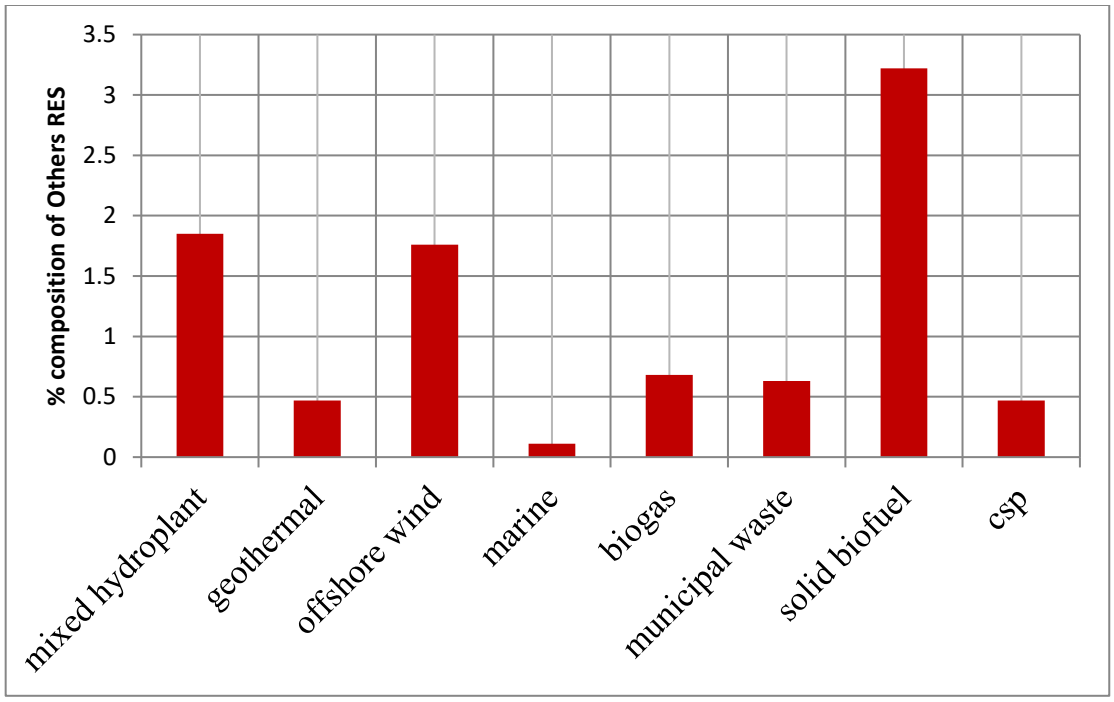

Figure 1.2 (b): Percentage share of 'Others' renewable energy technologies power plants in 2021. Data from (IRENA Technologies, 2021)

The passivated emitter rear contact (PERC), passivated emitter rear locally-diffused (PERL), passivated emitter rear diffused (PERT), inter-digitized back contact (IBC), and the hetero-junction with an intrinsic thin layer (HIT) are examples of silicon solar cell technologies that have made bifacial solar cell operation a working reality today (Jaeckel et al., 2018).

The Perovskite tandem technology is promising and gaining research interest since it is less susceptible to self-heating and produces more energy (Khan et al., 2021). Figure 1.3 shows the market share of different cell technologies. The bifacial modules were first conceived in the 1960s and were deployed in applications such as space exploration, telecommunication, and rural electrification (Lorenzo, 2021). However, economic and technical barriers kept them out of the main stream. Conventional modules have an opaque backside and absorb direct, diffuse, and reflected irradiance only at the front.

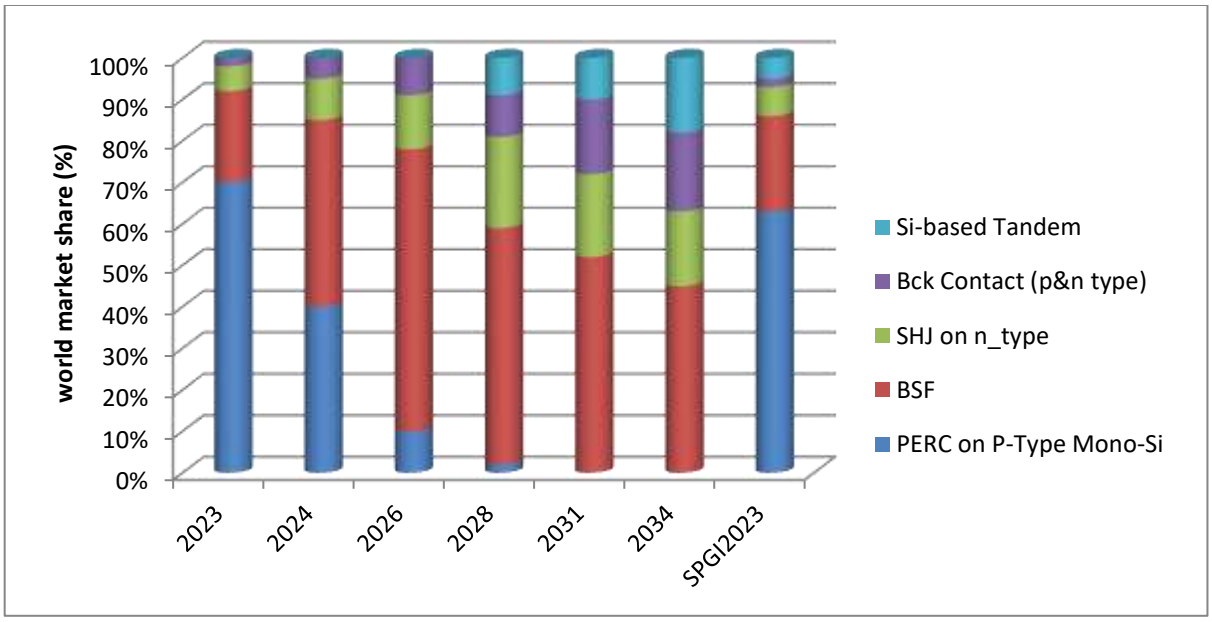

Figure 1.3: Projected different solar cell technology markets (Source: ITRPV, 2024)

In contrast, bifacial PV modules can convert irradiance into electrical energy on both the front and rear sides, depending on mounting conditions and ground albedo of the surroundings, resulting in a higher yearly energy yield for the same module area used by monofacial modules.

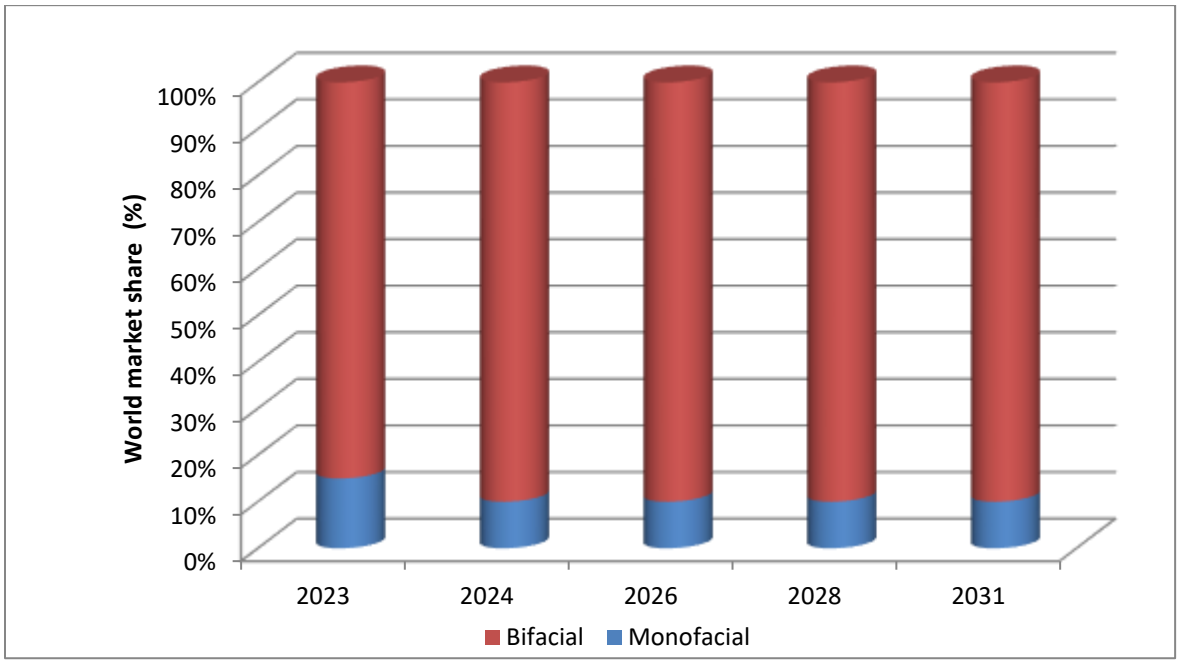

Figure 1.4: Projected bifacial cell technology market. Source: IRENA Technologies, 2021.

Consequently, the power density increases (Mesquita et al., 2021) and, as a result, can lower the Levelized cost of energy (Leonardi et al., 2022). Because bifacial module technology is likely to gain ground in the worldwide market, accurately estimating the performance of bifacial PV systems is important (Guerrero-Lemus et al., 2016).

To ensure the commercial success of bifacial modules and systems, a solid set of industry benchmarks for rating, characterization, modelling, and safety must be developed (Kopecek et al., 2015). Accurate and validated models of module and system performance are necessary. However, bifacial module technology introduces additional challenges regarding to the reproducible and comparable module characterization because most of the irradiance that strikes the module at the back comes from the ground albedo, which can be affected by shadow, mounting structure, and other modules within the field (Shoukry et al., 2016).

A critical understanding of ideal module structure; module tilt, orientation, spacing, and elevation is required to estimate the power generation of bifacial modules. The specification measures the current voltage (I–V) characteristics of bifacial photovoltaic systems in natural or simulated sunshine. Additionally, the specification applies to single PV cells, sub-assemblies of such cells, and whole PV modules (IEC Technical Specification, 2024). Several investigations on harnessing the energy yield from bifacial modules have been conducted using experimentation, modelling, and simulation. This study aims to synthesize prior work on bifacial PV characterization, modelling approach, energy performance evaluation, and applications at telecom base stations as energy-sought alternatives, and identify research gaps and prospects for bifacial PV systems. Despite the privatization of the Power Holding Company of Nigeria (PHCN), Nigeria's energy demand, which is always exponentially rising, still far outweighs the supply which is quite erratic. Adopting solar PV technology of bifacial module on a large scale will reduce the national consumption of fossil fuel and its related products, boosting its availability and sustainability (Schmitt et al., 2009). It is estimated by (Marsan et al., 2013) that when 1% of Nigeria's land area is covered with a solar technology of 5% efficiency, about 333,480 MW of electricity may be produced at about 26% capacity factor. This electricity generation capacity will be more than enough for the country up to 2050.

1.2 STATEMENT OF THE PROBLEM.

Telecommunication network base stations in Nigeria face significant energy challenges due to unreliable grid power electricity in urban areas and lack of grid electricity in rural areas. With the abundance of solar irradiation in the country, Solar-powered solutions offer a promising alternative. For long now, mobile network operators has adopted the MFPV module as the solar sort solution at telecom base stations but the monofacial solar panel systems have limitations. MFPV require large space for its installation. In the urban centres where cost of land is high, this has often increased the installation cost of the panel. MFPV tracks solar radiation only from one side of the panel, hence providing not enough power for powering the equipment at telecom base station site. Consequently, in making sure that there is 24-hr power supply at base station site, mobile operator employs diesel generators to back up the MFPV. The use of diesel generators as a backup at TBS site increases the Capital Expenditure (CAPEX) and poses great threat to the environment due to uncontrolled CO_2 emission. Beyond the imagination of the mobile operators, the inclusion of diesel generators at TBS site does not provide the 24-hr power supply due to system failure which may result from lack of preventive maintenance of the generator set, fuel pilferage and component failure. MFPV has no optimal energy harvesting strategy, as a result of its configuration, hence providing less power output at optimal level and no control and monitoring strategies. Additionally, MFPV has Lower Return on Investment (ROI) because of higher maintenance costs.

1.3 THE RESEARCH OBJECTIVES

The main objective of this research is the Optimization and Control of Solar-Powered Telecommunication Network Base Stations in Nigeria Using Standalone Bifacial Photovoltaic Module. Its specific objectives are:

i. To derive the mathematical models of a Single and double diode MFPV and rear-side irradiation models for BFPV module.

ii. Determination of the load profile of a micro-base station.

iii. Simulation of MFPV with MATLAB/SIMULINK and BFPV module with PVSyst to determine the maximum power point and its energy output at site selected from each of the six geopolitical zone of Nigeria.

iv. To develop optimization and control strategies for maximizing energy yield and minimizing energy costs using PVsyst and HOMER.

1.4 JUSTIFICATION OF THE RESEARCH

The justification of this research is based on the following situation;

i. Energy Challenges in Nigeria: Nigeria faces significant energy challenges, including inadequate power supply, frequent outages, and high energy costs. Telecommunication network base stations are particularly vulnerable to these challenges, as they require reliable and constant power supply to operate.

ii. Renewable Energy Potential: Nigeria has abundant solar energy resources, making solar power a viable alternative to traditional energy sources. Standalone bifacial solar panel systems offer a promising solution for powering telecommunication network base stations.

iii. Technical and Economic Benefits: Optimizing and controlling standalone bifacial solar panel systems can lead to significant technical and economic benefits, including increased energy yield, reduced energy costs, and improved system reliability.

iv. Environmental Benefits: Solar-powered telecommunication network base stations can reduce greenhouse gas emissions and contribute to a cleaner environment.

v. Knowledge Gap: There is a knowledge gap in the optimization and control of standalone bifacial solar panel systems for telecommunication network base stations in Nigeria. This research aims to fill this gap by providing insights into the technical and economic feasibility of these systems.

vi. Practical Applications: The findings of this research can be applied in practice to optimize and control standalone bifacial solar panel systems for telecommunication network base stations in Nigeria, leading to improved energy efficiency, reduced costs, and enhanced environmental sustainability.

vii. Contribution to Sustainable Development: This research contributes to the United Nations' Sustainable Development Goals (SDGs), particularly SDG 7 (Affordable and Clean Energy), SDG 9 (Industry, Innovation, and Infrastructure), and SDG 13 (Climate Action).

1.5 SCOPE OF THE RESEARCH

This research is based on the optimization and control of solar-powered communication network base stations using bifacial PV modules. Its scope is limited to telecommunication base stations in Nigeria. The research will focus on the development of an efficient energy management strategies and control algorithms for solar-powered telecommunication network base stations, employing a mixed-methods approach, combining simulation, and analytical methods and models of maximum power point tracking (MPPT) using PVsyst version 7.4.8 software and HOMER. In conducting this research, data from field measurements generated from NASA were used, while simulations will be used to achieve the research objective.

CHAPTER TWO

LITERATURE REVIEW

2.1 OVERVIEW

Renewable energies are those sources of energy that can be obtained naturally without depleting the planet's resources. These sources include solar, wind, hydro, geothermal, biomass, and biofuels. Unlike non-renewable energies, such as oil, gas, and coal, which are finite and emit large amounts of greenhouse gases, renewable energies are cleaner and more sustainable. Additionally, the technologies to capture and utilize these energies have improved in recent years, making their use increasingly viable and economical. Renewable energies are a key solution to combating climate change and reducing dependence on fossil fuels (Kharrich et al., 2021). By investing in these energy sources, jobs can be created and sustainable economic development can be promoted. In summary, renewable energies are a key alternative to ensure a cleaner and safer future for future generations.

Hybrid renewable energy systems are those that combine two or more renewable energy sources to generate electricity. These systems are especially useful in places where there is no access to the conventional electrical grid, or where the connection is limited or unstable (Dipti, 2018). An example of a hybrid system combines solar and wind energies. During the day, when the sun shines, solar panels generate electricity that is stored in batteries for later use. At night, when there is no sun, wind energy conversion systems (WECS) harness the wind to generate additional electricity and charge the batteries (Roy et al., 2022). Another example of a hybrid system combines solar and hydro energies. During the day, solar panels generate electricity that is used to pump water from a river or lake to a dam. At night, when there is no sun, the water stored in the dam is released through a hydro turbine to generate additional electricity (Nema et al., 2008).

Hybrid renewable energy systems can be more efficient and reliable than systems that use a single energy source (Singh, 2018). Additionally, they allow for a better use of available resources and reduce the cost of generated energy. For these reasons, hybrid systems are becoming increasingly popular worldwide, especially in rural or remote areas (Ganjei et al., 2022).

The studies conducted on HRESs mostly address the methods to use the different structures for power distribution. To date, there are three variants, which are used depending on the application chosen by the system designer. These configurations are DC microgrid, AC microgrid, and AC/DC

microgrid. A DC microgrid is a power system that uses direct current for power distribution instead of alternating current. It is composed of various renewable energy sources, energy storage systems, and DC loads. The use of DC for power distribution has several advantages, such as the elimination of AC–DC–AC conversions required in AC microgrids, which improves efficiency and reduces energy losses. In addition, eliminating the need for distributed generator (DG) synchronization also simplifies system designs and reduces costs. DC microgrids can also integrate energy storage systems to improve efficiency and energy independence (Pourbehzadi et al., 2019).

In an AC microgrid, an AC-to-DC converter is used to power the DC loads. Other renewable energy sources can also be incorporated through the appropriate interface of power converters. Each power source is connected to the AC bus through a separate power converter, allowing them to continue to operate even if one of them is disconnected, and improving system reliability. However, synchronization is a major obstacle in this configuration (Roy et al., 2022).

The AC/DC microgrid combines the advantages of AC and DC microgrids to facilitate the integration of AC and DC loads with their corresponding sources. It can be used in two modes, off-grid or grid-connected, and is suitable for use in smart grids alongside the current grid. In addition, voltage transformation, economic viability, and harmonic control are other advantages of this configuration. Although it has some major benefits, in terms of overall performance, the hybrid AC/DC microgrid is a good option to address operational problems and challenges as it outperforms other types of microgrids (Pourbehzadi et al., 2019).

Battery energy storage systems (BESSs) are a crucial part of the system for good optimization, as they allow electrical energy to be stored for later use when needed. This makes them especially useful for the integration of renewable energy sources, such as solar and wind power, into the power grid. In this way, the BESSs can balance the variability of renewable energy generation and provide power when demand is high or when power generation is low (Hidalgo-Leon et al., 2017).

Battery energy storage systems (BESSs) have several advantages over other forms of energy storage. First, they are highly efficient and can store large amounts of energy. Second, they are flexible and can be used in a variety of applications, including backup power systems and energy management systems. Third, they are capable of providing grid services, such as frequency control and voltage control, making them valuable for grid stability. In addition, BESSs have a longer lifetime than other forms of energy storage and are less prone to failure. Overall, BESSs are an important part of the transition to a more sustainable and secure energy system (Singh, 2018).

Optimization techniques are fundamental to achieve an efficient and reliable energy management and storage system. These techniques consist of designing appropriate strategies to balance power generation and load demand, even when uncertain renewable sources are used. This is achieved through the use of control algorithms that can predict the availability of renewable energy and adjust the load accordingly. In addition, these techniques can also help optimize the use of energy storage systems, such as BESSs, to ensure that energy is stored and released effectively and efficiently. Overall, choosing the right optimization technique is crucial to maximize energy efficiency and system stability (Vishakha et'al., 2020). The modelling and optimization approaches used for HRESs can be classified into intelligent methods, iterative methods, and computational methods (Singh, 2018).

To achieve an optimal HRESs design, economic and technical criteria are considered. The economic criteria seek to minimize the costs associated with HRESs implementation, including energy cost and net present cost, while the technical criteria focus on the reliability, efficiency, and environmental benefits of HRESs. Overall, the goal is to find a compromise solution between the costs and benefits of HRESs (Roy et al., 2022)

2.2 OPTIMIZATION OF HYBRID RENEWABLE ENERGY SYSTEMS (HRES)

In energy systems, the optimization of the size of the individual systems can be made in a variety of ways, depending upon the choice of parameters of interest (Habib et al., 1999). Energy Optimization models are employed as a supporting tool to develop energy strategies as well as outline the likely future structure of the system under particular conditions. This will help to provide insights into the technological paths, structural evolution and policies that should be followed (Mattsson & Clas-Otto, 2023). Several studies have been done to evaluate the competitiveness of renewable energy systems as alternatives to the diesel generator such as by (Schmid et al., 2004) and feasibility of the standalone systems (Shaahid & Elhadidy, 2004). While it is found that the renewable energy system is competitive and feasible for off-grid application, single source renewable usually leads to component over-sizing, which increases the operating and life cycle costs (Bagul et al., 2023). A combination of one or more resources of renewable energy, called hybrid, will improve load factors and help in saving on maintenance and replacement costs as the renewables can complement each other (Kaldellis et al., 2006). High

initial capital of the system is a barrier to adopt the system thus the needs for long-lasting, reliable and cost effective system (Kellogg et al., 1996) is an added advantage. Designing an energy system would require correct components selection and sizing, with appropriate operation strategy (Borowy & Ziyad, 1994). Initial optimization and component sizing methods are based on worst month scenario and leads to non-optimal design with excess capacity. BFPV systems can offer great abilities in the production of energy based TBS. A Diesel generator is often used so that energy needs are covered in case of insufficient meteorological conditions in some areas. A battery can also be used with the systems for storage of energy when its production is more than the required loads. In regions where sunshine is good, the combined use of BFPV and Battery has great results for most of the day-night period and also for a very large period of a year. (Deepak et al., 2011) proposed a system that consists of micro hydro plant, wind turbine and solar photovoltaic (PV) panels. Diesel generator and battery bank were included as part of back-up and storage system. The authors adopted a new approach to the PV/Wind/diesel hybrid system including a hydro resource and compared the results. The renewable energy sources in collaboration with diesel generator were evaluated to determine the feasibility of the system. Their results show that on a cloudy day, when solar photovoltaic cells are producing lower levels of energy, a battery is producing a lot of energy to the loads to meet peak load demands. More so, the contribution of electrical power by diesel generator increases in the absence of micro-hydro plant. A lot of research has been conducted on the performance of power systems and experimental results have been published in many articles. The energy output of a BFPV system can be enough for the demands of a house placed in regions where the extension of the already available electricity grid would be financially unadvisable (Elhadidy & Shaahid, 2004). Such hybrid systems can also be used in various other applications, such as telecommunications.

Fossil fuels like coal, oil and natural gas are currently the world's primary energy sources. The heavy dependence on the fossil fuel in 20th century largely reduced the natural reserve of it. Aware of its finite reserve and adverse effect on environment, engineers and scientists are increasingly trying to find and use alternative energy sources. The three most widely used renewable alternative energy sources are hydro, wind and photovoltaic (PV). For isolated and remote places where chances of reaching national grid is minimum because of technical and economic constraints, renewable energy system is considered as an attractive alternative and thus preferred in many regions and countries.

Such system can also have backup devices like diesel generator and battery bank to meet peak hour demand. Electric power is vital for both economic and personal well-being (Binayak et al, 2015). A well-engineered renewable energy system can be cost effective, highly reliable and can improve the quality of life. In most cases, solar and wind energy complement each other, however both are unpredictable because of instantaneous fluctuation of solar irradiation and wind speed. A new hybrid system comprising of solar-wind and hydro were implemented by (Bhandari, 2013) in the remote village of Nepal (Bhandari et al., 2014) (Ahn et al., 2014) explored the characteristics of an off-grid hybrid renewable energy system (HRES) and their implications regarding the reliability of the system. HRES optimization criteria can be divided into two categories: economic and reliability and the selection of each depend on the research objectives and the desired tolerance level. Economic criteria refer to the cost or size of the system, while reliability criteria focus on ensuring the continuity of load power supply.

Hybrid systems with energy storage in batteries have been studied by various authors. These systems have been installed for a number of decades, although their systems would be substantially improved if optimization methods were applied (Bernal-Agustín et al., 2009). Numerous papers have been written about the optimum economic designs of PV and/or Wind and/or hydro and/or Diesel systems with energy storage in batteries. Usually, the optimum design is carried out minimizing the Net Present Cost (NPC). NPC is the investment costs plus the discounted present values of all future costs during the lifetime of the system) or by minimizing the Levelized Cost of Energy (LCE). LCE is the total cost of the entire hybrid system divided by the energy supplied by the hybrid system.

2.3 HRES OPTIMIZATION METHODS

Energy optimization is very paramount in the design of a system that could deploy the best available energy options at any GSM base stations in cellular mobile communications (Razak et al., 2009). Energy Optimization of a GSM base station system looks into its sizing and the process of selecting the best components to provide cheap efficient, reliable, environmentally friendly and cost effective power supply. The techno-economic analysis looks at both environmental cost and the cheapest cost of energy produced by the system components. This

review focuses on the implementation and simulation of BFPV module, as well as the optimization of the systems using software.

A well designed simulation program permits to determine the optimum size of battery bank, PV array, Wind turbine, Hydro generation capacity and other generation system for an autonomous or grid integrated HRES for a given load and a desired LPSP based on various criteria. Some of the criteria are minimum cost of the system, minimum capacity of system and storage devices, maximum power generation, and minimum LPSP and minimum LOLP. Various optimization techniques such as graphical construction, probabilistic approach, iterative technique, artificial intelligence (AI), dynamic programming, linear programming and multi-objective were used by researchers to optimize hybrid PV/wind energy system. Table 2.1 shows detail of optimization techniques used by various authors. Various optimization techniques for energy system have been reported in Renewable and Sustainable Energy Reviews (Bernal-Agustín & Rodolfo, 2009), such as graphic construction methods, probabilistic approach, iterative technique, artificial intelligence methods, multi- objective design. Using feasible optimization method, optimum configurations which meet the load requirement can be obtained (Yang, 2008).

2.3.1 Graphical Construction

Problem with two design variables can be solved by observing graphically how they change with respect to one another. All constraint functions are plotted in the same chart. By visual inspection of the feasible region, the optimized point on the graph can be identified after objective function contours are drawn. (Markvart et al, 2006) used a long time series of solar radiation where the optimal sizing was determined by a superposition of contributions from climatic cycles of low daily solar radiation. (Ai et al, 2003) presented method for optimum size of hybrid PV/wind energy system. Performance of hybrid PV/wind energy system was determined on hourly basis; by fixing the wind generators capacity. Annual LOLP with different capacity of PV array and battery bank were calculated and optimum configuration (cost and LPSP) was found by drawing a tangent to the trade-off curve

2.3.2 Probabilistic Approach

In this approach, randomness is present depending on the collected data thus variable states are not described by unique values, but rather using one of the statistical tools. Optimum size of hybrid PV/wind energy system can be calculated on an hourly basis or daily average power per month, the day of minimum PV power per month, and the day of minimum wind power per month. Two advantages of this method are that the cost and time of environmental and load data collection are minimum.

2.3.2.1 hourly average generation capacity method

In this method, the hourly average wind, insolation, and power demand are used for optimization of the system sizing. This calculation is based on the average annual monthly data of sun and the wind. The size of the photovoltaic and wind components is given by the following equations. Most unfavourable month method

In this method, the size of the PV and Wind generators is calculated in the most unfavourable month. The unfavourable irradiation month and unfavourable wind speed month are determined based on the available data (El-Khadimi et al., 2004) (Kusakana & Vermaak, 2013).

2.3.2.2 deterministic approach

In deterministic approach, every set of variable states is uniquely determined by parameters in the model and by sets of previous states of these variables, thus there is always unique solution for given parameters, unlike probabilistic approach (Bhandari & Stadler, 2011) calculated system size and cost for PV system.

2.3.2.3 iterative approach

Iterative approach is a mathematical procedure generally performed using computer that generated a sequence of improving approximate solution for the optimization problem until a termination criteria is reached. As the number of optimization variables rises, the computation time increases exponentially when using this approach. (Li et al., 2012) used this approach to optimize PV-wind-battery HRES based on the minimization of life cycle cost.

2.3.2.4 artificial intelligence (AI)

AI is the branch of computer science that studies and develops intelligent machines and software. Russell and Norvig94 define AI as "the study and design of intelligent agents" where an intelligent agent takes actions that maximize the chance of success. AI consists of branches such as artificial neural networks (ANN), genetic algorithms (GA), fuzzy logic (FL) and hybrid systems combining two or more of the above branches. The appropriate use of intelligent technologies leads to useful systems with improved performance or other characteristics that cannot be achieved through traditional methods (Liu and Jordan, 1963).

GA is a dynamic search technique used in computing to find true or approximate solutions for the optimization and search problems. GA is categorized as global search heuristics. GA is a particular class of evolutionary algorithms that use techniques inspired by evolutionary biology such as inheritance, mutation, selection and recombination. A typical GA requires two things to be defined: A genetic representation of the solution domain and, A fitness function to evaluate the solution domain. GA might be useful in problem domains that have a complex fitness landscape that a traditional hill climbing algorithm might fail(Xu et al., 2005) used GA with elitist strategy for optimally sizing a standalone hybrid PV/Wind power system for a year (8760 hours).

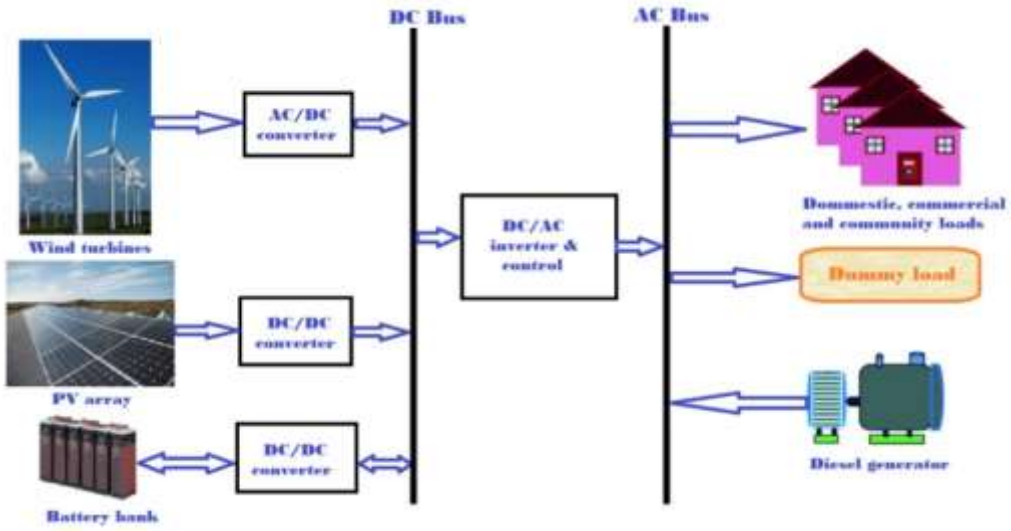

Figure 2.1: diagram of Optimization of hybrid renewable energy power systems. Source: Xu et al, 2005.

Their main objectives were to minimize the total capital cost of the system with constrained LPSP. Similarly, figure 2.1 is the diagram of Optimization of hybrid renewable energy power systems.

2.3.2.4.1 software based approach

One of the popular commercial software for designing and analysing hybrid power system is HOMER of National Renewable Energy Laboratory (NREL)/USA. Solar insolation, electrical load, hybrid generator technical details, costs, constraints, controls and type of dispatch strategy are used as the input to the HOMER software. (Hrayshat, 2009) carried out a detailed techno-economic analysis using HOMER software to design an optimal hybrid PV-diesel-battery system for remote house in Jordan.

2.4 OPTIMIZATION SOFTWARE TOOLS FOR RENEWABLE ENERGY SYSTEMS

Simulation programs are the most common tools for evaluating performance of the systems. By using computer simulation, the optimum configuration can be found by comparing the performance and energy production cost of different system configurations. Several software tools are available for simulation of the energy systems, such as HOMER, HYBRID2, HOGA, etc.

2.4.1 HOMER

This is the Hybrid Optimization Model for Electric Renewables, developed by National Renewable Energy Laboratory (NREL) USA. It is the most-used optimization software for hybrid systems (http://homerenergy.com/) (Bernal-Augustine & Rodolfo, 2009). HOMER software can simulate a wide variety of micro power system configurations. A micro power system is a system that generates electricity to serve a nearby load. Such a system may employ any combination of electrical generation and storage technologies. It is able to optimize hybrid systems consisting of a photovoltaic generator, batteries, wind turbines, hydraulic turbines, AC generators, fuel cells, electrolysers', hydrogen tanks, AC–DC bidirectional converters, and boilers. The loads can be AC, DC, and/or hydrogen loads, as well as thermal loads. The simulation is carried out using 1-hour intervals, during which all of the parameters (load, input and output power from the components, etc.) remain constant. Two types of dispatch strategies are available in HOMER. In the 'load following' strategy, the generators supply just enough power to service the loads whenever there is insufficient renewable energy contribution. In the 'cycle charging' strategy, the

generator (if present) runs at full power and excess electricity is used for charging the batteries (Lal & Atul, 2012). The control strategies are based on four proposed strategies: frugal dispatch, load following, State of Charge (SOC), set- point, and operation strategy (Barley & Byron, 2022). For systems that include batteries or fuel-powered generators like diesels, the software decides the strategy to operate generators and charging/discharging of batteries.

The analysis and design of distribution systems can be challenging, due to the large number of design options and the uncertainty in key parameters, such as load size and future fuel price. Renewable power sources add further complexity because their power output may be intermittent, seasonal, and non-dispatchable, and the availability of renewable resources may be uncertain. This software was designed to overcome these challenges. HOMER performs three principal tasks namely simulation, optimization, and sensitivity analysis. The simulation process determines how a particular system configuration, a combination of system components of specific sizes, and an operating strategy that defines how those components work together, and would behave in a given setting over a long period of time. Its higher-level capabilities, optimization and sensitivity analysis rely on this simulation capability. The simulation process serves two purposes. First, it determines whether the system is feasible. Also, it considers the system to be feasible if it can adequately serve the electric and thermal loads and satisfy any other constraints imposed by the user second, it estimates the life-cycle cost of the system. The quantity used to represent the life-cycle cost of the system is the total net present cost (NPC). This single value includes all costs and revenues that occur within the project lifetime, with future cash flows discounted to the present. The total net present cost includes the capital cost of the system components, the cost of any component replacements that occur within the project lifetime, the cost of maintenance and fuel

2.4.2 HYBRID 2

This is the Hybrid Power System Simulation Model which was developed by the Renewable Energy Research Laboratory (RERL) of the University of Massachusetts (Green & James, 1995). It is a hybrid systems' simulation software. The hybrid systems may include three types of electrical loads, multiple wind turbines of different types, photovoltaic generators, multiple diesel generators, battery storage, and four types of power conversion devices. Other components, such as, fuel cells or electrolysers', can be modelled in the software. The simulation is very precise, as

it can define time intervals from 10 min to 1 h. The possibilities with regard to control strategies are very high, but it does not optimize the system. NREL recommends optimizing the system with HOMER and then, once the optimum system is obtained, improving the design using HYBRID2.

2.4.3 HOGA

Hybrid Optimization by Genetic Algorithms is a hybrid system simulation and optimization program developed in C++ by José L. Bernal-Agustín and Rodolfo Dufo-López of the Electric Engineering University of Zaragoza, Spain (http://www.unizar.es/rdufo/hoga-eng.htm). The optimization is carried out by means of Genetic Algorithms, and can be Mono-Objective or Multi-Objective. It allows optimizing of hybrid systems consisting of a photovoltaic generator, batteries, wind turbines, hydraulic turbine, AC generator, fuel cells, electrolyser, hydrogen tank, rectifier, and inverter. The loads can be AC, DC, and/or hydrogen loads. The simulation is carried out using 1-hour intervals, during which all of the parameters remained constant. The control strategies are optimized using Genetic Algorithms. It can be downloaded and used free of charge

2.5 COMPONENT SIZING

In order to efficiently and economically utilize the renewable energy resources, an optimum sizing method is necessary. The optimum sizing method can help to guarantee the lowest investment with full use of the system component, so that the hybrid system can work at the optimum conditions in terms of investment and system power reliability requirement. With continuous research and development efforts, it has been established that the hybrid systems, if optimized properly, are both cost effective and reliable compared with single power source systems (Laidi et al., 2012).

Solar, hydro and wind energy systems are among the most developed renewable energy systems (RES), with diesel generator and have been widely applied in both stand- alone and grid-connected applications. The sizing tool performs dimensioning of the system: given an energy requirement, it determines the optimal size of each of the different components of the system. In a hybrid system, 40% of the total energy loss is due to the non-optimal sizing of the system. Simulation tools can be used for sizing. Simulation programs are the most common tools for evaluating performance of the hybrid systems. This requires that the user correctly identify the key variables and then repeatedly run the simulation, adjusting the variables manually to converge on an acceptable sizing. Some packages automate this process. A lot of research work has been

carried out to optimize their size and evaluate their performance. (Chedid & Rahman, 2020) developed a linear programming model to optimize the size of a hybrid system with battery storage and diesel sets. However, the solution provided did not consider system's expansion over a future horizon. Kellogg et al (Kellogg et al., 2023) presented a simple numerical algorithm to determine the optimum size of system's components for three different configurations: wind alone, photovoltaic (PV) alone and hybrid wind/PV. (Karaki et al., 2021) presented a probabilistic model of a stand-alone wind/PV power system. The model takes into consideration system stability, outages due to the primary energy fluctuations and hardware failure. (Gavanidou & Bakirtzis, 2019) developed a multi-objective planning technique to design a hybrid system based on minimization of both capital investment and loss of load probability (LOLP). They applied the tradeoff/risk method which rejected inferior plans and gave a set of robust scenarios to the designer. (Karaki et al., 2021) tried to determine the optimum size of a hybrid system and to assess its economic and technical merits against single PV and wind stand-alone systems. Gavanidou & Bakirtzis (2019) reported an algorithm based on energy concept to optimally size solar PV array in a PV/wind hybrid system. In this study, HOMER simulation was used to find the optimum combination and sizing of components. When working with stand-alone hybrid systems for the generation of electricity, various aspects must be taken into account (Karaki et al., 2021). Reliability and cost (economic and environmental) are two of these aspects. (Yiew et al., 2011) studied the technical and economic feasibility of implementing a Solar-wind Power Plant in Malaysia. A comparison was made between the hybrid system and a conventional standalone PV based system. From their analysis, a solar-wind hybrid power plant was highly feasible and improves the reliability and sustainability of existing standalone solar power plants. (Muselli et al., 2000) proposed the optimal configuration for hybrid systems should be determined by minimizing the kilowatt-hour (kWh) cost. Studies on genetic algorithm (GA) are done to find the optimum sizing as well as the suitable operation strategies to meet different load demand by, among others, (Dufo-Lopez & Bernal- Augustin, 2023), (Gavanidou & Bakirtzis, 2019) carried out the optimization of PV–Wind–Battery systems, modifying the size of the batteries until a configuration that ensures sufficient autonomy is achieved. (Elhadidy & Shaahid, 2023) had studied the effect of the size of the batteries on the operation hours and on the energy provided by the diesel generator in Wind–Diesel–Battery systems. The diesel generator works only when the wind turbines do not provide sufficient energy and, additionally, the batteries are unable to supply

the demand. By changing the size of the batteries, economic optimization of the system is carried out. (Koutroulis, et' al, 2006) presented a paper for economic optimization by means of Genetic Algorithms on PV–Wind–Battery systems. Elhadidy & Shaahid (2023) studied the performance of possible variances of PV–Wind–Diesel–Battery systems; Schmidt & Patterson (2018) studied the effect of energy demand management on PV– Wind–Diesel–Battery systems

2.6 CHOICE OF THE SOFTWARE

Among the various software discussed in this research, we have chosen the PVsyst version 7.4.8 for solar tracking and HOMER for optimization process. This software is users' friendly that can be easily configured, and as for the managed information, it is complete too. It is also the software that can be used to simulate BFPV module and at the same time conduct the energy optimization of any designed project. This software is a computer modelling tool that can evaluate different situations to determine the system configuration that will provide acceptable reliability at the lowest lifecycle cost. In addition to sizing the components of the any system, the software also does a comparison between two simple dispatch strategies. PVsyst dispatch strategies are Load profile monitoring and Cycle Charging. The user is able to choose between different sources of the solar project, such as standalone with generator, standalone without generator, grid connected system, pumping system and, electric vehicle system.

2.7 OPTIMIZATION TECHNIQUES

2.7.1 Multi-Objective Design of Standalone Energy Systems

In any engineering field, to carry out a design, it is possible to have several objectives simultaneously, being typical that some of them conflict with each other (Collette & Patrick, 2003). Multi- Objective optimization attempts the simultaneous minimization of various objectives. In the optimum sizing of the systems, we wish to carry out the design considering simultaneously at least two objectives (costs and pollutant emissions). These two objectives are in conflict, since a reduction in design costs implies a rise in pollutant emissions and vice versa. Therefore, the task of getting good results in problems of this kind (multi-objective) is complicated. Given the complexity of this kind of problems, because of the large number of variables that are usually considered and of the mathematical models applied, classic optimization techniques may consume excessive Central Processing Unit (CPU) time or even being incapable of taking into account all the characteristics associated to the posed problem. In the literature (Dufo-López, 2005) the design

of these systems is usually done by searching the configuration and/or controls that yields the lowest total cost through the useful life of the installation. However, the environmental issues associated to this type of installations should also be taken into account during the design process. Until now, usually, the pollutant emissions have been calculated after obtaining the design that minimizes costs. In some cases, as in the HOMER program, it is possible to consider the pollutant emissions by economically evaluating them, and therefore becoming a part of the costs objective function. This mapping of costs to emissions is subjective, and decisively influences the results of the design. The method that the software uses for the multi-objective design is known as the method of the weights (Dufo-Lopez, 2008). Multi-Objective Evolutionary Algorithms (MOEAs) stand out in the multi-objective design task, being applied in numerous papers (Pelet et al., 2005). (Coello et al., 2007) carried out an application of MOEA for the optimization of system cost and CO_2 emissions for a stand-alone system in which three hotels and a town in the Tunisian Sahara were thermally and electrically supplied. The system consisted of photovoltaic panels, diesel generators, thermo-solar panels, a hot water accumulator, and a cooling tower (Ranking cycle). (Bernal-Agustín et al., 2006) presented a multi-objective optimization (NPC versus CO_2 emissions) to hybrid a Solar-wind-diesel system with battery storage based on MOEAs. In a similar development, (Dufo-López & Bernal-Agustín, 2008) presented a triple multi-objective optimization to minimize simultaneously the total cost throughout the useful life of the installation, pollutant emissions (CO_2) and unmet load.

Multi-objective optimization deals with such conflicting objectives. It provides a mathematical framework to arrive at optimal design state which accommodates the various criteria demanded by the application. The process of optimizing systematically and simultaneously a collection of objective functions are called multi-objective optimization (MOO). The similarity between single- and multi-objective optimization makes it possible to use the same optimization algorithms as for the single-objective case. The only required modification is to transform the multi-objective problem into a single criterion optimization problem. But the resulting solution to the single objective optimization problem is usually subjective to the parameter settings chosen by the user (Mohammad, 2005). Moreover, multi-criteria optimization requires simultaneous optimization of multiple often competing or conflicting criteria (of objectives). A multiple criteria decision making (MCDM) process is a system that helps with making decisions under multiple, but conflicting criteria. The conflict of these objectives or criteria arises because improvement in one objective

can only be made to the detriment of one or more of the other objectives. It can also be described as a migrated system with an analyzing technique called multi-criteria decision analysis (MCDA). MCDA provides a systematic procedure to help decision makers choose the most desirable and satisfactory alternative under uncertain situations (Steven, 2000). For instance, in order to select a new automobile vehicle, many criteria need to be considered including the cost, speed, interior capacity, comfort level, and reliability. There is no optimal solution for this vehicle selection problem. One might want to choose a fast but inexpensive vehicle, while others might want a comfortable and reliable one. Therefore, using MCDA, a decision can be made according to the decision maker's preference. A multiple-criteria problem begins when a decision maker has a situation that requires a decision. There are a number of criteria that the decision maker should be concerned with, and several different courses of action may be available to address most or all of the criteria in some way. The problem the decision maker is faced with is to determine which course of action or alternative would best satisfy the criteria and fully satisfy the constraints (Rao & Davin, 2008). According to many authors for instance MCDM is divided into Multi-objective Decision Making (MODM) and Multi-attribute Decision Making (MADM). MODM studies decision problems in which the decision space is continuous. A typical example is mathematical programming problems with multiple objective functions. On the other hand, MADM concentrates on problems with discrete decision spaces. In these problems the set of decision alternatives has been predetermined. Alternatives represent the different choices of action available to the decision maker. Usually, the set of alternatives is assumed to be finite, ranging from several to hundreds. They are supposed to be screened, prioritized and eventually ranked. Each MADM problem is associated with multiple attributes. Attributes are also referred to as "goals" or "decision criteria". Attributes represent the different dimensions from which the alternatives can be viewed.

2.8 RELATED LITERATURE ON THE OPTIMIZATION OF HYBRID ENERGY SYSTEM

The hybrid energy system based on renewable energy (RE-HES) has advantages of high efficiency, economy and low carbon emission, and is considered to be one of the effective & Chee, 2019) (Yi et al., 2021). RE-HES has high degree of flexibility and diversity, it provides a good platform for the comprehensive utilization of various energy sources (Mala & Rajeshwer, 2020), including the complementarity of continuous energy and intermittent energy (Merei et al., 2013), the complementarity of high-carbon energy and low carbon energy (Yongpin et al., 2016) (Junjie et

al., 2022), the complementarity of electricity and gas (Merei et al., 2013), the complementarity of electricity and heat (Zeng et al., 2016), and so on. RE-HES have many application scenarios, such as residential communities, office buildings, commercial areas, campuses, hospitals, and airports. Another potential application scenario is the data center (Pei et al., 2020).The data center consumes a large amount of energy (Caishan et al., 2021). RE-HES can provide efficient green energy for data centers to meet its power and cooling needs. At the same time, the large amount of waste heat generated by the data center can also be combined with RE-HES to further improve the overall efficiency and economy of the system (Howard and Shengwei, 2019). The performance of RE-HES in various application scenarios must first be guaranteed through configuration optimization. During the system configuration process, various energy sources are added as needed, the type and capacity of each device are selected, and its operation strategy is determined to make the final configured production system more economical, energy efficient, and environmentally friendly (Seyed et al., 2022). RE HES have numerous devices, diverse structures, and flexible operation strategies, which bring great challenges to the configuration optimization of the hybrid energy system. To this end, many literatures focus on the configuration optimization problem of RE-HES (Barun & Mahmudul, 202) (Lin et al., 2017). Performance evaluation, model building, and model solving are the three main elements of a configuration optimization problem. In terms of performance evaluation, most researches are based on economic, energy saving, and environmental protection indexes (Liu et al., 2022), but in order to analyze system performance more comprehensively, many new evaluation indexes have also been developed in recent years (Ni et al., 2020) (Zhong et al., 2021). The construction of the model is closely related to the research object and research needs. In addition to the need to reasonably construct the objective function (mainly based on the research results of evaluation indexes), it is more important to reasonably describe the constraints (Wei et al., 2017) (Cao et al., 2018). The constraints here include not only the internal constraints of the system and the physical interaction constraints between the system and the outside world, but also various non-physical constraints, such as economic constraints, human preference settings, etc. (Ahmad, 2021). The solution of the model also deserves attention. The configuration optimization model of the hybrid energy system is usually complex, which brings many challenges to the research of the solution algorithm. Many solving algorithms have been proposed, including classical algorithms (Yunfei et al., 2020), intelligent algorithms (Paliwal et al., 2014) and hybrid algorithms (Askarzadeh, 2013).

2.9 INTEGRATED STRUCTURE OF RE-HES

According to the current literature, the most basic integration methods of hybrid energy systems can be divided into two categories. One is series integration, the other is parallel integration. In the series integration type, the two energy sources do not work independently, but are strongly coupled in the same device and work together. As shown in figure 2.3, based on gas steam combined cycle, solar collector is used to heat the outlet water of high-pressure economizer. In this system, the solar collector plays a role like the steam drum of the heat recovery steam generator in the gas steam combined cycle.

The two energies converge at the inlet of the super-heater of the heat recovery steam generator, and then jointly drive the steam turbine to do work (Antonanzas et al., 2014). In the parallel integration type, the various energy sources are less coupled during the energy conversion process, but only converge before being supplied to the user, as shown in figure 2.4.

The integration structure of the former is more complicated with stronger coupling, so the current research mainly focuses on the integration mechanism and performance analysis. Although the integration structure of the latter is relatively simple, it has many types of units and complex combinations, which makes the integration optimization more difficult and becomes the focus of current research.

2.10 Series integration

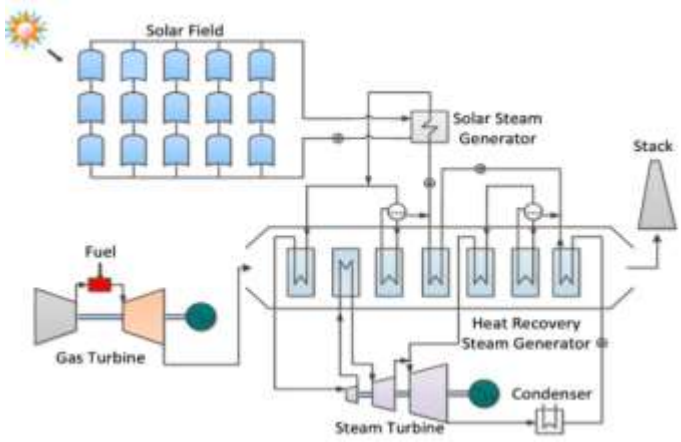

Figure 2.2: Series-integrated multi-energy complementary system. Source: Askarzadeh, 2013

In hybrid energy systems, the integration of solar energy and natural gas is the most common. In addition to the integrated forms shown in figure 2.2, solar energy is also used for the synthesis and de-carbonization of gaseous fuels (Wei et al., 2011). In this system, natural gas reacts with water vapor under the high temperature heating of solar energy to generate H_2 and CO_2, and the H_2-rich fuel can be obtained by removing CO_2. According to the literature, not only 92% CO_2 can be removed, but also the power generation efficiency of the gas turbine reaches 39.2%, which is 7.9% higher than the reference system. Similarly, (Augusto et al., 2013) also uses solar energy for the synthesis of gaseous fuel, and then the synthesis gas is mixed with natural gas and then enters the gas turbine to be burned and do work. This study shows that when all syngas is used as fuel, about 20% of natural gas can be saved, which is quite close to the study by Wei et al., (2011) Solar and gas turbines are more closely integrated in Felsmann et al., (2015).

Part of the air at the outlet of the compressor is heated by solar energy, mixed with the high temperature flue gas at the outlet of the combustion chamber, and then enters the turbine to do work. In another proposed scheme, the solar collector directly replaced the function of the combustion chamber. All air at the compressor outlet is heated by solar energy to high temperature air and then goes directly to the turbine to do work. This scheme actually goes beyond the combination of solar energy and natural gas and can be classified as a pure Solar System. Another way of integrating solar energy into gas turbines is given in Soltani et al., (2014). Part of the air at the outlet of the regenerator is heated by the solar collector and then enters the combustion chamber, and the solar collector plays the role of secondary heating of the air here. In addition to pure power generation systems, solar energy is also often introduced into cogeneration or combined cooling, heating and power systems. For example, Yagoub et al., (2006) studies the system performance of solar energy integrated with a gas boiler and turbine type cogeneration unit. In this study, solar energy was used to heat the exhaust flue gas of the boiler, and then combined with the high temperature flue gas from the combustion chamber to enter the boiler to heat the working fluid. It can be seen from the above research that the series integration of solar and natural gas distributed energy systems is very diverse. Solar energy can penetrate from the fuel end of the natural gas distributed energy system to the waste heat recovery end. In contrast, the series integration of wind energy, geothermal energy, etc. with the natural gas distributed energy system is much less, and its integration is mainly at the waste heat recovery end. Parallel integration is a relatively common way to realize the complementary utilization of these energies

2.10.1 Parallel integration

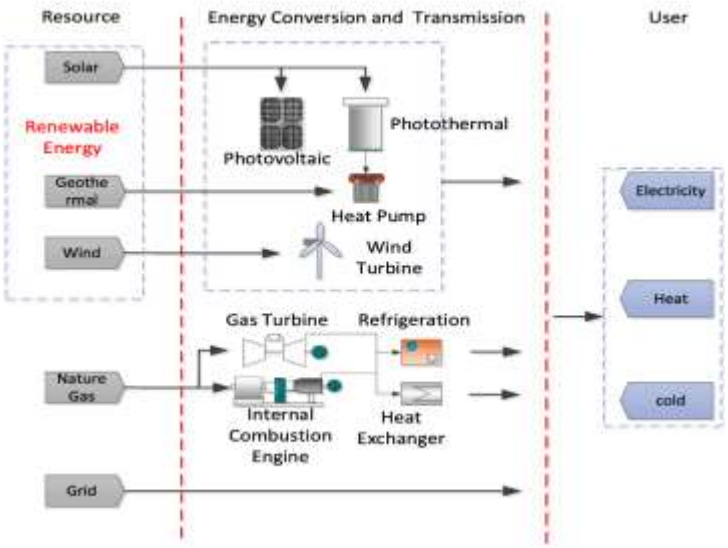

Figure 2.3: Parallel-integrated multi-energy complementary system. Source: Antonanzas et al., 2014

Compared with the series integration method, the parallel integration method is much more flexible as shown in figure 2.3. Through parallel integration, multiple energy sources can work together on the same platform to meet the user's cooling, heating and power load needs. Kalantar & Mousavi, (2010) integrates 195 kW wind turbine, 85 kW solar power generation, 230 kW micro gas turbine and 2.14kAh lead-acid battery and realizes the capacity optimization and operation control of the system. A similar study was conducted in Mousavi, (2012). The introduction of renewable energy can significantly reduce greenhouse gas emissions from natural gas energy systems. This is fully reflected in the research in Braslavsky et al., (2015). In this thesis, DER-CAM tool was used to establish an economic optimization model for the integrated system, which includes natural gas combined cooling, heating and power plant, photovoltaic power generation, solar collectors, etc., and the minimum cost and minimum CO_2 emissions are used as the objective function (Yongpin et al., 2016) (Yinghong et al., 2008), PV-wind-Battery hybrid energy system (Garima et al., 2017), PV-Wind-Diesel-Battery hybrid system (Mohammad et al., 2017), wind-diesel system with compressed air storage (Ibrahim et al., 2011). In the comprehensive utilization of multiple energy sources, it can be further subdivided according to whether each energy source is equal or has

priority such as the solar-assisted coal-fired power generation system based on coal-fired power generation (Yongpin et al., 2016), solar thermal integration in combined cycle gas turbines (Antonanzas et al., 2014), and hybrid energy system with natural gas as main fuel (Hossein et al., 2017).

2.11 CONFIGURATION OPTIMIZATION ARCHITECTURE OF HE-RES.

The optimal configuration of a system means that the system has the best combination of equipment and capacity, which can optimize the overall performance of the system by optimizing operation under the expected load demand. Therefore, the configuration optimization of the hybrid energy system needs to solve two problems at the same time: one is the configuration problem, i.e., to determine the type and capacity of each device in the system; the other is the operation problem, i.e., to determine the optimal operation strategies of the system under the expected load demand. These two issues are not independent but affect each other (Ryohei et al., 2015).

2.11.1 Centralized architecture

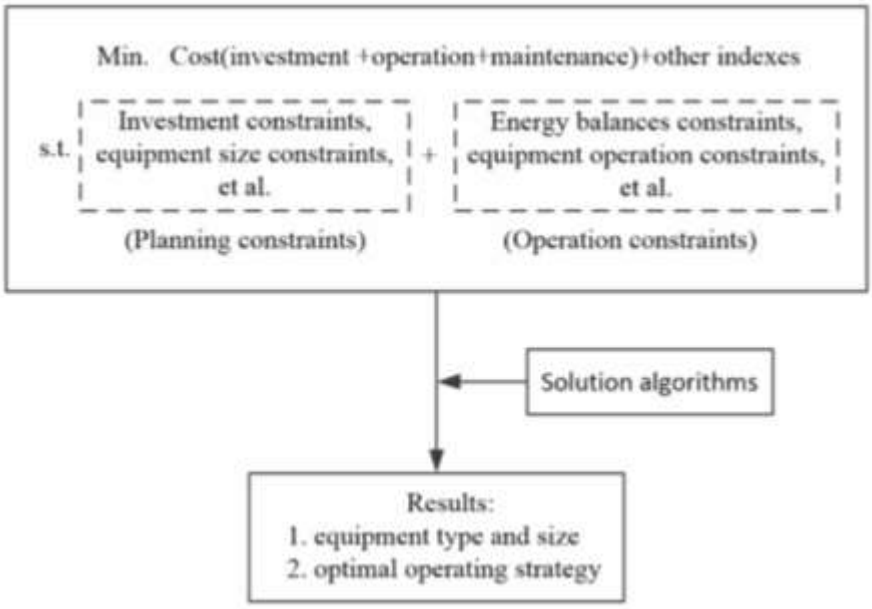

Figure 2.4: Centralized architecture for RE-HES configuration optimization. Source: Wang et al, 2019a

The centralized architecture refers to the unified construction and solution of the model to obtain the equipment type and size and the optimal operation strategy, as shown in figure 2.4. Based on the centralized architecture, many studies have been carried out on hybrid energy systems. Yi et al., (2022) proposed a mixed integer nonlinear programming (MINLP) model to obtain the optimal configuration of a solar-assisted natural gas distributed energy system with energy storage (Jianli et al., 2021). The advantage of the centralized architecture is that the construction of the model can be closer to the original appearance of the problem, and there is no need to worry about the loss of information that may be caused by the separation of the planning optimization model and the operation optimization model in the layered architecture. Therefore, with the support of efficient solving algorithms, the Centralized architecture is more likely to obtain theoretical optimal values than the layered architecture. However, as the complexity of the problem increases, the shortcomings of the overall architecture will become more and more obvious. The model obtained based on this method may be difficult to solve, and the accuracy of the model description and the solution efficiency are not easy to balance, which eventually leads to the problem of the quality of the optimization results.

2.11.2 Layered architecture

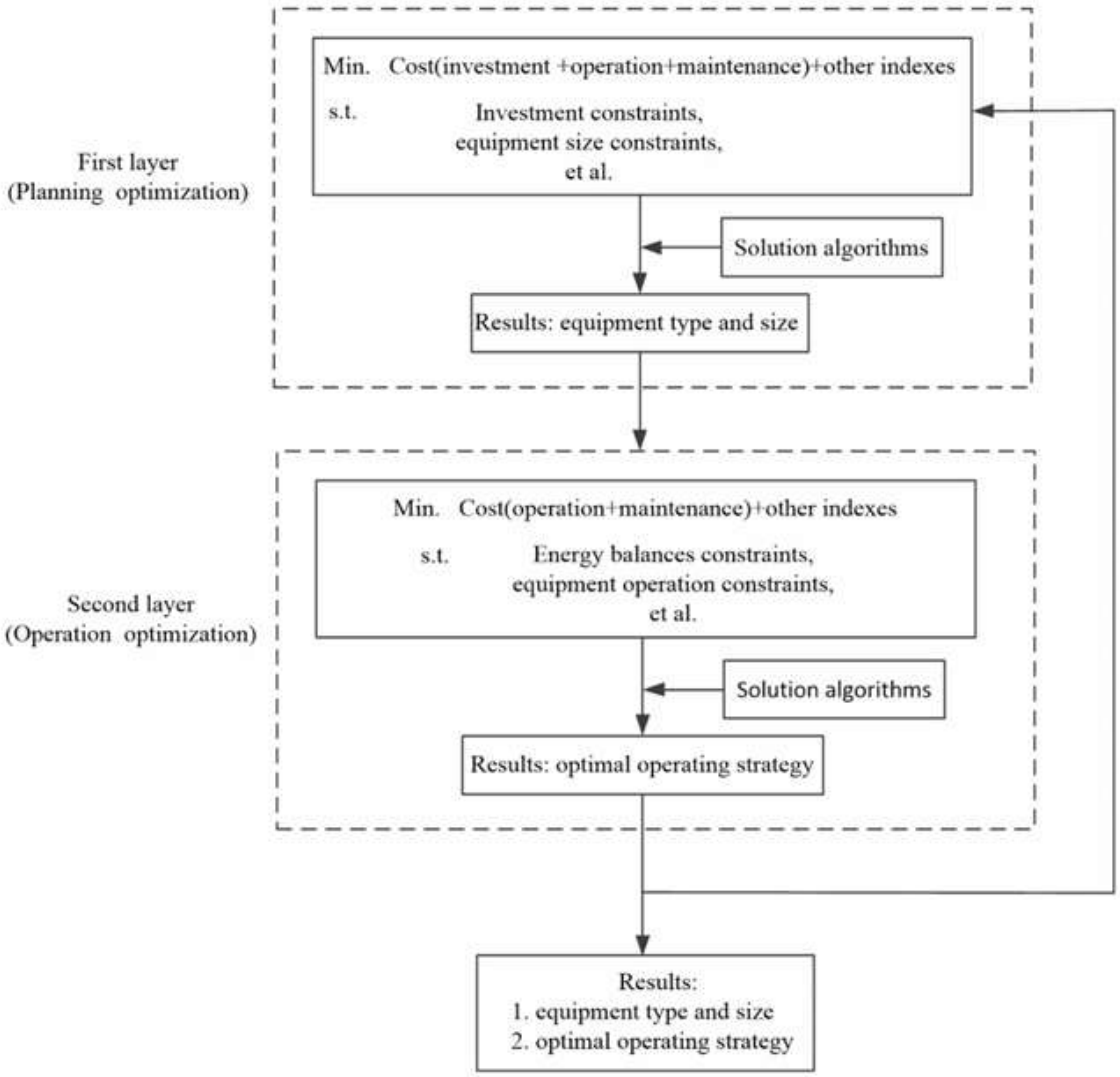

Figure 2.5: Layered architecture for RE-HES configuration optimization. Source: (Source: Yuxuan et al., 2022)

The layered architecture refers to dividing the configuration optimization problem into multiple problems to model and solve separately, as shown in figure 2.5. In the layered architecture, the configuration problem is divided into the planning problem layer and the operation problem layer. These two layers can be modeled and solved separately, but the coupling problem between the two layers needs to be properly handled. The layered architecture has greater flexibility than the centralized architecture, and the choice of modeling and solution methods can be more free and targeted. Therefore, many researches have been carried out based on this architecture in recent years. Aiming at an isolated grid energy system composed of hydropower stations, hydrogen

production equipment, hydrogen storage devices and fuel cells, a configuration optimization model based on a two-layer structure is designed in Huang et al., (2021), in which the upper layer aims to minimize the investment cost, and the lower layer aim for minimal operating costs. The Asynchronous Advantage Actor-Critic (A3C) reinforcement learning algorithm and Gurobi are used to solve the model. To solve the problem of optimal configuration of park integrated energy system under the influence of uncertainty, Min et al. (2022) proposes a two stage robust optimization model based on a dynamic programming strategy. Wang et al. (2019a) presents a two stage optimal configuration method. The first stage determines the capacity size, equipment selection and the number of units; the second stage considers the operation constraints, verifies and compares the reliability and economy of the configuration scheme, so as to obtain the optimal capacity configuration scheme. For multi-objective optimization, more layers can be used. Since multi-objective optimization problems are often handled with a two-layer structure (Xu et al., 2020a), in the first layer, the multi-objective optimization results are obtained; in the second layer, the weight coefficients of each objective are determined. Therefore, if the multi-objective optimization results are computed in the first layer using the layered architecture, the entire optimization problem actually adopts a three-layer structure. Problems at different levels can be solved by different algorithms, which provide more possibilities for the combination of more algorithms to solve the problem. It is worth noting that the more layers are divided, the easier the optimization problem may be to solve, but the more difficult it is to obtain the theoretical optimal value.

2.12 MODEL DESCRIPTION AND CONSTRUCTION OF RE-HES

2.12.1 Model construction method

The construction of an optimization model is one of the keys whether a centralized architecture or a layered architecture is adopted. In the process of model establishment, in addition to accurately describing various influencing factors of the system, the logic of model expression and the convenience of solution should also be considered. There are many structural forms of the hybrid energy system, and the operation strategy is also very flexible, especially in the case of the coupling of multiple energy flows, the system configuration optimization results have many possibilities. This brings great difficulties to the efficient construction of the model. An efficient solution is to

use a superstructure-based method (Tetsuya & Ryohei, 2014), where all possible or mainly possible structures are put into an overall structure, resulting in more structural forms than required for the actual system. Then describe the characteristics of each device, the logic between each device, the relationship between each energy flow, etc., so as to construct models such as mixed integer nonlinear programming (Juan et al., 2016) (Zheng et al., 2022) and mixed integer linear programming (Yun et al., 2015a). The advantage of this method is that it can make the logical description of the optimization model clearer and reduce the impact of meaningless structures. Based on this method, Yun et al., (2015b) establishes a mixed integer linear programming model of the coupled system of distributed energy and energy distribution network and realizes the optimal annual total cost of the system. It should be noted that when the system is more complex, the scale of the superstructure should be properly defined (Philip et al., 2012). The size of the scale affects the optimization results and efficiency of the solution. When the scale is small, it is easier to solve, but the optimal value may have been excluded from the structure. When the scale is large, although the chance of obtaining the optimal solution is greater, it may also introduce many meaningless structures, making the model difficult to solve.

2.12.2 Performance evaluation indexes of RE-HES

The performance evaluation index of the hybrid energy system is the basis for constructing the configuration optimization objective function, which has a significant impact on the configuration optimization results. Among the existing index, the three most commonly used indexes are economic, energy and environment related indexes and their combination. In recent years, with the increase in the proportion of renewable energy in the system, it is important to improve the reliability and flexibility of the system, and the related performance evaluation index has therefore received more attention.

2.12.3 Economic, energy, and environment related indexes

2.12.3.1 Economic

In most configuration optimization studies, the influence of economic index is considered when constructing the objective function. For example, Askarzadeh, (2013) established a configuration optimization model for photovoltaic, wind, and battery hybrid energy systems with the annual total cost as the optimization goal. Ryohei et al., (2015) optimizes the number of photovoltaic panels

and wind turbines in the wind-solar hybrid system with the lowest cost as the optimization goal. Yi et al., (2022) takes the minimum annual cost as the optimization goal optimizes and optimizes the configuration of a solar-assisted natural gas distributed energy system (DES) with energy storage. In these literatures, it can be found that the economic evaluation of the system is basically carried out with the lowest total annual cost. This index mainly includes two parts; one is fixed cost, such as equipment investment cost. The other is variable cost, such as fuel cost. Since the fuel cost of photovoltaic, wind power and other renewable energy utilization devices is basically negligible (except for biomass), and the investment cost of the equipment has been decreasing in these years, the configuration optimization results of RE-HES based on economic index tend to increase the proportion of the renewable energy consumption.

2.12.3.2 Energy energy-related indexes

This can be divided into two categories, one based on the first law of thermodynamics and the other based on the second law of thermodynamics.

Based on the first law of thermodynamics, the performance evaluation index based on the first law of thermodynamics mainly considers how much energy is lost in the process of energy utilization. In order to solve the problem that the traditional system cycle thermal efficiency and other evaluation indexes are difficult to scientifically evaluate the performance of the hybrid energy system, Yawen et al., (2014) puts forward the relative efficiency evaluation index of solar complementary power generation, which provides a new idea for the integrated design and optimization of solar complementary power generation. Yixun et al., (2017) considers the multi-energy f low characteristics of the integrated energy system and the influence of renewable energy access, and proposes a comprehensive energy utilization index suitable for multi energy collaborative remote energy efficiency evaluation, which reflects the utilization level of renewable energy and non-renewable energy in the park. Like energy efficiency, primary energy consumption is often used as a performance evaluation index for configuration optimization (Xiaomin et al., 2017). No matter which index form is adopted, the index based on the first law of thermodynamics fails to take into account the difference in energy quality, which may lead to insufficient improvement of the performance of the system.

Based on the second law of thermodynamics, compared with the single-energy energy system, the energy conversion structure of RE-HES is more complicated and the energy form of RE-HES is

more diversified, which means, not only the amount of energy but also the energy grade needs to be considered. Therefore, many scholars have conducted research based on the second law of thermodynamics. Baghernejad and Yaghoubi, (2010) study the integrated system of solar energy and gas-steam combined cycle with exergy analysis method and obtains the main exergy loss components of the research object. Another paper further established the exergy economic optimization model of this type of system (Baghernejad & Yaghoubi, 2011), and used genetic algorithm to optimize it, which reduced the power generation cost of steam turbine and gas turbine by 7.1% and 1.17%, respectively. Calderón et al., (2011), Sayem and Ibrahim (2014) both apply the energy analysis method to the wind-solar hybrid power generation system. In addition to the necessary exergy analysis, the latter literature also conducts research from the perspective of exergy and exergy economics to more fully demonstrate the performance of such systems. Integrating renewable energy with conventional coal-fired systems is a type of system that has received a lot of attention in recent years (Yinghong et al., 2008) (Xuemin et al., 2015) (Rongrong et al, 2016). For a more comprehensive analysis of the performance of the hybrid energy systems (Suresh et al., 2010) even discusses the technical and economic feasibility of such systems from the perspective of 4E (Energy, Exergy, Environment, and Economy).

2.12.3.3 Environment environmental indexes.

This has received great attention in recent years. Many studies have proved that the hybrid energy system has advantages in increasing the penetration rate of renewable energy and reducing carbon emissions in the social production process. Xue et al., (2017) proposes a comprehensive energy utilization index by adding the energy non-renewable coefficient to the evaluation index of the multi-park hybrid energy system, which can reflect the impact of renewable energy in primary energy, and through case calculation and comparative analysis, It verifies the consistency between the comprehensive energy utilization index and the economic index, and can improve the penetration rate of renewable energy in the hybrid energy system. In order to improve the renewable energy penetration rate of the system, in addition to directly establishing the optimization index considering the nonrenewable coefficient of energy, many scholars try to add carbon trading mechanism to the hybrid energy system. Wei et al., (2016) proposed to introduce a carbon trading mechanism into the hybrid energy system of electricity-gas interconnection, taking the minimum sum of carbon trading cost and power generation energy cost as the objective

function of the system, and combining the carbon trading mechanism with the collection of carbon taxes and other factors. Mechanisms were compared, and it was verified that the carbon trading mechanism can reduce the cost of power generation more effectively and has a good development prospect. Qu et al., (2018) verifies the feasibility of the carbon trading mechanism in the multi-regional hybrid energy system and establishes the optimization goal of the multi-regional hybrid energy system considering the carbon transaction cost. The results show that under the background of low coal prices in my country, the multi-regional hybrid energy system can make each regional energy system actively use low-emission technologies such as cogeneration and other clean energy through the carbon trading mechanism game. Wang et al. (2019b) further considers the impact of the combination of LCA energy chain and carbon trading mechanism on the optimization of the hybrid energy system, and solves the difficulty in calculating the total carbon emissions caused by the mutual conversion of various energy sources in the hybrid energy system. This ensures the effective operation of the carbon trading mechanism. In addition, studies have also considered the impact of carbon taxes (Wang et al., 2021) and renewable energy subsidies (Liu et al., 2021) on hybrid energy systems. Shebaz et al., (2021) conducts a study on the optimal configuration of solar and wind hybrid renewable energy systems with and without energy storage for environmental and social criteria.

2.12.4 Reliability and flexibility System

Reliability and flexibility become important due to the presence of large amounts of renewable energy.

2.12.4.1 Reliability.

In the practical application of the hybrid energy system, not only its environmental protection performance needs to be better than that of the traditional energy system, but also its reliability must be guaranteed. This is one of the keys to the large-scale commercial application of hybrid energy systems by establishing the reliability evaluation index of the hybrid energy system to evaluate the reliability of the equipment. It is helpful to find the deficiencies of the system and improve them effectively (Li et al., 2021). Some studies do not consider the influence of randomness and quantify the influence of the failure of each device on the reliability of the hybrid energy system by establishing the fault correlation matrix of each device (Zhao et al., 2022). However, affected by the characteristics of renewable energy, the operating state of each device

has certain randomness. Therefore, some scholars have carried out reliability assessment based on probabilistic operating state modeling for hybrid energy systems. Usually, the Monte Carlo method is applied to reliability evaluation, and a new reliability evaluation index is proposed (Cao et al., 2022) (Fang et al., 2022). Optimizing based on reliability alone may result in system redundancy. Therefore, the reliability index needs to be used together with other indexes such as economics. Yin et al., (2021) proposed a two-layer optimization method based on the reliability objective and the economic objective. The minimum outage capacity is converted into the minimum outage penalty cost, which is the reliability cost. The reliability cost and the economic cost are integrated to a new optimization target to realize the comprehensive optimization of the system reliability and economy.

2.12.4.2 Flexibility

Due to the stochastic of renewable energy, the hybrid energy system needs to have higher flexibility than the traditional energy system to ensure the energy supply and demand balance of the system, the higher the flexibility of a hybrid energy system, the better the ability to utilize renewable energy (Liu et al., 2019). Wang et al., (2022a) combines the power grid with the hydrogen grid by adding electricity-to-hydrogen equipment in the hybrid energy system and improve the flexibility of the system, helping the grid to absorb the uncertainty of renewable energy generation, smoothing the output power of renewable energy. Cui et al., (2022) cited the flexibility index of air source heat pump with waste heat recovery considering dynamic characteristics in integrated energy system. Hao et al., (2022) further studies the impact of energy storage devices on the flexibility of the hybrid energy system. In addition to the influence of equipment characteristics in the hybrid energy system on the flexibility index, the variability of the load side also has an impact on the flexibility index of the hybrid energy system. Chen et al., (2021), Zhang et al., (2021) respectively study the flexibility of hybrid energy systems from the perspective of load elasticity and load excitation response. The former's flexibility takes into account the maximum variation range of the load and is a definite value. The latter's flexibility is based on the value obtained from the game of incentives and market transaction mechanisms.

2.12.5 Multiple indexes

The configuration and development of hybrid energy systems are affected by various factors such as technology, cost, and policy. Therefore, the performance index of the hybrid energy system usually adopts the index based on thermodynamics, economy, environmental protection and so on (Wang et al., 2022b). In Xinjie et al., (2021) research, the synthesis of three indicators of energy efficiency, cost rate and emissions are considered for a novel hybrid solid oxide fuel cell (SOFC) solar hybrid CCHP residential system. Arnette and Zobel, (2012) consider both greenhouse gas emissions and annual operating costs. The minimum outage capacity in Yin et al., (2021) is converted into the minimum outage penalty cost, which is a combination of reliability indexes and economic indexes. The low-carbon indexes in Wei et al., (2016) are also represented by carbon transaction costs, which are ultimately reflected in economic goals. Zhong et al., (2021) builds a model that includes six evaluation indexes: energy saving rate, energy loss, new energy proportion, new energy consumption rate, and operation and maintenance cost. The system can be more comprehensively evaluated and optimized through multiple indexes, but how to reasonably determine the weight of each index is still one of the basic challenges of current multi-objective configuration optimization.

2.13 UNCERTAINTY AND DYNAMIC CHARACTERISTICS IN OPTIMIZATION.

The system characterization has a significant impact on the configuration optimization model and its optimization results. Most of the existing configuration optimization studies ignore the uncertainty and dynamic characteristics of the system when describing the system. For hybrid systems that do not contain renewable energy, this treatment may not have a noticeable effect on the results. However, for systems with renewable energy sources, ignoring uncertainties and dynamics may lead to large deviations in system configuration results.

2.13.1 Considering uncertainty

For the treatment of uncertainty, the commonly methods used are stochastic optimization methods and robust optimization methods.

2.13.1.1 Stochastic optimization methods

The main idea of the stochastic optimization method can be summarized as: based on a large amount of historical data, typical scenes are obtained by clustering, then the probability of

occurrence of each scene is calculated, and finally the mathematical expectation model is solved. Stochastic optimization is mainly based on the probability prediction information of uncertain variables. The uncertain variables usually obey a certain probability density distribution, such as the wind speed obeys the Weinbull distribution (Villanueva et al., 2011), and the forecast errors of wind power and photovoltaic output obey the normal distribution (Lange, 2005) (Abedi et al., 2011). Using stochastic optimization method, Yi et al., (2022) established an optimization model for the hybrid energy system and the uncertainty of cooling, heating and power load and the stochastic of renewable energy are described by Monte Carlo simulation method. Amirhossein et al., (2017) established a two stage stochastic programming model for hybrid energy system configuration based on typical scenarios obtained by Monte Carlo sampling and K-Means clustering.

2.13.1.2 Robust optimization methods

Unlike stochastic optimization methods, which have higher requirements on historical data, robust optimization methods have much lower requirements on it. The method only needs to determine a reasonable fluctuation range of random variables to ensure the feasibility of configuring results within this range (Cao et al., 2018) (Zugno & Conejo, 2015). Robust optimization methods can be summarized as traditional robust optimization methods and distributed robust optimization methods.

2.13.1.3 Traditional robust optimization method

The traditional robust optimization method is mainly to find the worst scenario in the uncertainty interval and calculate the optimal solution in this scenario. According to this idea, (Chen et al., 2019) established a robust optimization model considering the uncertainty factors of load demand and used the Benders algorithm to solve it. The optimization results obtained in the worst case are very conservative. To reduce the conservativeness of the method, a two-stage robust model is proposed. Based on two-stage robust method, Zeng & Zhao, (2013) propose a column-and-constraint generation (C&CG) algorithm based on the Benders decomposition method. By continuously introducing optimal cut sets and feasible constraints in the loop, it can quickly solve two-stage robust optimization problems. To further improve the robustness, Yan et al., (2021) uses box uncertainty sets, ellipsoid uncertainty sets, and convex uncertainty sets to describe the

distribution of uncertain factors and establishes a two-stage robust optimal configuration model.

2.13.1.4 Distribution robust optimization method

To achieve the balance of performance such as economy and conservatism, distributed robust optimization methods have been proposed and developed in recent years. The distribution-robust optimization (DRO) method is mainly to find the decision results under the worst probability distribution of uncertain parameters (Wang et al., 2018). It is mainly divided into two methods: probability density and distance information. DRO methods based on probability density mainly include three forms: multi-discrete scene (He et al., 2019), Wasserstein distance (Zhu et al., 2019) and KL divergence (Chen et al., 2018). DRO methods based on range information mainly include two forms: deterministic range (Chen et al., 2016) and indeterminate range (Alvarado et al, 2019) (Lu et al, 2018a). The mathematical description of the DRO method based on distance information is more accurate, but the conversion and solution process are complicated. The DRO method based on probability density has the advantages of simple mathematical logic and easy solution, so it is currently used more in hybrid energy systems.

2.13.2 Considering dynamic characteristics

To cope with the uncertain influence of load demand and renewable energy output, the dynamic tracking performance of the system needs to be improved (Chen & Pan, 2021). Existing studies are mainly based on the steady-state characteristics of the system, and the improvement of system dynamic tracking performance by advanced control methods is limited (Blaud et al., 2020). Therefore, ignoring the dynamic tracking performance in the capacity configuration may result in the inability of the hybrid energy system to track the load demand in time. For scheduling optimization problems, some studies have considered the influence of dynamic characteristics, mainly the influence of thermal network and thermal inertia of buildings (Wei et al., 2017) (Yang et al., 2020).

However, the impact of considering dynamic properties in configuration optimization has only recently received attention. Existing studies have shown that the system exhibits more advantageous performance after adopting an optimized configuration that considers the dynamic characteristics (Yuxuan et al., 2022; Bingle & Xiao, 2022). With the increasing proportion of renewable energy in the system and the in-depth understanding of the dynamic characteristics of

the hybrid energy system, considering the dynamic characteristics in the configuration and scheduling optimization are expected to bring more benefits to the system (Bingle & Xiao, 2022)
.

2.14 MODEL SOLUTION ALGORITHMS FOR RE HES'S CONFIGURATION.

The model solution algorithm plays an important role in the configuration optimization of the hybrid energy system. At present, a variety of solution algorithms have been developed, which can be mainly divided into two basic categories: classical optimization algorithms and intelligent optimization algorithms. There are also some studies using commercial solver to solve optimization models. Such Gurobi (Jiang et al., 2022) and CPLEX (Zhou et al., 2022), are widely used due to their superior performance. Other solvers such as MOSEK (Zhang et al., 2018), XPRESS (Andrychowicz and Olek 2016), can be used LINGO (Xu et al., 2020b) (Ibrahimi et al., 2019). However, the core algorithms of these solvers are also based on classical algorithms or intelligent algorithms or hybrid algorithms of classic and intelligent. This paper mainly focuses on these two basic algorithms.

2.14.1 Classical optimization algorithms

The configuration optimization problem of RE-HES is essentially a nonlinear programming problem. When considering the discrete characteristics of the problem, such as discontinuity of equipment size, start-stop logic of equipment, etc., the problem becomes a nonlinear mixed integer programming problem. In practical applications, for the convenience of solving, nonlinear programming (or mixed integer nonlinear programming) problems are often transformed into linear programming (Peng et al., 2016) or mixed integer linear programming (Jiang et al, 2022) (Mazaheri et al, 2021) problems through simplification or linearization. When using traditional solving methods, different solving algorithms are used for different models. For example, sequential quadratic programming methods can be used to solve nonlinear programming problems (Ahmad, 2021) (Lu et al., 2018b); branch and bound methods and cutting plane methods can be used to solve mixed integer programming problems (Yi et al., 2022), etc. Different from the generality pursued by some intelligent methods, traditional methods are generally more targeted to the problem, and the algorithm can often be improved according to the characteristics of the problem (Ryohei et al., 2015). For example, Lahdelma & Hakonen, (2003) establish a linear programming model for the cogeneration problem and propose an improved simplex method

according to the characteristics of the model, which achieves good results. Then, a TCS algorithm suitable for solving the linear programming model of the tri-generation system is proposed Rong & Lahdelma, (2005). The enumeration method may also be an effective method when the model complexity is low or the value range of the decision variable is small (Shaneb et al., 2012) (Sanaye et al., 2008).

2.14.2 Intelligent optimization techniques

The rapid development of intelligent optimization techniques in recent years has been clearly reflected in the comprehensive optimization of hybrid energy systems. Various novel and hybrid algorithms are selected and proposed to solve complex integrated optimization problems of hybrid energy systems. Paliwal et al., (2022) applies particle swarm optimization (PSO) to the study of capacity allocation optimization of wind-solar-diesel-storage hybrid energy systems. Mei et al., (2022) uses a multi-objective particle swarm algorithm to optimize the regional hybrid energy system. Arabli et al., (2013) studies the integrated optimization problem of the heating ventilation system (HVAC) powered by wind-solar storage and uses the genetic algorithm (GA)-based two-point estimation method to optimize the model. Chen et al., (2020) established an exergy analysis model for the hybrid energy system using an adaptive genetic algorithm and verified the validity of the model for the Bali hybrid energy system model. There are also some other new algorithms that can also be used to solve the configuration optimization problem of hybrid energy systems, such as ant colony algorithm (Abdolvahhab & Ehsan, 2015), big bang–big crunch algorithm (Saeedeh & Shirzad, 2016) and bee swarm algorithm (Akbar & Alireza, 2014). Due to the limitations of a single algorithm, some studies use a combination of multiple algorithms to improve the optimization performance. Shilaja, (2021) combines the chaotic particle swarm optimizer and the gravitational search algorithm to deal with the power flow calculation problem in the hybrid energy system. Askarzadeh, (2013) combines chaos search (CS), harmony search (HS) and simulated annealing (SA), and proposes a new discrete chaotic harmony-based simulated annealing method (DCHSSA) to solve the configuration optimization model of hybrid energy systems. At present, the effective combination of intelligent algorithms and configuration optimization models is still insufficient. This is a general problem that deserves attention. Compared with the traditional method, the intelligent method does have better generality, but the excessive pursuit of generality will inevitably lead to the difficulty of improving the algorithm in

combination with the specific characteristics of the model. To solve this problem, in addition to improving the intelligent algorithm itself, it is also an effective method to combine the intelligent algorithm with the traditional method.

2.15 STANDALONE SOLAR POWER SYSTEMS

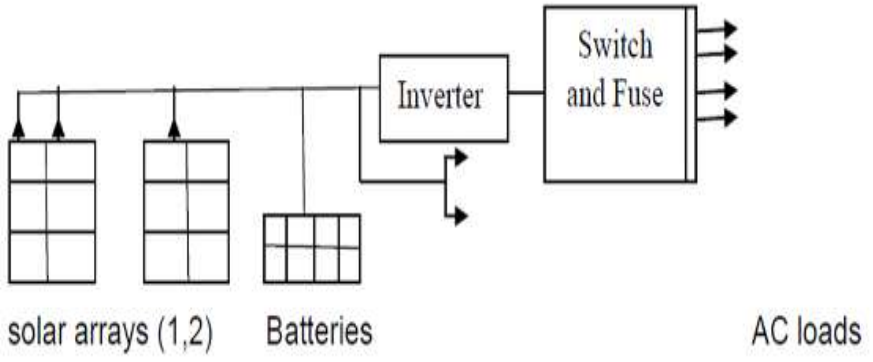

Figure 2.6: block diagram of a standalone solar power system. Source: Goshwe et al., 2015

Standalone are solar power systems that are not connected to the utility grid. They are made from the combination of batteries, inverter, switches, and solar arrays. The power from PV rays passes to batteries, from the batteries it passes to the inverter which converts the DC to AC. From the inverter the power passes to the base-station. Figure 2.6 represent the diagram of a Standalone Solar Power System. For the hybrid Systems, multiple power sources are used (Chinnu & Athulya, 2014).

2.16 SOLAR ENERGY SURVEY OF NIGERIA

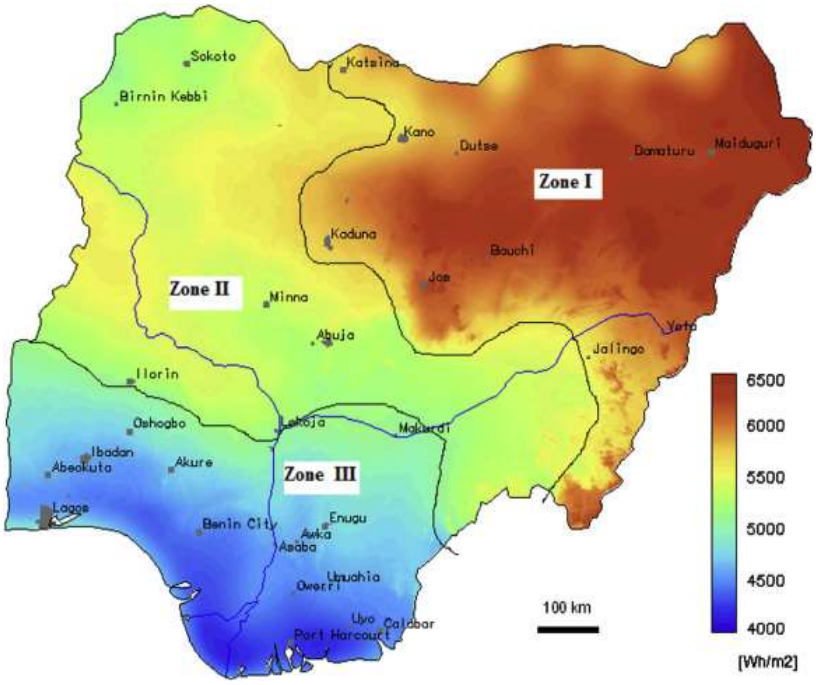

Figure 2.7: Solar radiation map in Nigeria. Source: Ohunakin et al., 2014.

Nigeria lies within longitude 8°E and latitude 10°N on the equator, having wet and dry seasons. These seasons have affected the adoption of different Renewable Energy Resources (RER); for instance, the different seasons in the country affect hydropower stations because of variations in water availability and level. Even thermal-powered stations have been affected by lack of adequate supplies of natural gas from the Niger Delta gas wells (Charles & Meisen, 2014); this makes the use of petrol and diesel-powered generators the unavoidable sources easy way out for telecommunication industries in the country. Sunlight is an excellent renewable energy source and it is in abundance in most African countries like Nigeria. Therefore, using solar-generated energy for powering cellular base stations should be an energy solution, particularly for rural dwellers where power grid is not available. The clarion call for clean energy globally should be a driving force for the Nation to harvest this naturally available energy source. The solar photovoltaic cell operates based on the principle of conversion of sunlight into electricity.

Figure 2.7 show that Zone I and Zone II receive the highest sun irradiation annually, while Enugu receives the least. Practically, the average sun Irradiation annually is about 1000 to 2200 watts per square meter (Abdul et al., 2019). With typical crystalline solar cell efficiencies of around 14-

16%, we can expect to generate about 140-160W per square meter if solar cells are exposed to maximum sun irradiation.

In the early part of 2000, Nigeria identified RE as an additional source to improve electrical power generation. This alternative energy has been somewhat introduced on a small scale to local economies, but it has not yet been implemented into the national grid on a larger scale (Mas'ud et al., 2015). Continual increases in the cost of oil, global warming, and the constant need for power supply has made the Nigerian government improve efforts towards adopting Photovoltaic Technology (PVT).Presently, solar PV systems are used as an alternative source of power to specific areas like telecom masts, street lights, parks, etc. in moments of fluctuating power supply or power outage (Njok et al., 2020). Irrespective of the presence of fossil fuels, Nigeria needs to promote the growth of the energy mix from RE sources. This energy mix will promote its continuous foreign exchange earnings from exporting these raw materials, keeping in mind that the worldwide percentage growth in demand for these raw materials will keep reducing (Sambo, 2005).

Therefore, there should be a dire need for research, development, and demonstration activities within key research centres all over the country, as well as identifying interested groups in other local and international institutions. To promote this, there should be Local craftsmen's training on designing, constructing, operating, and maintaining solar energy production devices, and the implementation of less-interest soft loans to drive production and adoption is a solution for this problem.

2.17 SOLAR MODULES TECHNOLOGY

A Solar module is a device that converts light from the sun, which is composed of particles of energy called "photons", into electricity that can be used to power electrical loads. The development of solar energy goes back more than 100 years. In the early days, solar energy was used primarily for the production of steam which could then be used to drive machinery. But it wasn't until the discovery of the "photovoltaic effect" by Edmond Becquerel that would allow the conversion of sunlight to solar electric energy (Bayod & Antonio, 2019). Becquerel's discovery then led to the invention in 1893 by Charles Fritts of the first genuine solar cell which was formed by coating sheets of selenium with a thin layer of gold. Russel Ohl, an American inventor on the

payroll of Bell Laboratories, patented the world's first silicon solar cell in 1941. Ohl's invention led to the production of the first solar panel in 1954 by the same company. Solar panels found their first mainstream use in space satellites. For most people, the first solar panel in their life was probably embedded in their new calculator - circa the 1970s (Luceño & Antonio, 2019). Today, solar panels and complete solar panel systems are used to power a wide variety of applications. Solar panels in the form of solar cells are still being used in calculators.

Solar panels are comprised of several individual solar cells which are themselves composed of layers of silicon, phosphorous (which provides the negative charge) (Qazi, 2017), and boron (which provides the positive charge). Solar panels absorb the photons and in doing so initiate an electric current. The resulting energy generated from photons striking the surface of the solar panel allows electrons to be knocked out of their atomic orbits and released into the electric field generated by the solar cells which then pull these free electrons into a directional current. This entire process is known as the Photovoltaic Effect. An average home has more than enough roof area for the necessary number of solar panels to produce enough solar electricity to supply all of its power needs, excess electricity generated goes onto the main power grid, paying off in electricity use at night.

2.18 TYPES OF SOLAR PANELS

Three main types of solar panels are commercially available today. They are monocrystalline solar panels, polycrystalline solar panels, and thin-film solar panels. There are also several other promising technologies currently in development, including bifacial panels, organic solar cells, concentrator photovoltaic, and even Nano-scale innovations like quantum dots solar panels.

Each of the different types of solar panels has a unique set of advantages and disadvantages that consumers should consider when choosing a solar panel system. It is evident from the table that solar panels made from pure silicon are the most reliable with the longest life span, followed by panels made from silicon crystal melted together. The less efficient one is the thin-film solar panel (Source: Luceño & Antonio, 2019).

2.18.1 Monocrystalline Solar Panels

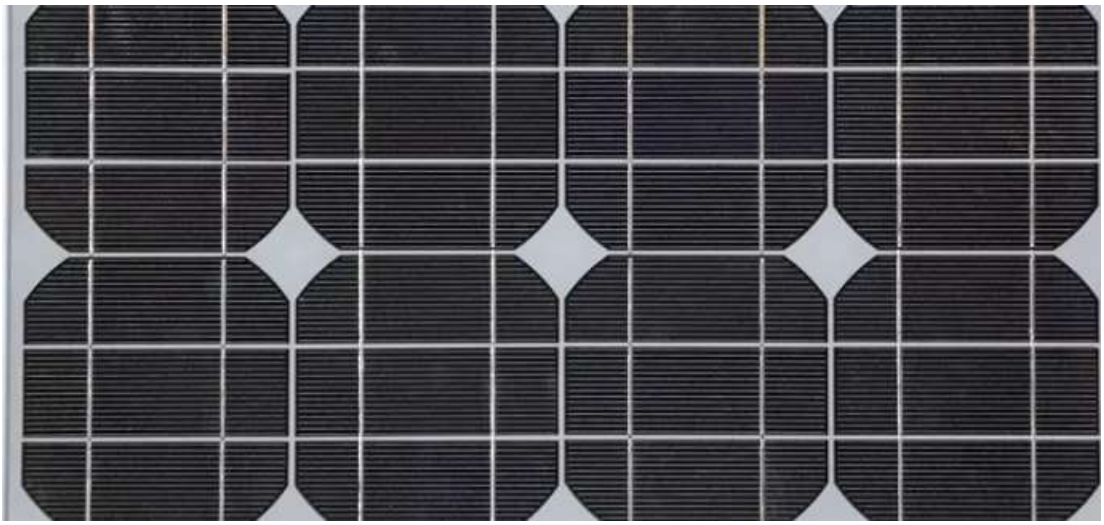

Plate 2.1: monocrystalline solar PV. Source: Bayod & Angel Antonio, 2019

This type of solar panel has many advantages over others making them the most commonly used solar panels on the market today (Luceño & Antonio, 2019). About 95% of solar cells being sold in the market are made of silicon as the semiconductor material (Qazi, 2017). Silicon is abundant, stable, non-toxic, and works well with established electric generation technologies.

Originally developed in the 1950s, monocrystalline silicon solar cells are manufactured by first creating a highly pure silicon ingot from a pure silicon seed using the Czochralski method. A single crystal is then sliced from the ingot, resulting in a silicon wafer that is approximately 0.3 millimeters (0.011 inches) in thickness (Taraba, 2019) (Bayod & Antonio, 2019)

Monocrystalline solar cells are slower and more expensive to produce than other types of solar cells due to the precise way the silicon ingots must be made. To grow a uniform crystal, the temperature of the materials must be kept very high. As a result, a large amount of energy must be used because of the loss of heat from the silicon seed that occurs throughout the manufacturing process (Luceño & Antonio, 2019). Approximately, 50% of the material can be wasted during the cutting process, resulting in higher production costs for the manufacturer (Askari, 2015). These types of solar cells maintain their popularity for several reasons. First, they have a higher efficiency than any other type of solar cell because they are made of a single crystal, which allows electrons to flow more easily through the cell. Because they are so efficient, they can be smaller than other solar panel systems and still generate the same amount of electricity. They also have the longest

life span of any type of solar panel on the market today (Taraba, 2019). One of the biggest downsides to monocrystalline solar panels is the cost (due to the production process). In addition, they are not as efficient as other types of solar panels in situations where the light does not hit them directly. And if they get covered in dirt, snow, or leaves, or if they are operating in very high temperatures, their efficiency reduces drastically (Taraba, 2019) while monocrystalline solar panels remain popular, the low cost and rising efficiency of other types of panels are becoming increasingly appealing to consumers.

2.18.2 Polycrystalline Solar Panels

Plate 2.2: Polycrystalline solar PV module. Source: Taraba, 2019.

Polycrystalline solar panels are made of cells formed from multiple, non-aligned silicon crystals (Taraba, 2019). The first-generation solar cells are produced by melting solar-grade silicon, casting it into a mould and allowing it to solidify. The moulded silicon is then sliced into wafers to be used in a solar panel. These types of solar cells are less expensive to produce than monocrystalline cells because they do not require the time and energy needed to create and cut a single crystal. While the boundaries created by the grains of the silicon crystals result in barriers for efficient electron flow. They are more efficient in low-light conditions than monocrystalline cells and can maintain output when not directly angled at the sun. They end up having about the same overall energy output because of this ability to maintain electricity production in adverse conditions (Askari, 2015).The cells of a polycrystalline solar panel are larger than their monocrystalline counterparts, as a result, the panels may take up more space to produce the same amount of electricity (Qazi, 2019). They are also not as durable or long-lasting as other types of panels, although the differences in longevity are small.

2.18.3 Thin-Film Solar Panels

Plate 2.3: Thin-film solar PV (Source: Bayod & Angel Antonio, 2019).

The high cost of producing solar-grade silicon led to the creation of several types of second- and third-generation solar cells known as thin-film semiconductors. Thin-film solar cells need a lower volume of materials, often using a layer of silicon as little as one micron thick, which is about 1/300th of the width of mono- and polycrystalline solar cells. The silicon is also of lower quality than the kind used in monocrystalline wafers (Askari, 2015)

Many solar cells are made from non-crystalline amorphous silicon. Because amorphous silicon does not have the semi-conductive properties of crystalline silicon, it must be combined with hydrogen to conduct electricity. Amorphous silicon solar cells are the most common type of thin-film cell, and they are often found in electronics like calculators and watches (Qazi, 2019)

Other commercially viable thin-film semiconductor materials include cadmium telluride (CdTe), copper indium gallium diselenide (CIGS), and gallium arsenide (GaAs). A layer of semiconductor material is deposited on an inexpensive substrate like glass, metal, or plastic, (Taraba, 2019) (Bayod & Antonio, 2019) making it cheaper and more adaptable than other solar cells. The absorption rates of the semiconductor materials are high, which is one of the reasons they use less material than other cells. Production of thin-film cells is much simpler and faster than first-generation solar cells, and there are a variety of techniques that can be used to make them, depending on the capabilities of the manufacturer. Thin-film solar cells like CIGS can be deposited on plastic, which significantly reduces its weight and increases its flexibility. CdTe holds the

distinction of being the only thin film that has lower costs, higher payback time, lower carbon footprint, and lower water use over its lifetime than all other solar technologies (Bayod & Antonio, 2019)

However, the downsides of thin-film solar cells in their current form are numerous. The cadmium in CdTe cells is highly toxic if inhaled or ingested, and can leach into the ground or water supply if not properly handled during disposal. This could be avoided if the panels are recycled, but the technology is currently not as widely available as it needs to be. The use of rare metals like those found in CIGS, CdTe, and GaAs can also be an expensive and potentially limiting factor in producing large amounts of thin-film solar cells (Taraba, 2019) (Bayod & Antonio, 2019).

2.18.4 Other Types

The variety of solar panels is much greater than what is currently on the commercial market. Many newer types of solar technology are in development, and older types are being studied for possible increases in efficiency and decreases in cost. Several of these emerging technologies are in the pilot phase of testing, while others were proven only in laboratory settings. Here are some of the other types of solar panels that have been developed.

2.18.5 **Concentrator Photovoltaic module Technology**

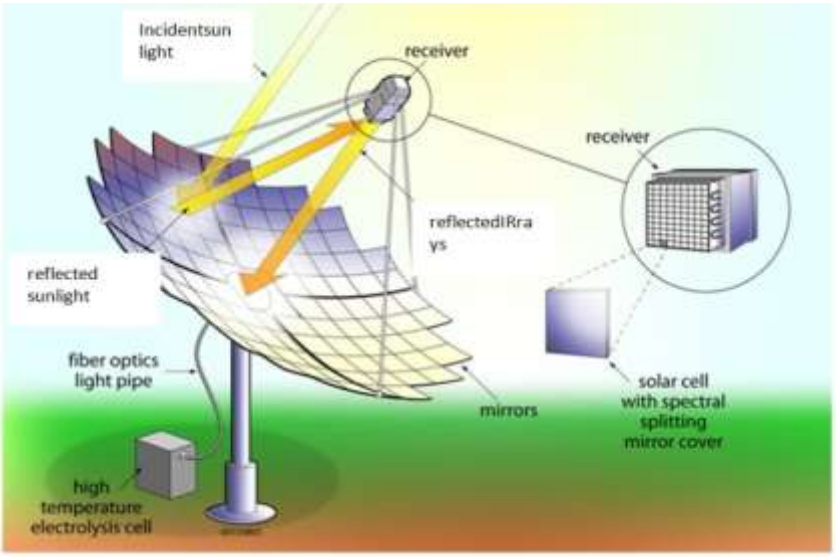

Plate 2.4: Pictorial diagram of concentrator Photovoltaic. Source: McConnell et al, 2005.

This Solar system was first developed in Australia and it uses a dish concentrator that reflects sunlight onto a focal point. The reflected infrared radiation is gathered by a fibre optics "light pipe" and conducted to the high-temperature solid-oxide electrolysis cell (Algora, 2004). The power output of the solar cells in addition powers the electrolysis cells.

About 120 megajoules are needed, either in electrical or thermal form, or both, to electrolyze water and generate 1kg of hydrogen (Archimedes, 2011). This results in more of the solar energy being used for hydrogen production. The costs of the components of this hybrid solar- concentrator, the spectral splitter, and the fibre-optic light pipe, are very small compared with the boost in hydrogen production. Plate 2.4 shows a Schematic of the system showing sunlight reflected and focused on the receiver, with reflected infrared directed to a fibre-optics light pipe for transport to a high-temperature solid-oxide electrolysis cell. Solar electricity is sent to the same electrolysis cell that uses both heat and electricity to split water (Backus, 2003).

A spectral splitter at the focal point reflects infrared solar radiation and transmits the visible sunlight to high-efficiency solar cells behind the spectral splitter (McConnell, et al, 2005b) (Faiman et al., 2005,) (McConnell et al, 2005a,) (McConnell et al., 2005b,) (McConnell et al.,2008,) on a small scale.

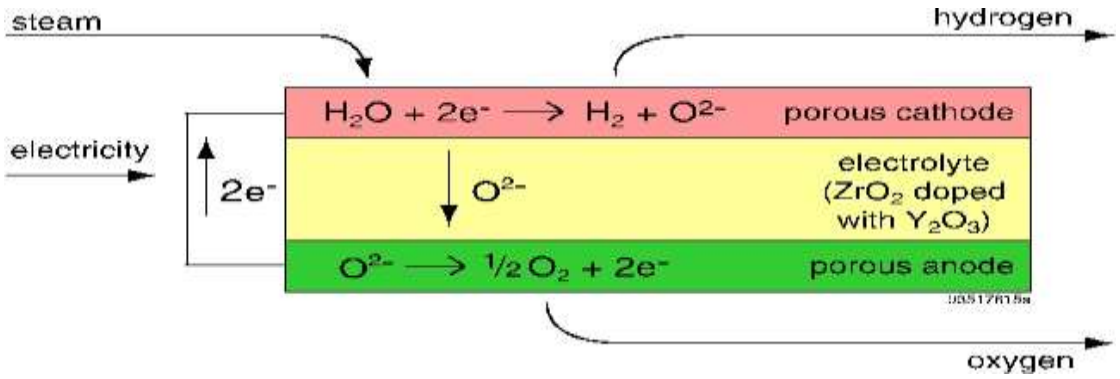

Figure 2.8: mode of Schematic of high-temperature electrolysis in a solid-oxide cell. Source: McConnell et al., 2005b

The solar concentrator is a large disc 1.5 m in diameter with two-axis tracking, and capable of more than 1000-suns concentration. The full dish was not needed and portions were appropriately shaded. At that time, the solar cell was a GaAs cell with an output voltage of 1 to 1.1V at maximum

power point with a measured efficiency of about 19%. The voltage was an excellent match for direct connection to the electrolysis cell when operating at 1000^{o} C (Lewis, 2006). The tubular solid-oxide electrolysis cell was fabricated from yttria-stabilized zirconia (YSZ); the cell had platinum electrodes since the test temperature was higher than that of typical solid-oxide cells. Figure 2.8 shows a schematic of the operation of solid-oxide electrolysis cells. Operating the electrolysis cell in reverse corresponds to electricity and heat production in solid-oxide fuel cell operation. In its internal structure, a metal tube is used to surround the cell to uniformly distribute the solar flux over the cell's surface (Thompson et al., 2005). The test occurs within two hours of operation with an excess of steam applied to the electrolysis cell. The output stream of unreacted steam and generated hydrogen will pass through water, and the hydrogen is collected and measured. Combining the optical efficiencies of the concentrator dish (85%), solar-cell efficiency, and thermal-energy boost, the efficiency of the total system in converting solar energy to hydrogen will be about 22% (Whisnant et al., 1986) (Licht, 2003). Therefore, Concentrator photovoltaic technology (CPV) uses optical equipment and techniques such as curved mirrors to concentrate solar energy in a cost-efficient way. Because these panels concentrate sunlight, they do not need as many solar cells to produce an equal amount of electricity. This means that these solar panels can use higher quality solar cells at a lower overall cost (Wang et al., 2011).

2.18.4.1 Organic photovoltaic

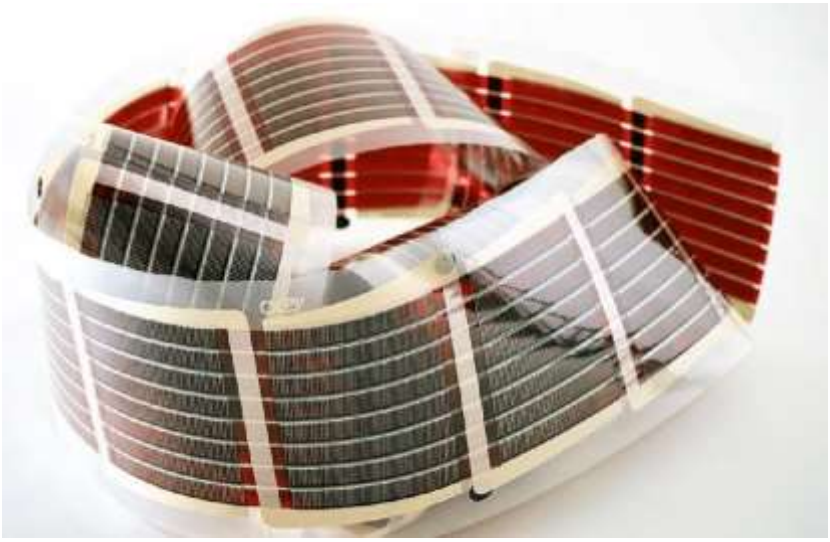

Plate 2.5: Organic Photovoltaics. Source: Katagiri et al., 2001

Organic photovoltaic cells use small organic molecules or layers of organic polymers to conduct electricity. These cells are lightweight (Plate 2.5), flexible, and have a lower overall cost and environmental impact than many other types of solar cells (Taraba, 2019).

Future trends in photovoltaic panel manufacturing Development and research in the solar energy field focus on increasing the efficiency of photovoltaic panels and the reduction of the production cost (Katagiri et al., 2001). The photovoltaic panel fabrication industry is developing better alternatives than traditional sources of energy, for example, fossil fuels. The early dominance of silicon in research programs has recently spread out to the wholesale of commercial modules (Global Market Outlook, 2011).

2.18.4.2 Perovskite cells

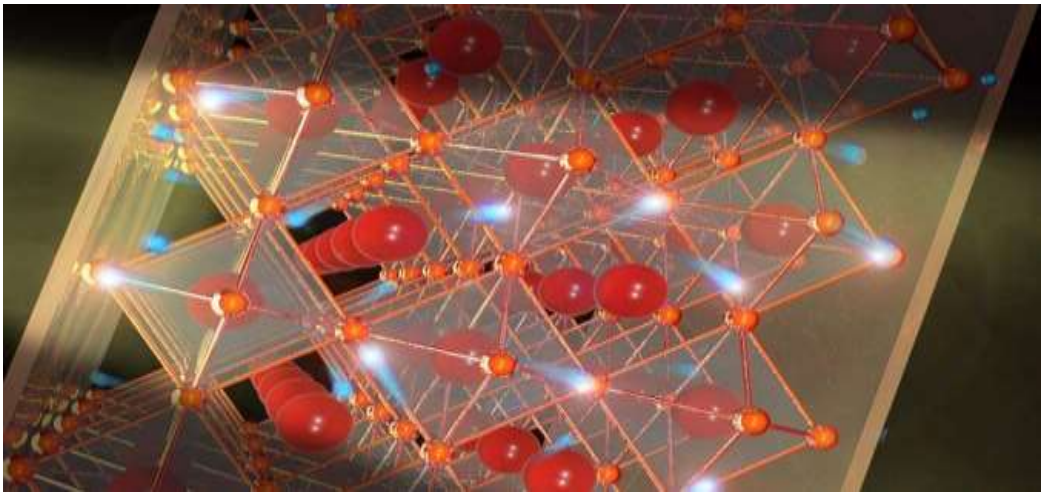

Plate 2.6: Perovskite cells. Source: Qazi, 2015

The Perovskite crystalline structure of the light-collecting material gives these cells their name. They are low-cost, easy to manufacture, and have a high absorbance. They are currently too unstable for large-scale use (Qazi, 2015). Perovskites are hybrid compounds that are produced from metal halides and organic constituents. Their attractive structural and electronic properties have placed them at the forefront of materials research, with enormous potential for transforming a wide range of applications, including solar cells, LED lights, lasers, and photo-detectors. For example, metal-halide perovskites in particular show great potential as light harvesters for thin-film Photovoltaics.

2.18.4.4 Dye-Sensitized Solar Cells (DSSC)

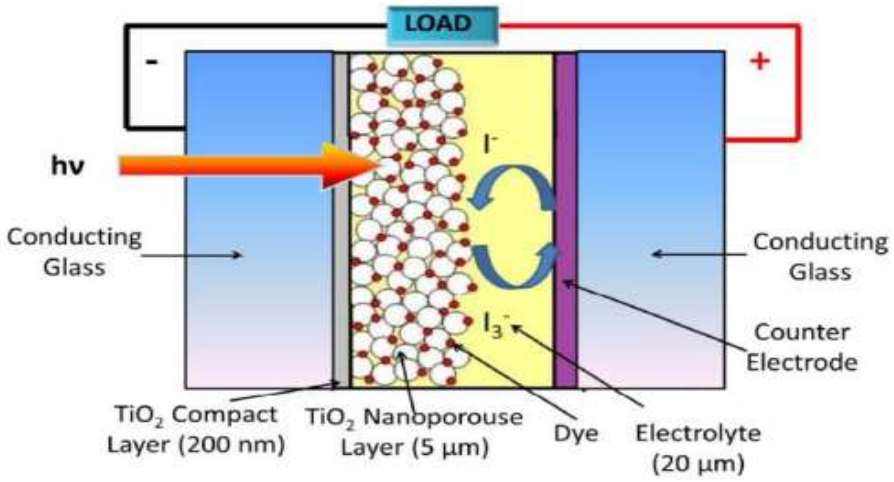

Figure 2.9: The structure of dye-sensitized solar cells (DSSCs). Source: Zekâi, 2009.

These five-layered thin-film cells use a special sensitizing dye to help the flow of electrons which creates the current to produce electricity as shown in figure 2.9. DSSCs have the advantage of working in low light conditions and increasing efficiency as temperatures rise, but some of the chemicals they contain will freeze at low temperatures, which makes the unit inoperable in such situations (Raina et al., 2019).

Generally, a DSSC consists of four elements: a photo-electrode with a thin layer of nanostructured wide band-gap semiconductor (usually TiO2, ZnO, SnO2 or Nb2O5) attached to the conducting substrate (fluorine-doped tin dioxide, FTO), a monolayer of dye adsorbed on the surface of the semiconductor, electrolyte containing a redox couple and a counter electrode (platinized FTO) (Fthenakis, 2012).

This type of solar cell is known for its relatively high efficiency exceeding 11% of full sunlight and low fabrication cost (1/10–1/5 of silicon solar cells) (Grätzel, 2004). Since the birth of DSSCs, great efforts have been made to make these devices more efficient and stable. Long-term stability tests have shown good prospects of DSSCs for domestic devices and decorative applications recently (Wang, et al, 2003) (Wang, et al, 2005).

2.18.4.5 Quantum Dots

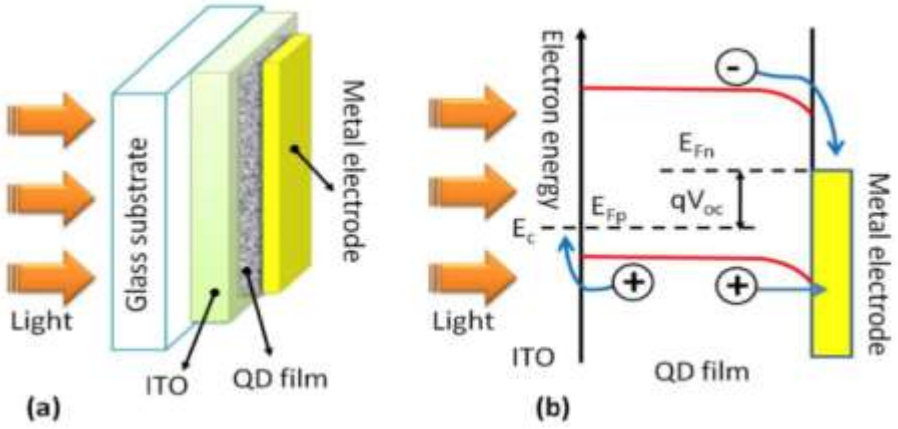

Figure 2.10: (a) Schematic of Schottky barrier quantum dots based solar cell, (b) band diagram of Schottky solar cell. Source: Pattantyus-Abraham, 2008

This technology has only been tested in laboratories, but it has shown several positive attributes. Quantum dot cells are made from different metals and work on the Nano-scale as shown in figure 2.10, so their power production-to-weight ratio is very good. Unfortunately, they can also be highly toxic to people and the environment if not handled and disposed of properly (Taraba, 2019).

Layer-by-layer fabrication of quantum dots film is prepared by layer-by-layer dip coating of the substrate. For instance, in the layer-by-layer fabrication of PbSe quantum dots films, quantum dots film prepared by dip-coating, alternating between PbSe NCs in hexane and then 0.1 M EDT in anhydrous acetonitrile, allowing the film to dry between each layer (Luthar et al., 2008). Table 2.4 shows the evolution of of photovoltaic module technology. A device with 140 nm-thick QD film achieved an efficiency of ~2.2 % (Luthar et al., 2010) hetero-

junction solar cell has been investigated by sputtering 150 nm layer of ZnO and growing layers of PbS quantum dots fabricated in the air (4.1 mg/mL concentration of PbS 820 nm NC in hexanes); 1mM solution of 1, 2-ethanedithiol in an acetonitrile layer-by-layer deposition for 20 cycles (~ 120nm PbS film thickness). Tested devices showed good air stability over ~1,000hrs with a cell power efficiency of 1.53 % (Yakubu et al., 2024).

PV panels generally absorb short-wave solar irradiance, and these panels convert them to DC electricity which charges batteries and operates base stations. "A 1-kW PV panel typically has a $5m^2$ area, and the lifetime of a typical PV panel may exceed 25 years" (Osinowo et al., 2015).

The panel's DC rating, tilt angle, and geographic location or solar irradiation profile of the site can affect the power generated by the PV panel, and Panels rated 1 kW are valued at about $1000 (Alsharif & Kim, 2016).

2.19 SOLAR-POWERED TELECOM BASE-STATION

Base stations are made up of several antennas mounted on a metallic tower and a house of electronics at the base of the tower (George, 2009). Many people in emerging markets like Nigeria live in rural areas with no access to the electricity grid and unreliable supply in the urban centres. This presents a significant barrier to expanding network coverage (for rural dwellers) and unstable network due to erratic power supply (in urban centres) in these areas as mobile phone base stations rely on a secure supply of power. The use of diesel generators to power base-stations requires regular maintenance, expensive to run, and cause air pollution. By utilizing solar power to run the base-stations, operators will be able to reduce their operational cost and thus allows for deeper penetration of mobile networks (Goshwe et al., 2015).

In recent years, the telecoms sector has shown an increased interest in the adoption of solar technology to generate power for cellular base stations. The large amount of operating a mobile cellular base station (MCB) generators, and its bad impact of greenhouse gas emissions on the environment have made the solar PV renewable energy source a sought after. The cost and environmental factors, abundant supply of solar radiation in Africa, and the drive to reduce the emission of carbon dioxide by the year 2030 and to enhance the quantity of power supply are also part of many advantages to power communication base station systems with solar PV cells. Therefore, solar PV-powered base stations have become an important integration into a mobile cellular network (Banjo et al., 2017).

For an operator of a mobile cellular network to provide seamless and continuous mobile services to the subscribers, many BSs must be installed, hence, the increase in the number of BSs globally. Energy-wise, a single BS contributes to about 75-80% of the total cost of energy consumption in mobile cellular networks as proven (Hassan et al., 2013), consuming 25 MWh of electrical energy per year per an estimated 4 million deployed BS worldwide (Josip & Ivana, 2013). Hence, mobile cellular BS has been the paramount reason for the increase in energy consumption, greenhouse gasses (GHG), and emissions, leading to a huge cost of operation in the mobile cellular network

(Olwal et al., 2016).Today, developing countries like Nigeria are witnessing a growth of mobile telecoms given network coverage and tremendous impact on the operating cost of running systems, since the electric power infrastructure and grid energy supply for remote telecom networks (RTNs) are unavailable (Olatomiwa et al., 2015). However, RTN has enlarged to eloigned deserts and forests where connectivity is an exigency, and may not exist and/or power grids are unstable (Allah et al., 2021).

Decades ago, the bulk of the growth in the deployment of cellular base stations has been in parts of the developing countries of Africa and Asia where the penetration of cellular communication is still low, particularly the rural dwellers. Research shows that out of the 4,00,000 base stations in Africa, more than 70% face power outages for more than eight hours a day. Because of this, the telecom industry in Africa consumes more than 2 billion litres of diesel per year, spending around US$ 1.4 billion and producing more than 5 metric tons of carbon dioxide emission (Jhunjhunwala et al., 2012). Currently, there are about 3, 20,100 off-grid and 7, 01,000 bad-grid (i.e. connected to a grid supply with frequent power outages, loss of phase, or fluctuating voltages) BSs globally (Smertnik, 2014). The off-grid and bad-grid BSs grew by 22% and 13% by the year 2020, respectively. About 80% of these would be installed in African and Asian countries with many of the countries in these regions having poor grid-connected power, rich in terms of solar resources. Therefore, solar-powered BSs are a viable and attractive option in these Asian, Sahara-African, and Sub-Sahara-African regions.

Globally, Cellular mobile technology has witnessed tremendous growth in recent times. The rising acceptance and accessibility of mobile broadband services are motivating a change in the engagement patterns of mobile users from basic voice to data-centric services. One of the challenges facing the operators in extending the networks' coverage to meet the rising demand for cellular mobile services is the power sources used to supply cellular towers with energy, especially in remote areas. Airtel Nigeria has embarked on upgrading 250 diesel-powered stations on–site. The company regretted that the non-availability of regular grid power supply to sites across the country is responsible for over 70% of downtime, resulting in poor Quality of Service (Supriya & Siddarthan, 2011). MTN Nigeria, one of the four mobile telecommunications operators with 4,798 base stations spends a whopping $82.8 million on generator acquisition almost every three years and $3.5 million monthly on diesel oil and generator maintenance (Tamm et al., 2010). However,

several problems related to low conversion efficiency, high-cost level of PV panels, and multiple local peaks of energy caused by partial shading conditions (PSCs) may be met (Naseem et al., 2021) (Olabi et al., 2023) (Novas et al., 2021). The future hope in SPV generations and its abundant cheap energy will for no doubt solve the energy crisis in most developing countries where accesses to the grid electricity are unavailable. This will encourage and promote economic activities in such areas, particularly in the telecommunication industries which is gradually expanding every day in the rural areas. If mobile subscribers can harness and make use of this natural golden opportunity in solar energy by using it to power their base stations in the rural areas where grid access in not present, their broadband connectivity will increase (Osuji & Onwughalu, 2024). In recent years, mobile operators who tried to harness this technology used Monofacial PV (MFPV) panel with backup generator, which still, confirm completely the global clean energy agenda.

2.20 BIFACIAL PV MODULE TECHNOLOGY

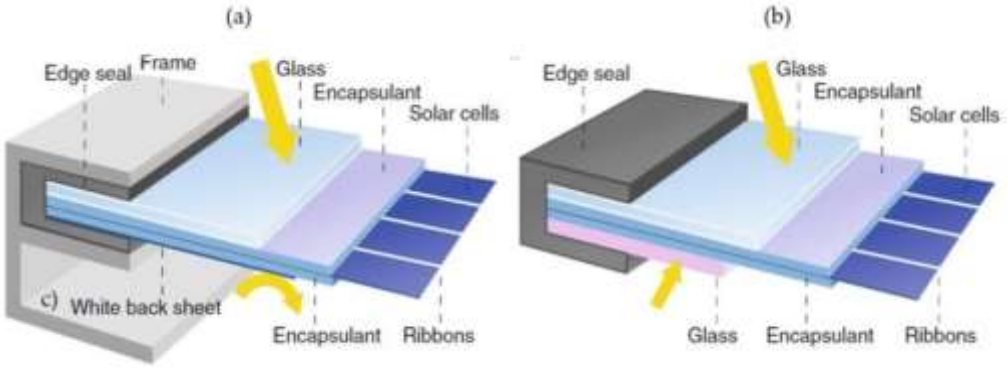

Figure 2.11: Differences between PV modules: (a) monofacial (upper left) and (b) bifacial (upper right). Source: IEA, 2021.

Differences between monofacial and bifacial cell and module design occur mostly on the rear side but can in some cases occur on the module edges. Figure 2.11 shows a monofacial module and solar cell on the left side and a bifacial module and solar cell on the right side (IEA, 2021). In bifacial modules, the rear-side cover consists of either glass or a transparent polymer back sheet. When back sheets are used, the module must be supported by an aluminium frame. However, in some cases, the rigidity of glass-glass modules makes a frame unnecessary, and the edges are

merely sealed. Bifacial modules are one of the older developments in solar panel technology, dating back to the 1960s. It is also one of the latest advances to take hold. According to many experts, however, it is now on track as the latest trend to sweep the solar industry and will soon become the standard. Bifacial photovoltaic (BPV) module technology is becoming increasingly attractive, with a market share of around 20% in 2020 which is expected to increase by more than 70% over the next ten years (Francia, 2015) (International Technology Roadmap for Photovoltaic, 2020). The cost of MFPV and BFPV from 2016 to 2022 is shown in figure 2.13. This technology uses similar fabrication methods as monofacial PV cells and implementation only requires minor and affordable changes in the manufacturing process (Guerrero-Lemus et al., 2016) (Salim et al., 2021).

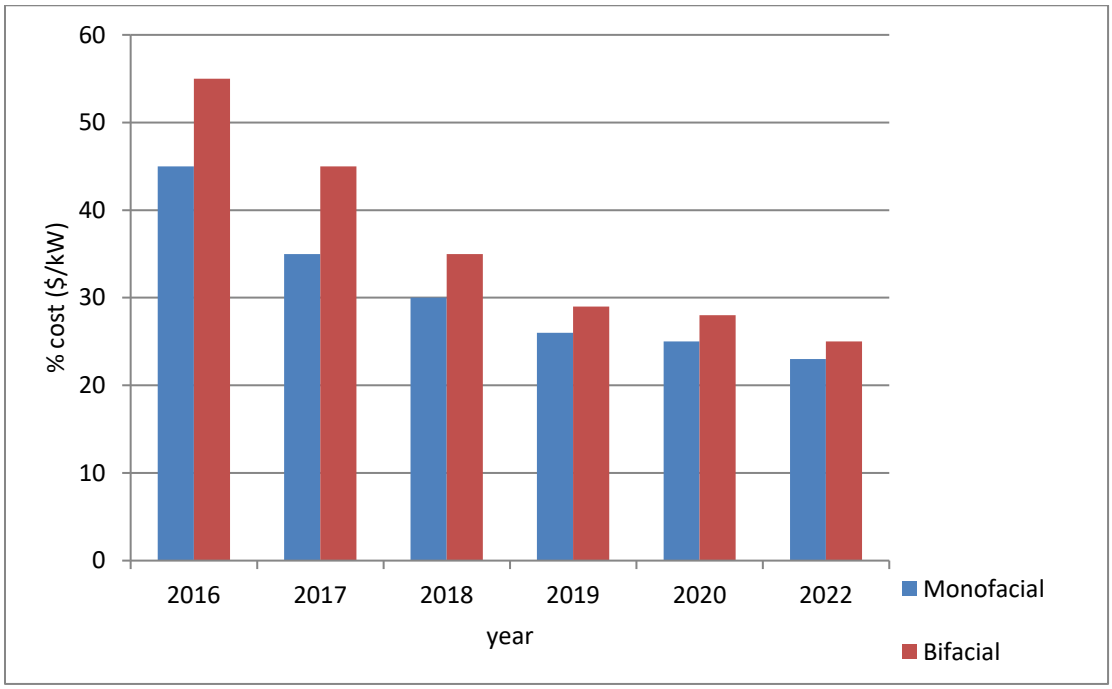

Figure 2.12: cost of MFPV and BFPV from 2016 to 2022. Source: Guerrero-Lemus et al., 2016

Like standard solar modules, the cost of bifacial modules has fallen precipitously over the last two decades. Notably, as costs have decreased, so too has the cost gap between mono and bifacial modules. Figure 2.12 shows one of the main reasons why bifacial module market share is predicted to continue to increase. As the cost gap becomes smaller and bifacial production increases, the extra production costs resulting from producing the rear side of bifacial modules can compensate for additional costs (Jang & Kyungsoo, 2020). For instance, there are many design elements unique

to bifacial systems that contribute to higher overall installation costs; in particular, the rear side of the modules. The DC design, site location, and installation can be more challenging for a bifacial plant versus one with monofacial modules, and this can create problems for investors (Lawin et al., 2019). It is also quite difficult to accurately predict the increased output for a system design, due to the many variables that affect rear-side production. Results and studies have shown that bifacial modules can produce additional power between 10-20% over monofacial panels. If conditions are optimized and single-axis trackers adopted, the additional power can be as high as 30-40% (Ajayi et al., 2014) (Lawin et al., 2019).\

The production of BPV requires the use of transparent material at the back side of the module, (Nussbaumer, et al, 2019) such as a transparent back sheet or glass, which may increase the cost slightly (Pelaez, 2019) (Deline et al., 2019). It has the advantage of different mounting concepts, including building-integrated vertically mounted scenarios, etc. (Viola et al., 2019) (Kopecek et al., 2019). Bifacial modules have been around since the 1960s, yet it has been the development of PERC (passivized emitter rear cell) technology that has significantly increased their efficiencies and created the potential for them to be a disruptive player in the solar PV market. That said, many variables must be addressed before bifacial modules can claim a significant market share. Cost is one of the biggest factors particularly in the case of monofacial modules (Augustine et al., 2009). It is important to bear in mind that we are looking for the optimum LCOE (levelized cost of electricity), not the maximum power possible. There are several ways to increase power production, but many of these options are not cost effective and, therefore, not practical in the market. For example, dual axis tracking can increase power production, but it is still too costly to be recommended. So a major obstacle for bifacial modules in the market is the difficulty in creating accurate simulations and thereby satisfying financial queries regarding the additional costs (Emmanuel et al,, 2021) (Augustine et al., 2009).

Improved testing and improved Modelling have been underway for years, and improvements in available data regarding irradiance and geospatial data have contributed greatly to improvements in these simulations. There have also been many bifacial test sites built, bifacial studies undertaken, and bifacial installations completed providing real data. In fact, despite all the obstacles and uncertainties, bifacial installations have grown rapidly in the last half decade, from only 97MW of installed global capacity in 2016, to almost 6 GW in 2019 (Augustine et al., 2009).

The largest bifacial plant to date is 224 MW was completed in late 2019. That growth is predicted to continue. According to Wood Mackenzie Consultancy, bifacial modules will account for 17% of the global market for solar panels in 2024. With all of the data from tests and completed installations, we do have a model of how to make bifacial panels work for a lower LCOE. Figure 2.13 is the pattern of solar radiations on the surface of BFPV panel.

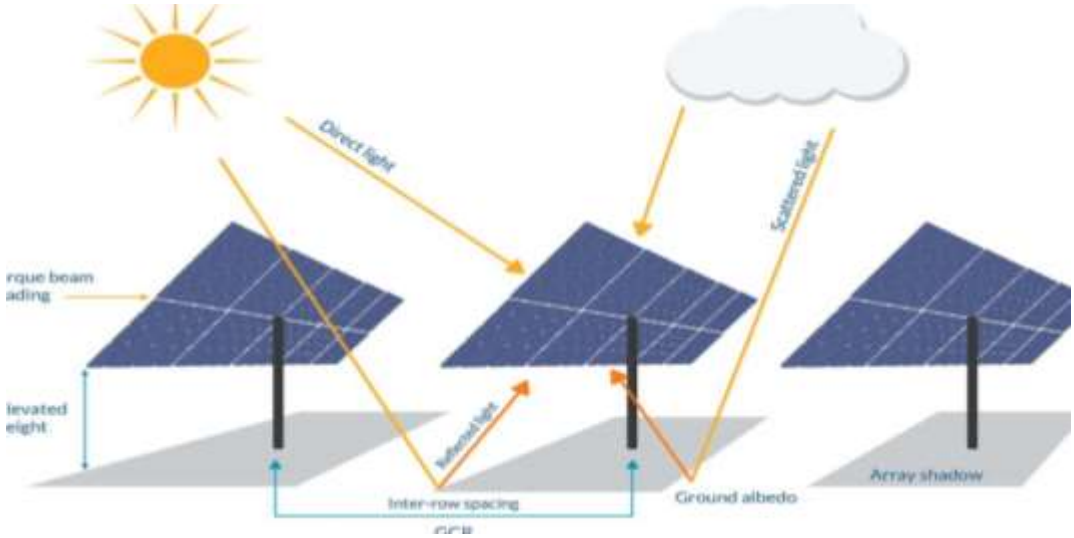

Figure 2.13: pattern of sun's irradiation on bifacial PV module. Source: Schmitt et al., 2009.

However, the performance of bifacial PV modules depends on the irradiance at the rear side, which is strongly affected by the installation setup and environmental conditions. In this research, attention is made to a bifacial PV module and a bifacial PV system by varying the size of the reflective material, vertical installation, temperature mismatch, and concentration of particulate matter (PM) (Jang & Kyungso, 2020). Bifacial solar panels have solar cells built on both sides as shown in Figure 2.14 to allow them to collect not only incoming sunlight but also albedo or reflected light off the ground beneath them. They also move with the sun to maximize the amount of time that sunlight can be collected on either side of the panel. A study from the National Renewable Energy Laboratory shows that there is a 10% increase in efficiency over single-sided solar PV panels (U.S. Department of Energy, 2021).

2.21 BIFACIAL ALBEDO EFFECT

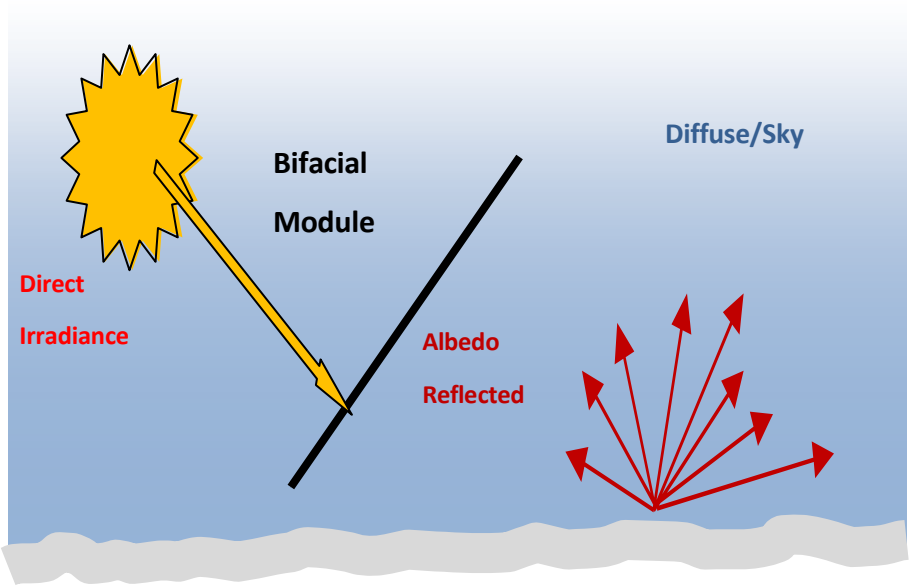

Plate 2.7: Solar irradiance components. Source: Schmitt et al., 2009.

Albedo is not directly dependent on illumination due to the changing amount of incoming light proportionally changing the amount of reflected light, unless in some circumstances where a change in illumination causes a change in the Earth's surface at that location.

Practically, albedo and illumination vary with latitude. Its magnitude is highest near the poles and lowest in the subtropical regions, maximum in the tropics (Schmitt et al., 2009). When the back of the module is introduced to increased light conditions, the output of the module is increased. By selecting installation conditions that maximize the light reflected onto the back of the module from ground and sky components, the energy generated by the backside of the module will increase. An albedometer is an instrument used to measure albedo, which is simply a configuration of two similar pyranometers measuring simultaneously, one facing upwards and one facing downwards, either back-to-back or in a single housing as shown in Figure 2.14.

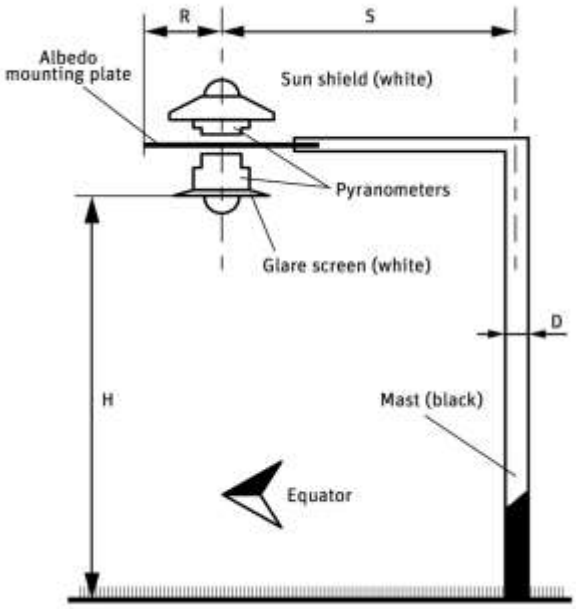

Figure 2.14: Installation of an albedometer on the mast. Source: Kipp & Zonen, 2015.

Historically, albedometer were mounted horizontally and used in meteorological stations and climate research institutes to validate satellite data like monitoring the increasing absorption of solar irradiation by polluted glaciers, heating the surface, and speeding up melting. Albedo is calculated as the ratio between surface irradiation to the incoming solar radiance. It is approximately between $3x10^{-7}$m to 3 x 10^{-6}m, although some instruments have a spectral range begins at 2.8 x 10^{-7}m and others ending at 2.8 x 10^{-6}m. The albedometer is installed upon a flux tower at a specific height above a black mast depending on the vegetation of the ecological region (Susan, 2019). With the upcoming growth in the application of bifacial modules, albedo measurement is also very interesting for the solar energy market but tilted in the plane of an array of modules instead of horizontally (Kipp & Zonen, 2015). For tracked installations, the albedometer is normally mounted on the support structure and moves with the modules. For single-sided, monofacial, PV modules the albedo effect (ground-reflected light reaching the panel) is often neglected unless the modules are at quite a high tilt angle but, even then, it is estimated and not measured. For bifacial modules, the backside can contribute 10 to 25% to the total energy production, so the albedo of the surface must be taken into account (Laudani et al., 2018).

To measure the incoming plane of array irradiance for performance ratio purposes the positioning of the pyranometers is generally well understood. However, for measuring the reflected radiation

coming into the back of a module there are few guidelines. It is important to select the right location, where the pyranometer is parallel to the module and receives light representative of the array. It might not be coincident with the position of the POA pyranometer. If the conditions affecting the amount of light reflected vary along a row, it may be necessary to average over two or more downwards-facing pyranometers. The local albedo is not a fixed number but is dependent on solar angle and weather conditions, such as rain or frost on the surface (otthydromet.com, 2018)

It is important to make the reflected radiation measurement part of the continuous plant monitoring system along with the incoming POA and GHI irradiance. For site prospecting it can be interesting to measure the tilted albedo at different heights and angles and also horizontally, to compare with satellite data.

2.22 ENERGY SCENARIO IN NIGERIA TELECOMMUNICATION INDUSTRIES

The overdependence on fossil fuel over the years has resulted in global warming (Mahalik et al., 2021). Therefore, it is necessary then for countries to diversify their sources of energy and adopt renewables whilst also ensuring that energy remains sustainable, accessible, and affordable (Liu et al., 2022) (Chapman et al., 2021). As of 2021, renewable energy generation stood at an all-time high of 30 % with advances to 50 % and 80 % expected by 2030 and 2050 respectively (IEA, 2021), but for the growth of renewables and to decrease reliance on fossil fuels and the emissions of greenhouse gases, levels of which in the decade 2010–2019 were higher than any level previously recorded (Taghizadeh-Hesary et al., 2019), investment in green energy is crucial. Many years now, solar photovoltaic (PV) energy has been part of the solution; however, its energy density is lower than many other alternative energy sources. Hence, it is necessary to try and increase the energy density of solar PV where possible. This brings the introduction of BFPV module, the first examples of which showed up in the early 1980s (Garrod & Ghosh, 2023) (Gu et al., 2020). The market share of BFPV is expected to be around 70 % by 2030, meaning that detailed knowledge of the performance of BFPV systems is essential (Gu et al., 2020). The systems are able to produce more energy than their monofacial counterparts due to their ability to exploit irradiance incident on both the front and rear sides of the panel (Aydan et al., 2024). The advantage of BFPV systems depends on specific site characteristics such as ground albedo. When applied in a real-world situation, in a ground-mounted system, BFPV systems can provide 25% to 30 % additional power output when installed in an optimised configuration (Raina & Sinha, 2022). In

the process of exploring the BFPV technology, several researches have been carried out around the globe. In one such attempt in Canberra, Australia, it was found that BFPV on a rooftop can result in an energy gain of up to 22.6 %, implying a considerable potential for optimizing solar energy production (Ernst et al., 2024). In another study carried out in Catania, Italy where the experimental setup was employed, it was observed that under operating conditions BFPV exhibits more heat as compared to monofacial. This was estimated to be between 9^0C and 12^0C, depending on the season though there was a significant increase in the energy yield (Leonardi et al., 2022).

Global System for Mobile (GSM) Communications is the most popular wireless cellular communication technique, used for public communication. The GSM standard was developed for setting protocols for second generation (2G) digital cellular networks. It initially started as a circuit switching network, but later packet switching was implemented after integration General Packet Radio Service (GPRS) technology as well. The widely-used GSM frequency bands are 900 MHz and 1800MHz. In Europe and Asia, the GSM operates in 900 to 1800 MHz frequency range, whereas in United States and other American countries, it operates in the 850 to 1900 MHz frequency range. It uses the digital air interface wherein the analogue signals are converted to digital signals before transmission. The transmission speed is 270 Kbps.

Global System for Mobile Communications (GSM) is currently used by about 80% of mobile phones across the worlds. There are about more than three billion users of this technology. The standard GSM was first developed in 1982 by a committee of Conference Europeenne des Postes et Telecommunications (CEPT) (Recent – European Telecommunications Standard Institute), the European Standard Organization, as a new mobile communications standard in the 900 MHz frequency band (Taha et al., 2002). The mobile station is generally the mobile phone which consists of a transceiver, display and a processor. Each handheld or portable mobile station consists of a unique identity stored in a module known as SIM (Subscriber Identity Chip). It is a small microchip which is inserted in the mobile phone and contains the database regarding the mobile station (Taha et al., 2002).

Energy costs are one of the largest operating expenses for telecommunication network operators. Energy costs account for more than half of the telecom operating expenses and about 65% of this is for the tower site equipment in remote and rural areas (Agbo et al., 2021). As the number of subscribers of mobile networks increases in the country, the challenges related to providing electricity to these expanding networks are becoming paramount.

Telecommunication networks are still driven largely by fossil fuel energy and the energy costs represent a significant item. The present research shows that global systems for mobile communication (GSM) operators have spent over N12, 000,000 (twelve million Naira) in 2002 (NCC, 2002) and over N300, 000, 000, 000 (three hundred and sixty billion) in 2023 (NCC, 2023) on diesel generators per year in each of their base stations with costs being transferred to subscribers in terms of billing (Agbo & Ekpo, 2021).

Base stations have been massively deployed nowadays to afford the explosive demand to infrastructure-based mobile networking services, including both cellular networks and commercial Wi-Fi access points. To maintain high service availability, backup battery groups are usually installed on base stations and serve as the only power source during power outages, which can be prevalent in rural areas or during severe weather conditions such as hurricanes or snow storms. Communication base station equipment has been used to replace the previous lead-acid batteries, LiFePO4 batteries, and scenery complementary power generation equipment combined, suitable for the lack of power supply network in the communications base station, to achieve the independent work of the system.

2.23 BASE STATION ENERGY ROAD MAP FOR MOBILE OPERATORS

Bifacial photovoltaic (PV) modules take advantage of the fact that it has rear-surface irradiance. This unique property enables them to produce more energy than monofacial PV modules. Irrespective of this advantage, the performance of bifacial PV modules mainly depends on the irradiance at the rear side of the module which is strongly affected by the installation setup and environmental conditions. Particularly, the size of the reflective material, vertical installation, temperature mismatch, and concentration of particulate matter (PM), are among the major determinants of the performance of the bifacial PV module. As of 2021, renewable energy generation stood at an all-time high of 30 % with advances to 50 % and 80 % expected by 2030 and 2050 respectively (IEA, 2021), but for the growth of renewables and to decrease reliance on fossil fuels and the emissions of greenhouse gases, levels of which in the decade 2010–2019 were higher than any level previously recorded (Taghizadeh-Hesary et al., 2019), investment in green energy is crucial. For many years now solar photovoltaic (PV) energy has been part of the solution, however, its energy density is lower than many other alternative energy sources. Hence, it is

necessary to try and increase the energy density of solar PV where possible. This brings the introduction of BFPV module, the first examples of which showed up in the early 1980s (Garrod & Ghosh, 2023) (Gu et al., 2020).

Over the years, it was shown that the specific yield increased by 1.6% when the reflective material size was doubled. When the PV module was installed vertically, the reduction of power due to the shadow effect occurred, and thus the maximum current was 14.3% lower than the short-circuit current (Guerrero et al., 2016). This shows that the bifacial PV module will provide more dependable solar energy power than the traditional monofacial module when used at telecom base stations in off-grid rural dwellers (Sng et al., 2021).

Plate 2.8: Field installed BFPV module. Source: Sng et al., 2021

The commonly seen panels are the monofacial panels which only collect irradiance from the front surface, the new BF PV module collects irradiance from both the front and the rear surface of the module which produces more power compared to the traditional monofacial panels. Bifacial PV technology was first introduced as a new concept in 1960 to improve the output of PV systems. It then quickly leads to the development of the first Bifacial PV cell which can capture irradiance from both the front and the rear simultaneously (Guerrero et al., 2016). This development quickly grew and captured much attention after a group of researchers from Spain presented results which shows that high efficiency and gain in bifacial PV cells in 1980. Subsequently, it is accepted that bifacial solar cells can increase the power output of a module compared to the traditional Monofacial solar cells with the implementation of cost-effective solutions at the same time. The

Bifacial PV technology came to be even more aware globally when many companies started to commercialize it in the 2010s. A bifacial PV power plant was built in Japan in 2013, an increased gain of 21.9% was observed when compared to a traditional monofacial power plant of similar size even though the installation was sub-optimal (Guerrero et al., 2016). Modelling and simulation are commonly used to analyse the performance of the module, the front surface of the bifacial module is simulated the same way as the front surface of the monofacial module. The rear surface of the module, however, is simulated along with many different factors such as the mounting structure, the albedo of the ground, and the reflectance of the surroundings which differs from location to location. These factors become the challenges in predicting the rear irradiance accurately (Razongles et al., 2016) (Sng et al., 2021). Ray Tracing is a technique that can trace the path of light and accurately simulate the way light bounces off an object. Compared to View Factor, Ray Tracing is much harder to use and implement due to the amount of effort required but can simulate results that View Factor cannot. Like View Factor, Ray Tracing is also widely used to simulate Monofacial modules, it is mostly used when geometry is irregular and mounting structure and in place and can produce accurate results where View Factor becomes complex to use when dealing with irregular geometry (Guerrero et al., 2016). Although Ray Tracing is more accurate when compared to View Factor, it is very resource-demanding and would require a lot of time and effort to produce results for large-scale simulations. In addition, Ray Tracing can also be used to find the efficiency of the design of the module (Liliana et al., 2016). The view Factor method is used to create a 2D model to simulate the front and rear irradiance of the bifacial module while taking into consideration the reflections from its surroundings (Sng et al., 2021).

Understanding the technology and the economics requires the ability to predict the performance of bifacial PV systems. Compared to monofacial PV systems, this requires also modelling the irradiance received by the backside of the PV module. The beam and diffuse sky irradiance components received on the backside may be modelled with the same model used for the front side, such as the Perez tilted surface model and using the appropriate tilt angle. Unless the PV module is mounted vertically, the ground-reflected radiation received by the backside is significantly greater than the beam and diffuse sky radiation received. It is also significantly more difficult to determine because the radiation received by the ground is reduced by shadows from the array and a restricted view of the sky. Additionally, the PV array support structure may prevent ground-reflected radiation from reaching the backside of the PV module. Ray-tracing software,

such as radiance (Guerrero et al., 2016) has been used successfully for modelling the backside irradiance (Deline et al., 2014) but the execution time is too great an obstacle for routine use for modelling the performance of bifacial PV systems. To facilitate reasonable execution times, our backside irradiance model uses configuration factors (CFs). A CF is the fraction of irradiance leaving a surface that is incident on a receiving surface (Guerrero et al., 2016). For ground-reflected radiation for the backside of the PV module, shadows disrupt the isotropic assumption, but the ground area may be divided into areas with equal irradiance distribution and CFs applied separately (Razongles et al., 2016), and then summed to determine the resultant ground-reflected irradiance. A similar technique may be used to determine the diffuse sky irradiance received when the view of the sky is partially obstructed (Singh, 2013). The presented model can give a similar trend to the measured data and predict accurate results only at specific times. The experiment only tested the modules in 0˚ and 30˚ at fixed height which does not give a relation between different configurations and the gain produced. Similar works have also been done by other researchers to predict the gain at both sides of the module at different rows but using View Factor and Ray Tracing (Iliana et al., 2016) (Bayod& Angel, 2019).

Presently, the market for bifacial photovoltaic (PV) modules and their applications is rapidly on the increase year by year (Sng et al., 2021). However, the International Technology Roadmap for Photovoltaic (ITRPV) predicts that the global market share of bifacial PV cells will increase to 80% by 2030 (ITRPV, 2019) (Khan et al., 2017). A bifacial module is particularly more influenced by the diffuse irradiance factor (DIF), height, and albedo than a monofacial PV module. Many researchers have analyzed the output performance based on reflective materials such as white clothes, vegetables, and gravel (Baumann et al., 2019) (Kenny, et al; 2014). There are also increasing applications of the bifacial PV module in a vertical form by integrating them into structures such as noise barriers and fences (Mahmud et al., 2018) (Faturrochman et al., 2020). Previous studies have analysed the simulated output performance, including the albedo, of bifacial modules based on the parameters of the installation setup, such as the tilt angle and height with good module output (Khan et al., 2017). In addition, these simulated output performances were analyzed based on latitude and region, which affect environmental conditions (Kreinin et al., 2016) (Meyer, 2019). Analyses of the output performance of bifacial PV modules at a vertical tilt were also carried out, but through simulations (De Jong et al., 2018) (Asgharzadech, 2018). Generally, before studies can take place, they are usually analyzed using simulations. Moreover, an energy

performance analysis of a bifacial PV module in conditions with high particulate matter (PM) concentrations is yet to be published (Kreinin et al., 2016) (Meyer, 2019).

Extra energy due to bifacial characteristics allows for cost and area savings (Taraba, 2015) as high energy density in the case of bifacial modules correlates to enhanced energy for the same area. This further implies a lower Levelized cost of energy (LCOE) (Luceño & Antonio, 2019). Consequently, bifacial modules also present an opportunity for increased savings and subsequent reduction in payback time. Research about the development of photovoltaic devices can be traced back to the 1950s when William B. Shockley presented an explanation of the method of the functioning of p-n junctions and thus laid the theoretical foundations of the solar cells employed today. Based on this theory, scientists in Bell Labs developed the first silicon cells with an area of 2 m^2 and efficiency of up to 6 % in 1954. In the following years, the efficiency of photovoltaic cells was raised to 10 %. It was in the 1960s, with the development of Photovoltaics as an energy resource for use in satellites, which bifacial PV technology came to the forefront (Bayod & Antonio, 2019). Since the start of a new decade, bifacial modules have gained significant traction in the market, which is expected to grow further in the coming years as bifacial modules are projected to achieve low LCOE in conjunction with tracking systems installed in utility-scale applications. The share of bifacial PV in land-based applications, like agro photovoltaic (AgroPV), building integrated PV (BIPV), carports, etc., as well as water-based applications like photovoltaic, is further expected to grow (Gu et al., 2020).

2.24 REVIEW OF RELATED WORKS.

Many Researchers have attempted to analyse experimentally, by modelling, and through simulation of several factors that can affect the design, characterization, and optimization of bifacial solar cells, modules, and PV installations using front nominal power (at STC) in both indoor and outdoor conditions (Kreinin et al., 2010). According to the number of light sources, indoor and outdoor performance characterization can be classified into single and double-side illumination (Gu et al., 2020). This is mainly used to assess and account for current-voltage characteristics when a bifacial cell is illuminated on one or both sides. Furthermore, when just one side is illuminated, the irradiance on the non-illuminated area should be maintained to a minimum by covering the backside with a non-reflective plate (Roest et al., 2018). This is done to avoid the non-illuminated side being exposed to stray light. In a single-sided illumination procedure, the PV

module's front side is exposed to the solar simulator one side at a time (Liu et al., 2022). In a double-sided illumination procedure, the PV module's front and back sides are simultaneously exposed to the solar simulator. In Schmid et al., (2017), they established that most laboratories cannot measure the I–V curve under bifacial illumination. Moreover, the double-sided illumination method is quite expensive (Zhang et al., 2018) and a single-sided illumination with a flash solar simulator at standard test conditions (STC) is required for the essential characterization of bifacial modules to assess the module parameters for each side (Mahalik et al., 2021). The market share of BFPV is expected to be around 70 % by 2030 (GU et al., 2020), meaning that detailed knowledge of the performance of BFPV systems is essential. The systems are able to produce more energy than their monofacial counterparts due to their ability to exploit irradiance incident on both the front and rear sides of the panel (Aydan et al., 2024). The advantage of BFPV systems depends on specific site characteristics such as ground albedo. When applied in a real-world situation, in a ground-mounted system, BFPV systems can provide 25% to 30 % additional power output when installed in an optimised configuration (Raina & Sinha, 2022). In the process of exploring the BFPV technology, several researches have been carried out around the globe. In one such attempt in Canberra, Australia, it was found that BFPV on a rooftop can result in an energy gain of up to 22.6 %, implying a considerable potential for optimizing solar energy production (Ernst et al., 2024). In another study carried out in Catania, Italy where the experimental setup was employed, it was observed that under operating conditions BFPV exhibits more heat as compared to monofacial. This was estimated to be between 9^0C and 12^0C, depending on the season though there was a significant increase in the energy yield (Leonardi et al., 2022). In South Korea, when monofacial and BFPV modules were installed in a solar carport system and studied for a year, it was estimated that the total annual energy yield for bifacial was 3.08 % higher. The low yield was determined to be the attribution of the low bifaciality of the cell and the shading experienced (Hwang et al., 2023). As the technologies continue to develop and integrate with other sectors, the employment of bifacial has proved to increase the electricity yield in the field like floating PV where modules can increase productivity due to reflection from water (Garrod et al., 2024) and agrivoltaics by providing partial shading for shade-tolerant crops (Ghosh, 2023). In a study performed, it was determined that using bifacial vertically mounted agrivoltaics almost doubled the energy yield compared to monofacial (Arena et al., 2024).

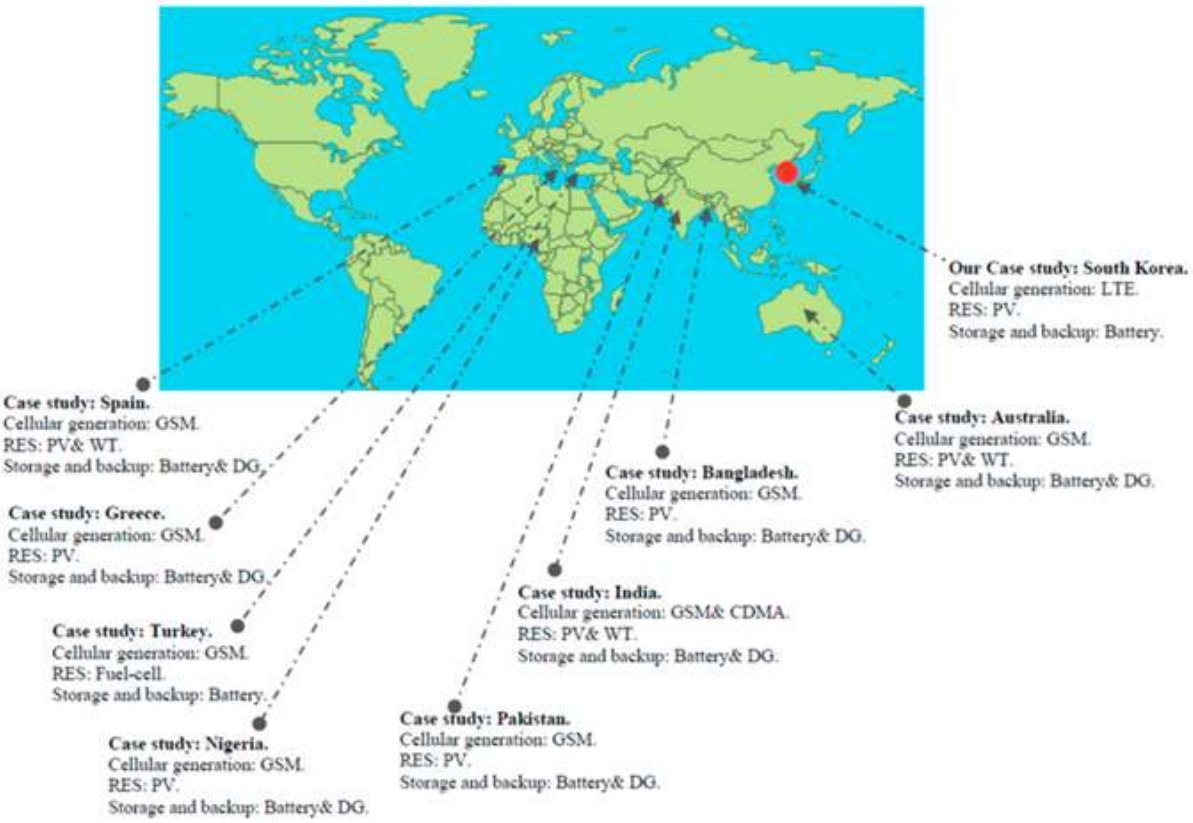

Plate 2.9: Summary of related works on energy optimisation strategies for cellular base stations. Source: Mohammed & Jeong, 2016.

In an experimental analysis, the performance of building integrated PV façade was examined, where the impact of ventilation on the temperature of the BFPV and monofacial PV modules was investigated. It was observed that the module efficiency increased at the same time decreasing the thermal load, at the same time the temperature recorded on the back side of the BFPV was higher as compared to its counterpart during the day (Ersagun & Mahir, 2022).

In South Korea, when monofacial and BFPV modules were installed in a solar carport system and studied for a year, it was estimated that the total annual energy yield for bifacial was 3.08 % higher. The low yield was determined to be the attribution of the low bifaciality of the cell and the shading experienced (Hwang et al., 2023).

As the technologies continue to develop and integrate with other sectors, the employment of bifacial has proved to increase the electricity yield in the field like floating PV where modules can increase productivity due to reflection from water (Garrod et al., 2024) and agrivoltaics by

providing partial shading for shade-tolerant crops (Ghosh, 2023). In a study performed, it was determined that using bifacial vertically mounted agrivoltaics almost doubled the energy yield compared to monofacial (Arena et al., 2024). In an experimental analysis, the performance of building integrated PV façade was examined, where the impact of ventilation on the temperature of the BFPV and monofacial PV modules was investigated.

It was observed that the module efficiency increased at the same time decreasing the thermal load, at the same time the temperature recorded on the back side of the BFPV was higher as compared to its counterpart during the day. However, much of the previous work done on BFPV performance has been simulation studies (Yusufoglu et al., 2015) however, previous studies have measured the electrical performance of BFPV modules for various applications such as building applied/integrated, agrivoltaics, floating (Campana, et al, 2021) as well as a summary of several ground-mounted BFPV simulations are mentioned (Lopez-Garcia et al., 2019) evaluates BFPV electrical performance; however, it focuses on indoor conditions and does not use conventional panel ground mounting. Table 2.10 states previous BFPV studies and their outcomes, focusing on ground-mounted systems. The UK currently has limited experimental papers evaluating BFPV performance, and only one simulation-based study (Gul & Puxty, 2024). It is therefore vital that this growing technology be evaluated for a country like Nigeria whose solar industry is seen as a promising source of clean and affordable energy (Mandys et al., 2023).

Given the UK's temperate climate, it could be thought that it would be a beneficial place to make use of BFPV due to the technology making more use of its bifacial gain under irradiance conditions dominated by diffuse light (Jouttijarvi et al., 2022). The specific location of a PV system concerning its latitude, longitude, and typical climate will have a significant effect on its overall performance (Yunus et al., 2020) this has the potential to be especially true with respect to climatic conditions when considering BFPV systems, due to the different characteristics concerning temperature performance (Lamers et al., 2018) and the earlier mentioned improved bifacial gain under diffuse light conditions (Aydan et al., 2024). None of which have been conducted in the United Kingdom, which as stated earlier could be an ideal location for the use of the BFPV technology due to its ability to perform better under diffuse dominant conditions. Also, the panel temperature model of the BFPV system for the temperate climatic condition of United Kingdom is also not available.

However, few articles have covered the area of the modelling and parameter identification of BPV modules. Extracting BPV model parameters is advantageous in terms of many application aspects, including the design of the optimal size of the PV system, calculating the annual energy yield, forecasting the produced energy and studying the system reliability and stability. The mobile cellular networks on Africa continent remains one of the fastest growing industries in the world. This growth has made the network to expand beyond the supply capacity of grid electricity system only. Thus, prompting the network providers to deploy many of their equipment in the areas where there is limited access to electric grid system according to the 1168 IEEE African 2017 Proceedings Groupe-Speciale Mobile Association (GSMA), explanation and research (GSMA, 2014). The GSMA further estimates that the total percentage of mobile cellular networks coverage across sub Saharan Africa remains 70% as a result of BS tower of 240,000 which is expected to increase to a total number of 325,000 at the end of the year 2029. The GSMA further stated that Africa has about 145,000 deployed off grid BS sites which are expected to grow to 189,000 by the end of 2029. Out of the number estimated - 84,000, expected to grow to 100,000, are said to be on faulty bad-grid (GSMA, 2014). This is the major cause of unreliable power, frequent power outage, voltage fluctuation, loss of phase and degradation of mobile signal coverage and capacity in the developing countries of the world. Consequently, the use of diesel generating set as a power backup which causes high cost of operation and emission of carbon oxides. However, further, observation shows that most of these countries in Africa region have abundant solar energy resource as compared to other sources of renewable energy such as the wind, fuel cells, etc. Hence, energy harvested from the solar seems to be a viable option to power the BS. Of all the Renewable Energy Sources (RES), energy harvested from the solar irradiance converted by the means of the PV panel has become a major energy source to power BS. Solar PV energy source is usually supported by an array of batteries to store extra energy harvested. Some advantages of using solar PV system in mobile cellular operation are; Self sustainability nature of solar energy, its availability virtually in all locations, little or no emission of CO_2, and affordable to implement. Solar PV energy source also requires little maintenance. Hence, for most developing countries, solar BS implementation is seeing as an alternative means of powering BS. Other advantages of using solar PV to powered mobile cellular BS were also highlighted in (Okundamiya et al., 2015) (Deruyck et al., 2011). Solar PV utilization is not new in Nigeria. However, little has been done towards powering the mobile cellular base station. Therefore, it is the focus of this research to

present an overview of using solar PV powered mobile cellular BS in Nigeria using bifacial PV module with the aim of encouraging its adoption and deployment. Currently a lot of research and studies have been carried out on the powering telecom base stations with solar PV. These studies can be grouped into the categories of system planning or design, operation and control. To a large extent studies and development efforts carried out so far have focused on monofacial PV (MFPV) module. This is because MFPV modules are commonly deployed as a backup power provider in case of grid electricity and generator failures. Another reason is that MFPV module offer a far better option for providing reliable electricity than putting large sums of money in purchase of backup generators. However, research on powering telecom base stations, economic aspects and operation as well as value propositions of these technologies still modest. Furthermore, solar PV based station especially those designed for rural purposes in developing countries face a lot of issues as regards their implementation (Zhu, et al, 2015). These fall into the categories of general, technical, economic and financial, legal and regulatory, institutional, social and sustainability issues. Various researchers have highlighted these issues (Parhizi et al., 2015) (Buchana & Ustun, 2015). A number of researchers have tried to address some of the above mentioned issues in their studies but additional research is needed in the areas of solar powered telecom base stations economics, appropriate technical designs and socio-economic analysis of solar-powered telecom base station deployments (Parhizi et'al., 2015). Furthermore, research is needed to clarify the expectations from solar PV for in remote areas as regards reliability as they may not be as reliable as the main grid. Research is needed to show that a well-designed, optimized and economically feasible Solar PV model can function in remote areas. When this is achieved it will provide network provider with the energy solution of running their base station without generator and thus scale up the Teledensity rates of mobile subscribers in developing countries. This will enable governments to deliver on their targets in line with the United Nations Sustainable Development Goal 7 (SDG 7).Taking an example of Nigeria as one of the developing countries with an aggressive action agenda for its Sustainable Energy for all initiative, it is important to come up with ways in which projects aimed at achieving these targets can be scaled up.

Over the course of the next twenty years, the research on bifacial PV technology did not pick pace as was expected at the time. It wasn't until Taraba and Cuevas published their work in 2020 highlighting their achievement that combining bifacial devices, capable of utilizing the surrounding albedo light, with a concentrating device could increase electricity production by

50 %. The 1980s ′s saw a high flux of scientific articles focussed on high efficiency and high gain bifacial PV cells and modules. Such increased interest enabled the concept of bifaciality to become prominent among researchers through the next decade, focusing on proposing cost-effective solutions for various niche applications. Parhizi et'al., (2015) presented a model for a two-sided collection of solar energy from a bifacial panel. They augmented their setup with a white-painted plane which produced diffuse reflections of the incoming irradiation. For such an augmentation, a practical gain of up to 59 % was achieved when compared to monofacial cells. Their work prompted researchers to develop models and correlations to estimate accurately the various components of irradiance incidents on a surface (Parhizi et al., 2015). Evaluation of bifacial PV performance, through simulation and novel test beds, became prevalent throughout the 1990s ′s and the first decade of the 21st century. Jaeger, et al: 2020, demonstrated experimental results derived from newly developed albedo collecting modules, manufactured using thin film silicon MIS inversion layer solar cells. They coupled their modules with white back diffusers and achieved a 33 % gain in power. Shoukry et al, 2016 analyzed the benefits of bifacial response phenomena by developing certain modifications in the PVFORM software package and determined that without any additional features, an increase of up to 20 % in annual energy can be generated. Their simulation provided insights into the performance of bifacial PV modules during high summer peaks and days with dense clouds. The chronological development of bifacial PV technology can be tracked through the years, starting from the development of the first PV cell to the early 2000′s wherein novel structures to achieve bifacial characteristics were designed and tested. The last decade oversaw research and development activities on developing models to assess bifacial PV's performance, evaluate feasibility, and find niche applications for bifacial PV (Chieng et al., 1993). On these lines, an extensive review has been carried out and systematically presented, which covers all facets of bifacial PV technology, from design to modelling followed by addressing the challenges and concluding with a discussion on the future applications of bifacial technology.

As the research into the benefits of the property of bifaciality of PV cells and modules gained pace through the years, researchers devoted their focus to developing novel structures that were in way modifications of existing PV cell structures. Parhizi et'al., (2015) developed bifacial cells for use in a concentrator module by using a new fabrication process, wherein they made use of the conventional mass production process while incorporating modifications in the boron diffusion (Ohtsuka et al., 2000).The difficulty in accurately measuring the bifacial PV cell and modules'

performance arises due to the external contributions of light reflections to the rear of the modules. This extra light can significantly increase the total current generated. Typically, the electrical characteristics of bifacial PV cells and modules are reported by individually irradiating the front and rear sides and quantifying the output (Mertens, 2018). A common method to do so is by securing the PV cell in a metal chuck and exposing it.

Modelling the performance of bifacial modules has been summarized as a three-step process in literature. Initial calculations for total available irradiance on the plane of array (G_{POA}), i.e., cumulative of front and rear irradiance are followed by the determination of module temperature (T_{MOD}) using available thermal models. For the thermal and optical models, the solar meteorological data i.e., GHI, DHI, wind speed (V_W), ambient surrounding temperature (T_{AM}), and local geographical conditions (Wong et al., 2001. While bifacial PV technology was initially developed in the 1960s ′s, advanced research, and development in recent decades have resulted in a significant increase in the efficiencies of bifacial PV modules and have allowed it to become a disruptive player in the PV market. However, several variables need to be addressed to ensure that bifacial PV cells and modules can account for a significant share of the PV market. Among the variables, cost is one of the most significant factors that will govern (Appelbaum, 2016)
Since the start of a new decade, bifacial modules have gained significant traction in the market, which is expected to grow further in the coming years as bifacial modules are projected to achieve low LCOE in conjunction with tracking systems installed in utility-scale applications. The share of bifacial PV in land-based applications, like agro Photovoltaics (AgroPV), building integrated PV (BIPV), carports, etc., as well as water-based applications like Photovoltaics, is further expected to grow (Gu et al., 2020)

BF PV power plant was built in Japan in 2013, and an increased gain of 21.9% was observed when compared to a traditional monofacial power plant of similar size even though the installation was sub-optimal (Guerrero et al., 2016). Modelling and simulation are commonly used to analyse the performance of the module; the front surface of the bifacial module is simulated the same way as the front surface of the monofacial module. The rear surface of the module, however, is simulated along with many different factors such as the mounting structure, the albedo of the ground, and the reflectance of the surroundings which differs from location to location. These

factors become the challenges in predicting the rear irradiance accurately (Razongles et al., 2016) (Sng et al., 2021).

Research gaps

i. The racking system of MFPV module is not efficient

ii. MFPV panel occupies large area of land than BFPV panel.

iii. There is no proper Optimization model for MFPV systems (combination of PVsyst, Heliscope and HOMER give the best solution).

iv. The presence of diesel generator as a power backup requires regular System Check and Maintenance.

v. The use of predictions in allocating data during simulation is not reliable

CHAPTER THREE

MATERIALS AND METHODS

3.1 MATERIALS

In establishing the goal of this research, the following materials was used**;** Hardware modules and Software systems. The tracking system is modelled with the help of hardware modules and software control systems.

3.1.1 Hardware modules materials.

The hardware modules used in the simulation are;

i. Site map (figure 3.1) of telecommunication base station (figure 3.2) at FUTO

ii. Load profile data of the site.

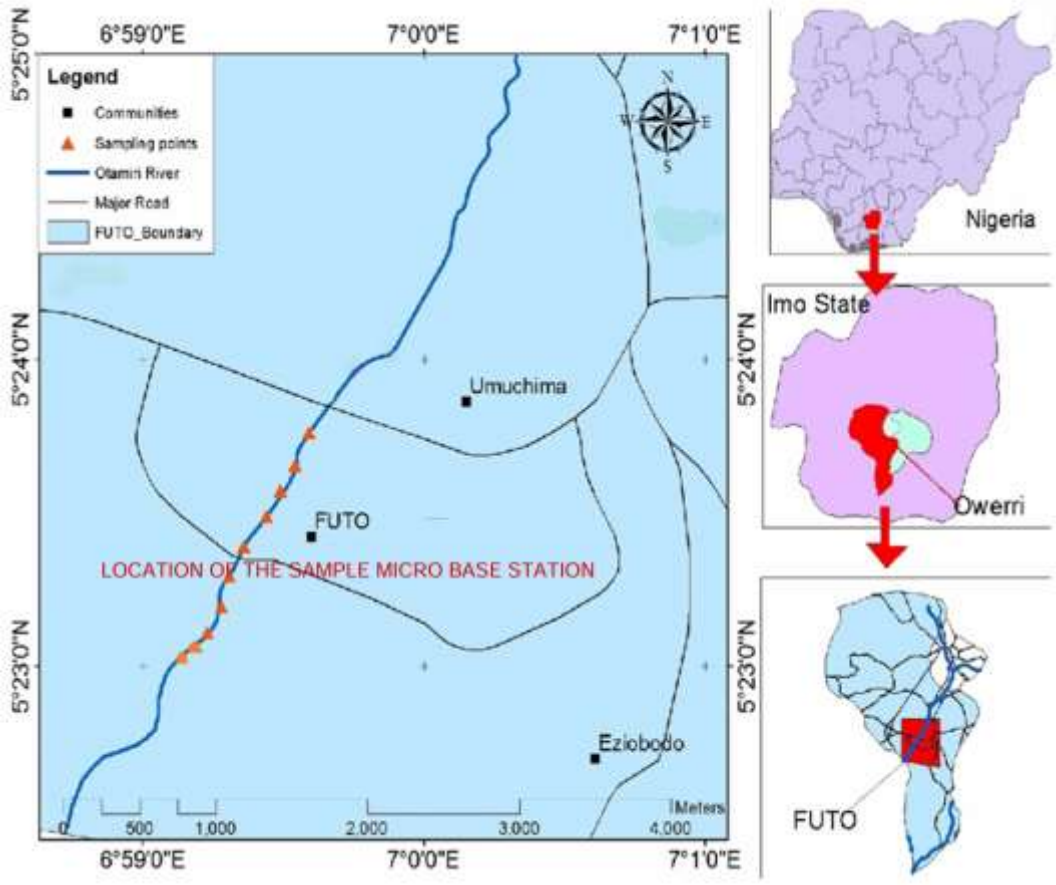

Figure 3.1: map of ihiagwa showing FUTO for the sample micro base station. Source: MTN, 2019

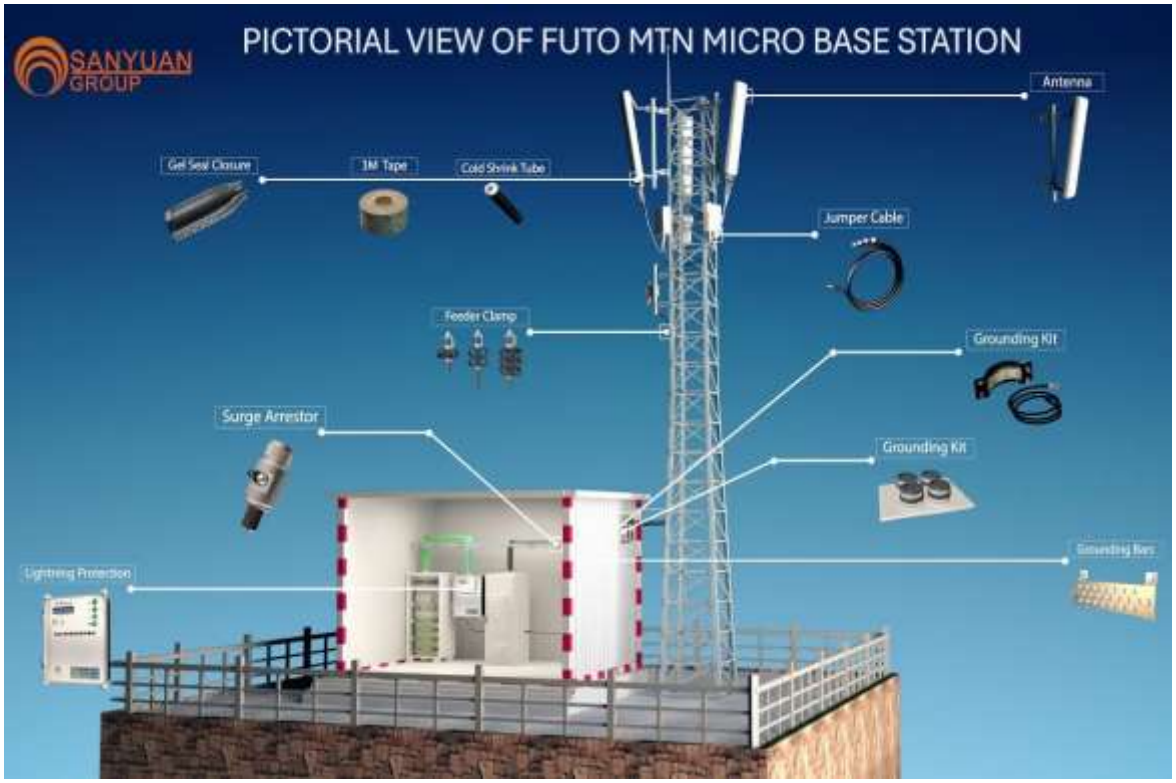

Figure 3.2: pictorial view of components at the sample micro base station. Source: MTN, 2019

3.1.2 Software and control systems materials

The software module and control systems materials used in this work are Matlab/Simulink, PVsyst version 7.4.8 and HOMER software. The Matlab/Simulink models were used to actualise the output performance of a single diode model of a monofacial solar PV. The PVsyst was used for the simulation of the bifacial module selected, and HOMER was used for the optimization process of the systems configuration. The energy performance of the selected sites was used to monitor each base station for twelve calendar moths of the year under review (2024).

3.2 METHODS

i. Control methods adopted

1. Maximum Power Point Tracking (MPPT): MPPT was used to control the power conditioning system to maximize energy output of the MFPV module.

2. Power Conditioning System (PCS) Control: PCS control was used to regulate the output power of the bifacial solar panels to match the load demand by two-axis tracking.

3. Energy Storage System (ESS) Control: ESS control was used in both PVsyst and HOMER to regulate the charging and discharging of the energy storage in order to minimize energy costs.

4. Supervisory Control and Data Acquisition (SCADA) System: SCADA system was used in PVsyst and HOMER to monitor and control the solar-powered telecommunication network base station remotely.

ii. Optimization method adopted

The multiple objective systems were the optimization method adopted in this research. Figure 3.3 shows that of the HOMER software. This software is able to optimize the cost, energy, solar irradiation and data analysis for the solar system. The PVsyst is divided into; grid-connected systems, standalone systems with generator and battery backup, standalone systems with battery backup only, pumping systems, and direct current networks for public transportation (DC-grid). PVsyst also features a database extensive and diverse meteorological data sources, as well as solar system component data.

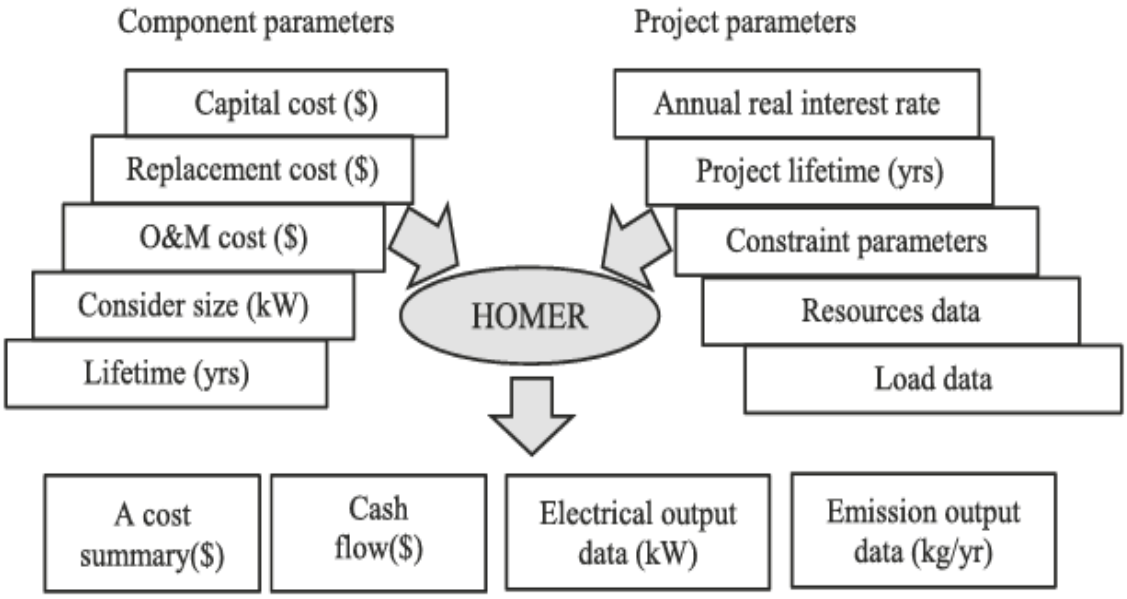

Figure 3.3: HOMER architecture software.

The simulation of a solar power plant depends on several factors explained on a theoretical basis, such as the choice of geographic location, PV modules, inverter quality, and solar panel orientation. Therefore, this research adopted many methods to realise the research objectives.

3.2.1 Development of a single and double diode mathematical model of MFPV and rear-side irradiation models for BFPV module.

Stand-alone photovoltaic systems are the best solutions for providing clean energy to telecommunication system, water pumping and low power appliances in rural area. Such systems are consisting of a PV generator, energy storage devices, AC or DC consumers and elements for power conditions. PV module represents the fundamental power conversion unit of a PV generator system. The output characteristic of PV module depending on the irradiance intensity and the cell's temperature is nonlinear, so it is necessary to model it for the simulation of maximum power point tracking. One-diode equivalent circuit is employed to investigate I-V and P-V characteristics of a typical solar module.

3.2.1.1 Single diode modelling

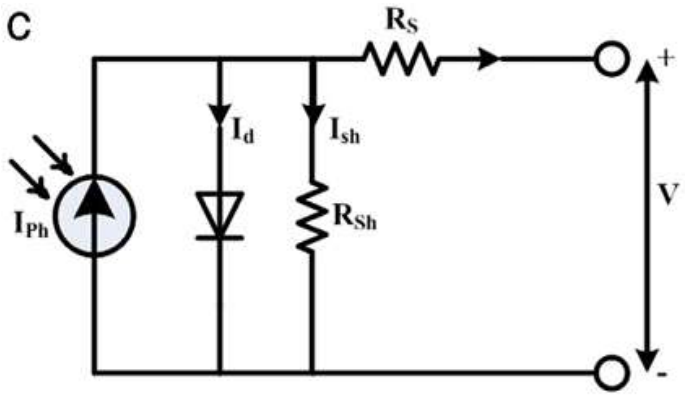

Figure 3.4: Single diode with shunt resistor.

Solar energy cells for the generation of electricity are built in cells called module. A module is the interface, which converts light energy into electrical energy (Jose, et'al, 2016). Modelling of a PV module requires taking weather data (irradiance and temperature) as input variables. In this research, the variables to investigate are the I–V and P–V characteristics and the maximum point power tracking point (MPPT) using simulation and MATLAB tools. The solar PV device can be represented as an ideal solar cell with a current source I_{ph} parallel to the diode as illustrated in figure 3.4. On this figure, applying current law (KCL) Kirchhoff's law we give us;

$$I = I_{phc} - I_{sh} - I_d \tag{3.1}$$

I_{PV} is the current generated by the solar cell, I_d is the diode current, I_{sh} is the current that is flowing through the shunt resistor and I is the photo current. Practically, the diode current I_d is given by the expression;

$$I_d = I_{sc}\left\{exp\left(\frac{V + IR_S}{aV_{TV}}\right) - 1\right\} \tag{3.2}$$

V_{TV} is the thermal voltage of the diode and is given as $V_{TV} = \frac{kT}{q}$. The terms $k, T\ and\ q$ are defined in table 3.1

Table 3.1: constant parameters used in the modelling

Parameters	
Maximum power	(P_m)
Open circuit voltage	(V_{oc})
Voltage at maximum power	(V_m)
Short circuit Current	(I_{sc})
Current at Maximum power	(I_m)
Power tolerance	(P_T)
Number of cells in series	(C_s)
Number of cells in parallel	(C_P)
Operating Temperature	(T)
Ideality factor	(A)
Electron Charge	(q)
Irradiation	(G_r)
Short circuit current temperature coefficient	(k_t)
Band gap	(B_g)
Boltzmann's constant	(k)
Shunt current	(I_{sh})

The current through the shunt resistor, I_{sh} is given as;

$$I_{sh} = \frac{V + IR_S}{R_{sh}} \tag{3.3}$$

$$\text{Photo current } (\mathrm{I_{phc}}) = \frac{[I_{sc} + k_t(T - T_r)]G_r}{1000} \tag{3.4}$$

Substituting equation 3.3 and 3.4 in equation 3.1 it becomes,

$$I = I_{phc} - \frac{V + IR_S}{R_{sh}} - I_{rs}\left\{exp\left(\frac{V + IR_S}{nV_{TV}}\right) - 1\right\} \tag{3.5}$$

$$\text{Reverse saturation current } (\mathrm{I_{rs}}) = \frac{I_{Sh}}{exp\left(\frac{qV_{oc}}{nkT}\right) - 1} \tag{3.6}$$

$$\text{Saturation current } (\mathrm{I_S}) = I_{rs}\left[\frac{T}{T_r}\right]^3 exp\left[\frac{qB_g}{nk}\left\{\frac{1}{T_r} - \frac{1}{T}\right\}\right] \tag{3.7}$$

$$I_{Sh} = short - circuit\ current$$

Therefore, the current output of the PV module which flows through the Rs, is given by;

$$I = I_{phc} - I_S\left\{exp\left[\frac{q(V + IR_S)}{nkT}\right] - 1\right\} - \frac{V + IR_S}{R_{sh}} \tag{3.8}$$

At open circuit condition,

$$0 = I_{phc} - I_s\left\{exp\left[\frac{q(V_{oc} + IR_S)}{nkT}\right] - 1\right\} - \frac{V_{oc} + IR_S}{R_{sh}} \quad (3.9)$$

At short-circuit condition,

$$I_{sh} = I_{phc} - I_s\left\{exp\left[\frac{q(I_{sh}R_S)}{nkT}\right] - 1\right\} - \frac{I_{sh}R_S}{R_{sh}} \quad (3.10)$$

At maximum power point condition,

$$I_{mpp} = I_{phc} - I_s\left\{exp\left[\frac{q(V_{mpp} + I_{mpp}R_S)}{nkT}\right] - 1\right\} - \frac{V_{mpp} + I_{mpp}R_S}{R_{sh}} \quad (3.11)$$

3.2.1.2 Double diode modelling

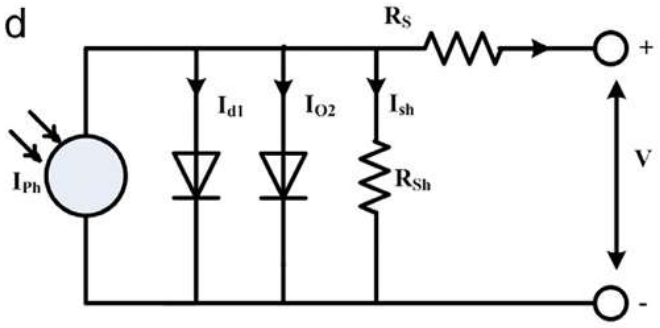

Figure 3.5: Solar PV cell double diode model

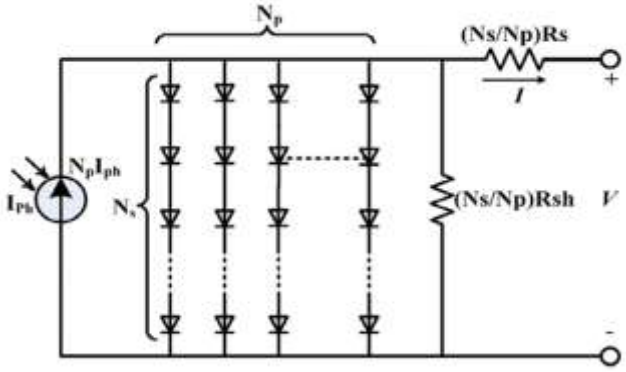

Figure 3.6: Equivalent circuit model of PV array

Irrespective of the improvement in single diode model, its accuracy is not reliable. To overcome this problem, a two diode model is introduced. It consists of two diodes connected in parallel to the current source, as shown in figure 3.5. The current I_{d1}, through the first diode is the current component same as I_d in single diode model. The current through the second diode I_{d2}, is the

combined current in space charge region. The equivalent circuit for a typical PV array is as shown in figure 3.6.

Figure 3.5 suggests that two Shockley terms contribute to the saturation currents of a solar PV cell. Series resistance Rs, and shunt resistance R_{sh}, are same as defined for single diode model. The double diode model of a SPV cell is highly accurate at low insolation levels. The double diode model can be represented by the following equation;

$$I = I_{phc} - I_{s1}\left\{exp\left[\frac{q(V + IR_S)}{n_1 kT}\right] - 1\right\} - I_{s2}\left\{exp\left[\frac{q(V + IR_S)}{n_2 kT}\right] - 1\right\} - \frac{V + IR_S}{R_{sh}} \qquad (3.12)$$

From figure 3.4, the monofacial PV output current for single diode model is given as;

$$I = N_p\left[I_{phc} - I_S\left\{exp\left[\frac{q\left(V + IR_S\left[\frac{N_s}{N_p}\right]\right)}{nkT}\right] - 1\right\}\right] - \left[\frac{V + IR_S\left(\frac{N_s}{N_p}\right)}{R_{sh}\left(\frac{N_s}{N_p}\right)}\right] \qquad (3.13)$$

and for double diode model is given as ;

$$I = N_p k_1 - N_p k_2 - k_3 \qquad (3.14)$$

$$k_1 = I_{phc} - I_{s1}\left\{exp\left[\frac{q\left(V + IR_S\left[\frac{N_s}{N_p}\right]\right)}{n_1 kT}\right] - 1\right\} \qquad (3.15)$$

$$k_2 = I_{s2}\left\{exp\left[\frac{q\left(V + IR_S\left[\frac{N_s}{N_p}\right]\right)}{n_2 kT}\right] - 1\right\} \qquad (3.16)$$

$$k_3 = \left\{\frac{V + IR_S\left[\frac{N_s}{N_p}\right]}{R_{sh}\left[\frac{N_s}{N_p}\right]}\right\} \qquad (3.17)$$

3.2.1.3 Single diode mathematical model of BFPV module

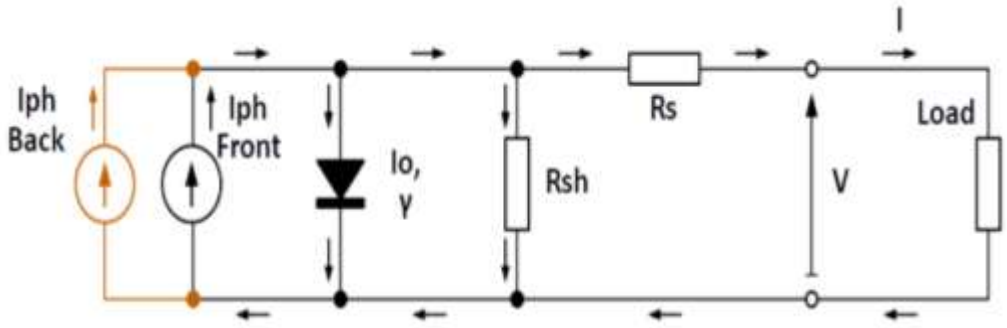

Figure 3.7: circuit diagram of a bifacial single diode PV module.

Figure 3.5 represents the electrical circuit diagram of a BFPV module. In bifacial modules, the top solar cells functions as in traditional monofacial modules; they directly capture sun rays and convert them into electricity. The modification is that bifacial modules come with a transparent backside that are able to generate electricity from the sun shining directly on them and also from the sunlight reflected on the opposite side or underneath the panel or off the ground. While the original light is called incident light, the reflected light is called albedo light. They come from diffused light from clouds, buildings or other objects from which light rays can bounce off and hit the backside of the bifacial modules. In a BPV module, the rear side acts as an additional current source. Since the front side current $I_{phfront}$ and the back side current I_{phback} are in parallel as shown in figure 3.5, the total current from a BPV module is given as;

$$I_{total} = I_{phfront} + I_{phback} \tag{3.18}$$

Careful experiments conducted on three different and standard albedo conditions (white surface, green grass land, and snow) show that $0.5I_{ph\ front} = I_{ph\ back}$ at Standard Test Condition (STC). Consequently, equation 3.18 becomes;

$$I_{total} = I_{ph\ front} + 0.5I_{ph\ front} = 1.5I_{phfront} \tag{3.19}$$

Unlike the monofacial module, this research work anchors the performance of a bifacial PV module based on the installation setup and environmental conditions in the mounted field area and the albedo. Here, the albedo used was collected from satellite data at standard test condition. To model a bifacial module for determining the energy output, a lot of sub-models should be considered. The electrical circuit shows that the bifacial module can be modelled using the one

diode model. In this process, the second diode is in parallel with the current source. The current versus voltage (I-V) relationship is given as;

$$I = I_{Ph}(Front + Back) - I_0\left[exp\left(\frac{V + IR_s}{nV_{TV}}\right) - 1\right] - \frac{V + IR_s}{R_{sh}} \quad (3.20)$$

In terms of bifaciality factor, it is given as;

$$I = I_{Ph}(1 + \varphi) - I_0\left[exp\left(\frac{V + IR_s}{nV_{TV}}\right) - 1\right] - \frac{V + IR_s}{R_{sh}} \quad (3.21)$$

Substituting equation 3.4 into equation 3.20 it becomes;

$$I = \frac{[I_{sc} + k_t(T - 298)]G}{500} - I_0\left[exp\left(\frac{V + IR_s}{nV_{Tv}}\right) - 1\right] - \frac{V + IR_s}{R_{sh}} \quad (3.22)$$

$$P_{PV} = \frac{P_{STC\ front}\{(I_f + I_r)\varphi f_1[(1 + \gamma)(T_c - 25)]\}n_{inv}[(1 - \beta_0 - \alpha\beta_1)(1 - \mu)]}{1000} \quad (3.23)$$

$P_{STC\ front}$ is the power output of the panel with light reaching their front side only, φ is the bifaciality factor, f_1 is the spectra irradiance contribution, γ is the power temperature coefficient, and T_c is the cell temperature. As the cell depreciates, β_0 is the initial cell degradation, and β_1 is the yearly degradation rate of the module while α is the age of the panel in years at the time of installation. For this research project, $\alpha = 25years$, μ is the Ohmic and shading losses. The solar spectra irradiance f_1 changes throughout the day and as well influences the performance of the module especially in large band gap semiconductor materials Therefore,

$$f_1 = [a_0 \times a_1 \times AM_a] + [a_2 \times (AM_a)^2] + [a_3 \times (AM_a)^3] + [a_4 \times (AM_a)^4] \quad (3.24)$$

AM_a is the absolute air mass which can be approximated using equation 3.24 as;

$$AM_a = e^{AM(-0.0001184)} \quad (3.25)$$

AM is the air mass based on Kasten's research from which results can be obtained from zenith angle up to 90^0

$$AM = \frac{1}{\cos Z + 0.50572(96.07995^0 - Z)^{-1.6364}} \quad (3.26)$$

T_c is given as;

$$T_c = T_a + \left(\frac{I_{front} + I_{rear}}{800}\right)(T_{INOPT} - 20) \quad (3.27)$$

T_a is the ambient temperature, and T_{INOPT} represents the installed normal operating temperature, which largely depends on the mounting structure, as it affects the dissipation of heat by the solar panel. I_{front} and I_{rear} are the front and rear irradiation of the panel

$$T_{INOPT} = T_{NOPT} + x_{mount} \quad (3.28)$$

$T_{NOPT}$is the normal operating temperature of the cell, and x_{mount} is a coefficient whose value is based on the mounting structure (Rodríguez-Gallegos, et al, 2018). Therefore, as years goes by, the PV system begins to degrade in value and its electrical performance starts to drop.

Alternatively, the current produced from the irradiance received in the rear-side (G_{rear}) is modelled as an extra current source besides the front irradiance (G_{front}), which can be simplified to a single current source with irradiance input G_{front} and G_{rear} weighted by the cell's bifaciality factor φ ;

$$G = G_{front} + \varphi G_{rear} \quad (3.29)$$

The variable φ is defined as follows;

$$\varphi = bifaciality\ factor = \frac{Rear\ irradiation}{front\ irradiation} \quad (3.30)$$

3.2.1.4 Rear-side irradiation model of a BFPV module

To model the electrical performance of the rear-side of a BFPV module, we have to model the parameters that affect the electrical performance of the rear-side.

3.2.1.5 Plane array of irradiance modelling (PAOI)

The irradiance incident on the surface of a cell, or array is important to module performance. Irrespective of the size of the PV system, this incident irradiance on its surface is known as Plane of Array Irradiance. The PV system can be fixed or variable through time like on tracking systems. The POAI includes the direct irradiation (Irr_{Beam}) and diffuse irradiations ($Irr_{Diffused}$), as well as ground reflectance (Irr_{Ground}). Therefore;

$$Irr_{POAI} = Irr_{Beam} + Irr_{Diffused} + Irr_{Ground} \quad (3.31)$$

To calculate the POA irradiance, the Angle of Incidence (AOI) formed between the normal of the PV array and the sun's position must be known as indicated in equation 3.32

$$AOI = cos^{-1}\{cos(\theta_z)\, cos(\theta_\beta)\} + sin(\theta_z)\, sin(\theta_\beta)\, cos(\theta_{azimuthsun} - \theta_{sazimuth}) \quad (3.32)$$

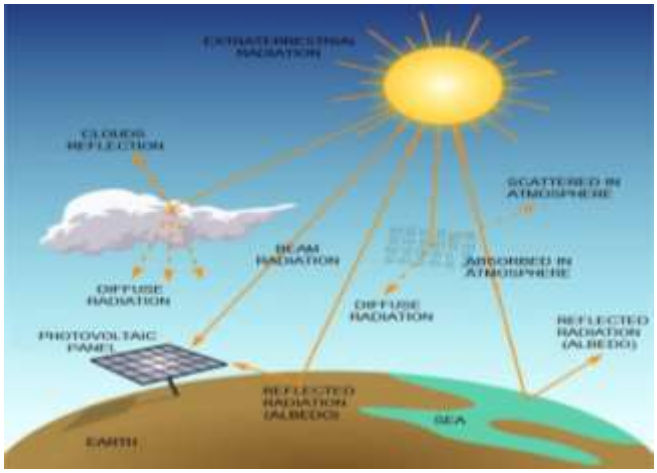

Plate 3.1 (a): Solar Radiation component. Source: Muriele et al., 2019

In equation 3.32, θ_z is the sun's zenith angle, β is the surface tilt of the PV array, and γ is the surface azimuth of the PV-array, defined from North pole at 0° as shown in plate 3.1 (b).

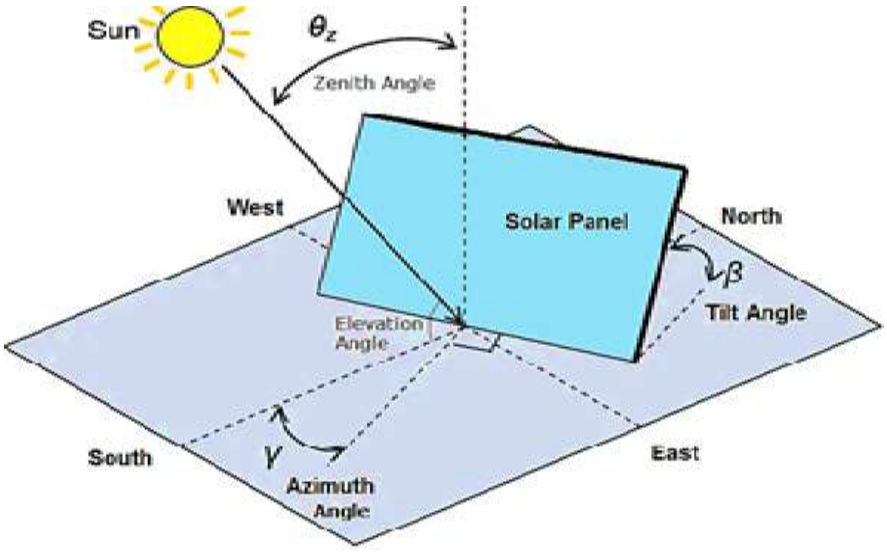

Plate 3.1 (b): diagram showing sun azimuth angle, surface tilt of the PV and surface azimuth angle. Source: Muriele et al., 2019

For arrays that are perpendicular to the south pole, $\theta_z = 180^0$. For a surface at any tilt of β, the components of the POAI assuming an isotropic diffuse sky is given as (Stein, 2018);

$$Irr_{Beam} = DNI\ cos(\theta_{AOI}) \tag{3.33}$$

$$Irr_{Diffused} = DHI\left(\frac{1 + cos(\theta_\beta)}{2}\right) = 0.5DHI\left[1 + cos(\theta_\beta)\right] \tag{3.34}$$

$$Irr_{Ground} = GHI \times \alpha \times \left(\frac{1 - cos(\theta_\beta)}{2}\right) = 0.5\alpha GHI\left[1 - cos(\theta_\beta)\right] \tag{3.35}$$

The ground-reflected irradiance component Irr_{Ground} considers the albedo (α) of the ground. The assumptions for equation 3.35 are that the array is infinitely long, and that GHI on the ground is uniform and evenly reflected in all the directions. Plates 3.1 (c) and (3.2) are the diffuse and ground components for flat and tilted module respectively (Silvana, 2019). Plate 3.1(c) is a flat module with an unobstructed view of the whole sky-hemisphere, so they are able to capture all diffuse radiation. No ground-reflected component makes its way to the front surface of the module in this position. Plate 3.2 is tilt module which receive only a fraction of diffused radiation, but they also receive ground-reflected irradiance (Source: Honsberg & Bowden, 2014) (Silvana, 2019).

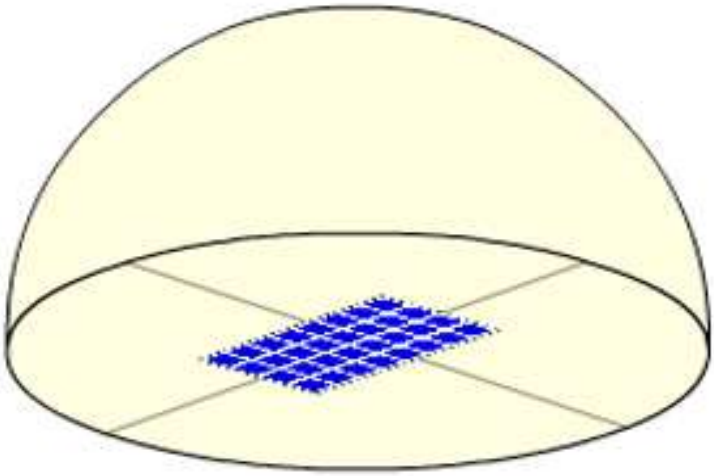

Plate 3.1 (c): Flat modules with an unobstructed view of the whole sky-hemisphere. Sources: Honsberg & Bowden, 2014.

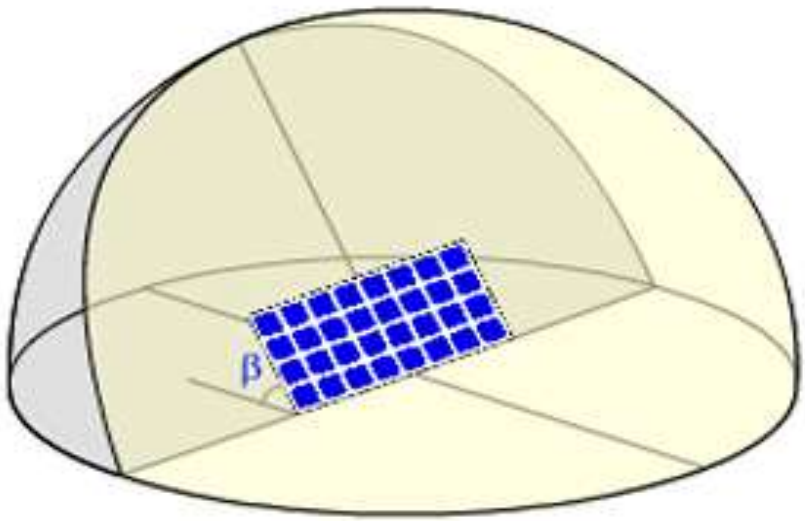

Plate 3.2: Tilted module Source: Honsberg & Bowden, 2014.

To evaluate the performance of a BFPV module, $IPOA$ must be known or calculated from one or various measurements at the plane of the array, or from horizontal irradiance measurements as shown in plate 3.3. With two detectors at the POA, one measuring diffuse by blocking the solar path (removing direct illumination), and another one measuring global irradiance on the detector, DNI can be calculated.

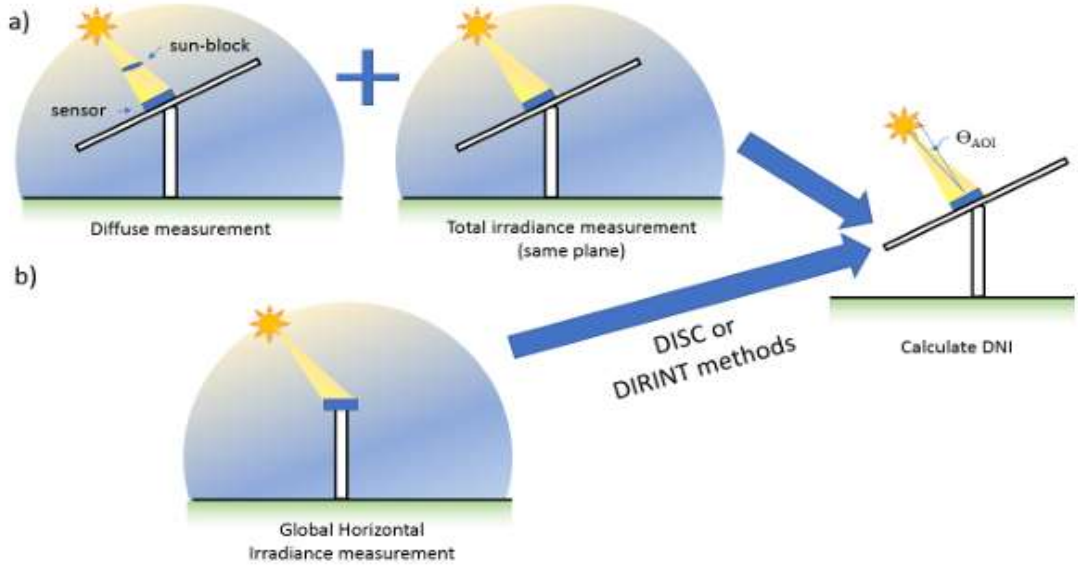

Plate 3.3: Two methods for measuring and calculating DNI for modelling of irradiance on the plane of the array (a) require diffuse and global irradiance co-planar measurements. (b) To calculate DNI from GHI. Source: Silvana, 2019.

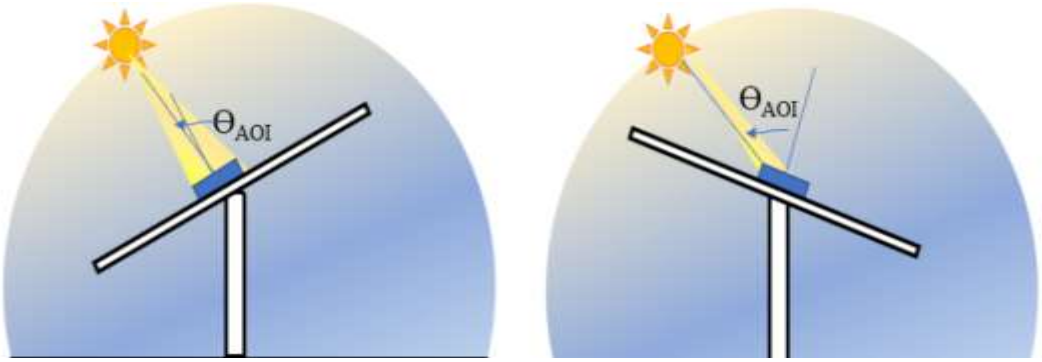

Plate 3.4: plane array of irradiance (Source: PV-tutorials, 2022).

From plate 3.4, each irradiance component is considered separately when modelling POA irradiance. For example, calculating the component of direct irradiance (DNI) that is incident on a panel is solved with straightforward geometry based on the angle of incidence. Finding the POA component of diffuse irradiance (DHI) is more complex and can vary based on atmospheric conditions. Many models, ranging from simple models with lots of assumptions to strongly empirical models, have been published to transpose DHI into the diffuse POA component. A third component of POA irradiance is light that reflects off the ground before being collected by the PV panel.

The most straightforward measurement to perform is Global Horizontal Irradiance since it only requires a detector with a wide field of view, such as a pyranometer, placed horizontally with an unobstructed view. Pyranometers have a true-cosine response to incident angle due to a diffuser over the detector. Reference cells are also used, but they do not exhibit the true cosine response. If only GHI is known, DNI and DHI can be approximated through the DISC or its improved version DIRINT models Honsberg & Bowden, 2014. However, these two methods do not have high accuracy, and for this dissertation, DNI and DHI measurements were obtained from NASA.

3.2.1.6 Diffuse sky modelling

Simplified models consider the sky as an isotropic source with a 180° divergence angle when calculating the POA contribution of diffuse sunlight. However, diffuse radiation is not uniform over the sky, particularly in the regions near the solar disk and near the horizon, which are brighter. More complex models divide diffuse radiation into an isotropic component, a circumsolar diffuse component, and a horizon brightening component, and they estimate the POA diffuse irradiance with a combination of these components obtained through semi-empirical approaches. For

example, to account for these components the Sandia Model (Lave et al., 2015) adds an empirical correction term to equation 3.34 as;

$$Irr_{Diffused} = DHI\left(\frac{1+cos(\beta)}{2}\right) + GHI\left[\frac{(0.012\theta_z - 0.04)(1-cos\,\beta)}{2}\right] \quad (3.36)$$

The Hay and Davies model of equation 3.37 (Hay & Mckay, 1985), as well as the Reindl model of equation 3.38 (Reindl et al., 1990) uses an anisotropic index Ai in their model to calculate the diffuse sky. Ai is the ratio of DNI to the extra-terrestrial radiation. Reindel's model extends Hay and Davies by adding an additional factor for the horizon brightening as;

$$Irr_{Diffused} = DHI\left[A_i\left(\frac{cos(\theta_{AOI})}{cos\,\theta_z}\right) + (1-A_i)\frac{(1+cos\,\beta)}{2}\right] \quad (3.37)$$

$$Irr_{Diffused} = DHI\left[A_i\left(\frac{cos\,(\theta_{AOI})}{cos\,\theta_z}\right) + \left\{(1-A_i)\frac{(1+cos\,\beta)}{2}\left(1+\sqrt{\frac{DNI+cos\,\theta_z}{GHI}}\right)sin^3\left(\frac{\beta}{2}\right)\right\}\right] \quad (3.38)$$

3.2.1.7 Perez Diffuse Sky Model

Perez Sky diffuse model is a more complex model to calculate the diffuse contribution to the POA. It relies on six empirical coefficients f11 through f23 as shown in Table 3.2 to determine eight specific bins of clearness ε, which is calculated from DNI, DHI, and sun position.

$$\varepsilon = \frac{\left[(DHI+DNI)/5.535\times10^{-6}{\theta_Z}^3\right]}{1+5.535\times10^{-6}{\theta_Z}^3} \quad (3.39)$$

While the sky diffuse model presented up to this point separated the isotropic, circumsolar, and horizon components explicitly, Perez developed a more complex model that relies on a set of empirical coefficients for each term.

The basic form of the model is:

$$E_D = DHI\left[(1-F_1)\left(\frac{1+cos(\beta)}{2}\right)\right] + F_1\left(\frac{a}{b}\right) + F_2\,sin(\theta_T) \quad (3.40)$$

F_1 and F_2 are complex empirically fitted functions that describe circumsolar and horizon brightness respectively.

$$a = max(0, cos\,(AOI)), and\ b = max(cos\,(85^0), cos\,(\theta_Z)).$$

DHI is diffuse horizontal irradiance, AOI is the angle of incidence between the sun and the plane of the array, θ_Z is the solar zenith angle., and θ_T is the array tilt angle from horizontal.

$$F_1 = max\left[0, \left(f_{11} + f_{12}\Delta + \frac{\pi\theta_z}{180^0} f_{13}\right)\right] \quad (3.41)$$

$$F_2 = f_{21} + f_{22}\Delta + \frac{\pi\theta_z}{180^0} f_{23} \quad (3.42)$$

Equation 3.39 can be rewritten as;

$$\varepsilon = \frac{\left[(DHI + DNI)/q{\theta_Z}^3\right]}{1 + q{\theta_Z}^3} \quad (3.43)$$

DNI is direct normal irradiance and q is a constant equal to 1.041 for angles in radians, or 5.535×10^{-6} for angles in degrees.

$$\Delta = \frac{DHI \times AM_a}{E_a} \quad (3.44)$$

where AM_a is the absolute air mass, and E_a is extra-terrestrial radiation.

Table 3.2: Perez model coefficients for irradiance

bin	f11	f12	f13	f21	f22	f23
1	-0.008	0.588	-0.062	-0.06	0.072	-0.022
2	0.13	0.683	-0.151	-0.019	0.066	-0.029
3	0.33	0.487	-0.221	0.055	-0.064	-0.026
4	0.568	0.187	-0.295	0.109	-0.152	-0.014
5	0.873	-0.392	-0.362	0.226	-0.462	0.001
6	1.132	-1.237	-0.412	0.288	-0.823	0.056
7	1.06	-1.6	-0.359	0.264	-1.127	0.131
8	0.678	-0.327	-0.25	0.156	-1.377	0.251

(Source: Perez, et al, 1990)

Table 3.3: Sky clearness bins.

Bin	Lower Bound	Upper Bound
1 Overcast	1	1.065
2	1.065	1.230
3	1.230	1.500
4	1.500	1.950
5	1.950	2.800
6	2.800	4.500
7	4.500	6.200
8 Clear	6.200	—

(Source: Perez, et al, 1990)

Perez has published a number of different versions of the f coefficients fitted to various data sets (Perez, et'al 1988). Table 3.3 shows the f coefficient values published in (Perez, et al, 1990) for irradiance. The bin refers to bins of clearness, ε, defined in Table 3.3

3.2.1.8 Module elevation

It is important to secure enough space between the module and the ground for more sunlight reflectance, resulting in a greater bifacial gain. Thus, the height of the module is also one of the main factors that have a significant impact on bifacial gain. Plate 3.5 represents a BFPV panel on module elevation.

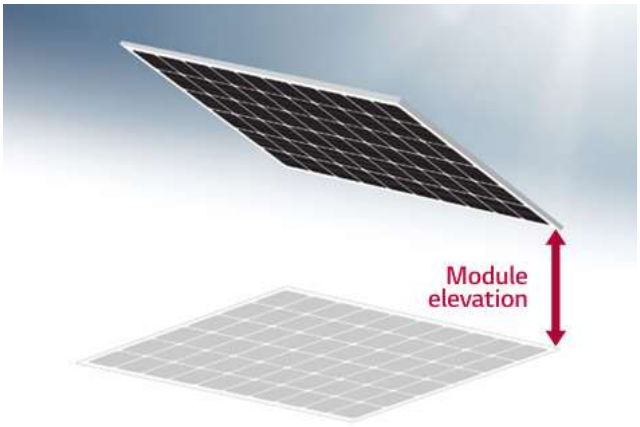

Plate 3.5: Bifacial module on elevation. Source: LG Electronics, 2017.

The module elevation is defined as the distance between the bottom of the lowest part of the module and the ground surface as shown in plate 3.5.

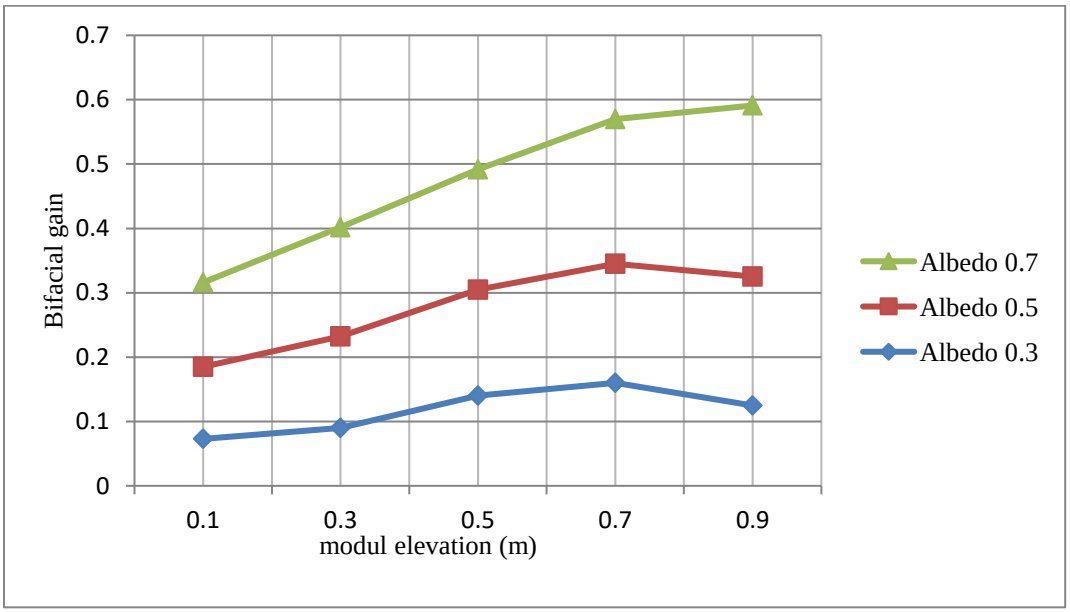

Figure 3.8: effect of module elevation on the bifacial gain of PV module. Source: LG Electronics, NASA, 2017.

The module elevation is one of the factors that affect the amount of irradiation reaching the rear-side of a BFPV module. Figure 3.8 shows the variation of module elevation with bifacial gain at different surface albedo. It is evident from the figure that the higher the soil albedo, the higher the bifacial gain. It is paramount to note here that beyond module elevation of 1m, the bifacial gain would begin to drop due to that fact that most of the reflected sunrays from the ground would diffuse into the atmosphere. This is a practical situation that should be considered when installing a BFPV module.

Not only does it affect the irradiance on the backside, the module height also affects the reflected light uniformity. If the module height is low, the amount of irradiance on the backside is different on certain parts of the module due to its own shadow. The cells near the top edge of module absorb more light than the cells on the rest of the module.

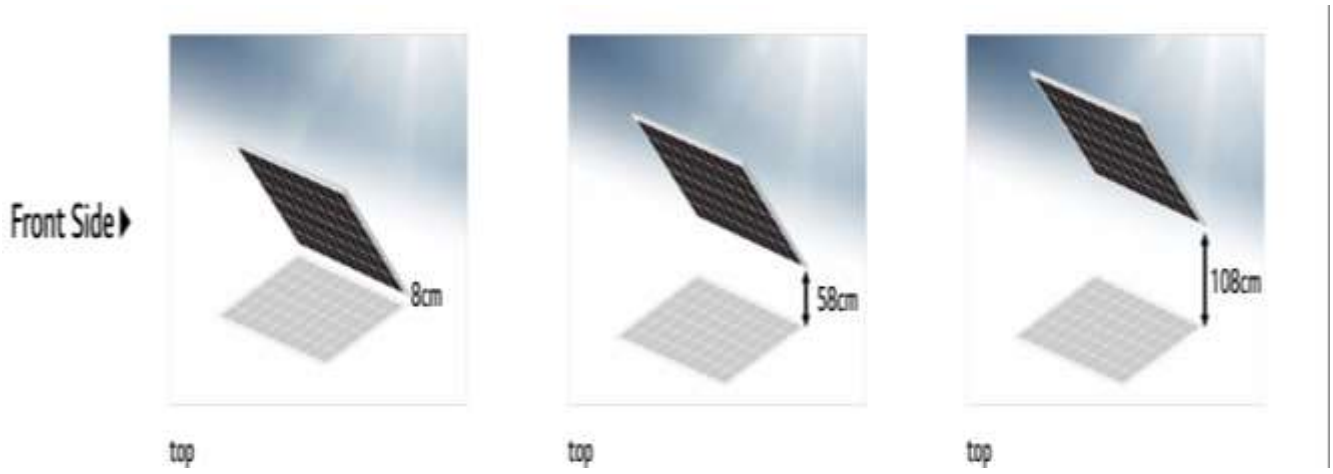

(a) (b) (c)

Plate 3.7: module elevations (a) elevation 8cm (b) elevation 58cm (c) elevation 108cm. Source: LG Electronics, 2017.

When the module elevation is at 0.5m, the range of irradiance exposed to the backside of the module is rather larger (plates 3.7 (a-c) and 3.8 (a-c)) the highest measurement is 5 times higher than the lowest value recorded. As module elevation increases, the irradiance values are more uniform throughout the module. This is important because irradiance uniformity results in mismatch loss from the module and array, which ultimately leads to energy loss.

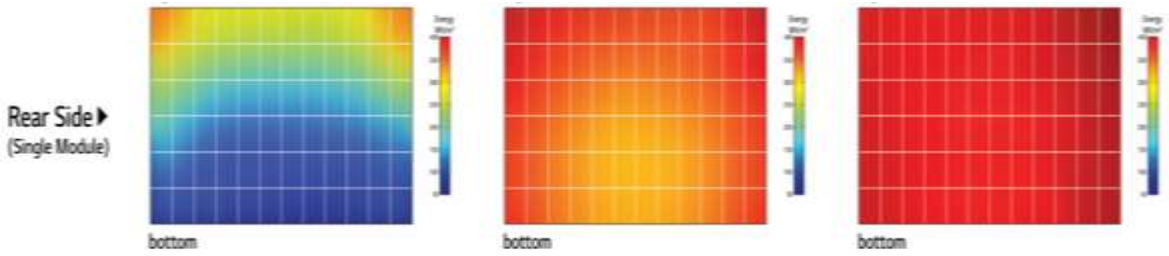

(a) (b) (c)

Plate 3.8: irradiance distribution of backside in single module, (a) 66-328W/m^2 (5 times difference) (b) 360-3390W/m^2 (within 10% difference) (c): 400W/m^2 (uniform distribution). Source: LG Electronics, 2017.

There is also an irradiance uniformity difference by module location due to elevation in an array regardless of the array being fixed tilt or single axis tracker.

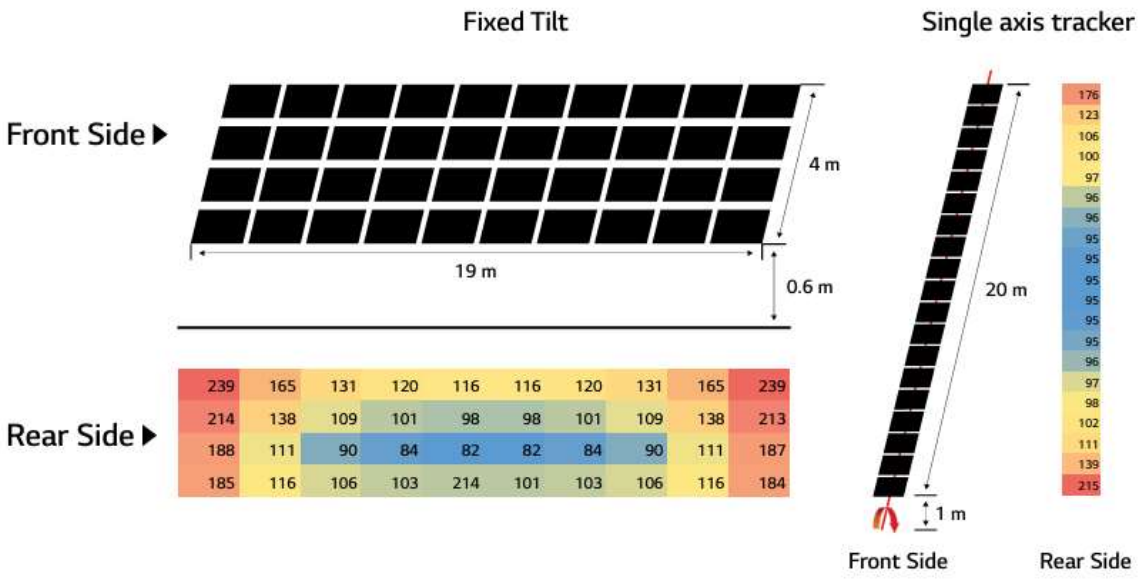

Figure 3.9: module elevation for single axis tracking. Source: Fakhfouri, 2015

The bifacial gain of the array or system is determined by the module performance with the lowest irradiation. It is very helpful to understand irradiance distribution on backside of array to plan cable routes in series and reduce mismatch loss.

3.2.1.9 Bifaciality factor

Monofacial cells and modules are characterized under standard test conditions (STC) of 1000 W/m^2 and 25°C, with an incident spectrum corresponding to Air Mass 1.5 Standard spectrum (Gueymard, 1995). Under these same standard conditions, the power produced by the front- versus the rear-side of a bifacial PV module will differ due to semiconductor properties, the amount of back contact metallization, and shading from the module's junction box. This is quantified with a bifaciality factor φP_{mp} (Fakhfouri, 2015). After characterizing the rear-side and front-side with a non-irradiated background for the module, the only light contribution is from the side being tested by placing a black-absorbing surface behind the module, the bifaciality factor can be established as:

$$\varphi_{I_{sc}} = \frac{I_{I_{sc-rear}}}{I_{I_{sc-front}}} \tag{3.45}$$

$$\varphi_{V_{oc}} = \frac{V_{oc-rear}}{V_{oc-front}} \tag{3.46}$$

$$\varphi_{P_{mp}} = \frac{P_{pmp-rear}}{P_{pmp-fornt}} \quad (3.47)$$

V_{oc} for the rear and the front show little difference for bifacial modules, as they depend more directly on module temperature than irradiance levels. Isc between the front and the rear of the module is the value that varies the most and gives the lower bifaciality factor. However, when the rear-side of the module is shaded by junction-boxes or has a poor design, the bifaciality factor determined from maximum-power point will be the one displaying the lowest value (Fakhfouri, 2016). Thus, the IEC TS 60904-1-2 standard determines that the overall bifaciality factor to be used will be the lower bifaciality factor between the short-circuit current and maximum-power:

$$\varphi = Min(\varphi_{SC}, \varphi_{pmp}) \quad (3.48)$$

Bifaciality factors can reach as high as 0.99 (Schulte-Huxel, et al, 2016). In commercial modules, it ranges from 0.6-0.9 in their bifaciality factor (Bub, et al, 2018). However, these values were established from before the standard was released, so their accuracy must be revised before further modelling or comparison with newer research since they might refer to the bifaciality factor derived from I_{sc} or P_{mp}, and not necessarily the lower value of the two.

3.2.1.10 Bifacial gain.

The additional power produced by bifacial cells/modules over monofacial cells/modules is known as bifacial gain BG and is used as a metric to evaluate bifacial PV module performance (Ayala, et al, 2018). The bifacial gain is an electrical parameter, but for a simple calculation of the output of a module, it can be considered as an optical parameter as well, considering the front and rear-side irradiance values on the module G_{front} and G_{rear}:

$$Bifaciality\ Gain\ [B_G(\%)] = \varphi\left(\frac{G_{rear}}{G_{front}}\right)(1 - \mu_{loss}) \quad (3.49)$$

The term μ_{loss} represents power losses caused by non-uniform rear-side irradiance and/or rear shading. For simplified calculations, φ = 100% and μ_{loss}, which accounts for additional bifacial loss terms such as shading loss and irradiance mismatch, is assumed to be zero. Also, BG can be calculated with modelled values $G_{rear,\ modelled}$ and $G_{front,\ modelled}$, or with measured values $G_{rear,measured}$ and $G_{front,measured}$, and both will be distinguished as in which case it will be labelled $BG_{modeled}$ or $BG_{measured}$ in this research.

3.2.1.11 Mismatch effects

Just as with front irradiance, non-uniform rear-side irradiance and rear shading can affect power and energy production. Reference cells matched for spectrum and incidence angle are used on experimental setups and on-field systems to measure the front-side and rear-side irradiance values (Meydbray, et al, 2012). To evaluate uniformity, more than one sensor is needed for each side, and is calculated with the maximum and minimum rear-side irradiance values:

$$non - uniformity = \frac{maxG_{rear} - miniG_{rear}}{\frac{1}{2}(maxG_{rear} + miniG_{rear})} \quad (3.50)$$

Modelling has shown that there is a minimal effect on performance due to non-uniformity of rear-side irradiance (Bailey & Jaubert, 2018) and this effect might be significant for certain low-light conditions and deployments of bifacial PV. However, by definition, rear non-uniformity is not more impactful on performance than front non-uniformity, but due to reduced irradiance values in the rear, the non-uniformity effect is diminishing because the front irradiance still dominates heavily. For most performance modelling in this dissertation, G_{rear} represents averaged rear irradiance over the collector width.

3.2.1.12 Albedo

Practically, albedo is determined by positioning two pyranometers 180◦ apart. The maximum uncertainty for the albedo measurement value in a day is fixed at 2% (Kipp & Zonen, 2016). The accuracy of albedo measurements is mainly influenced by the measurement setup and the reflecting properties of the surroundings. The radiation events in the region where the shadows of the bars are captured are assumed to be atmospheric hemispherical diffused radiation. Reflected radiation from shaded and unshaded areas is combined and constitutes celestial radiation. In this thesis, we adapted satellite measured albedo from each geographical site and calculated albedo using a glass rectangular prism as shown in figure 3.10 using the equation 3.51.

$$\text{Albedo} = \frac{\text{reflected ray}}{\text{incident ray}} \quad (3.51)$$

Here, the specular reflection represents the GHI and diffused reflection represents the DHI. Figure 3.11 shows the practical set-up for measuring ground albedo using pyranometer.

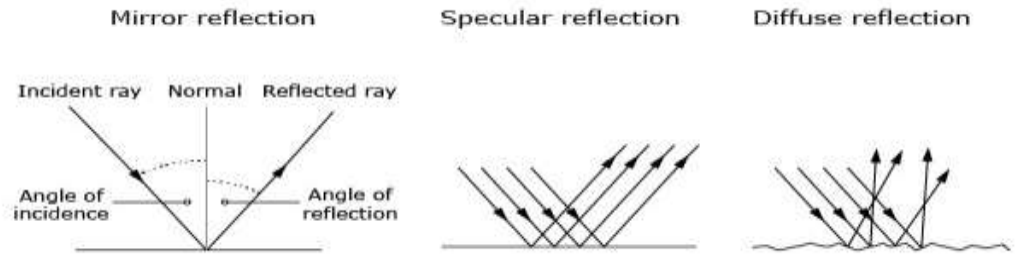

(a) (b) (c)

Figure 3.10: (a) mirror reflection (b) normal reflection (c) diffused reflection. Source: Kipp & Zonen, 2016

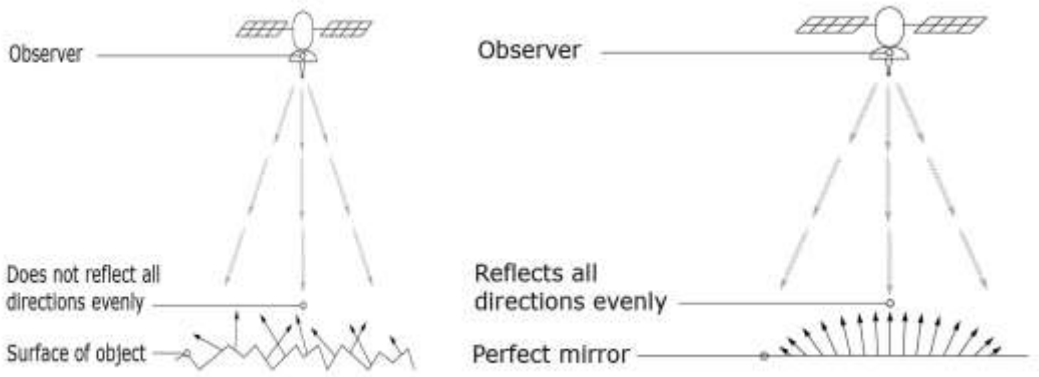

(a) (b)

Figure 3.11: (a) pyranometer measuring incident ray (b) pyranometer measuring reflected ray. Source: Kipp & Zonen, 2016

The upward facing pyranometer measures the global solar radiation, while the downward facing pyranometer measures the reflected solar radiation. The ratio of the reflected radiation to the global radiation is the regions albedo. The height of instalment of the albedometer is very important because of errors due to self-shading. The measurement accuracy of an albedometer can be affected because the device casts a shadow onto the ground it is measuring, resulting in a slightly lower albedo value of the measured ground. Albedo is a measure of soil's reflectivity. It is the ratio of the solar radiation reflected by a surface to the total incoming solar radiation. Albedo can either be expressed as a ratio or as a percentage. The higher the value, the more energy is reflected back

to the source. Complete reflection is 1 or 100%, and complete absorption is 0. Surfaces that have a low albedo such as rocks or water are dark colour and will absorb more incoming solar radiation. High albedo surfaces are light, such as snow, ice, or sand, and reflect most of the incoming solar radiation back into the atmosphere. Incoming solar radiation is measured in Watt/m^2, and the instrument that is used for the measurement is called a pyranometer. Since pyranometers are very expensive, the following experiment will be done with lightmeters. Lightmeters provide a measure of the light intensity (measured in the unit, lux), a good approximation of solar radiation.

Once the shadow/unshadow ratio and the net albedo are calculated, the next step is to perform the calculation of equation 3.51. To carry out the result, it is necessary to know the global horizontal irradiance GHI and the value of its main components: the Direct Normal Irradiance, DNI and the Diffuse Horizontal Irradiance DHI. The relationship between these components is,

$$\mathrm{GHI} = \mathrm{DHI} + \mathrm{DNI}\cos(\mathrm{Z}) \tag{3.52}$$

where Z is the solar zenith angle.

This computation is more accurately managed using well known astronomical equations and a clear sky model, like the one used in PVsyst and PVsol software. Therefore, starting from a Typical Meteorological Year (TMY) irradiance data file or even from averaged monthly data, it is possible to build a yearly profile of irradiance for both sides of the module. If there is no availability of hourly irradiance data, it is still possible to create an irradiance profile using solar distribution models. The Global Rear Irradiance (GRI) is the radiant flux received by the backside of the bifacial PV module, and Global Front Irradiance (GFI) is the radiant flux received by the front face. The sum of these two components, defined as GBI, (Global Bifacial Irradiance, represents the total amount of solar energy received by the bifacial PV module. Since any bifacial module does not convert the energy with the same efficiency on both its faces, we multiply the GRI for the BFF (φ) term, (Bifaciality Factor) i.e. the ratio of the power output at standard test condition (STC) from the rear side upon the power output at STC from the front side. The global bifacial irradiance can now be written as:

$$\mathrm{GBI} = \mathrm{GFI} + \varphi\mathrm{GRI} \tag{3.53}$$

The complete method of calculation, bifacial layout view factors and irradiance are taken care of in the PVsyst 7.8.4 version software used in this research. This computed composite irradiance is used to determine the energy produced by a bifacial module given its STC electrical characteristics.

The software produces an output in standard CSV format that can be imported by other design tools and used as irradiance descriptor file. When measuring the albedo of PV modules, any performance model used must be clearly stated. Some performance models require the albedo as ground surface property while other models use the reflected irradiance as input for the albedo. Common albedo for different surfaces is shown in figure 3.12.

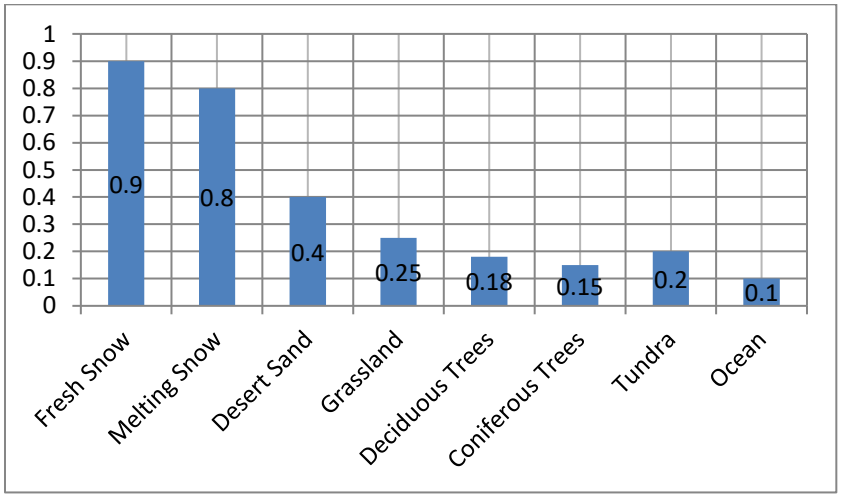

Figure 3.12: the effect of ground albedo on bifacial gain

$$a = \frac{E_{reflected\ Solar\ radiation}}{E_{incident\ Solar\ radiation}} \tag{3.54}$$

3.2.1.13 Pitch:

This is the distance apart from lower part of module elevation of a panel to the lower part of module elevation of the next panel at different row or column of a BFPV module as shown in figure 3.13. Pitch is directly correlated with the Ground Coverage Ratio (GCR). The GCR is the ratio of the area covered by PV modules to total ground area considered for the installation.

$$\text{GCR} = \frac{\text{modul area}}{\text{Total ground Area}} \tag{3.55}$$

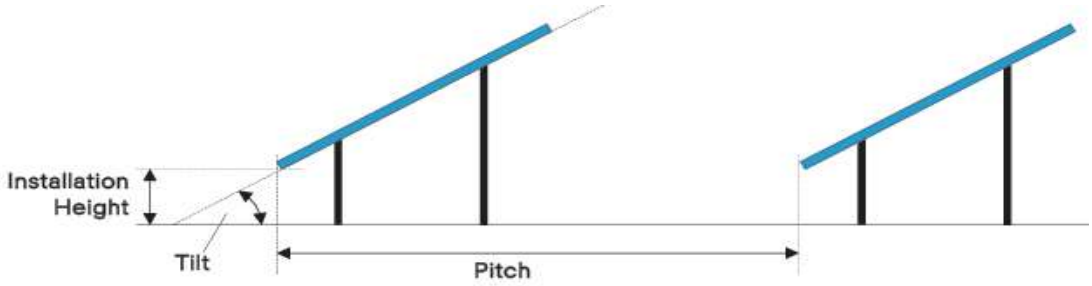

Figure 3.13: Fixed tilt systems: Row-to-row distance (pitch), module tilt and installation height. As the value of GCR increases, both the Pitch value as well as the installation area decreases. Pitch is another important factor that affects the bifacial gain. A high Pitch value which produces a low GCR provides a greater possibility of more energy production. As a result, the Pitch should be considered while designing the system.

3.2.1.14 Shading

The mounting structure, especially the mounting rail, blocks reflected sunlight that comes to the backside of module contribute to the blocking of sunray that reflect at the rear-side of the BFPV solar module. The shading produced by the mounting structure decrease the bifacial gain. The loss of the backside gain depends on various factors associated with the module and the mounting structure. These include; rail thickness and width, number of rails below module, rail design.

One of the most significant and testing tasks for MPPT Controller is track MPP under Partial shading condition (PSC). PSC's is a phenomenon that happens in a PV array because of uneven exposure of light to the solar panels. These situations may arise because of the entry of clouds, bird droppings, trees and building shadows (Ratnakar et al., 2020). The size of the array depends mostly on the power required by the application. Under uniform irradiance, same insolation strikes the panel results in the same output current from all panels. During PSC's, shading of at least one array results in the generation of less current, which directly accounts for the power loss. The dependence of this operating point on environmental parameters like angle of solar insolation, temperature, and shading makes the process a bit complex. As these parameters vary continuously, MPP also varies (Verma et al., 2016). Whenever, the configuration made of numerous solar cells combined in series to form a module, variable insolation on one cell leads to rupture the lamination if not attended properly. So, as to decrease the effect from this operational condition, bypass diodes are connected in anti-parallel to the cells. As an outcome,

significant voltage differences will not emerge in the reverse-current direction of solar cells. At least one anti-parallel diode is sufficient for 15–20 cells in the configuration. These diodes are helpful in the flow of current through the PV module, especially during the shaded condition and at deficient levels of voltage and power. Hence, the particular shaded panels are bypassed using anti-parallel diodes which also mitigate hot-spot (increase of heat in particular area) effects on the panel. In the same manner, blocking diode is used to block the penetration of surges into the system. Simulation results give multiple peaks, i.e. Various MPPs due to the presence of shading as shown in figure 3.14.

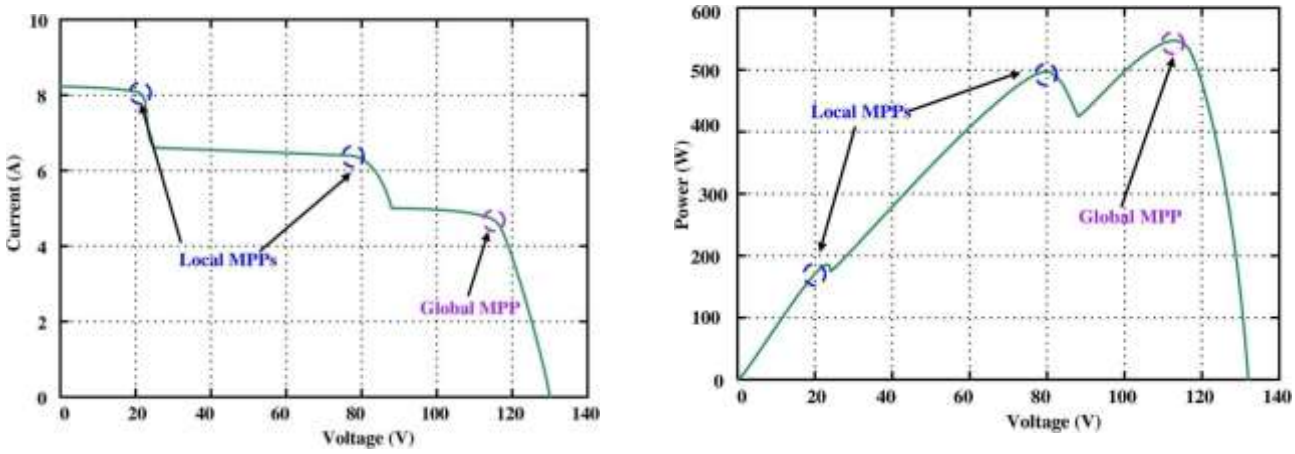

(a) (b)

Figure 3.14: (a) Characteristic I–V curve of the PV configuration (b) Characteristic P–V curve of the PV configuration. Source: Ratnakar et al, 2020.

Out of these MPP's, one is Global MPPG (MPP) and remaining is Local MPP (LMPP) for the whole array (Pendem et al, 2020) and their presence in resultant I–V and P–V curves for the shaded panel are shown in figures 3.14 (a) & (b) respectively. For numerical analysis of the MPP, Batzelis et'al (2015) shows the MPP in unshaded and shaded conditions precisely considering all the parameters. During MPP, the derivative of output power P w.r.t output voltage V equals zero. Therefore, the MPP is tracked according to the load line with the use of appropriate MPPT technique.

3.2.2 Determination of the load profile of a micro-base station.

The TBS, a centrally located set of equipment used to communicate with mobile units and the backhaul network, consists of multiple transceivers (TRXs), which in turn consist of a power

amplifier (PA) that amplifies the input power, a radio-frequency (RF) small-signal transceiver section, a baseband (BB) for system processing and coding, a DC-DC power supply, a cooling system and an alternating current (AC)-DC unit for connection to the electrical power grid. Table 3.4 summarises the power consumption of the different pieces of macro-BS equipment for a 2 × 2 MIMO configuration, and three sectors where the total input power (Pin) needed by the –macro-BS is 6695W.

Table 3.4: Load demand and power rating per hours used in (4G) site

S/N	Unit	Qty.	Power consumption per unit (W)	Total power Consumption (W)	Hours of operation	Daily Energy Consumption (kWh/day)
1	Transceiver (4G) (DC)	6	120	720	24	17.28
2	Base band unit (DC)	1	180	180	24	4.32
3	Air conditioner (AC)	2	1200	2400	24	57.6
4	Indoor light (AC)	4	15	60	12	0.72
5	Security light (AC)	4	25	100	12	1.2
6	Rectifier (AC)	1	2400	2400	24	57.6
7	Microwave antenna (DC)	5	5	25	24	0.6
8	GSM Antenna (DC)	3	20	60	24	1.44
9	Multiplexer (DC)	1	240	240	24	5.76
10	Intermediate frequency links (DC)	9	20	180	24	4.32
11	Router (DC)	1	330	330	24	7.92
	Total			6695	240	158.76

Before estimating the size of the panel, the first step is to determine the total power and energy consumption of all loads that need to be supplied by the solar photovoltaic system at the base station. Therefore, the total energy requirement of the system is determined by multiplying the power consumption of each component that must be supplied by its working hours in order to obtain the energy requirement of the equipment, and then add all the energies of all equipment, and as shown in Table 3.4.

3.2.2.1 Determination of number of Solar Panels Required.

Table 3.5 shows the information on the nameplate of the chosen PV module. To calculate the number of solar panel for the base station, we should determine the average daily energy consumption in kilowatt-hours (kWh). In this research, the average daily energy consumption is 158.76kWh/day and the system performance ratio is 85%. 6 hours of sunlight per day is taken in geopolitical zones within the south and 8 hours in geopolitical zones within the North since it is not the same throughout the country. Hence an average of 7hrs is assumed in this research.

Table 3.5 information on the nameplate of the chosen PV module

Solar Module type: LG 450 bifacial 2W	Parameter
Module Size (kW)	0.45
Lifetime	25 yr
Derating factor	90%
Tracking system	East - West
Slope	30^0
Azimuth	0^0
Albedo	0.2

Therefore;

$$\text{Daily energy production requirement} = \frac{158.76\text{kWh}}{0.85} = 186.78\text{kWh}$$

$$\text{Solar panel capacity} = \frac{186.78\text{kWh}}{7\text{ hours}} = 26.68\text{kW}$$

With a derating factor of 85%, the actual solar panel capacity required will be;

$$\text{Actual panel capacity} = \frac{26.68\text{kW}}{0.85} = 31.39\text{kW}$$

In this research, the capacity of the solar panel is 450W. Therefore, the number of panels will be;

$$\text{number of panel} = \frac{\text{Actual panel capacity}}{\text{solar panel rating}} = \frac{31.39\text{kW}}{0.45\text{kW}} = 69.76\text{ panels} \sim 70\text{ panels}$$

The obtained number of panels is MFPV which will occupy large area of land. With the adoption of the standalone BFPV module, the number of panel becomes;

$$\therefore \text{Total number of bifacial panels needed} = \frac{70}{2} = 35 \text{ panels}$$

Therefore, the standalone system will require 35 BFPV modules of 5 rows and 7 columns.

3.2.2.2 Determination of size of inverter.

3.2.2.2.1 Daily energy supplied to inverter

In this research, the daily energy consumption by the load is 6695Wh. Note that the inverter has its efficiency, thus the energy supplied to the inverter should be more than the energy used by the load, so that the losses in the inverter can be compensated. In this work, we will use 90% efficiency was assumed. Therefore, the total energy supplied by the battery to the inverter would be given as;

$$\text{Energy supplied by the battery to the inverter input} = \frac{6695}{0.90} = 7438.9\text{Wh}$$

3.2.2.2.2 System voltage

The inverter input voltage is referred to as the system voltage. It is also the overall battery pack voltage. This system voltage is decided by the selected individual battery voltage, line current, maximum allowable voltage drop, and power loss in the cable. System voltage to be used here is 48V. By decreasing the current, power loss and voltage drop in the cable can be reduced; this can be done by increasing the system voltage. This will increase the number of batteries in the series. Therefore, one must choose between power loss and system voltage. Therefore,

$$\text{Total Load in kVA} = \frac{\text{load in kW}}{\text{pf}} = \frac{6.696}{0.8} = 8.37\text{kVA} \sim 10\text{kVA}$$

$$\text{Inverter rating in kW} = \frac{\text{load in kW} \times \text{loss factor}}{\text{efficiency}} = \frac{6695 \times 1.3}{0.9} = 9.670\text{kW} \sim 10\text{kW}$$

Thus the inverter rating required for the design is 15kW

3.2.2.3 Determination of battery size:

This step is also very important for reliability of the system because at night or cloud day, sufficient energy is required to operate the appliances. Battery sizing means calculating the number of batteries needed for a renewable energy system. This particularly depends on the Days of Autonomy required (DOA). DOA is the number of days a battery system will supply a load to the system without being recharged by a PV array. For non-critical load, DOA is between 2 to 3 days while for critical loads, 5 days of autonomy are recommended as used in this research. A critical

load is a load that must be used all the time. It is also important to note that when selecting battery size, battery's capacity decreases at lower temperatures and increase at higher temperature, and battery's life increases at lower temperature and decreases at higher temperature. For maximum performance, it is important to keep the battery's storage system at 25ºC. Therefore the size of the battery is calculated thus;

Consider our batteries of 48 V, 550 Ah with DOD of 50%. Therefore, the usable capacity of the battery is 550 Ah × 0.5 = 275 Ah. Hence, the charged capacity that is required is determined as follows;

$$\text{charge capacity } = \frac{\text{energy supplied by the battery to the inverter input}}{\text{system voltage}} = \frac{7438.9}{48} = 155\text{Ah}$$

From this, the number of batteries required can be calculated as;

$$\text{Battery capacity in Ah} = \frac{\text{energy in Wh} \times \text{days of aut} \times \text{hr of oprt}}{\text{DOD in \%} \times \text{DC Voltage}} \tag{3.56}$$

$$\text{Battery capacity in Ah} = \frac{7438.9\text{ Wh} \times 5 \times 14}{0.5 \times 48} = 21{,}696.8\text{Ah} \sim 21{,}697\text{Ah}$$

This is the minimum battery bank capacity size need at the base station to run a 6695Wh load daily for 14hours.

$$\therefore \text{No of Batteries required } = \frac{21697\text{Ah}}{550\text{Ah}} \sim 40 \text{ batteries}$$

Practically, there are variations in weather conditions within the country which affects the solar panel. During the dry season, dust particles coat the surface of the panels thereby increasing the batteries DOA. During the rainy and cloudy days, the solar panels do not get enough sunrays; this also increases the days of autonomy of the battery. To cushion this effect since the base station requires 24-hrs uninterrupted energy supply, we have to multiply the normal battery numbers by 50% of the calculated battery size and add it up to get the actual number of batteries required. Therefore, actual number of batteries required is obtained thus;

$$\text{Actual number of batteries for the system} = (0.5 \times 40) + 40 = 60 \text{ batteries}$$

Therefore, 60 batteries is required for the base stations in each of the geopolitical zones and the charging current for 550Ah batteries is 10% of Ah rating which is (0.1×550) = 55A;
But due to some losses, we take 60A for batteries charging purpose instead of 55A.
Hence require battery capacity is;

$$60 \times 24 \times 550 = 792{,}000\text{W} = 792\text{kW}$$

3.2.2.4 Determination of size of charge controllers.

Figure 3.15 uses only the energy generated by the MFPV panels to supply the load while BFPV supplies the energy at the same mode as shown in figure 3.16. Sometimes the energy available from this might be in excess of what is needed by the load and therefore the amount of energy supplied to the load must be matched to the load demand. This is called sliding control. There is however a possibility, a time that the amount of power required by the load is not able to be supplied by mode 1, then the program determines what element (batteries or diesel generator) have priority to supply energy.

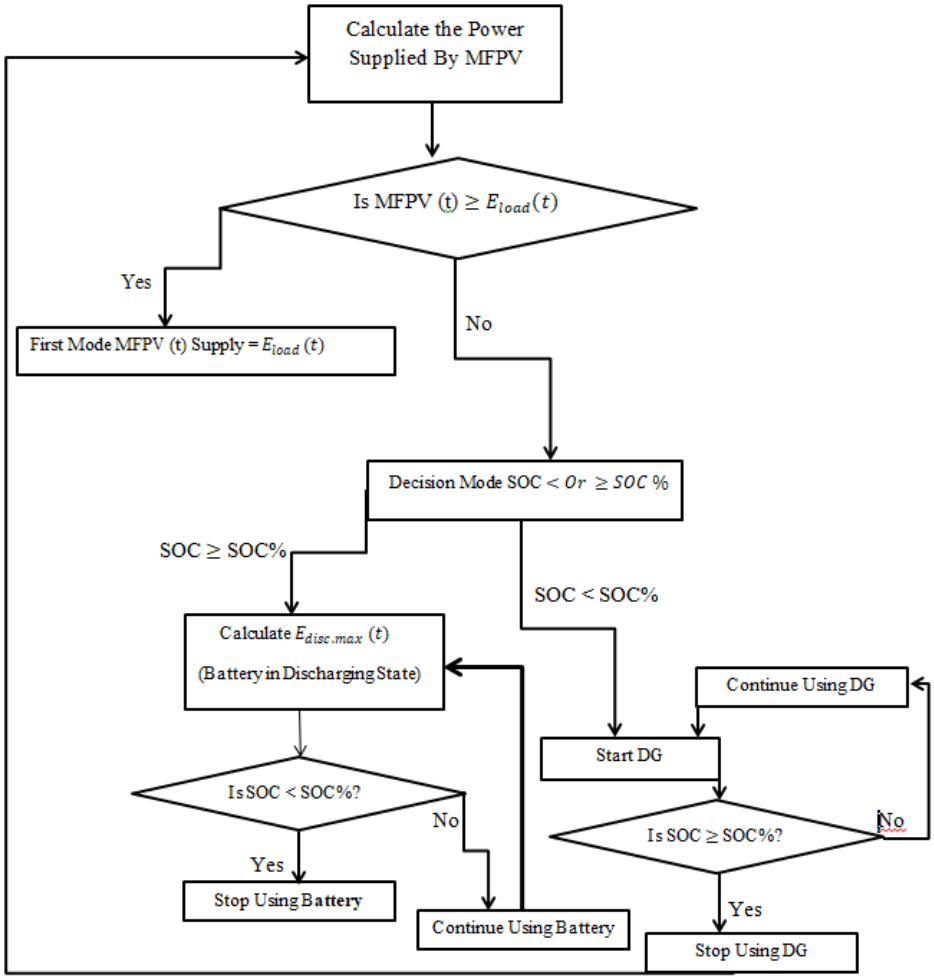

Figure 3.15: Flowchart of Decision Strategy of MFPV Controller and Mode 1 of Control for the System Operation.

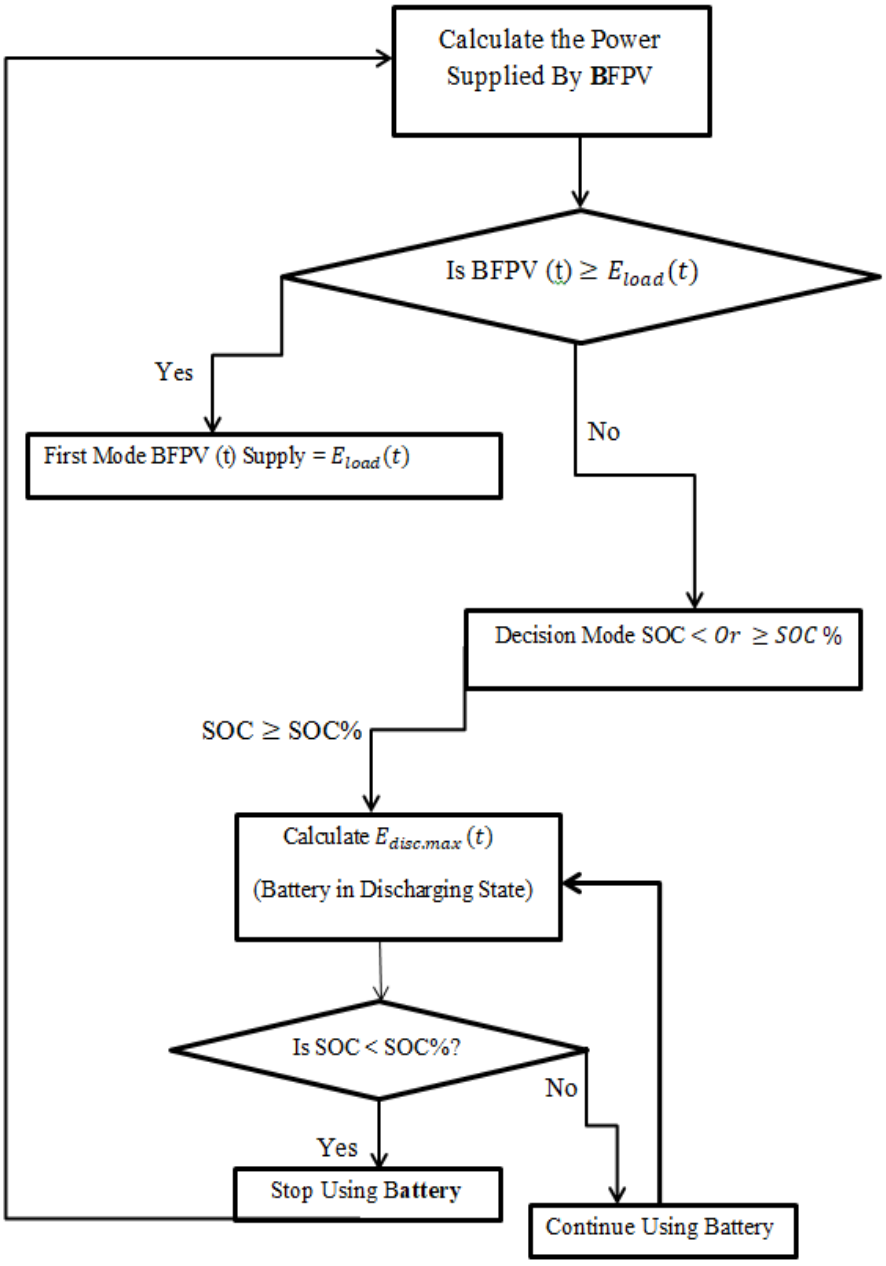

Figure 3.16: Flowchart of Decision Strategy of BFPV Controller and Mode 2 of Control for the System Operation.

The program determines what element has priority to supply energy based on:

i. If the SOC of the battery is greater than the minimum amount and therefore the battery is able to supply power to the load. The battery will be used.
ii. If the load cannot be supplied by the energy sources i.e. the combined power of the MFPV panels, not sufficient to supply the load and the battery is at its minimum SOC and therefore cannot be used to supply the deficit of power required. Then the diesel generator will be used.
From this control simulation we are able to see the performance of the system over the course of the year to see which modes the system spends most time in, the power supplied by each of the energy sources over the year, and the power required by the load over the year.
The charge controller rating should be 125% of the photovoltaic panel short circuit current. In other words, it should be 25% greater than the short circuit current of solar panel.

$$\text{Size of solar charge controller in amperes}$$
$$= \text{no. of panels} \times \text{Shortcircuit current of PV} \times 1.25 \text{ (Safety factor).}$$

This formula is not applicable on MPPT Solar chargers.

In this step we select the appropriate charge controller to match the voltage of PV array and the battery. In this study, PV module specifications, the short circuit current = 10.5A.

$$I_{rated} = 44 \times I_{sc} \times 1.25 = 44 \times 10.5 \times 1.25 = 577.5\text{A}$$
$$\text{Nominal system voltage} = 24\text{V}$$

Using a safety factor of 1.25 and a string of 4 PV modules per controller

$$\text{Nominal PV array current} = (24 \times 10.5) \times 1.25 = 315\text{ A}$$
$$\text{Nominal load current} = \frac{\text{Total load}}{\text{Nominal system voltage}} = \frac{158.76}{24} = 6.615\text{A}$$

3.2.2.5 Determination of converter size

Power converters are used to convert DC power from PV panels to AC power, which is required by most electrical appliances, and vice versa. Most common power conversion devices are electronic and include inverters (DC to AC). The four primary components for producing

electricity using solar power, which provides AC power for daily use, are: Solar panels, charge controller, batteries and inverter. Solar panels charge the battery, and the charge regulator insures proper charging of the battery. The battery provides DC voltage to the inverter, and the inverter converts the DC voltage to normal AC voltage. For the selected sites for the simulation, table 3.6 shows the respective soil or surface albedo.

Table 3.6: Six sites areas from six geopolitical zones in Nigeria under study.

Nature of Soil surface	albedo	region	State/locality
Dark wet soil	0.005-0.5	North-Central	Kwara/Oje/Illorin
Dry sandy soil	0.25-0.45	North-East	Borno/Baje/ Maiduguri
Dry sand	0.18	North-East	Sokoto/Kiso/Sokoto
Wet sand	0.09	South-South	Rivers/ Chokocho/Port-Harcourt
Green grass	0.16-0.27	South-East	Imo/Umuagwo/Owerri
Dark clay wet	0.02-0.08	South-West	Lagos/Kwame/Lagos

(Source: NASA, 2024)

3.2.3 Simulation of MFPV with MATLAB/SIMULINK and BFPV module with PVsyst.

3.2.3.1 Simulation of MFPV

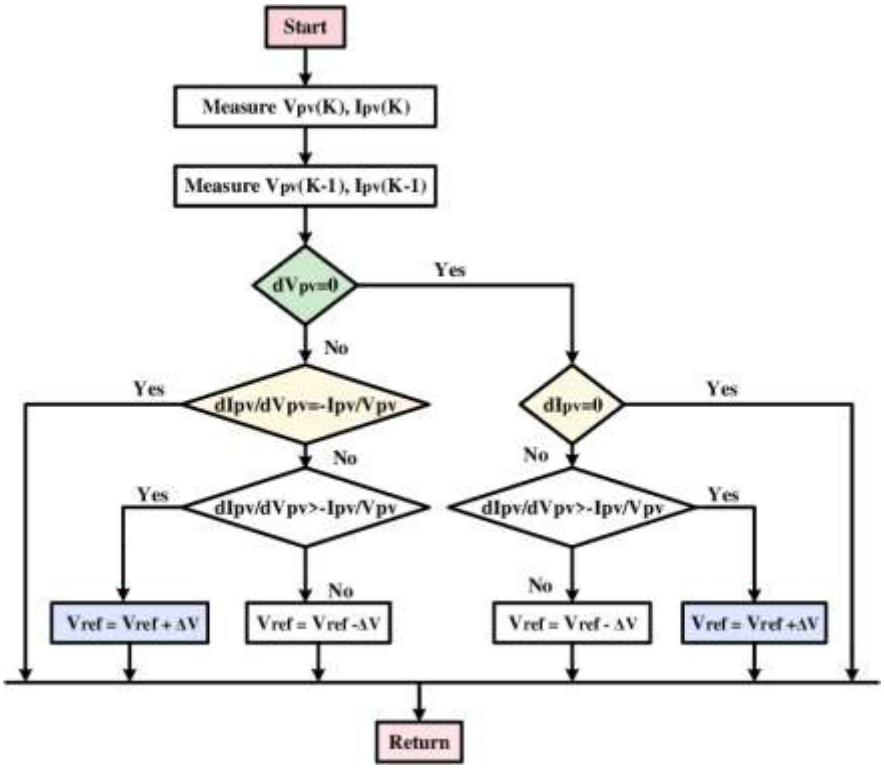

Figure 3.17: flowchart for perturb and Observation algorithm for MPPT of single diode model.

Tracking the maximum power point (MPP) of a photovoltaic (PV) array is usually an essential part of a PV system (Prasanna & Rajashekara, 2016). As such, many MPP tracking (MPPT) methods have been developed and implemented. The methods vary in complexity, sensors required, convergence speed, range of effectiveness, popularity, etc. In fact, so many methods have been developed, as it has become tedious to find which method, newly proposed or existing, is most appropriate for a given PV system (Hintz, et al, 2016). A MPPT is used for extracting the maximum power from the PV module and transferring that power to the load (Pandiarajan & Muthu, 2011). By changing the duty cycle of the PWM control signal, the load voltage varies and matches at the point of the peak power with the source so as to transfer the maximum power .A study in Germany, of PV system revealed that inverters contribute for 63%of failures, PV module 15% and other components 23% on an average, every 4.5 years .when PV module maximum power point comes into case of a real time is a well-known Tracking problem.

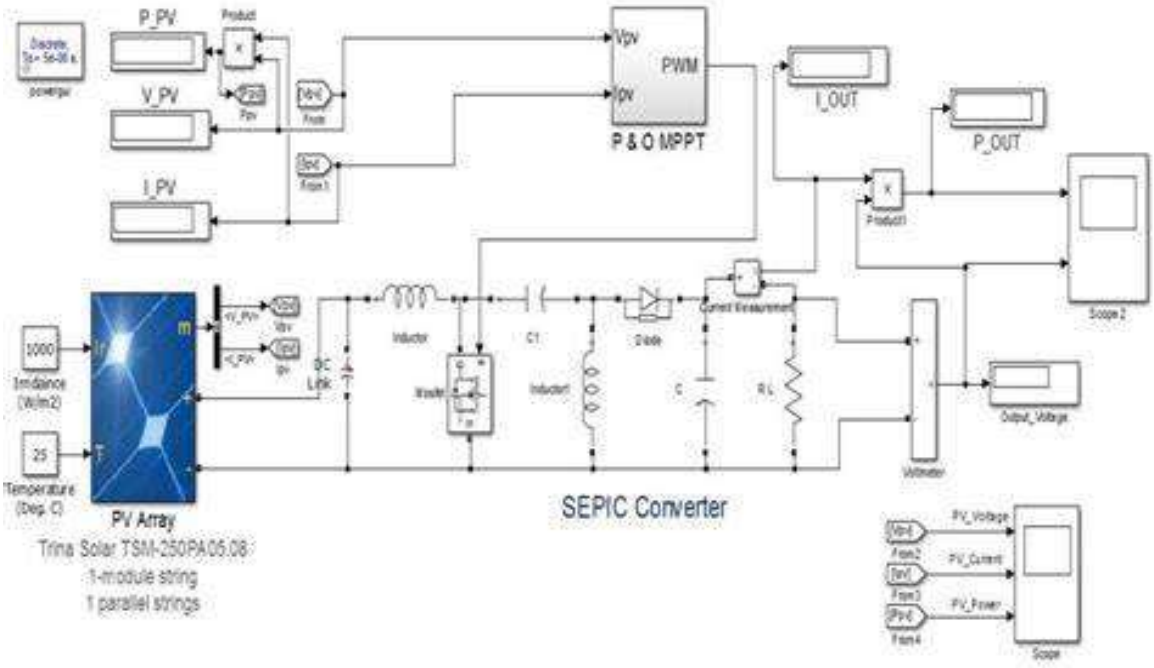

Figure 3.18: Simulink block model for the single diode model

Using a solar panel or an array of panels without controller that can perform Maximum Power Point Tracking will often result in wasted power. An efficient MPPT algorithm is important criteria to increase the efficiency of PV system to maintain the PV array's operating point at this MPP at all environment conditions. Therefore, MPPT techniques are needed to maintain the PV array's

operating at its MPPT. Many MPPT techniques have been proposed in the literature example are the Perturb and Observe (P&O) methods (Mohammed & Atkinson, 2012).

Using the mathematical model developed in section 3.2.1.1 above, we determined the I-V and P-V curves of a MFPV. The initial input irradiance to the PV array model is 1000 W/m^2 and the operating temperatures are 25^0C, 45^0C , 65^0C and 85^0C as shown in figure 3.18. At steady-state (i.e. at t = 0.15 sec.), figure 3.19 is the Simulink block model for the simulation of the saturation current.

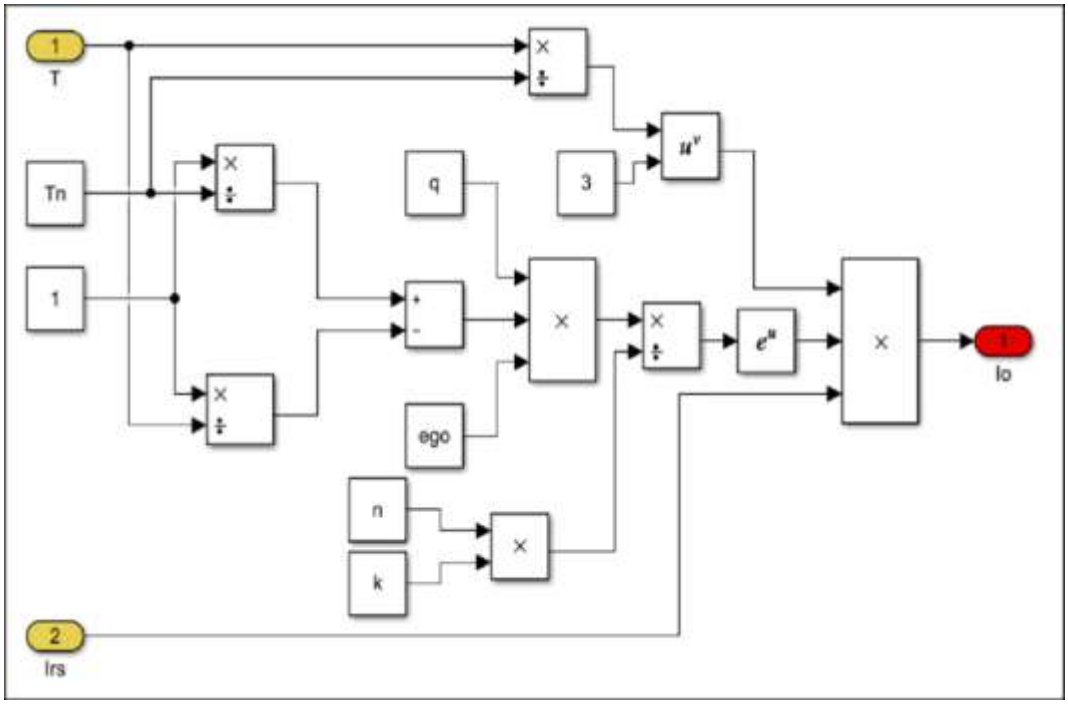

Figure 3.19: Simulink block model for the simulation of the saturation current

3.2.3.2 Simulation of standalone BFPV using PVsyst 7.4.8 version software

PVsyst is a software tool designed mainly for the bifacial solar energy industry. PVsyst creates, simulates, and analyses solar energy systems of all types. PVsyst is famous for its accuracy and flexibility because, it allows users to input specific data about their solar systems, simulate the performance of an energy system under various conditions which include solar panels' orientation, the site's location and climate, the electrical load and consumption patterns, etc.

In order to model a power system for any Base Station Site, we have to obtain some information about a particular remote location of the Base Station, such as the load profile that should be met

by the system. Such information includes: solar radiation for PV generation (availability of solar resources), cost for each component (diesel, renewable energy generators, battery, converter, etc.), cost of diesel fuel (price of fuel), annual interest rate, project lifetime, etc. Outlined below are suggestions of systems that could determine the best option for a Base station site in Nigeria.

Additionally, PVsyst offers a range of advanced customization options for PV system design. This includes modelling different panel technologies, incorporating shading and other site-specific factors, and optimizing system performance based on various criteria. The benefits of using this software include,

A. **Accuracy**: PVsyst uses advanced algorithms and databases to simulate solar energy systems' performance. Thus, users design optimized systems for their locations, meteorological data, and electrical load.

B. **Flexibility**: PVsyst allows users to input a wide range of data and customize their simulations to their needs. Optimizing system performance based on various circumstances saves the user money.

C. **Simplicity**: PVsyst makes it easy for solar energy professionals to input data, run simulations, and analyse results. The software also comes with comprehensive documentation and support resources to help users get the most out of the software.

This software has an edge over other software in that it can access satellite data, Google map, and information about a particular geographical area where the bifacial panel will be installed. It also helps to resolve the cost analysis of a BFPV installation. Before that, it is paramount to model important parameters that are inevitable when modelling a bifacial module which are embedded in the software. The simulation will be run at 60% bifaciality factor.

3.2.3.3 Solar radiation path of the respective Location.

Tables 3.7–3.12 show the monthly average global irradiation of the states in each of the six geopolitical zones in Nigeria.

Table 3.7: Monthly averaged global irradiation (kWh/m^2/mon) for North - Central Nigeria:.

Month	Abuja		Illorin		Jos		Lafia		Lokoja		Makurdi		Minna	
	H_{opt}	H_h	H_{opt}	H_h	H_{opt}	H_h	H_{opt}	H_h	H_{opt}	H_h	H_{opt}	H_h	H_{opt}	H_h
Jan	221.02	194.81	213.97	192.29	229.01	199.02	220.66	196.60	211.44	192.49	215.38	194.79	219.54	193.28
Feb	196.85	182.74	192.97	181.04	209.50	191.86	196.70	183.74	189.48	179.26	190.46	179.68	198.98	184.18
Mar	202.86	199.93	197.45	194.87	217.78	213.54	202.07	199.43	195.19	193.04	196.22	194.07	208.01	204.44
Apr	179.39	186.25	181.78	187.52	177.70	184.95	179.76	185.95	179.24	184.30	177.64	183.14	187.03	193.99
May	161.13	173.73	167.29	179.18	159.86	173.70	164.34	176.33	167.00	177.48	163.43	174.32	170.35	184.02
Jun	138.04	150.53	146.55	158.75	145.39	160.62	142.42	154.95	150.92	162.67	143.57	154.86	146.53	160.22
Jul	131.07	141.17	135.38	144.43	135.82	147.89	140.13	151.02	147.28	156.95	139.70	149.22	136.14	147.03
Aug	123.29	128.85	128.00	132.84	132.16	138.68	131.54	137.26	143.51	148.67	135.47	140.55	129.11	134.80
Sep	146.00	147.06	145.41	146.20	157.19	158.10	147.76	148.77	155.76	156.43	147.51	148.41	155.79	156.51
Oct	179.21	171.29	176.62	169.64	196.75	185.75	184.84	176.95	181.72	174.89	176.03	169.65	190.22	180.80
Nov	208.76	186.57	196.29	179.16	222.05	195.06	207.14	186.99	199.55	183.43	196.89	180.66	210.66	187.76
Dec	220.35	190.50	211.32	187.01	229.08	194.32	218.28	191.33	209.77	188.38	212.07	189.29	219.97	189.85
Average	175.66	171.12	174.42	171.08	184.36	178.62	177.97	174.11	177.57	174.83	174.53	171.55	181.03	176.40

The solar radiation map in figure 3.20 shows the distribution of solar irradiance in Nigeria in three zones while figure 3.21 represents the states in the geopolitical zones. Each of the solar zones of figure 3.20 represents two geopolitical zones, and this shows high values compared to other nations having high solar PV installed capacity. Figure 2.9 shows the solar irradiation in Nigeria indicating the three zones that constitute the six geopolitical zones. It is evident from the map that Zone I receives about 6000 kW/m^2 to 6500 kW/m^2 irradiance per annum, and Zone II is in the range of 5000 kW/m^2-5500 kW/m^2 of the sun's irradiation annually. For Zone III, the annual irradiation is 4000 kW/m^2-5000kW/m^2.

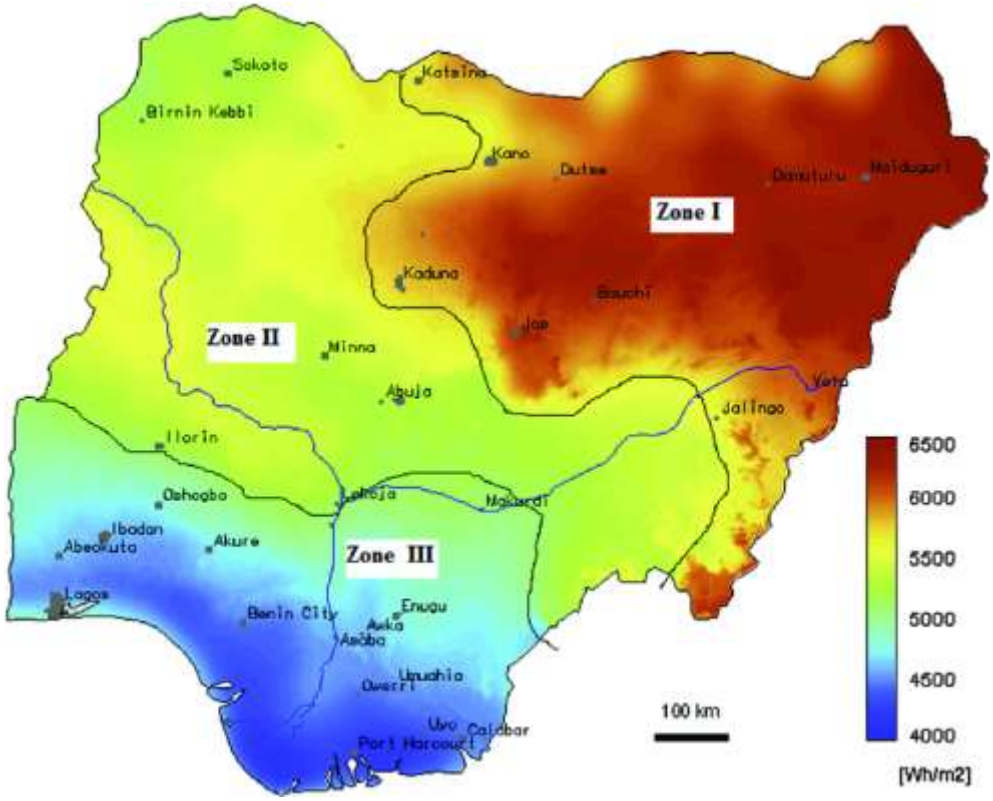

Figure 3.20: solar radiation zones of Nigeria. Source: Njok et al., 2020.

Figure 3.21: states in the six geopolitical zones. Source: Njok et al., 2020.

Table 3.8: Monthly averaged global irradiation (kWh/m^2/month) for North-Eastern Nigeria:

Month	Bauchi		Damaturu		Gombe		Jalingo		Maiduguri		Yola	
	H_{opt}	H_h	H_{opt}	H_h	H_{opt}	H_h	H_{opt}	H_h	H_{opt}	H_h	H_{opt}	H_h
Jan	226	197	227	195	226.45	198	225.70	199	229.00	196	225	199.81
Feb	210	192	211	191	208.97	192	205.25	190	211.52	191	206	191.63
Mar	222	217	227	221	221.34	216	213.84	210	227.75	221	218	214.13
Apr	195	202	205	212	196.58	203	189.22	196	205.73	213	193	200.04
May	180	195	191	207	182.18	196	168.91	182	190.11	206	174	188.02
Jun	164.19	180	172	190	165.30	181	149.32	163	167.67	185	159	174.73
Jul	157.16	170	168	183	158.22	171	137.68	148	164.14	179	153	165.73
Aug	153.47	160	161	169	149.12	155	133.90	139	158.27	165	148	155.70
Sep	174.89	175	182	181	173.42	173	153.43	154	181.82	181	167	167.70
Oct	208.48	196	213	199	207.28	195	192.92	183	213.43	199	202	191.94
Nov	219.98	194	220	191	218.38	193	215.18	192	220.08	191	217	194.73
Dec	224.23	192	223	188	223.28	191	223.94	194	225.13	188	224	194.81
Average	194.74	189	200	194	194.21	189	184.11	179	199.55	193	190	186.58

Table 3.9: Monthly averaged global irradiation (kWh/m^2/month) for North-Western Nigeria:

Month	Birnin Kebbi		Dutse		Gasau		Kaduna		Kano		Katsina		Sokoto	
	H_{opt}	H_h	H_{opt}	H_h	H_{opt}	H_h	H_{opt}	H_h	H_{opt}	H_h	H_{opt}	H_h	H_{opt}	H_h
Jan	222.43	190.35	223.29	193.06	222.75	191.06	225.92	195.73	222.50	191.73	222.53	189.44	220.04	187.48
Feb	207.15	187.41	208.50	189.64	209.92	189.89	208.16	190.33	208.91	189.60	210.84	189.52	207.93	187.16
Mar	223.70	216.84	225.14	218.89	225.43	218.73	219.08	214.30	225.86	219.35	230.47	222.62	225.11	217.59
Apr	204.35	211.11	205.47	212.29	203.10	210.15	193.90	201.57	206.26	213.16	208.91	215.84	207.39	214.06
May	188.85	204.79	189.93	205.37	187.58	203.49	175.79	190.88	190.56	206.06	194.77	211.55	193.25	209.64
Jun	170.74	188.65	171.75	188.91	169.42	187.13	151.86	167.00	172.33	189.78	176.60	195.23	175.81	194.39
Jul	165.70	180.95	166.64	181.39	162.48	177.16	143.31	155.31	168.08	183.18	172.64	188.59	171.14	186.91
Aug	159.53	167.11	164.99	172.78	158.22	165.85	138.15	144.68	164.70	172.55	168.07	176.17	164.58	172.36
Sep	181.01	180.06	183.70	183.06	182.57	181.91	163.00	163.57	185.63	184.89	192.26	190.93	187.62	186.25
Oct	215.07	199.93	214.06	200.09	212.97	198.39	199.52	187.98	215.80	201.29	219.12	202.89	215.53	199.65
Nov	214.63	186.57	218.13	190.89	218.39	189.73	219.15	192.30	218.01	190.22	219.23	189.01	215.57	186.23
Dec	220.03	184.58	219.90	186.48	221.77	186.23	225.78	191.40	220.07	185.95	220.90	184.03	218.33	182.31
Average	197.76	191.53	199.29	193.57	197.88	191.64	188.63	182.92	199.89	193.98	203.03	196.32	200.19	193.67

Table 3.10: Monthly averaged Monthly global irradiation (kWh/m^2/month) for South-Eastern Nigeria

Month	Abakiliki		Awka		Enugu		Owerri		Umuahia	
	H_{opt}	H_h	H_{opt}	H_h	H_{opt}	H_h	H_{opt}	H_h	H_{opt}	H_h
Jan	204.95	189.94	201.14	186.51	203.94	188.26	197.09	184.38	199.14	186.09
Feb	179.44	171.89	174.53	167.39	174.22	166.79	170.75	164.55	172.09	165.72
Mar	182.77	181.49	178.75	177.61	177.23	176.14	173.24	172.36	171.85	170.97
Apr	170.35	174.66	165.64	169.88	166.77	171.26	163.04	167.02	162.04	166.00
May	158.06	166.64	150.58	158.54	154.15	162.79	147.81	155.01	148.59	155.98
Jun	140.61	149.62	134.32	142.79	137.83	146.99	126.31	133.29	128.17	135.45
Jul	131.29	138.04	124.72	131.12	127.21	134.02	119.47	124.82	120.29	125.81
Aug	130.57	134.42	127.63	131.55	128.24	132.30	126.27	129.82	126.14	129.70
Sep	142.13	142.86	134.82	135.61	137.44	138.25	132.02	132.77	132.01	132.80
Oct	166.93	162.42	158.98	154.87	165.92	161.22	154.55	151.15	157.09	153.52
Nov	181.25	170.17	179.69	168.78	183.73	171.73	169.81	160.87	171.21	161.93
Dec	198.26	182.20	196.80	180.83	200.61	183.13	189.67	176.22	192.54	178.55
Average	165.55	163.70	160.63	158.79	163.11	161.07	155.84	154.35	156.76	155.21

The implication of this is that Nigeria receives a good amount of the sun's energy needed for PV generation per annum. Data shows that Nigeria receives about 4.85 x 10^{12} kW/h of this energy per day which comes from about 4 kW/m^2 - 8.5 kW/m^2 (an average of 7 days) hours per day of sunlight, which is equivalent to the energy produced from about 1.082 million tons of oil per day (Osueke & Ezugwu, 2011). This figure corresponds to about 4000 times the current daily crude oil production in the country and about 13,000 times the natural gas daily production, based on standard energy units.

The value of the total monthly horizontal irradiation H_h (kWh/m^2/mon) (hitting a horizontal plane) is collected and presented in tables 3.7, 3.8, 3.8, 3.10, 3.11, and 3.12 alongside H_{opt} for all state capitals in separate geopolitical zones. The nation can achieve enough in different sectors of the economy with this large, free, and sustainable clean energy. The solar energy outputs of Nigeria from the six geo-political zones are displayed in tables 3.13 to 3.18. The global radiation data for the optimally inclined planes (H_{opt}) of the PV module is the value of the summation of the monthly radiation energy incident on one square meter (1Sq-m) facing the direction of the equator. The

optimally inclined angle (angle of inclination) is the one that gives the highest annual irradiation in kWh/m^2.

Each table represents the six geopolitical zones in Nigeria; North Central (Table 3.7), North East (Table 3.8), North West (Table 3.9), South East (Table 3.10), South-South (Table 3.11), and South West (Table 3.12). The global total monthly radiation was collected, and the average was found for each month and resented for all state capitals of the different regions.

Table 3.11: Monthly averaged Monthly global irradiation (kWh/m^2/mon) for south-South Nigeria

Month	Asaba		Calabar		Benin City		Port Harcourt		Uyo		Yenagoa	
	H_{opt}	H_h	H_{opt}	H_h	H_{opt}	H_h	H_{opt}	H_h	H_{opt}	H_h	H_{opt}	H_h
Jan	199.70	186.40	196.36	184.14	195.16	181.88	190.67	179.21	193.07	181.53	193.04	180.84
Feb	171.80	165.34	168.21	162.39	169.55	162.94	162.03	156.67	164.37	158.93	163.32	157.61
Mar	176.88	175.80	162.70	162.07	173.07	171.93	157.61	157.01	161.22	160.60	162.76	162.11
Apr	168.75	172.73	150.18	153.84	163.91	167.82	150.16	153.90	153.88	157.50	149.59	153.44
May	155.98	163.88	143.38	150.53	153.16	160.99	136.63	143.24	141.63	148.27	134.41	141.15
Jun	138.25	146.36	115.93	122.09	132.08	139.83	106.83	112.28	116.40	122.48	111.32	117.40
Jul	127.39	133.40	102.07	106.37	119.87	125.47	104.52	108.85	107.34	111.85	107.86	112.65
Aug	130.47	134.11	106.51	109.26	123.43	126.97	113.64	116.66	114.90	117.91	117.76	121.18
Sep	138.15	138.81	118.46	119.19	130.73	131.36	116.23	116.97	120.44	121.13	116.63	117.42
Oct	162.04	157.95	143.14	140.38	158.32	154.29	137.64	135.01	143.42	140.59	139.76	136.88
Nov	179.44	169.26	153.45	146.35	172.05	162.42	149.89	142.90	157.87	150.44	158.91	150.72
Dec	194.24	179.88	184.80	172.32	187.41	173.37	182.31	170.32	184.54	172.36	186.29	173.19
Average	161.92	160.33	145.43	144.08	156.56	154.94	142.35	141.08	146.59	145.30	145.14	143.72

Table 3.12: Monthly averaged Monthly global irradiation (kWh/m^2/mon) for South-Western Nigeria

Month	Abeokuta		Ado-Ekiti		Akure		Ibadan		Ikeja		Osogbo	
	H_{opt}	H_h	H_{opt}	H_h	H_{opt}	H_h	H_{opt}	H_h	H_{opt}	H_h	H_{opt}	H_h
Jan	200.922	184.68	205.96	187.61	202.10	185.31	200.95	184.01	192.51	178.39	204.87	186.14
Feb	176.98	168.72	182.20	172.70	176.98	168.50	177.54	168.83	167.27	160.35	182.83	172.95
Mar	177.62	176.13	186.29	184.53	180.22	178.77	181.23	179.68	171.77	170.60	186.89	185.03
Apr	165.54	170.06	172.61	177.76	168.46	173.16	168.67	173.50	162.59	166.91	171.01	176.15
May	158.16	167.59	160.50	170.81	158.11	167.73	160.07	170.21	145.90	153.94	158.70	169.03
Jun	132.51	141.30	141.55	152.25	138.13	147.93	135.20	144.73	114.00	120.90	138.12	148.68
Jul	122.45	129.02	131.54	139.57	126.93	133.97	121.29	128.02	115.58	121.43	122.65	130.09
Aug	120.75	124.41	127.31	131.67	122.01	125.90	117.75	121.46	125.74	129.72	115.45	119.37
Sep	132.68	133.36	139.92	140.69	137.70	138.45	132.51	133.26	125.28	126.00	131.99	132.81
Oct	163.05	158.28	171.02	165.22	167.01	161.76	166.93	161.55	149.18	145.12	162.98	157.67
Nov	177.58	165.99	192.84	177.60	186.53	173.08	183.46	170.21	165.12	155.35	187.04	172.33
Dec	195.48	178.06	207.48	186.01	201.31	182.11	197.29	178.59	184.95	170.03	203.06	181.93
Average	160.31	158.13	168.27	165.53	163.79	161.39	161.91	159.50	151.66	149.89	163.80	161.01

It can be concluded that the Northern states have higher values of global solar radiation, which is in agreement with facts that the Northern States are hotter, and the Southern States generally have lower temperature values, mainly because of their closeness to the Atlantic Ocean. After using the total monthly global solar radiation, the estimated solar energy generation for all the six geopolitical zones presented in tables 3.13, 3.14, 3.15, 3.16, 3.17, and 3.18.

Table 3.13: Estimated electricity generation from 1kWp PV module in North Central Nigerian cities

City	Position	Angle of Inclination (degrees)	Averaged Monthly radiation Per annum for H_h (kWh/m^2/mo)	Averaged Monthly radiation Per annum for H_{opt} (kWh/m^2/mo)	Annual Electricity generation from H_h (kWh)	Annual Electricity generation from H_{opt} (kWh)
Abuja	9.063N, 7.489E	15	171.12	175.66	1,540.07	1,580.97
Illorin	8.491N, 4.549E	14	171.08	174.42	1,539.69	1,569.77
Jos	9.922N, 8.859E	17	178.62	184.36	1,607.62	1,659.21
Lafia	8.490N, 8.513E	15	174.11	177.97	1,566.99	1,601.73
Lokoja	7.800N, 6.744E	12	174.83	177.57	1,573.49	1,598.15
Makurdi	7.729N, 8.540E	13	171.55	174.53	1,543.98	1,570.77
Minna	9.617N, 6.547E	16	176.40	181.03	1,587.64	1,629.25
Average		14	173.96	177.93	1,565.64	1,601.41
Total		116	1217.72	1245.54	10,959.48	11,209.85

Table 3.14: Estimated electricity generation from 1kWp PV module in North-Eastern Nigerian cities.

City	Position	angle inclination (degrees)	Averaged Monthly radiation Per annum for H_h (kWh/m^2/mo)	Averaged Monthly radiation Per annum for H_{opt}(kWh/m^2/mo)	Annual Electricity generation from H_h (kWh)	Annual Electricity generation from H_{opt} (kWh)
Bauchi	10.308N, 9.843E	16	189.60	194.74	1,706.43	1,752.64
Damaturu	11.838N, 11.901E	17	194.35	200.41	1,749.11	1,803.73
Gombe	10.279N, 11.171E	15	189.23	194.21	1,703.09	1,747.89
Jalingo	8.967N, 11.309E	15	179.64	184.11	1,616.80	1,656.97
Maiduguri	11.837N, 13.156E	17	193.29	199.55	1,739.65	1,795.97
Yola	9.254N, 12.45E	14	186.58	190.93	1,679.22	1,718.33
Average		15.67	188.78	193.99	1,699.05	1,745.92
Total			1,132.70	1,163.95	10,194.31	10,475.52

Table 3.15: Estimated electricity generation from 1kWp PV module in North-Western Nigerian cities.

City	Position	Angle of Inclination (degrees)	Averaged Monthly radiation Per annum for H_h (kWh/m^2/mo)	Averaged Monthly radiation Per annum for H_{opt} (kWh/m^2/mo)	Annual Electricity generation from H_h (kWh)	Annual Electricity generation from H_{opt} (kWh)
Birnin Kebbi	12.454N, 4.198E	17	191.53	197.76	1,723.75	1,779.88
Dutse	11.751N, 9.341E	16	193.57	199.29	1,742.13	1,793.63
Gusau	12.164N, 6.663E	17	191.64	197.88	1,724.79	1,780.95
Kaduna	10.518N, 7.435E	17	182.92	188.63	1,646.27	1,697.70
Kano	12.000N, 8.532E	16	193.98	199.89	1,745.82	1,799.03
Katsina	12.988N, 7.600E	17	196.32	203.03	1,766.85	1,827.25
Sokoto	13.057N, 5.2360E	17	193.67	200.19	1,743.02	1,801.72
Average		16.71	191.95	198.10	1,727.52	1,782.88
Total			1343.63	1386.69	12,092.64	12,480.17

Table 3.16: Estimated electricity generation from 1kWp PV module in South-Eastern Nigerian cities

City	Position	Angle of inclination	Averaged Monthly radiation Per annum for H_h (kWh/m^2/mo)	Averaged Monthly radiation Per annum for H_{opt} (kWh/m^2/mo)	Annual Electricity generation from H_h (kWh)	Annual Electricity generation from H_{opt} (kWh)
Abakiliki	6.312N, 8.107E	11	163.70	165.55	1,473.27	1,489.96
Awka	6.218N, 7.083E	11	158.79	160.63	1,429.11	1,445.69
Enugu	6.463N, 7.542E	11	161.07	163.11	1,449.67	1,467.97
Owerri	5.490N, 7.034E	10	154.35	155.84	1,389.19	1,402.53
Umuahia	5.525N, 7.517E	10	155.21	156.76	1,396.89	1,410.86
Average		10.60	158.62	160.38	1,427.62	1,443.40
Total			793.12	1163.95	10,194.31	10,475.52

Table 3.17: Estimated electricity generation from 1kWp PV module in South-South Nigerian cities.

City	Position	Angle of inclination	Averaged Monthly radiation Per annum for H_h (kWh/m^2/mo)	Averaged Monthly radiation Per annum for H_{opt} (kWh/m^2/mo)	Annual Electricity generation from H_h (kWh)	Annual Electricity generation from H_{opt} (kWh)
Asaba	6.025N, 6.693E	10	160.33	161.92	1,442.95	1,457.31
Calabar	4.977N, 8.313E	10	144.08	145.43	1,296.69	1,308.88
Benin	6.325N, 5.607E	10	154.94	156.56	1,394.45	1,409.05
Port Harcourt	4.814N, 7.080E	10	141.08	142.35	1,269.76	1,281.14
Uyo	5.048N, 7.907E	10	145.30	146.59	1,307.70	1,319.31
Yenagoa	4.904N, 6.234E	10	143.72	145.14	1,293.45	1,306.22
Average		10.00	148.24	149.67	1,334.17	1,346.99
Total			889.45	1163.95	10,194.31	10,475.52

Table 3.18: Estimated electricity generation from 1kWp PV module in South Western Nigerian cities.

City	Position	Angle of Inclination	Averaged Monthly radiation per annum for H_h (kWh/m^2/mo)	Averaged Monthly radiation per annum for H_{opt} (kWh/m^2/mo)	Annual Electricity generation from H_h (kWh)	Annual Electricity generation from H_{opt} (kWh)
Abeokuta	7.155N, 3.339E	13	158.13	160.31	1,423.20	1,442.79
Ado-Ekiti	7.601N, 5.273E	13	165.53	168.27	1,489.81	1,514.41
Akure	7.258N, 5.218E	13	161.39	163.79	1,452.51	1,474.11
Ibadan	7.371N, 3.964E	13	159.50	161.91	1,435.54	1,457.17
Ikeja	6.626N, 3.361E	12	149.89	151.66	1,349.05	1,364.91
Osogbo	7.754N, 4.581E	114	161.01	163.80	1,449.13	1,474.19
Average		12.17	159.25	161.62	1,433.21	1,454.60
Total			955.47	1163.95	10,194.31	10,475.52

Similarly, the estimated electricity generation from 1kWp PV module for North Cental (table 3.13), North Eastern (table 3.14), North Western (table 3.15), South Eastern (table 3.16), South Southern (table 3.17), and South Western (table 3.18) Nigerian cities.

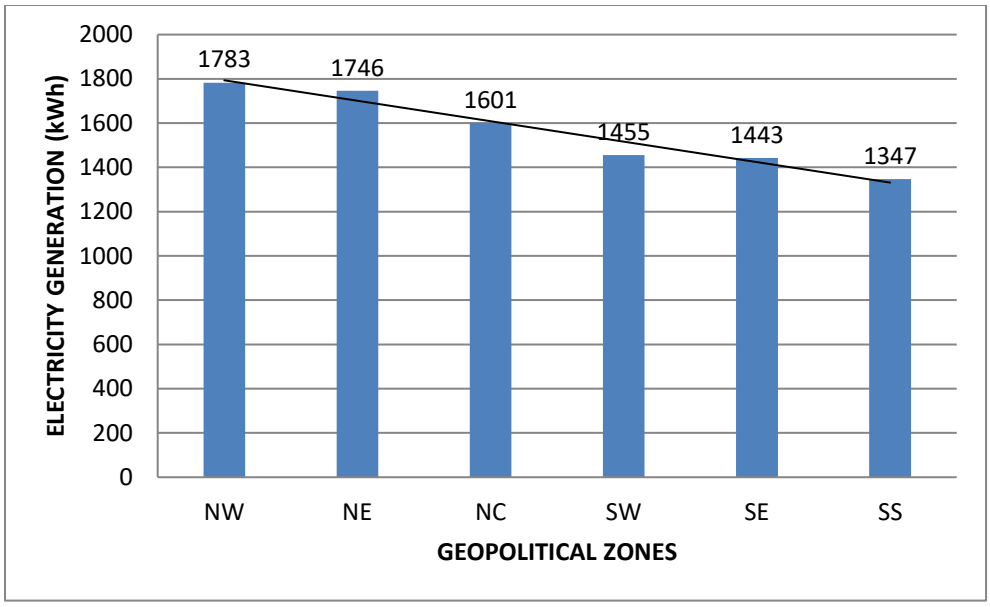

Figure 3.22: Average estimated electricity generation from each geopolitical zone in kWh. Source: Data from (Emanuel et al., 2021)

The tables show that the region with the higher potential for annual electricity generation from 1kWp PV modules is the Northern states. The Northern states are closer to the Sahara Desert, and these regions have higher elevations above the sea level than the cities located towards the South.

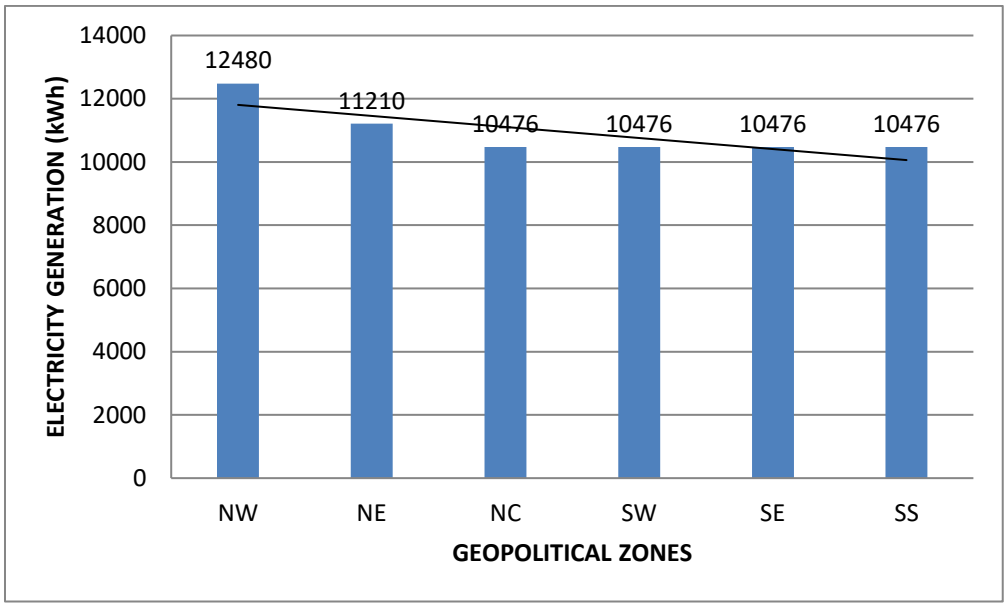

Figure 3.23: Total estimated electricity generation from each geopolitical zone in kWh.

Figure 3.22 clearly shows the average estimated electricity generation for each geopolitical zone while figure 3.23 shows the total estimated electricity generation for each geopolitical zone. The cities in the North-Western region produce the highest estimated electrical energy (about 12,480 kWh), and the cities in the Southern region all have the same estimated electricity generation (about 10,475 kWh).

However, there has been research on global solar radiation at different locations in the country for the geopolitical zones in these locations. Sunshine hours were used to calculate the electrical energy that can be generated from the sun by taking note of the Global horizontal Solar Radiation $Gh_i$and the extra-terrestrial irradiance Ho. Based on research, it has been proven that the geographical location and climatic condition of the region are the major factors affecting global solar radiation; this is related to the region's location. The major reason why most countries do not utilize this main source of energy is that they do not directly study and understand global solar radiation variation. The result of solar irradiance over Nigeria shows that the northern part of the country possesses more significant potential for solar energy electricity generation than other parts. To estimate the solar energy potential, either the solar irradiance data or the PV module can be applied to determine the solar energy potential. Mathematically,

$$E = ArGh_iP_R(kWh) \tag{3.57}$$

Where E represents the energy in kWh, A is the area (m^2) of the PV module, r is the yield (%) of the PV module, Gh_i is the average irradiation (kWh/m^2 /day) on the solar PV module at any specific angle and P_R performance ratio. P_R is given as;

$$P_R = \frac{(P_{measured}/P_{maximum})}{(E_{measured}/1000)} \tag{3.58}$$

$E_{measured}$ is the measured incident solar irradiance on the PV array, $P_{measured}$ and $P_{maximum}$ are the measured and maximum power from the PV array respectively. P_R is usually 0.75 for most systems. To estimate the solar energy generation potential from the daily values of solar irradiance, equation 3.59 can be applied.

$$E = 365P_{up}Gh_iP_R(kWh) \tag{3.59}$$

Equation 3.59 gives the total estimated annual energy output (E) by considering the average daily solar radiation data Gh_i, the performance ratio P_R, and the unit Peak P_{up} over 365 days of the year

assuming a unit peak power (P_k) of 1kWp for the PV module. To obtain the actual estimate of the annual energy output (E), the average monthly radiation data obtained from a PVGIS (Photovoltaic Geographic Information System) Satellite will be used. Therefore, the daily radiation data to estimate using equation 3.59 may not be entirely accurate since it will not take into account the leap years. Hence, equation 3.60 is more reliable.

$$E = 12P_{up}Gh_{i(mo)}P_R(kWh) \quad (3.60)$$

The "365" factor has been replaced with "12," which shows the 12 months of the year, which never changes, unlike 365 days which varies in leap years. $Gh_{i(mo)}$in equation 3.60 is the monthly solar radiation data for optimally inclined planes (kWh/m^2 /mon), P_R and P_{up} are the performance ratio of value 0.75 and the peak power of value 1kWp, respectively. Based on the Nigerian land area of about 924 km^2 and an average irradiance per unit area of 5.535 KWh/m^2, the country has been estimated to have an average of 1831.06 kWh (Kilowatt-hour) incident solar energy annually. The annual insolation of solar energy is valued at about 27 times the national conventional energy resources in energy units and also over 117,000 times the amount of electric power that was generated in 1998. To produce energy equal in quantity to the conventional energy reserve, about 3.7% of the nation's land area has to be utilized. Nigeria's ability to sustain energy production will be tested in the coming decades as her energy demand far outweighs her supply. The epileptic nature of the electric power supply has hindered her economic development and growth albeit, alas, it has vast natural resources and an abundance of solar insolation.

3.2.3.3.1 Geographical site: Umuagwo, Imo State: South-East

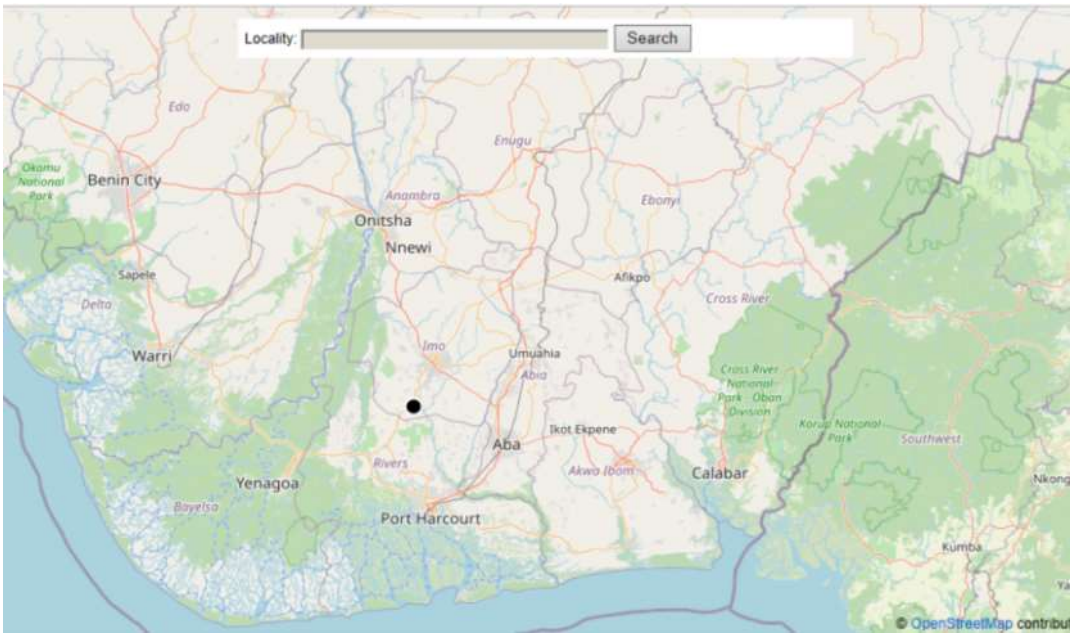

Plate 3.8: site location

Umuagwo, Imo State as shown in plate 3.8 is located on latitude 5.2906^0N and on longitude 6.9379^0E with an altitude of 44m. Figure 3.24 is the sun path of the site based on the azimuth angle.

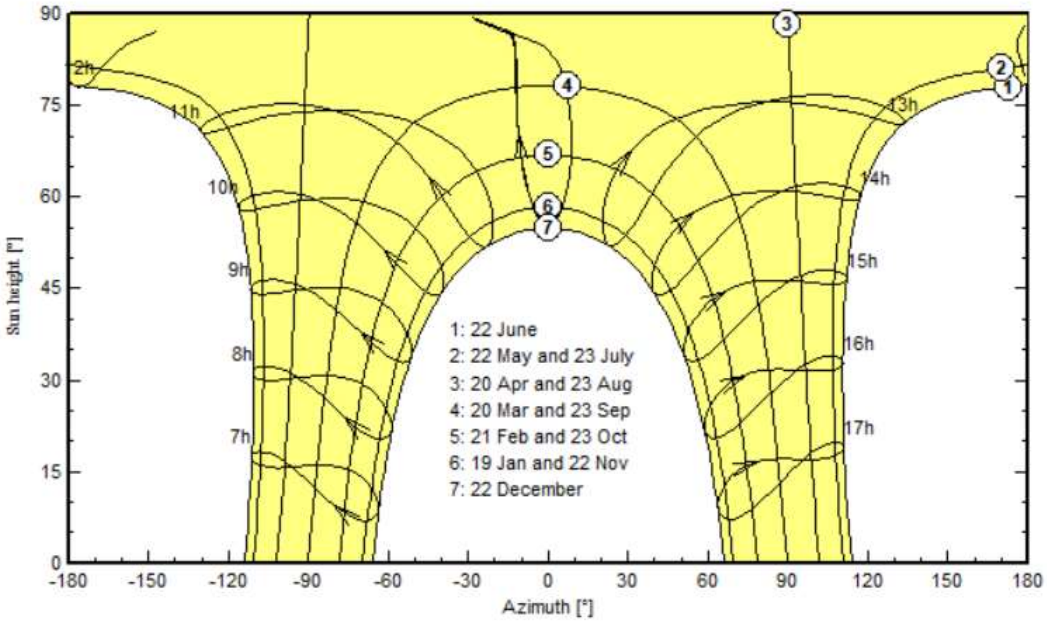

Figure 3.24: Sun paths for Umuagwo.

3.2.3.3.2 Geographical site: Chokocho, Rivers State: South-south

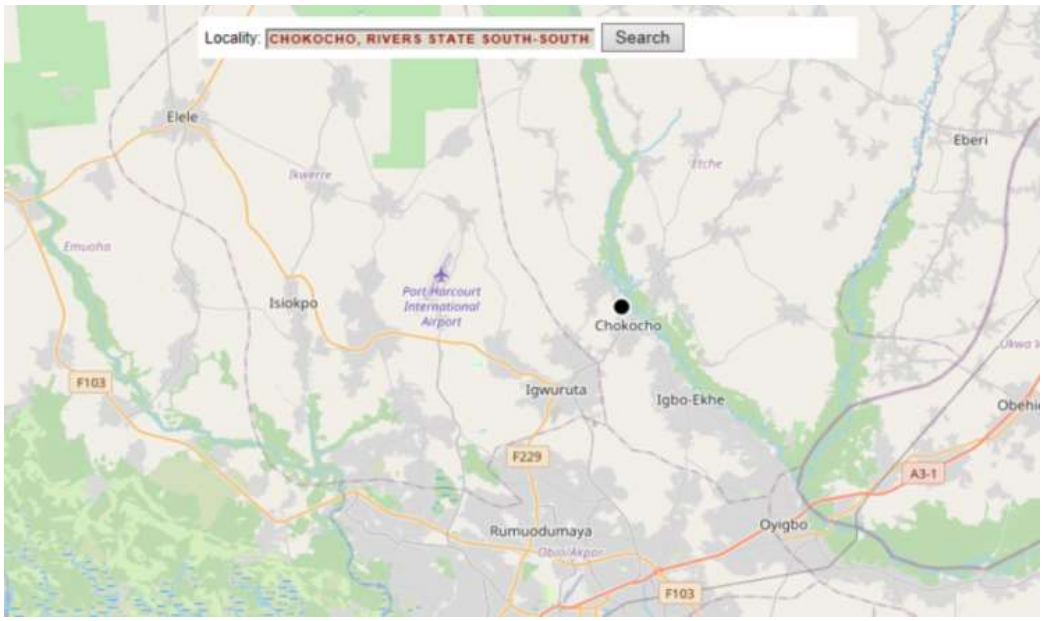

Plate 3.9: site location for Chokocho

Chokocho, Rivers State is located on latitude 4.900^{0}N and on longitude 7.047 ^{0}E with an altitude of 22m as shown in plate 3.9 while the sun's azimuth angle is shown in figure 3.25

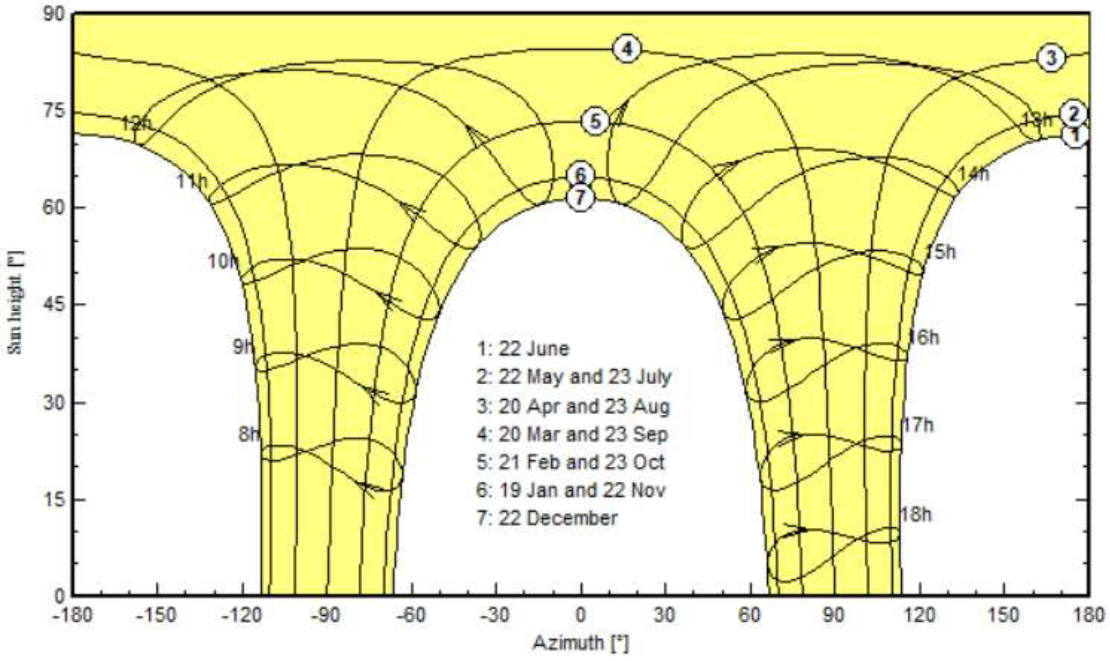

Figure 3.24: Sun paths for Chokocho.

3.2.3.3.3 Geographical site: Kwame, Lagos State: South-West

Plate 3.10: site location for Kweme

Kweme Lagos State is located on latitude 6.400^{0}N and on longitude 2.73 ^{0}E with an altitude of 10m as shown in plate 3.10 and the sun path shown in figure 3.26

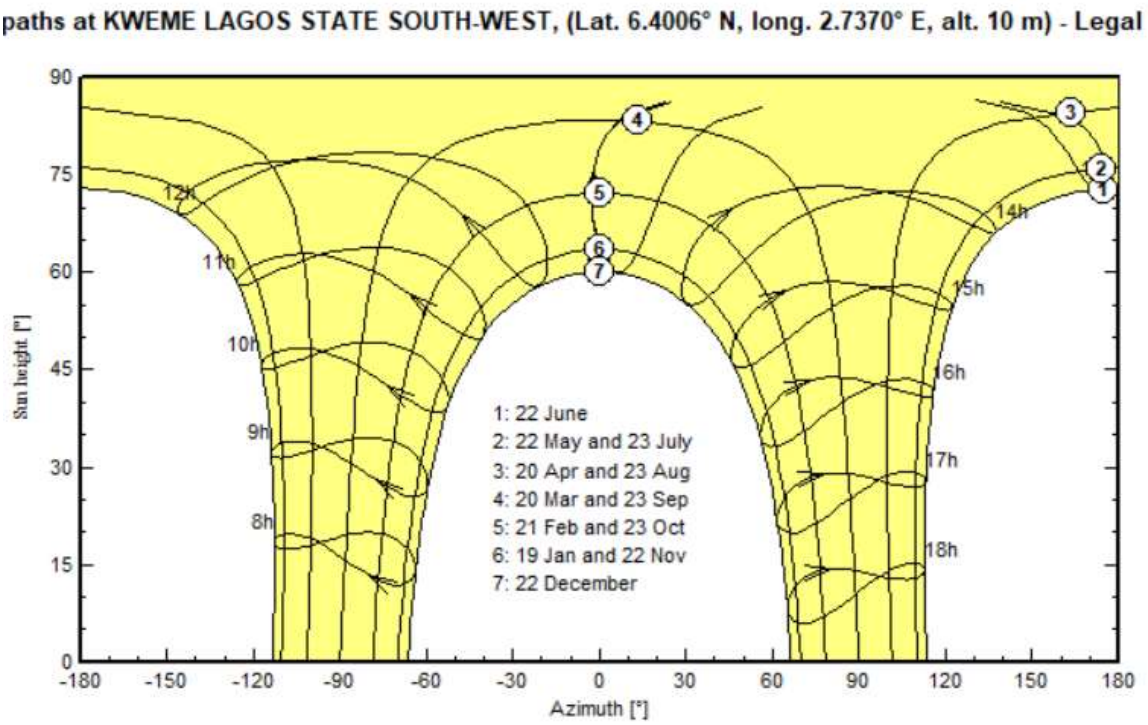

Figure 3.26: Sun paths for Kweme.

3.2.3.3.4 Geographical site: Oje, Kwara State: North-Central

Oje, Kwara State is located on latitude 8.442^{0}N and on longitude 4.733 ^{0}E with an altitude of 408m as shown in plate 3.11 and the sun path shown in figure 3.27

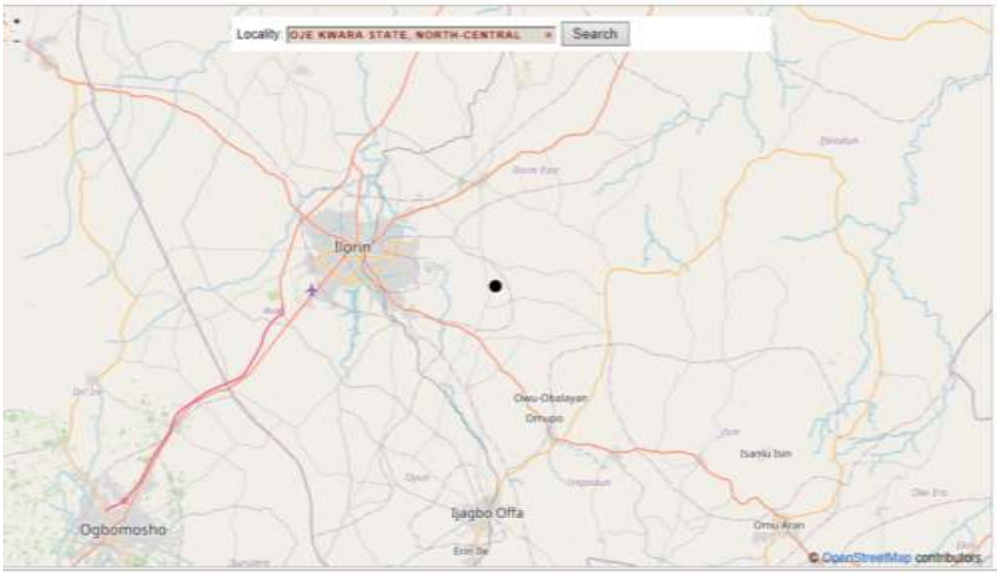

Plate 3.11: site location for Oje

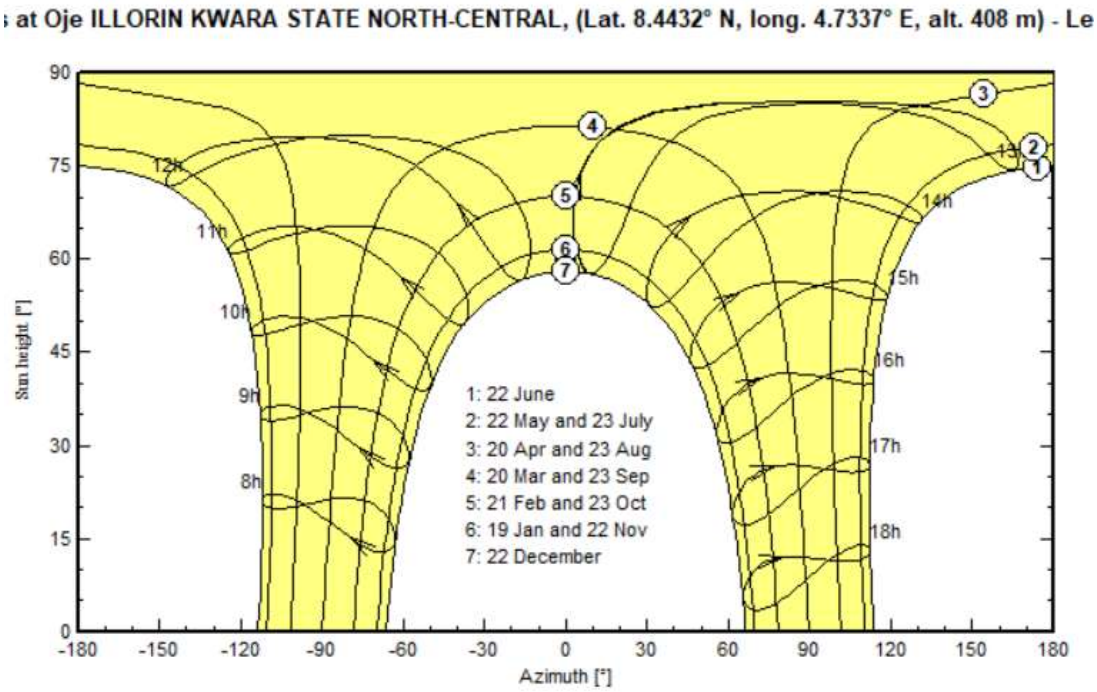

Figure 3.27: Sun paths for Oje.

3.2.3.3.5 Geographical site: Kiso, Sokoto State: North-West

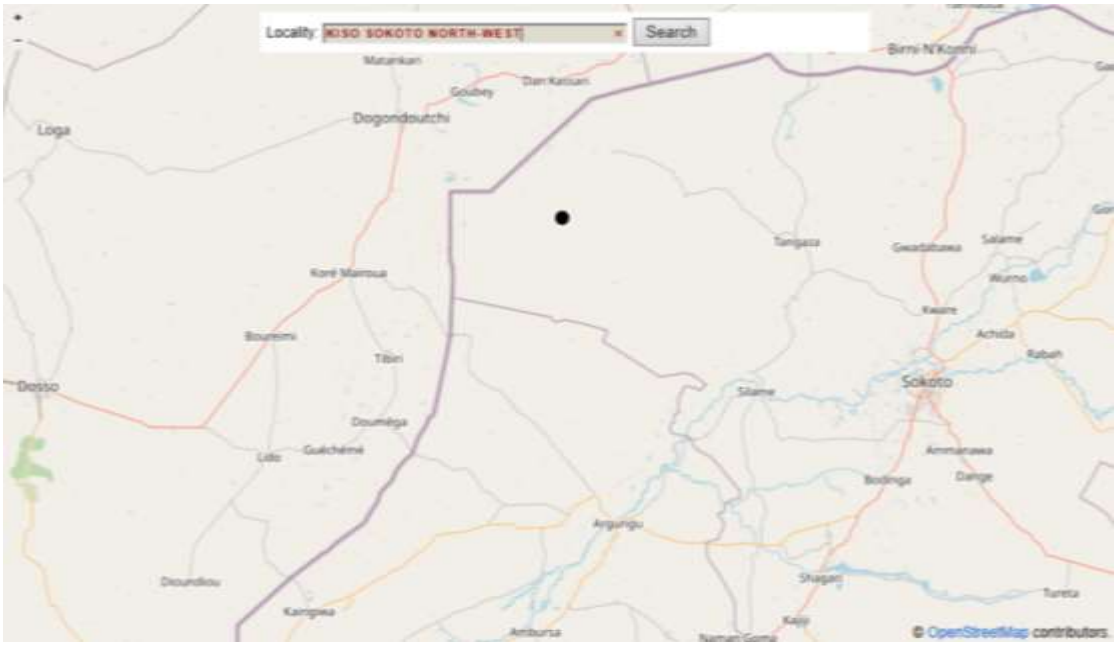

Plate 3.12: site location for Kiso

Kiso, Sokoto State is located on latitude 13.4^{0}N and on longitude 4.4 ^{0}E with an altitude of 241m as shown in plate 3.12 and the sun path shown in figure 3.28

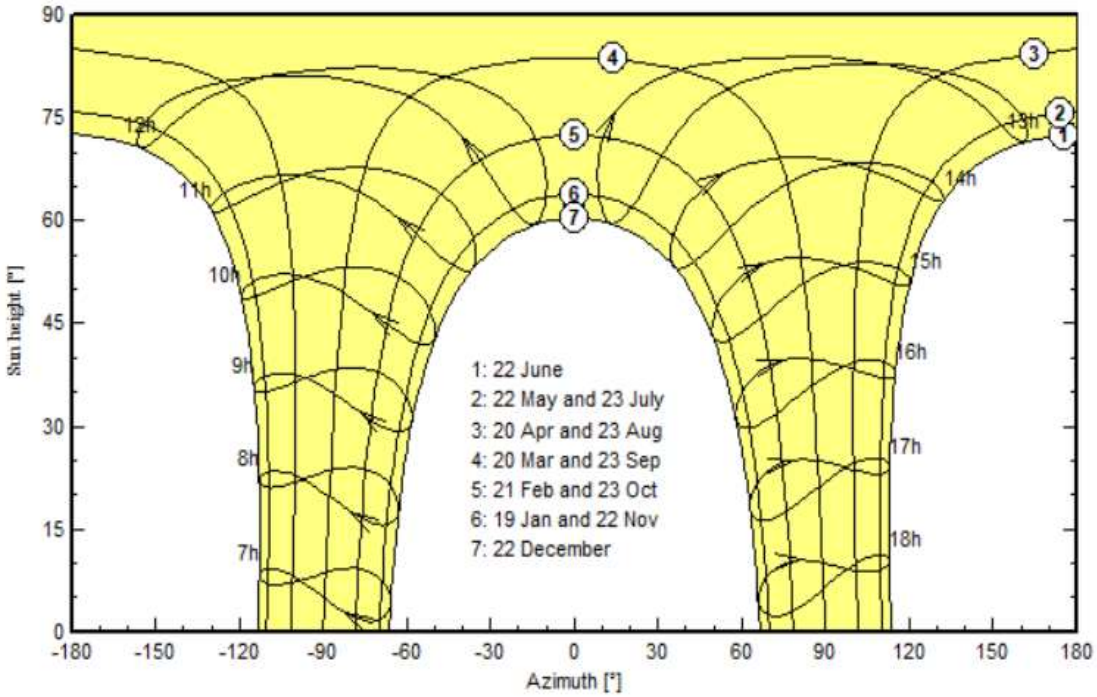

Figure 3.28: Sun paths for Kiso.

3.2.3.3.6 Geographical site: Baje, Bornu State: North-East

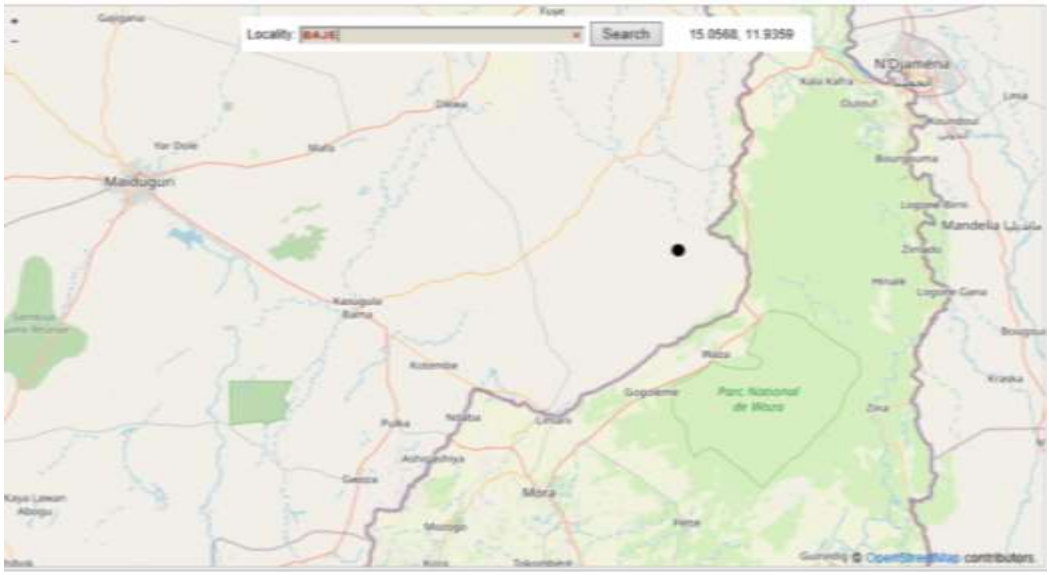

Plate 3.13: site location for Baje

Baje is located on latitude 11.59^{0}N and on longitude 14.49 ^{0}E with an altitude of 297m as shown in plate 3.13 and sun path in figure 3.29.

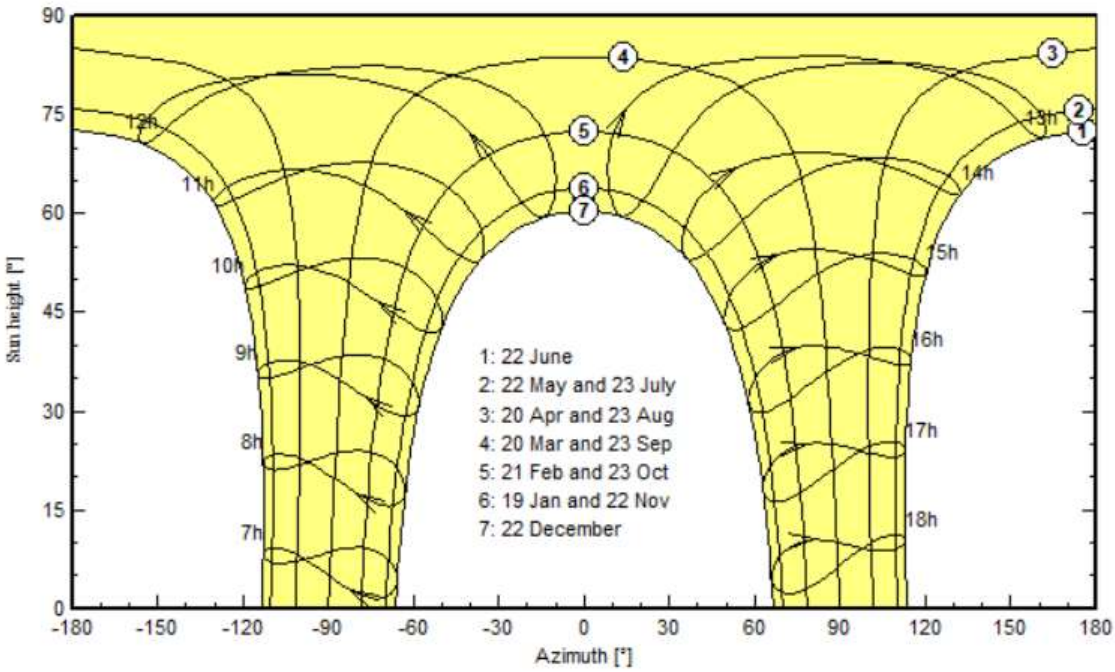

Figure 3.29: Sun paths for Baje

3.2.4 Development of an energy optimization model using HOMER for the three categories and select the one with the best optimal solution.

HOMER is used to design an optimal energy solution of hybrid power system based on comparative economic analysis. The HOMER software determines optimal hybrid systems using combinations of photovoltaic, wind turbines, micro-hydro, diesel generation, battery storage, and inverter capacity but this research will base its optimization on MFPV+DG+B and BFPV+B to optimize the cost, pollutant emission and land usage. HOMER like PVsyst also takes into account both seasonal and hourly load variations as well as variations in resource availability such as wind and sunlight. In addition, HOMER outputs multiple options ranked in order of least net present cost, which is based on a 25-yr lifecycle cost including interest as used in this work (Jang & Kyungsoo, 2020). Figures 3.30 and 3.31 shows the two energy configuration to be optimized with HOMER

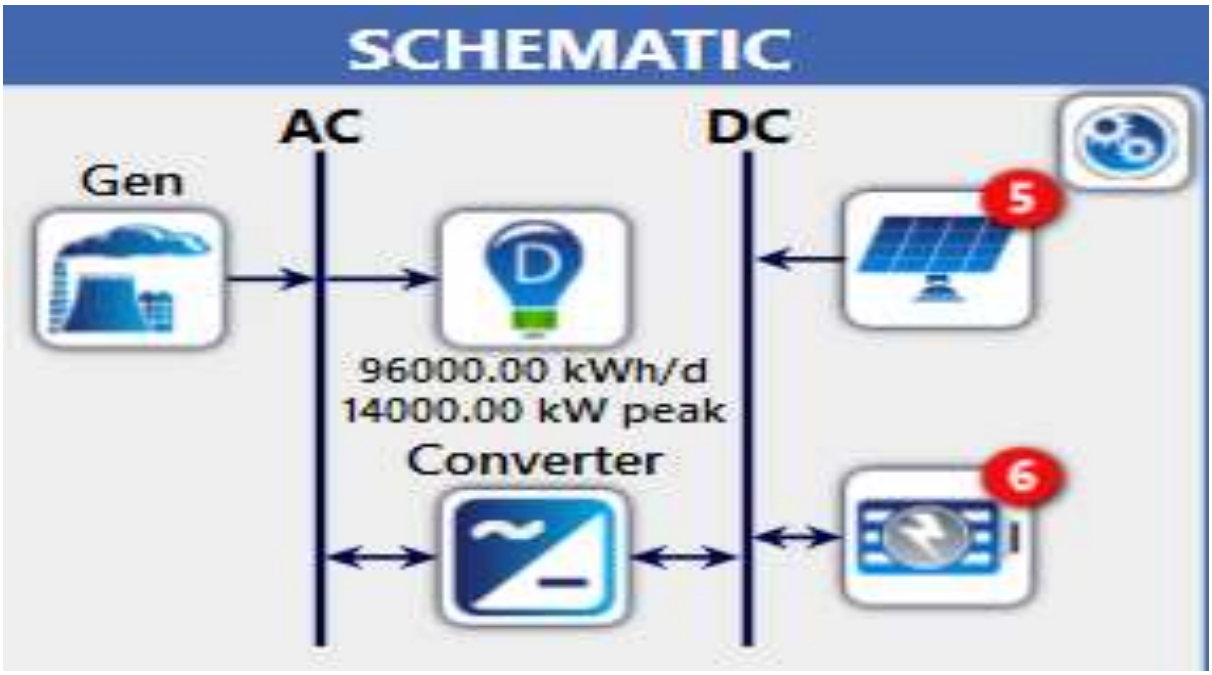

Figure 3.30: MFPV+DG+B (Energy system 1)

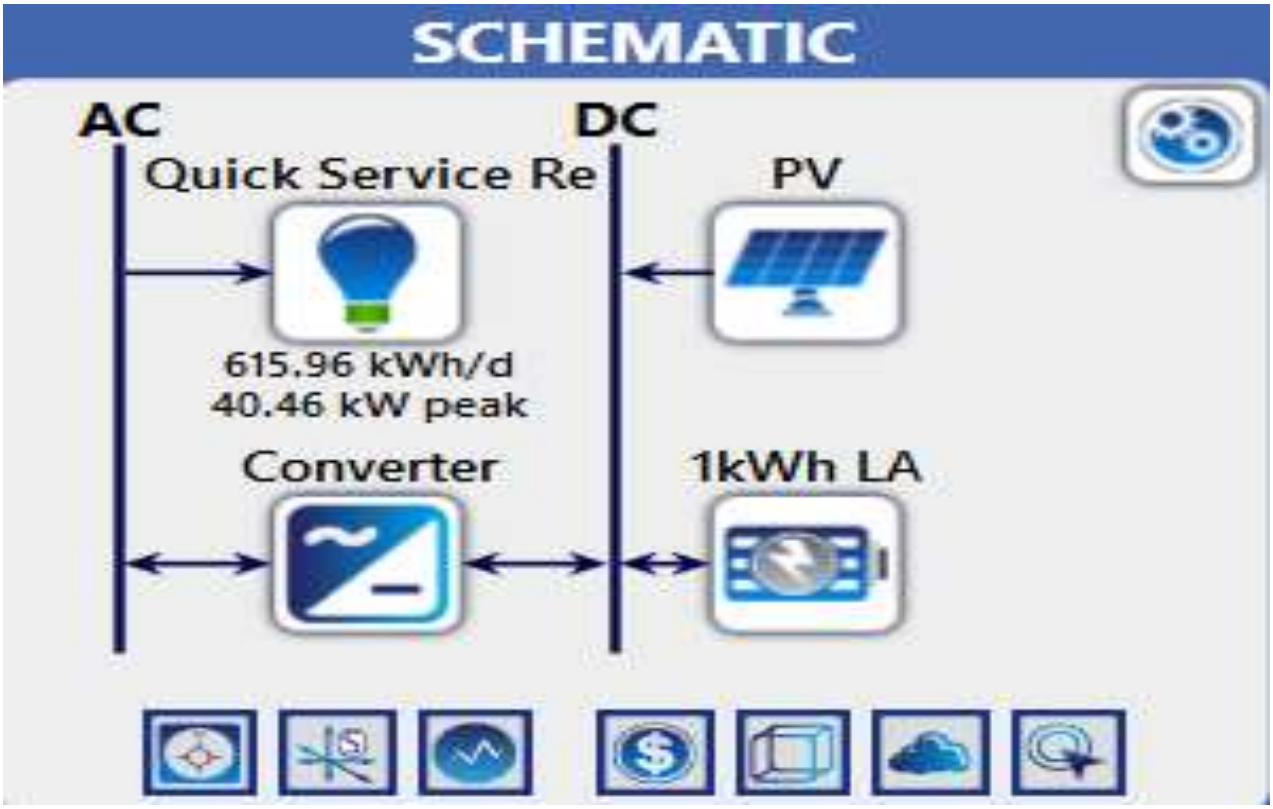

Figure 3.31: BFPV+B (Energy system 2)

Tables 3.19 and 3.20 show how the demand is met by the respective energy system MFPV+DG+B and BFPV+B. It shows how the sources were allocated according to the load demand and availability. It was observed that the variation is not only in the demand but also the availability of sources. The battery or the diesel generator compensates the shortage depending on the climatic condition. The results show that in the MFPV+DG+B combination, the PV, due to poor irradiation is not enough to charge the battery. Therefore, at that instance, the controller switches the generator on to compensate the load. The PV power supply is between 8:00 h to 19:00 h while the radiation peak is between 12:00 h to 14:00 h as can be seen in the Tables. Between 12:00 h and 14:00 h there is no deficit in the system and the renewable energy supplies the load and charges the battery.

3.2.4.1 Demand met by the two Energy System: MFPV/ Diesel/Battery and BFPV/Battery

I. MFPV+DG+B

Table 3.19: Power demand met by the energy system (MFPV/ Diesel/Battery) at the locations

Time (h)	Global solar (kW/ m^2)	Incident solar (kW/ m^2)	Wind Speed (m/s)	DC (kW)	MFPV Output (kW)	Diesel Output (kW)	Battery Input (kWh)	Battery state of charge (%)
0:00	0.000	0.000	2.505	10.667	0.000	0.000	-3.483	47.021
1:00	0.000	0.000	2.440	10.667	0.000	0.000	-3.299	46.774
2:00	0.000	0.000	1.332	10.667	0.000	0.000	-3.299	46.527
3:00	0.000	0.000	2.540	10.667	0.000	0.000	-3.299	46.281
4:00	0.000	0.000	2.430	10.667	0.000	0.000	-3.299	46.034
5:00	0.000	0.000	2.190	10.667	0.000	0.000	-3.299	45.788
6:00	0.000	0.000	2.385	10.667	0.000	0.000	-3.299	45.541
7:00	0.001	0.000	1.072	10.667	0.000	0.000	-3.299	45.295
8:00	0.126	0.223	1.431	10.467	2.146	0.000	-0.953	45.224
9:00	0.329	0.411	0.876	10.467	3.957	0.000	0.858	45.275
10:00	0.570	0.660	1.907	10.467	6.356	0.000	3.257	45.470
11:00	0.834	0.925	1.894	10.467	8.906	0.000	5.807	45.817
12:00	1.022	1.102	2.096	10.467	10.615	0.000	7.516	46.266
13:00	1.064	1.134	2.123	10.467	10.925	0.000	7.826	46.734
14:00	1.082	1.159	2.133	10.467	11.157	0.000	8.058	47.216
15:00	0.888	0.967	3.038	10.467	9.315	0.000	6.300	47.592
16:00	0.652	0.730	2.521	10.467	7.028	0.000	3.929	47.827
17:00	0.493	0.604	2.227	10.467	5.812	0.000	2.713	47.989
18:00	0.258	0.384	1.819	10.667	3.700	0.000	0.401	48.013
19:00	0.041	0.161	2.825	10.667	1.546	0.000	-1.715	47.885
20:00	0.000	0.000	3.571	10.667	0.000	0.000	-3.101	47.653
21:00	0.000	0.000	2.070	10.667	0.000	0.000	-3.299	47.407
22:00	0.000	0.000	2.537	10.667	0.000	0.000	-3.299	47.160
23:00	0.000	0.000	1.523	10.667	0.000	0.000	-3.299	46.914

II. BFPV+B

Table 3.20: Power demand met by the energy system (BFPV/Battery) at the locations

Time (h)	Global solar (kW/ m^2)	Incident solar (kW/ m^2)	DC Load (kW)	PV Output (kW)	Battery Input (kWh)	Battery state of charge (%)
0:00	0.000	0.000	10.667	26.5	15.053	74.248
1:00	0.000	0.000	10.667	26.5	15.053	74.864
2:00	0.000	0.000	10.667	26.5	15.053	75.479
3:00	0.000	0.000	10.667	26.5	15.053	76.095
4:00	0.000	0.000	10.667	26.5	15.053	76.711
5:00	0.000	0.000	10.667	26.5	15.053	77.326
6:00	0.000	0.000	10.667	26.5	15.053	77.944
7:00	0.002	0.000	10.667	26.5	15.053	78.574
8:00	0.141	0.260	10.467	26.5	15.053	79.355
9:00	0.417	0.543	10.467	26.5	15.053	80.297
10:00	0.687	0.791	10.467	26.5	15.053	80.570
11:00	0.940	1.025	10.467	26.5	15.053	80.975
12:00	1.062	1.126	10.467	26.5	15.053	81.437
13:00	1.061	1.113	10.467	26.5	15.053	81.893
14:00	0.978	1.028	10.467	26.5	15.053	82.299
15:00	0.846	0.901	10.467	26.5	15.053	82.632
16:00	0.679	0.748	10.467	26.5	15.053	82.884
17:00	0.464	0.544	10.467	26.5	15.053	83.011
18:00	0.208	0.257	10.667	26.5	15.053	82.963
19:00	0.043	0.165	10.667	26.5	15.053	82.840
20:00	0.000	0.000	10.667	26.5	15.053	82.594
21:00	0.000	0.000	10.667	26.5	15.053	82.347
22:00	0.000	0.000	10.667	26.5	15.053	82.101
23:00	0.000	0.000	10.667	26.5	15.053	81.854

There is likely to be deficit in other remaining hours due to poor radiation, and the deficit is being completed by either the battery or the diesel generator. The energy output from the configuration is sufficient at all the time. Here the BFPV follows the heliotropism process of the sunflower in charging the battery. The controller switches the batteries into charging mode whenever excess power is available from the PV, and this is only efficient in the BFPV+B configuration, during the Night, the battery takes over the system load. For the MFPV+DG+B configuration, at night, the controller turns on the diesel generator when the load demand cannot be met together by the PV and battery due to poor state of charge,

3.2.4.2 PV Costing of variable components

The initial costs of the PV array are the PV panel costs according to the size of the PV panel type, the percentage of capital costs added for installation and Balance of System (BOS) parts, and added fixed costs accounting for installation and BOS parts, respectively. Operation and maintenance of PV arrays can be described with monthly fixed costs and yearly costs as a percentage of capital costs. These payments can cover system inspection by a maintenance person. Replacement events of PV arrays for this research are assumed to occur after every 25 years, so for a project life of 25 years or less, there will be no PV replacement costs.

3.2.4.3 Diesel generator costing

The initial costs of the diesel gensets are the diesel generator cost according to the size of the diesel generator type, the percentage of capital costs added for installation and BOS parts for diesel generator type and the corresponding added fixed costs. The diesel generator operating costs comprise fuel costs, and maintenance, overhaul and replacement costs. The fuel costs occur whenever the fuel storage tanks are refilled. Overhaul is assumed halfway through the diesel lifetime. Replacement occurs after a certain number of diesel generators run time hours. The effective lifetime of a diesel generator is defined by the time until a mechanical overhaul becomes uneconomic (i.e. when overhaul costs exceed 60% of the replacement costs). Factors that affect the lifetime include the quality and regularity of maintenance, the average capacity factor and the number of start-ups. An air-cooled machine is likely to have a shorter life than a water-cooled unit that can keep the operating temperature down. Annualized Total Cost of running Diesel Generator only is calculated by considering the installation costs, balance of system costs;

fuel tank and shelter costs are included in the fixed costs or as a percentage of initial costs. The diesel fuel consumption varies according to generator size and loading factor and is non-linear.

3.2.4.4 Battery costing

The initial battery costs are the installation costs and balance of system costs which will be accounted for in the fixed costs or as a percentage of initial battery capital costs. The battery operation costs depend on the battery cycling during system operation and also include fixed costs and costs at regular intervals such as maintenance costs. Maintenance includes checking the battery electrolyte levels. Battery maintenance costs are often included in maintenance costs of the overall system or individual electricity generators. Replacement costs occur whenever a battery needs to be exchanged with a new or newer one.

3.2.4.5 Conversion devices

Power converters are used to convert DC power, e.g. from PV panels, and batteries, to AC power, which is required by most electrical appliances, and vice versa. Engine generators typically produce AC power which can be converted to DC power with the help of a rectifying battery charger in order to be used to charge batteries. The most common power conversion devices are electronic and include inverters (DC to AC), rectifiers (AC to DC) and bi-directional converters (both directions)

3.2.4.6 Optimization technique used

Various optimization techniques for hybrid system have been reported in Renewable and Sustainable Energy Reviews, such as graphic construction methods, probabilistic approach, iterative technique, artificial intelligence methods, and multiple-objective design. Using feasible optimization method, optimum configurations which meet the load requirement can be obtained. In this research, we will use the multiple-objective optimization which is inherent in the software for running the simulation.

3.2.4.7 Multi-objective optimization method

In any engineering field, to carry out a design, it is possible to have several objectives simultaneously, being typical that some of them conflict with each other. Multi- Objective optimization attempts the simultaneous minimization of various objectives. In the optimum sizing of solar, diesel systems, we wish to carry out the design considering simultaneously at least two objectives (costs, land and pollutant emissions). These three objectives are in conflict,

since a reduction in design costs implies a rise in pollutant emissions and vice versa.
Therefore, the task of getting good results in problems of this kind (multi-objective) is complicated. Given the complexity of this kind of problems, because of the large number of variables that are usually considered and of the mathematical models applied, classic optimization techniques may consume excessive Central Processing Unit (CPU) time or even being incapable of taking into account all the characteristics associated to the posed problem. However, the environmental issues associated to this type of installations should also be taken into account during the design process. Until now, usually, the pollutant emissions have been calculated after obtaining the design that minimizes costs. In some cases, as in the HOMER, it is possible to consider the pollutant emissions by economically evaluating them, and therefore becoming a part of the costs objective function.

3.2.4.8 optimization with genetic algorithm (GA)

GA is a dynamic search technique used in computing to find true or approximate solutions for the optimization and search problems. GA is categorized as global search heuristics. GA is a particular class of evolutionary algorithms that use techniques inspired by evolutionary biology such as inheritance, mutation, selection and recombination. A typical GA requires two things to be defined: A genetic representation of the solution domain and, a fitness function to evaluate the solution domain.

GA might be useful in problem domains that have a complex fitness landscape that a traditional hill climbing algorithm might fail. The flow chart of the GA optimization process for HRES is illustrated in figure 3.32 (Xu et al., 2005) used GA with elitist strategy for optimally sizing a standalone hybrid PV/Wind power system for a year (8760 hours). Their main objectives were to minimize the total capital cost of the system with constrained LPSP.

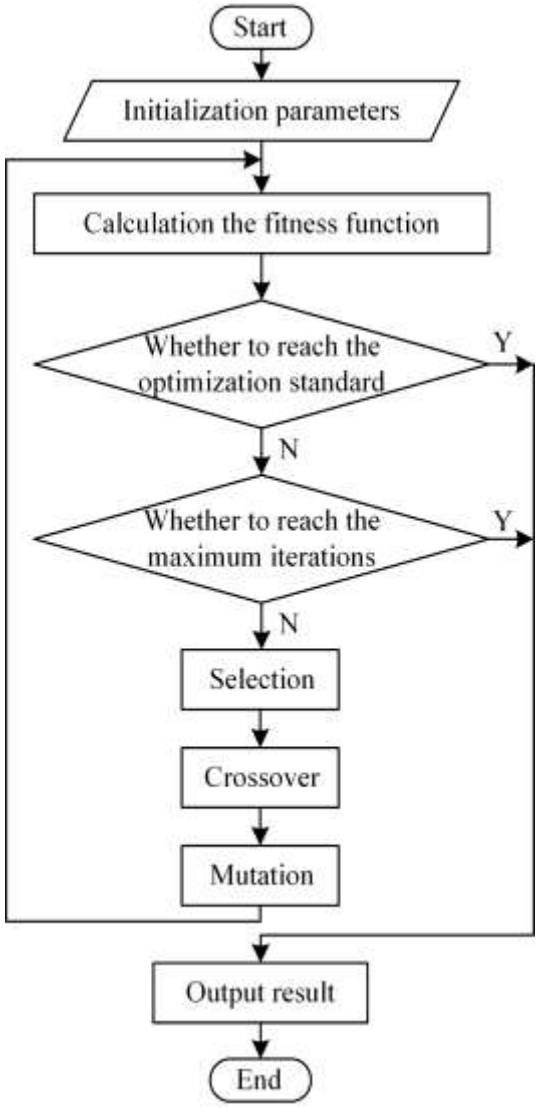

Figure 3.32: Flow chart of typical Genetic algorithm consisting of PV-Wind and Hydro models

3.2.4.9 System cost analysis

Several economic criteria exist, such as the Net Present Cost (NPC), Levelized Cost of Energy (LCOE) and life-cycle cost (LCC). The PVSyst Optimization Model for BFPV uses the total Net Present Cost (TNPC) to represent the life-cycle cost of the system, assumes that all prices escalate at the same rate and takes the ‘‘annual real interest rate” rather than the ‘‘nominal interest rate”. This method allows inflation to be factored out of the analysis. The NPC also takes into account any salvage costs, which is the value remained in a component of the system at the end of the project lifetime. PVSyst assumes a linear depreciation of components in its simulation process, meaning that the salvage value of a component is directly proportional to its remaining life. It also

assumes that the salvage value is based on the replacement cost rather than the initial capital cost. The LCOE is defined as the ratio of the total annualized cost of the system to the annual electricity delivered by the system. It has been extensively used as an objective term to evaluate the solar-generator system configurations. Other economical approaches, such as the Levelized Cost of System (LCOS) and LCC are also widely used. The mathematical model derived estimates the life-cycle cost of the system, which is the total cost of installing and operating the system over its lifetime. The life-cycle cost is a convenient metric for comparing the economics for different types of system configurations. Life cycle cost analysis is a tool used to compare the ultimate delivered costs of technologies with different cost structures. The initial costs are the costs incurred through purchasing equipment, and hiring labour, in order to install an energy system. A component purchase might also generate certain associated fixed costs for the user. For example, Seeling-Hochmuth indicate that regardless what kind of component size is purchased a certain type of transport would always have to be paid for, or a certain sized container etc. When installing equipment, certain costs arise due to installation, labour or required accessories. These costs depend on size and type of a component and are often given as a percentage of individual or overall equipment purchase costs. In general, the initial purchase costs of a component will depend on the size and type of a component, and on how many components are bought. For example, differently sized generators are available at varying costs due to different material and labour costs in producing a generator. In addition, similarly sized generators from different manufacturers might be priced differently due to the use of particular designs, materials, quality standards and mark-ups. The component size and type are subject to optimizing system design criteria. They are therefore selected as decision variables to be optimized in the developed system design model. The component initial cost is multiplied by the required number of components to be installed in the system in series (n_i, series) and in parallel (x_i, parallel). The number of components to be installed in series is often straightforward and determined by the nominal operating voltages of the system and the components. However, the number of components to be installed in parallel is subject to system design and its optimization and is therefore labelled with an ‘x’, as is the size of a component type. Therefore, in the initial cost modelling, the size and type of a component and the required number of parallel connected components are taken to be decision variables to be optimized in the developed system model. The operation costs describe costs incurred after installation in order to run the system for a certain

number of years, the so-called 'project life'. The project life is an important parameter for system designers as it helps to benchmark different life cycle costs or net present value costs for different designs. The operation costs include expenses for fuel, maintenance, components-overhaul and components replacement. As operation costs occur in the near and distant future and are only estimates, they are more difficult to determine than initial costs. It is also difficult to estimate component degradation as part of the replacement and maintenance costing. In the developed model the predicted timing for maintenance, overhaul and replacements is based on the number of hours or operational cycles a component has been operating which is influenced by the system size and system operation. Operation costs can be split into a number of contributing expenditures, mainly costs for maintenance, refueling, component overhaul, component replacement, and administration. In many projects, a maintenance person is employed to look after a system or several systems. This person's monthly salary or part of it will therefore occur in the maintenance costs. Often systems will need some kind of administrative support, and then monthly administrative costs will be included in the operation costs. The operation costs for either a component or the overall system can contain fixed costs and costs that are counted as a percentage of initial capital expenditure. From the above statement, we can see that the operation cost comprises of expenses for fuel, maintenance, and component replacement.

3.2.4.10 Energy Model of the system

3.2.4.10.1 MFPV Photovoltaic Generator

With the solar radiation available and ignoring the effect of temperature, the hourly energy output of the PV generator can be calculated using equation 3.61 as;

$$\mathrm{E_{PVG}} = \mathrm{G(t)} \times \mathrm{A} \times \mathrm{P} \times \eta_{\mathrm{PVG}} \qquad (3.61)$$

E_{PVG} is the energy output of the MFPV, $G(t)$ is the hourly sun irradiation measured in kwh/m^2, (A) is the panel cross-sectional area, P is the penetration level factor of the solar PV, and η_{PVG} is the efficiency of the panel.

3.2.4.10.2 Diesel Generator

The hourly energy output of the diesel generator $E_{DEG}(t)$ is given as;

$$\mathrm{E_{DEG}(t)} = \mathrm{P_{DEG}(t)} \times \eta_{\mathrm{DEG}} \qquad (3.62)$$

$P_{DEG}(t)$ is the rated power in kVA, and η_{DEG} is the efficiency of the diesel generator.

3.2.4.10.3 The converter

In the proposed scheme, a converter contains both rectifier and inverter. PV and battery sub-systems are connected with DC bus while diesel generating unit sub-system is connected with AC bus. The electric loads connected in this scheme are DC loads. The rectifier is used to transform the surplus AC power from the diesel electric generator to DC power of constant voltage. The diesel electric generator will be powering the load and at the same time charging the battery. Hence the rectifier model is given as;

$$\mathrm{E_{REC-OUT}(t)} = \mathrm{E_{REC-IN}(t)} \times \eta_{\mathrm{REC}} \quad (3.63)$$

$$\mathrm{E_{REC-IN}(t)} = \mathrm{E_{SUR-AC}(t)} \times \eta_{\mathrm{REC}} \quad (3.64)$$

At any time t,

$$\mathrm{E_{SUR-AC}(t)} = \mathrm{E_{DEG}(t)} - \mathrm{E_{load}(t)} \quad (3.65)$$

$\mathrm{E_{REC-OUT}(t)}$ is the hourly energy output from rectifier rated in kWh, $E_{REC-IN}(t)$ is the hourly energy input to rectifier in kWh, $E_{SUR-AC}(t)$is the amount of surplus energy from AC sources in kWh, η_{REC} is the efficiency of rectifier, $E_{DEG}(t)$ is the hourly energy generated by diesel generator, and $E_{load}(t)$ is the load.

3.2.4.10.4 Charge controller

In order to prevent overcharging of a battery, a charge controller is used to sense when the batteries are fully charged and to stop or reduce the amount of energy flowing from the energy source to the batteries. The model of the charge controller is given as;

$$\mathrm{E_{CC-OUT}(t)} = \mathrm{E_{CC-IN}(t)} \times \eta_{\mathrm{CC}} \quad (3.66)$$

$$\mathrm{E_{CC-IN}(t)} = \mathrm{E_{REC-OUT}(t)} - \mathrm{E_{SUR-DC}(t)} \quad (3.67)$$

At any time t,

$$\mathrm{E_{SUR-AC}(t)} = \mathrm{E_{DEG}(t)} - \mathrm{E_{load}(t)} \quad (3.68)$$

$E_{CC-OUT}(t)$ is the hourly energy output from charge controller rated in kWh, $E_{CC-IN}(t)$ is the hourly energy input to controller in kWh, $E_{SUR-DC}(t)$ is the amount of surplus energy from DC sources in kWh, η_{CC} is the efficiency of controller, $E_{REC-OUT}(t)$ is the hourly energy output from the rectifier in kWh

3.2.4.10.5 The Battery

The battery state of charge (SOC) is the cumulative sum of the daily charge/discharge transfers. The battery serves as an energy source entity when discharging and a load when charging. At any time, t, the state of battery is related to the previous state of charge and to the energy production and consumption situation of the system during the time from $(t-1)\ to\ t$. During the charging process, when the total output of all generators exceeds the load demand, the available battery bank capacity at time, t, can be described as;

$$\mathrm{E_{BAT}(t)} = \mathrm{E_{BAT}(t-1)} - \mathrm{E_{CC-OUT}(t)} \times \eta_{\mathrm{CHG}} \quad (3.69)$$

Where $E_{BAT}(t)$ the energy stored in the battery at time t is rated in kWh, $E_{BAT}(t-1)$ is the energy stored in the battery at time (t-1) in kWh, and η_{CHG} is the charging efficiency of the battery. On the other hand, when the load demand is higher than the generated energy, the battery bank will be in a state of discharge. Hence, the battery bank capacity that would be available at a time t is given as;

$$\mathrm{E_{BAT}(t)} = \mathrm{E_{BAT}(t-1)} - \mathrm{E_{NEEDED}(t)} \quad (3.70)$$

Where $E_{NEEDED}(t)$ is the available energy needed at a particular time t. is rated in kWh, $E_{BAT}(t-1)$ is the energy stored in the battery at time (t-1) in kWh, and η_{CHG} is the charging efficiency of the battery.

If d is the ratio of minimum allowable state of charge (SOC) voltage limit to the maximum SOC voltage across the battery terminals when it is fully charged. The Depth of Discharge (DOD) of the battery is given as;

$$\mathrm{DOD} = (1-\mathrm{d}) \times 100 \quad (3.71)$$

DOD is a measure of how much energy has been withdrawn from a storage device, expressed as a percentage of full capacity. The maximum value of SOC is 1, and the minimum SOC is determined by maximum depth of discharge (DOD).

$$\mathrm{SOC_{Min}} = 1 - \frac{\mathrm{DOD}}{100} \quad (3.72)$$

3.2.4.11 General Power Model of the entire System

For the standalone with generator and battery backup, the power model is given as;

$$P(t) = \sum_{PVG=1}^{N_{PV}} P_{PVG} + \sum_{DEG=1}^{N_G} P_{DEG} \quad (3.73)$$

N_{PV} is the number of PV unit and N_G is the number of generator unit. This generated power will feed the base station loads. The diesel generator has the constraint to always operate between 80 and 100% of their kW power rating. When this generated power exceeds the load demand then the surplus of energy will be stored in the battery bank. This energy will be used when deficiency of power occurs in order to meet the load demand. The charged quantity of the battery bank has the constraint $SOC_{Min} \leq SOC(t) \leq SOC_{Max}$. The dump load will draw excess energy produced by the renewable generators or diesel generators but unused when the load does not need all the energy and the battery has reached its maximum capacity and cannot store more energy. The approach involves the minimization of a cost function subject to a set of equality and inequality constraints.

3.2.4.12 Mathematical Cost Model (Economic & Environmental Costs) the Systems

In this research, we developed a mathematical model of a system that could deploy the best renewable energy options available at any base station located in any part of Nigeria. The term "**Best"** as used in this work shows the sum of the minimum economic and environmental costs of the considered options. For this proposal, we adopted the Optimization model for standalone BFPV and MFPV and compared two of them and determine the model that will give the optimal benefit to the telecommunication operators in terms of cost, environmental impact (health and safety), and land area as used in the PVSyst Version 7.4.8 software.

3.2.4.12.1 The Annualized Cost of a Component

The annualized cost of a component includes annualized capital cost, annualized replacement cost, annual operation and maintenance (O&M) cost, emissions cost and annual fuel cost (generator). Operation cost is calculated hourly on daily basis. In this, price of diesel per liter is taken as N1700.00 at a prevailing interest rate of 27.5% as listed by CBN in June, 2024.

3.2.4.12.2 Annualized Capital Cost

The annualized capital cost of a system component is equal to the total initial capital cost multiplied by the capital recovery factor. Annualized capital cost is given as;

$$\mathrm{C_{ACP}} = \mathrm{C_{CP}} \times \mathrm{CRF}\left(\mathrm{i}, \mathrm{R_{Proj}}\right) \tag{3.74}$$

C_{CP} is the initial capital cost of the component, and $CRF\left(i, R_{Proj}\right)$ is the capital recovery factor of the project.

3.2.4.12.3 Annualized Replacement Cost

This is the annualized is the annualized value of all the replacement costs occurring throughout the lifetime of the project, minus the salvage value at the end of the project lifetime. This is given as;

$$\mathrm{C_{ARep}} = \mathrm{C_{ReP}} \times \mathrm{f_{Rep}} \times \mathrm{SFF}\left(\mathrm{i}, \mathrm{R_{Comp}}\right) - \mathrm{S} \times \mathrm{SFF}\left(\mathrm{i}, \mathrm{R_{Proj}}\right) \tag{3.75}$$

C_{ReP} is the component replacement cost, f_{Rep} a factor arising because the component lifetime can be different from the project lifetime and it can be calculated using equation 3.76.

$$\mathrm{f_{Rep}} = \begin{cases} \mathrm{CRF}\left(\mathrm{i}, \mathrm{R_{Proj}}\right)/\mathrm{CRF}\left(\mathrm{i}, \mathrm{R_{Rep}}\right), & \mathrm{R_{Rep}} > 0 \\ 0 & \mathrm{R_{Rep}} = 0 \end{cases} \tag{3.76}$$

The replacement cost R_{Rep} can be calculated using equation 3.76 given as;

$$\mathrm{R_{Rep}} = \mathrm{R_{Comp}} \times \Gamma\left(\frac{\mathrm{R_{Proj}}}{\mathrm{R_{Comp}}}\right) \tag{3.77}$$

The symbol Γ used in equation 3.77 is an integer function, returning the integer portion of a real value. $SFF(\,)$ represents the sinking fund factor which is used to calculate the future value of a series of equal annual cash flows. It is given as;

$$\mathrm{SFF(i, N\,)} = \frac{\mathrm{i}}{(1+\mathrm{i})^{\mathrm{N}} - 1} \tag{3.78}$$

N in equation 3.78 is the number of years which is 25 years as used in this research. The salvage value (S) of the component at the end of 25 years which is the project lifetime is proportional to its remaining life is calculated using equation 3.80 as;

$$\mathrm{S} = \mathrm{C_{rep}}\left(\frac{\mathrm{R_{rem}}}{\mathrm{R_{com}}}\right) \tag{3.80}$$

Where R_{rem} the remaining life of the component at the end of 25 years is given as;

$$\mathrm{R_{rem}} = \mathrm{R_{com}} - \left(\mathrm{R_{proj}} - \mathrm{R_{rep}}\right) \tag{3.81}$$

3.2.4.12.4 Operating Cost per Annum

The operating cost is the annualized value of all costs and revenues other than initial capital costs and is calculated thus;

$$C_{aop} = \sum_{t=1}^{365} \left\{ \sum_{t=1}^{24} [C_{oc}(t)] \right\} \quad (3.82)$$

$C_{oc}(t)$ is the cost of operating the component at time t.

3.2.4.12.5 Cost of CO_2 for operating the diesel generator per annum

The emission of CO_2 to the environment has a huge impact in energy optimization of the proposed model. This will be calculated in United States Dollar ($) as used in the PVSyst software. This is calculated thus;

$$C_{emission} = \frac{c_{C0_2} A_{CO_2} + c_{C0} A_{CO} + c_{S0_2} A_{SO_2} + c_{UHC} A_{UHC} + c_{PM} A_{PM} + c_{N0_X} A_{NO_X}}{1000} \quad (3.83)$$

the parameters used in equation 3.83 are defined in table 3.21 as follows;

Table 3.21: Description of parameters

S/N	Parameter	Description
1	c_{C0_2}	cost for the emmission of CO_2 in $ per unit time
2	c_{C0}	cost for the emmission ofCO in $ per unit time
3	c_{UHC}	cost for the emmission ofunburned hydrocarbons in $ per unit time
4	c_{PM}	cost for the emmission particulate matter in $ per unit time
5	c_{PM}	cost for the emmission particulate matter in $ per unit time
6	c_{S0_2}	cost for the emmission of SO_2 in $ per unit time
7	c_{N0_X}	cost for the emmission of NO_X in $ per unit time
8	c_{N0_X}	cost for the emmission of NO_X in $ per unit time
9	A_{C0_2}	emmission of CO_2 per annum in kg/yr
10	A_{C0}	emmission of CO per annum in kg/yr
11	A_{UHC}	emmission of unburned hydrocarbons in kg/yr
12	A_{PM}	emmission of particulate matter in kg/y
13	A_{S0_2}	emmission of SO_2 per annum in kg/yr
14	A_{N0_X}	emmission of NO_X per annum in kg/yr

Table 3.21 shows the description of parameters. Therefore, for the purpose of this research and simulation, the following were considered;

Total Cost of a Component (TCC) = Economic Cost (EC) + Environmental Cost (EVC)

EC = Capital Cost (CC) + Replacement Cost (RC) + O&M Cost + Fuel Cost (FC)

EVC = Emission Cost (EMC)

The annualized cost of component is calculated using equation 3.68 as;

$$C_{acomp} = C_{acap} + C_{arep} + C_{aop} + C_{aemission} \quad (3.84)$$

The annualized total cost of component is calculated using equation 3.85 as;

$$C_{ann,tot,c} = \sum_{C=1}^{\mathrm{N}_C} \left(C_{acap,c} + C_{arep,c} + C_{aop,c} + C_{aemission,c}\right) \quad (3.85)$$

$C_{acap,c}$ is the capital cost of component per annum;

$C_{arep,c}$ is the replacement cost of component per annum;

C_{aop}, c is the operating cost of component per annum;

$C_{aemission,c}$ is the emission cost of component per annum;

Considering equation 3.81, we can derive the EC and EVC model by using the respective annualized total cost.

Therefore, the economic and environmental cost model for running a diesel generator alone is given as;

$$C_{ann,tot,g} = \sum_{g=1}^{N_g} \left(C_{acap,g} + C_{arep,g} + C_{aop,g} + C_{aemission,} + C_{afg}\right) \quad (3.86)$$

where;

$C_{acap,g}$ is the capital cost of diesel generator per annum;

$C_{arep,g}$ is the replacement cost of diesel generator per annum;

$C_{aop,g}$ is the operating cost of diesel generator per annum;

C_{afg} is the cost of fuel used by diesel generator per annum

The economic and environmental cost model for running a MFPV alone is given as;

$$C_{ann,tot,mf} = \sum_{mf=1}^{N_{mf}} \left(C_{acap,mf} + C_{arep,mf} + C_{aop,mf} + C_{aemission,}\right) \quad (3.87)$$

where;

$C_{acap,\mathrm{m}f}$ is the capital cost of MFPV per annum;

$C_{arep.mf}$ is the replacement cost of MFPV per annum;

$C_{aop,mf}$ is the operating cost of MPV per annum;

Economic and environmental cost model for running a BFPV alone is given as;

$$C_{ann,tot,bf} = K + Q \quad (3.88)$$

where;

$$K = \sum_{mf=1}^{N_{mf}} \left(C_{acap,mf} + C_{arep,mf} + C_{aop,mf} + C_{aemission,}\right)$$

$$\mathrm{Q} = 0.3\mathrm{K} \quad (3.89)$$

Economic and environmental cost model for running batteries alone is given as;

$$C_{ann,tot,b} = \sum_{b=1}^{N_b} \left(C_{acap,b} + C_{arep,b} + C_{aop,b} + C_{aemission,}\right) \quad (3.90)$$

where;

$C_{acap,b}$ is the capital cost of batteries per annum;

$C_{arep,b}$ is the replacement cost of batteries per annum;

$C_{aop,b}$ is the operating cost of batteries per annum;

Economic and environmental cost model for running converters alone is given as;

$$C_{ann,tot,cv} = \sum_{cv=1}^{N_{cv}} \left(C_{acap,cv} + C_{arep,cv} + C_{aop,cv}\right) \quad (3.91)$$

where;

$C_{acap,cv}$ is the capital cost of converters per annum;

$C_{arep,cv}$ is the replacement cost of converters per annum;

$C_{aop,cv}$ is the operating cost of converters per annum;

From the above equations, we can model the economic cost of running MFPV, Diesel Generator, Battery, and Converter thus;

Economic and environmental cost model for running MFPV + Diesel generator + Batteries + Converter is given as;

$$C_{ann,tot,(mf+g+b+cv)} = C_{ann,tot,mf} + C_{ann,tot,g} + C_{ann,tot,b} + C_{ann,tot,cv} \quad (3.92)$$

Economic and environmental cost model for running BFPV + Batteries + Converter is given as;

$$C_{ann,tot,(bf+b+cv)} = 1.3C_{ann,tot,mf} + C_{ann,tot,b} + C_{ann,tot,cv} \quad (3.93)$$

Equations 3.88 and 3.89 are the required model that will calculate the lifecycle cost optimization

of the proposed system. Note that in the model of BFPV, the effect of running the generator is not inclusive because the proposed standalone is without generator. Therefore, each of the equation will give the total cost of installing and operating the system over its operational life. The simulation result from PVSyst version 7.4.8 will give us the optimal configuration of the energy system of each model that takes into account technical and economic performance of supply options (rated power characteristics for solar Photovoltaic (MPV & BFPV), fuel consumption characteristics for diesel generators (DG) and minimum and maximum state of charge (SOC) of a battery bank, the 25-year life cycle cost (LCC) of equipment, locally available energy resources (hourly solar insolation data (kW/m^2), hourly DHI, GHI, and NHI (kW/m^2), albedo, tilt angle, azimuth angle, cost of fossil fuels, environmental costs, and system efficiency.

3.2.4.13. The energy optimization model

Optimization methods had been a major concern for man for many years (Waqas, 2011). Prior to this time, there were no defined scientific rules for optimum conditions. With the advancement in science and technology, everything was considered to be based on certain reasons or logics. Mathematical calculations involving process of optimization have become more famous in recent years. By optimization i s to find the best solution for a particular problem. A problems dealing with the cost will require the best cost to be as less as possible. Conversely, a problems dealing with profit will see the maximum value as the best answer. Therefore, 'Optimum' is the word which is used to demonstrate the meaning of best, and the process of finding the best solution to a particular problem is known as the process of optimization. To solve an optimization problem, we require an optimization algorithm. An optimization algorithm is the algorithm which is used to define an optimized solution for a particular function. Thus, for the standalone MPV/BPV system with constraints under study, we developed the following optimization algorithm.

For MFPV, Minimize,

$$\text{Cost} = \sum_{i} C_{MPV_i} N_{MPV_i} + \sum_{j} C_{G_j} N_{G_j} + \sum_{k} C_{B_k} N_{B_k} + \sum_{m} C_{c_m} N_{c_m} \qquad (3.94)$$

For BFPV and MFPV, Minimize,

$$\text{Cost} = 1.3\sum_{i} C_{MPV_i} N_{MPV_i} + \sum_{k} C_{B_k} N_{B_k} + \sum_{m} C_{c_m} N_{c_m} \quad (3.95)$$

Subject to the constrains;

$$\text{Load (MFPV)} \leq \sum_{i} E_{MPV_i} N_{MPV_i} + \sum_{j} E_{G_j} N_{G_j} \quad (3.96)$$

$$\text{Load (BFPV)} \leq 1.3\sum_{i} E_{MPV_i} N_{MPV_i} \quad (3.97)$$

$$\text{Maximum power } \leq \sum P_{C_n} N_{C_n} \quad (3.98)$$

The parameters are defined in table 3.22

Table 3.22: parameter description

S/N	PARAMETER	DESCRPTION
1	C_{MPV_i}	Cost of a MFPV module
2	N_{MPV_i}	Number of MFPV modules
3	N_{G_j}	Number of diesel generators
4	C_{G_j}	Cost of a diesel generator
5	C_{B_k}	Cost of a battery
6	N_{B_k}	Number of battery bank to be use.
7	C_{c_m}	Cost of a converter
8	N_{c_m}	Number of converters
9	P_{C_n}	Maximum output power of converter n
10	SOC_{min}	State of battery charge at minimum
11	SOC_{max}	State of battery charge at maximum
12	E_{MPV_i}	kWh generated by photovoltaic module i
13	E_{G_j}	kWh generated by a diesel generator j

In this optimization process, decision variables are the sizes of system components, and the

objective functions are the costs and emissions in the environment.

3.2.4.13.1 Objective function

The objective functions to be minimized are the total costs (in Naira) and the emissions of pollutant (kg of CO_2).

3.2.4.13.2 Costs

The costs objective function is the Total Net Present Cost of the system (NPC), which includes the cost of the initial investment plus the discounted present values of all future costs throughout the total life of the installation. The life of the system is usually considered to be the life of the PV panels, which have a longer lifespan. The costs to be considered are;

i. Cost for purchasing the MFPV panels, the batteries, the inverter, the charge regulator, and the Diesel generator.
ii. Costs of maintenance of the components.
iii. Costs of replacing the components throughout the life of the system.
iv. Costs of operation and maintenance of components throughout the life of the system.
v. Cost of the fuel consumed throughout the life of the system.

3.2.4.13.3 Pollutant Emissions

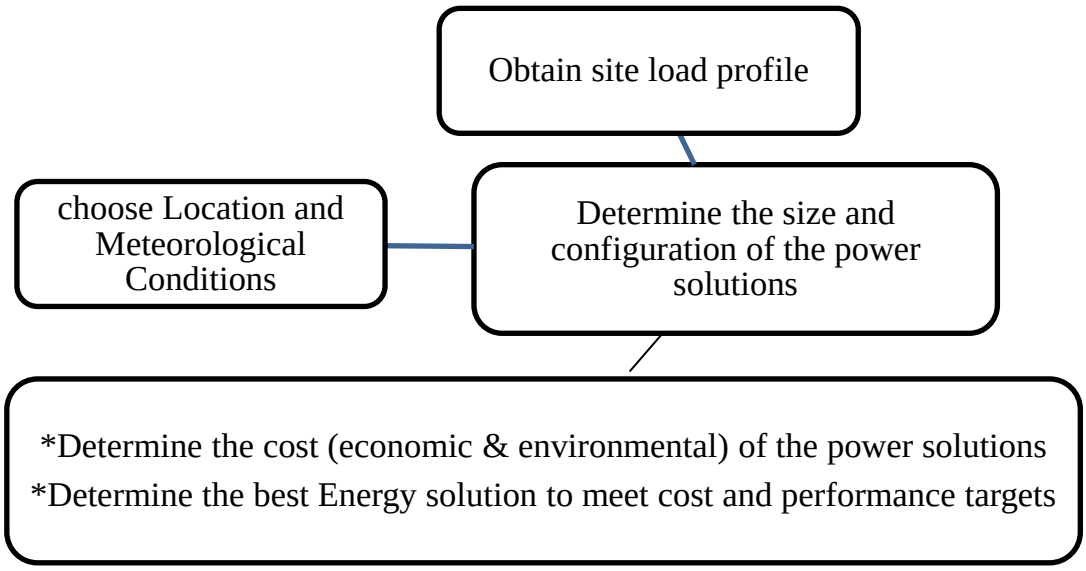

Figure 3.33: Model for choosing Power Solution for a BTS Site.

To measure the pollutant emissions, the weight of CO_2, in kg is considered; it represents the largest percentage of all emissions when fuel is burnt (Sonntag et al., 2023) and it is the main cause of the greenhouse effect. It is considered that the total amount of kg of CO_2 produced by the system in one year is the correct measure of the pollutant emissions and, therefore, it can be used as the objective to be minimized. The developed algorithm has as input data the number of kg of CO_2 produced per litre of fuel consumed by the diesel generator. This value depends on the characteristics of the diesel generator and of the characteristics of the fuel, and it usually falls in the range of 2.4-2.8 kg/l (Vodafone Germany, 2007).

In this research, the useful parameters for making the decision on the type standalone type of energy solution suitable for a site and its location are grouped into Total Cost of Energy Generation and Total Environmental impact of each energy solution. These two summarize all the factors we proposed for evaluating the suitability of energy solution for any BTS in Nigeria. The model is as shown in figure 3.33.

3.2.4.13.4 Net Present Cost (NPC) for each component

The total net present cost (NPC) of a system is the present value of all the costs that it incurs over its lifetime minus the present value of all the revenue that it earns over its lifetime. Revenues include salvage value and grid sales revenue. The Net Present Cost (NPC) for each component is derived using equation 3.99.

$$C_{NPC} = \frac{C_{ann,tot}}{CRF\left(i, R_{proj}\right)} \tag{3.99}$$

The capital recovery factor (CRF) is calculated using;

$$CRF = \frac{i \times (1+i)^N}{(1+i)^N - 1} \tag{3.100}$$

The economic optimization identifies the most financially attractive solution for two models, diesel generator, and solar power. Data for the two optimized scenarios are obtained and graphed to present the viability and financial impact of each scenario for adoption.

3.2.4.14 Calibration of the model

Without data validation coupled with optimization and modelling there is little reason to believe that the conclusions stated in any paper has applicability beyond the immediate circumstances stated. Before using the measured data gotten from NASA datasets in simulating the individual components of a MFPV/ Diesel system, we must establish the accuracy of the software used. If the simulated data predicted by the software programs do not fall within the bounds of the measured data, then there is either a problem with how the models are formulated or a problem with the models that the programs use. The algorithm that HOMER uses to synthesize solar data is based on the work of (Perez et al., 2022). The realistic nature of synthetic data created by this algorithm is demonstrated in the geographical site and daily sun-hour.

In carrying out this study, simulation was done by selecting a site from each of the six geopolitical zones based on their respective irradiation as obtained from NASA data sheet. HOMER software was used for these processes. It uses single axis tracking heliotropism process of a sunflower. In each case, electrical parameters of the selected module were used and daily sun irradiation used for the optimization are shown in figures 3.34 (a – f).

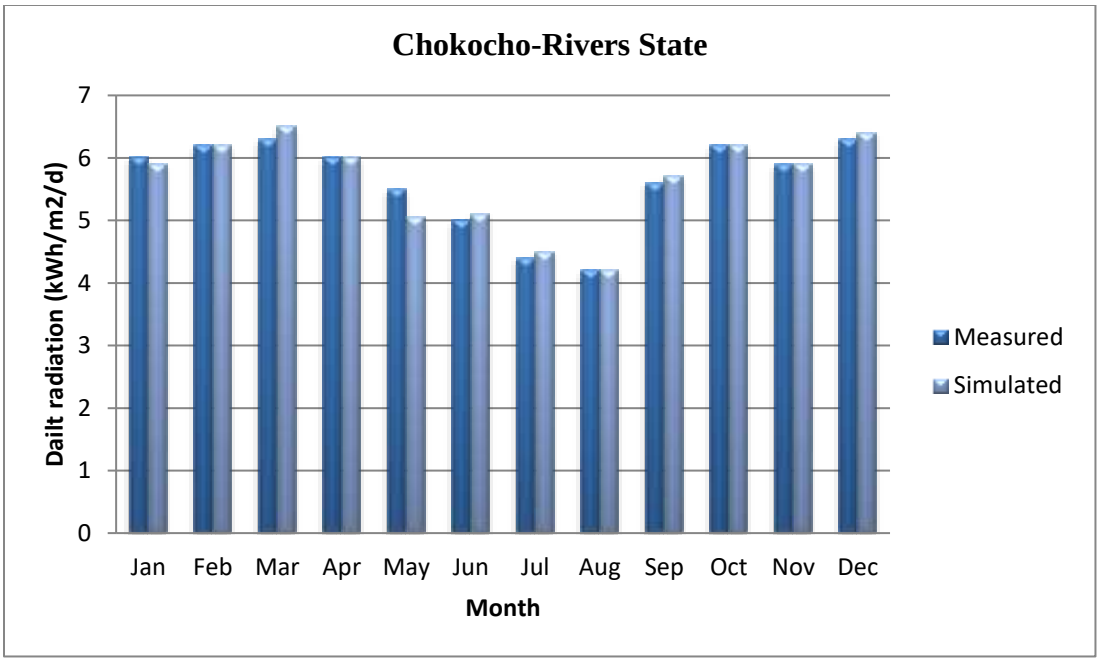
Chokocho-Rivers State
Dailt radiation (kWh/m2/d)
0
1
2
3
4
5
6
7
Jan
Feb
Mar
Apr
May
Jun
Jul
Aug
Sep
Oct
Nov
Dec
Month
Measured
Simulated

(a)

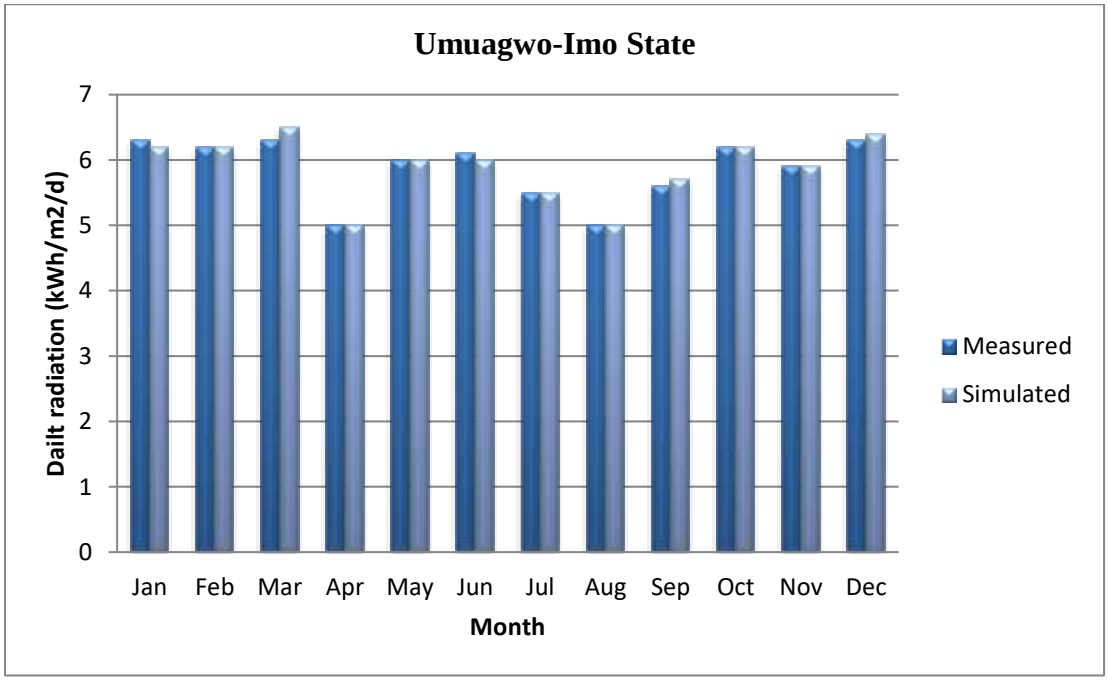
Umuagwo-Imo State
Dailt radiation (kWh/m2/d)
0
1
2
3
4
5
6
7
Jan
Feb
Mar
Apr
May
Jun
Jul
Aug
Sep
Oct
Nov
Dec
Month
Measured
Simulated

(b)

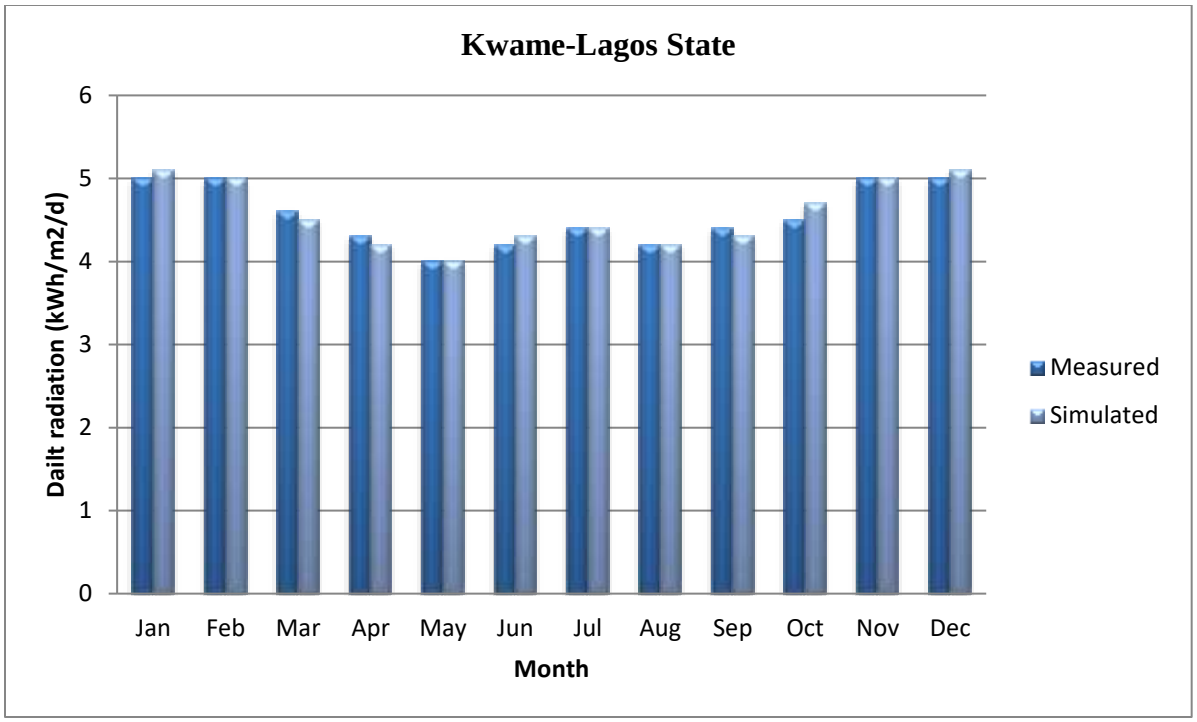
Kwame-Lagos State
Dailt radiation (kWh/m2/d)
0
1
2
3
4
5
6
Jan
Feb
Mar
Apr
May
Jun
Jul
Aug
Sep
Oct
Nov
Dec
Month
Measured
Simulated

(c)

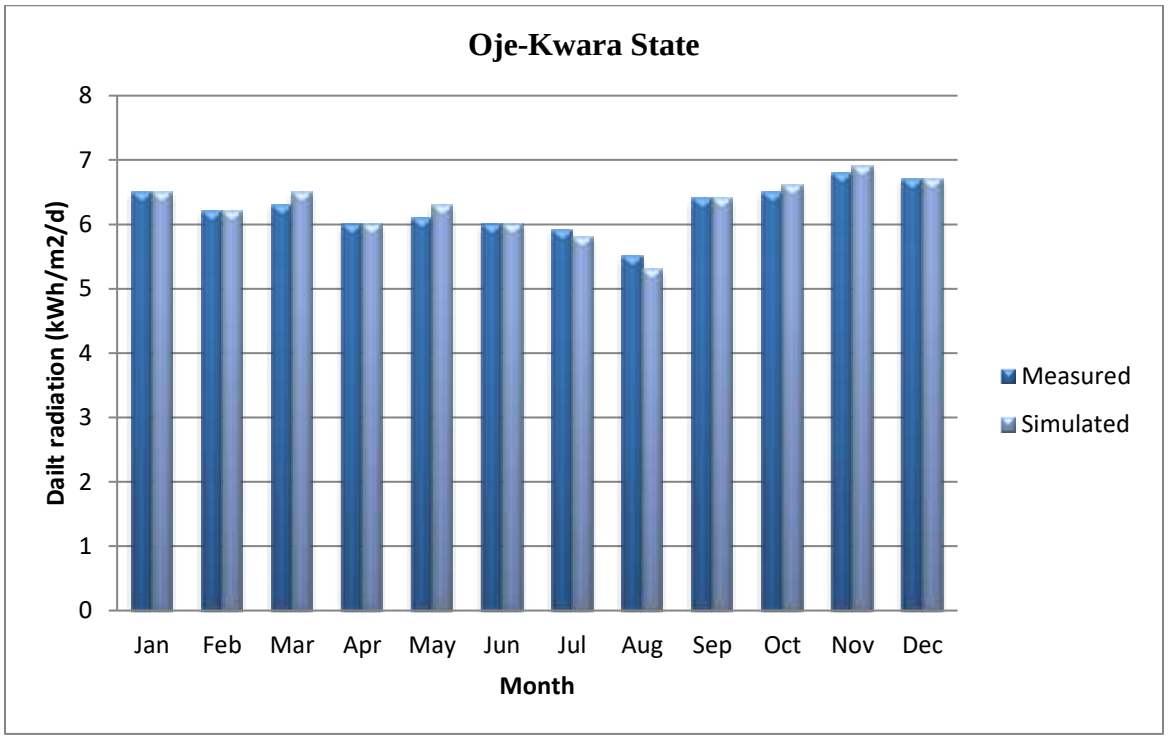
Oje-Kwara State
Dailt radiation (kWh/m2/d)
0
1
2
3
4
5
6
7
8
Jan
Feb
Mar
Apr
May
Jun
Jul
Aug
Sep
Oct
Nov
Dec
Month
Measured
Simulated

(d)

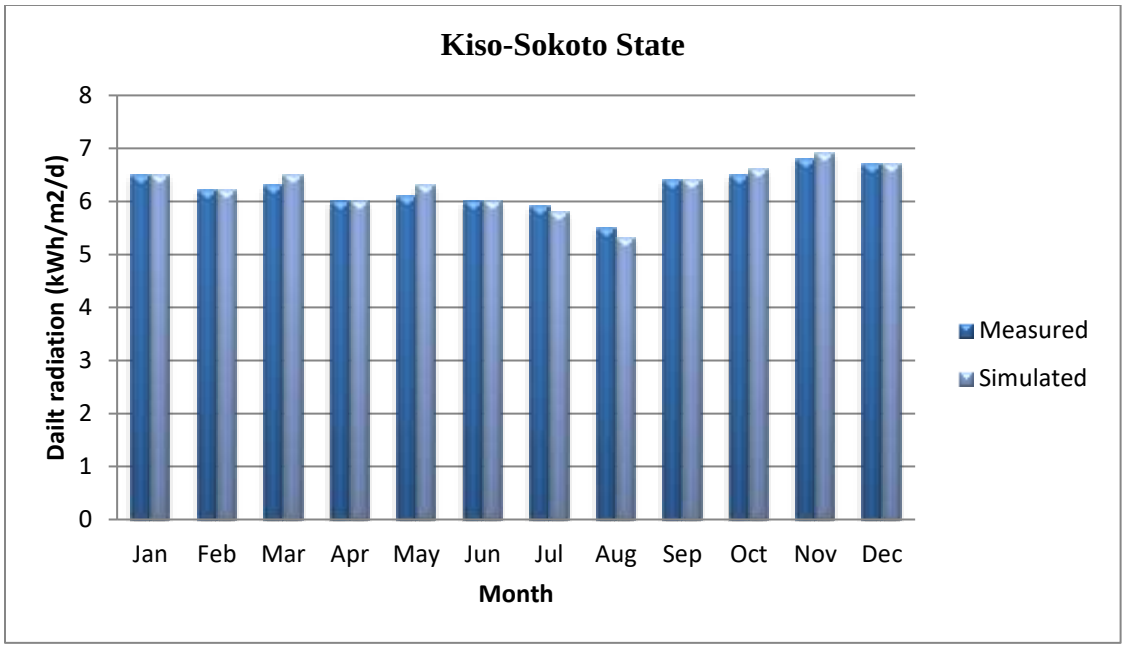

(e)

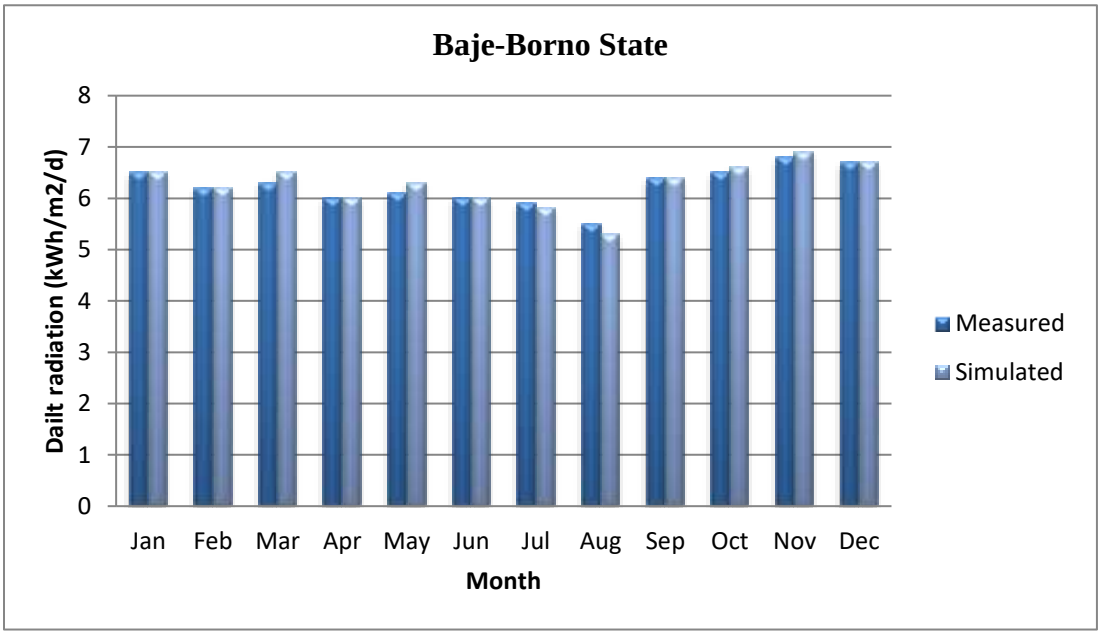

(f)

Figures 3.34: Array of power distribution in (a) Chokocho (b) Umuagwo (c) Kwame (d) Oje (e) Kiso (f) Baje.

Figures 3.34 shows the arrays power distribution from the months of January 01/01/2024 to December 31/12/2024 from the six locations. The deep blue colour shows the measured solar data from NASA for the locations, while the light blue colour shows the data created by specifying the study location's latitude and monthly average radiation values as shown in figure 3.34. The graphs, shows that the simulated data from HOMER fall within the bounds of the measured solar radiation which is an indication that solar data produce virtually the same simulation results as real data.

3.2.4.15 Daily Load Profile of a TBS

Hourly load demand of a Micro Base Station Site has been given as an input in HOMER and then it generates daily and monthly load profile for a year as shown in figure 3.35. It has been found that this site consumes energy around 254kWh/day with a peak demand of nearly 10.67kW. Table 3.23 shows the hourly load demand for radio base station and climate & auxiliary equipment.

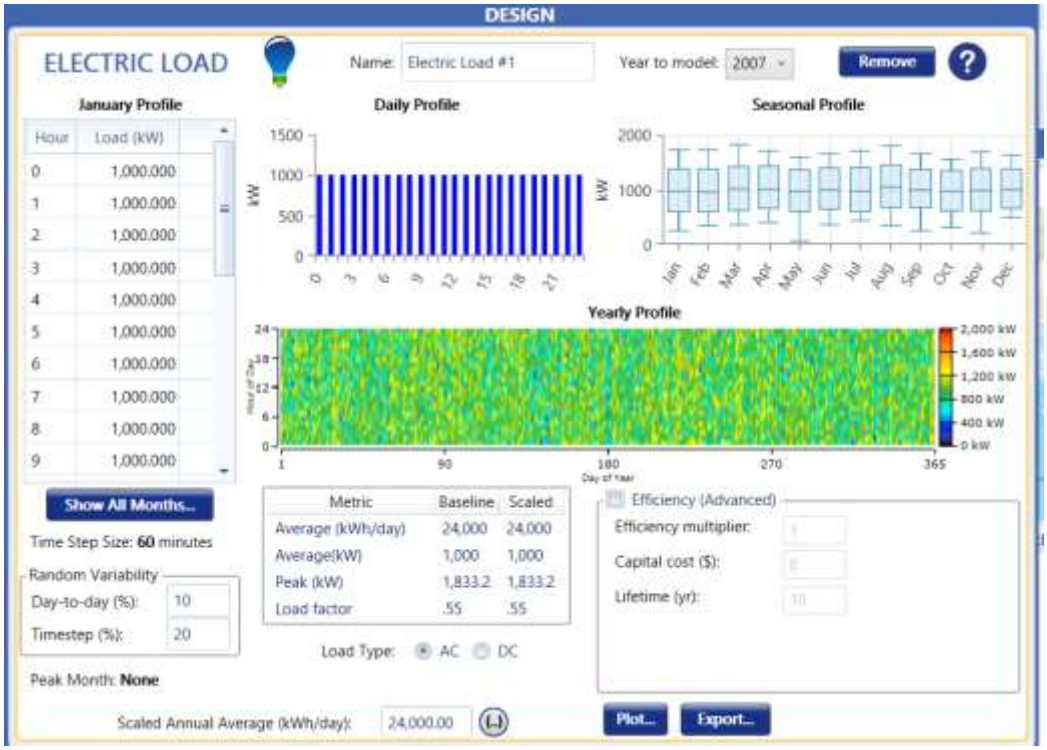

Figure 3.35: Overview of HOMER output graphic for DC Load of Radio Base Station Equipment.

From figure 3.35, the baseline load of the micro-base station is 24kW/h/day with a load factor of

0.55 and time step of 20 from January to December of the year under review. The solar irradiation for the daily and seasonal profile was maintained at 1000W/m^2 and temperature of 25^0C. For the yearly profile, the solar irradiation varies between 800W/m^2 to 1000W/m^2 throughout the year as shown in figure 3.35.

Table 3.23: Load Inputs for Radio Base Station, Climate and Auxiliary Equipment.

Hour	**Radio Base Station Baseline Data**	**Climate & Auxiliary Equipment Baseline Data**
	Load (kW)	**Load (kW)**
00:00 - 01:00	7.860	2.790
01:00 - 02:00	7.860	2.790
02:00 - 03:00	7.860	2.790
03:00 - 04:00	7.860	2.790
04:00 - 05:00	7.860	2.790
05:00 - 06:00	7.860	2.790
06:00 - 07:00	7.860	2.790
07:00 - 08:00	7.860	2.590
08:00 - 09:00	7.860	2.590
09:00 - 10:00	7.860	2.590
10:00 - 11:00	7.860	2.590
11:00 - 12:00	7.860	2.590
12:00 - 13:00	7.860	2.590
13:00 - 14:00	7.860	2.590
14:00 - 15:00	7.860	2.590
15:00 - 16:00	7.860	2.590
16:00 - 17:00	7.860	2.590
17:00 - 18:00	7.860	2.790
18:00 - 19:00	7.860	2.790
19:00 - 20:00	7.860	2.790
20:00 - 21:00	7.860	2.790
21:00 - 22:00	7.860	2.790
22:00 - 23:00	7.860	2.790
23:00 - 00:00	7.860	2.790
Average (kWh/d)	189	65.0

3.2.4.16 Model parameters for diesel generator

Diesel generator technology is widespread and the development of the power plant is relatively easy. The price of diesel fuel is ₦1800 ($1.2/L) based on federal government approved pump price in Nigeria as at August, 2024. This price varies considerably based on region, transportation costs, and current market price. The details of diesel generator model parameters are shown in table 3.24. The diesel backup system is operated at times when the output from solar systems fails to satisfy the load and when the battery drained.

Table 3.24: Model parameters of Diesel Generator

AC Generator type: 25kVA Diesel Generator	Value
Size Considered (kW)	20 (25kVA)
Number of generator	1
Lifetime	21,900 hrs (5yr x 12hr x 365ds)
Minimum load ratio	30 %
Heat recovery ratio	0 %
Fuel used	Diesel
Fuel curve intercept	0.08 L/hr/kW
Fuel curve slope	0.25 L/hr/kW
Fuel: Diesel	
Price	₦1800 ($1.2/L)
Lower heating value	43.2 MJ/kg
Density	820 kg/m^3
Carbon content	88%
Sulphur content	0.33%

3.2.4.17 Economics and Constraints

The project lifetime is estimated to last 25 years. The annual interest rate is fixed at 27.25%. There is no capacity shortage for the system and operating reserve is 10% of hourly load. The operating reserve as a percentage of hourly load was 10%. Meanwhile, the operating reserve as a percentage of solar power output 25%. Operating reserve is the safety margin that helps ensure reliability of the supply despite variability in electric load. The constraints inputs required by software are given in table 3.25.

Table 3.25: constrain input

Maximum annual capacity shortage:	**0%**
Minimum renewable fraction:	0%
Operating reserve as percentage of hourly load:	10%
Operating reserve as percentage of annual peak load:	0%
Operating reserve as percentage of solar power output:	25%

3.2.4.18 System Economics

The capital costs for all system components including PV module, diesel generator, inverter, battery and balance of system prices are based on quotes from PV system suppliers inherent in the software. The figures used in the analysis are therefore only indicative. The replacement costs

of equipment are estimated to be within 20% lower than the initial costs, but because decommissioning and installation costs need to be added, we assumed that they are the same as the initial costs of the PV array, diesel generator, Inverter and battery maintenance costs are estimates based on approximate time required and estimated wages for this sort of work in Nigeria. All initial costs including installation and commissioning, replacement costs and operating & Maintenance costs at site are summarized in Tables 3.26 to 3.31. All costs presented are converted to Nigerian Naira using the prevailing exchange rate of N1600/$ since the software cannot recognize the naira.

Table 3.26: Economic data for Diesel generator

SYSTEM COMPONENT	**PARAMETER**	**VALUE**
DG	- Sizes considered	25kVA (20kW)
	- Operational lifetime	25,000h
	- Intercept coefficient	0.08L/h/kW
	- Capital cost	N800,000/W
	- Replacement cost	N800,000/kW
	- O&M cost	N1600/h

Table 3.27: Economic data control parameters

SYSTEM COMPONENT	**PARAMETER**	**VALUE**
Control Parameters	- Annual interest rate	27.5%
	- project lifetime	25 years
	- dispatch system	cycling
	- battery initial state of charge	95%
	- Operating reserve as per cent of load, hourly load.	20%
	- Carbon emission penalty	N3520/t
	- Diesel price	N1920/L

Table 3.28: Economic data control BFPV module

SYSTEM COMPONENT	PARAMETER	VALUE
BFPV	- Size considered - Operational lifetime - Efficiency - System tracking - Capital cost -Replacement cost O&M cost per year	900W 25years 90% Two axis N6400W N6400/W 16000/W

Table 3.29: Economic data control MFPV module

SYSTEM COMPONENT	PARAMETER	VALUE
MFPV	- Size considered - Operational lifetime - Efficiency - System tracking - Capital cost - Replacement cost - O&M cost per year	450W 25years 80% MPPT N3200/W N3200/W 24000/W

Table 3.30: Economic data control Inverter

SYSTEM COMPONENT	PARAMETER	VALUE
Inverter	Size considered	15kW
	Efficiency	90%
	Operational lifetime	15years
	Capital cost	$0.5/W
	Replacement cost	N800/W
	O&M cost per year	N80/W

Table 3.31: Economic data control for LG battery

SYSTEM COMPONENT	PARAMETER	VALUE
LG battery	- Number of batteries	32
	- Round tripe efficiency	90%
	- state of charge	30%
	- Nominal voltage	48
	- Nominal current	550Ah at 20h
	- Nominal capacity	26.4kWh
	- Lifetime throughput	1,075kWh
	- Max. Charge rate	1A/Ah
	- Max. charge current	65A
	-Self-discharge rate	0.1 % per hour
	- operational lifetime	5years
	- Capital cost	N800,000
	- Replacement cost	N800,000
	O&M cost per year	N400,000

The economic data of the systems/components mentioned in tables 3.26 to 3.31 includes; Initial System Costs, Replacement Costs and Operating & Maintenance Costs) of all the components of the system used for the Simulation. The input parameters and system constraints, as described above, were used to simulate the system and perform optimization analysis. HOMER determines the optimal system by choosing suitable system components (system configuration) depending on parameters like solar radiation, diesel price and maximum annual capacity shortage. The feasibility of a configuration is based on the NPC and hourly performance. The results are presented graphically and tabular forms in chapter four of this research.

3.2.4.19 optimal model of the standalone system

The system configuration model to be described is the core of the simulation. Apart from correct costing and optimization, the quality and accuracy of the model and its implementation in the algorithm, greatly determines the usefulness of the simulation results. Figure 3.36 shows one-line diagram of the proposed standalone System.

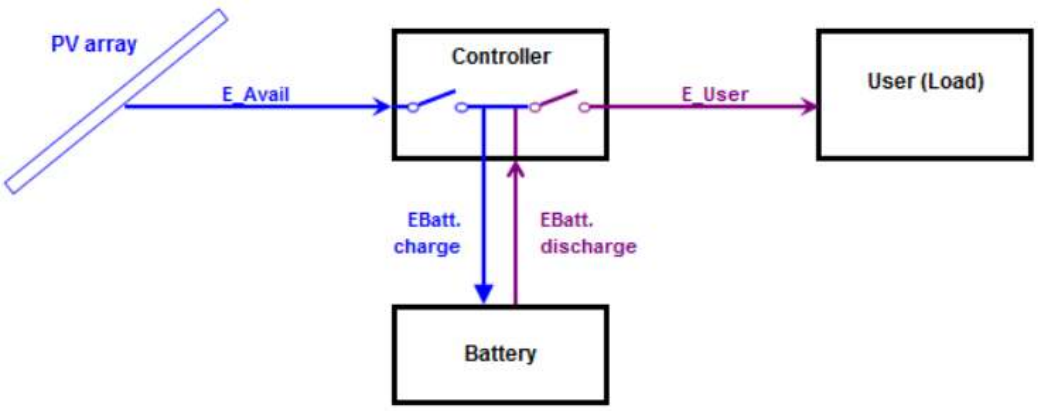

Figure 3.36: one line diagram of the proposed standalone System

This kind of installations is managed with very simple controllers, acting either by disconnecting the battery, or short-circuiting the PV modules when the battery is full. These controllers have always the ability of controlling the load when the battery is empty. Given the values of irradiation on tilted planes, and the consumption patterns previously described, the system behaviour can be simulated using an hourly time step. Based on a system energy balance and on the storage continuity equation, the simulation method used here is heliotropism process of sunflower.

Considering the battery charger output power $P_{chargerc}(t)$, the PV output power $P_p(t)$, and the load power $P_L(t)$ on the simulation step Δt, the battery energy benefit during a charge time Δt_1 is given by ($\Delta t_1 < \Delta t$):

$$C_1(t) = \rho_{ch} \int_{\Delta t_1} \{P_p(t) + P_{charger}(t) - P_l(t)\}\, dt \qquad (3.101)$$

The battery energy loss during a discharge time Δt_2 is given as $(\Delta t_2 < \Delta t)$;

$$C_1(t) = \frac{1}{\rho_{dch}} \int_{\Delta t_2} \{P_p(t) + P_{charger}(t) - P_l(t)\}\, dt \qquad (3.102)$$

The state of charge of the battery defined during the time of simulation time-step Δt is;

$$C(t) = C(t - \Delta t) + \ C_1(t) + C_2(t) \qquad (3.103)$$

When C(t) gets to the stopping threshold (SAR) with an energy benefit $C_2(t)$ within the charge time with the engine generator working, the generator has to be shot down and the charge time Δt_1 during Δt can be calculated using equation 3.104 given thus;

$$\frac{\Delta t_1}{\Delta t} = \left| \frac{SAR - C(t - \Delta t)}{C_1(t)} \right| \qquad (3.104)$$

However, if during the discharge period when the engine generator is stopped and C(t) gets to its Starting threshold (SDM), the motor is started and the discharge time Δt_2 during Δt is calculated using equation 3.105.

$$\frac{\Delta t_2}{\Delta t} = \left| \frac{C(t - \Delta t) - SDM}{C_2(t)} \right| \qquad (3.105)$$

As an input of a simulation time-step Δt (taken as 1h), several variables must be determined: PV output power, load power, battery state of charge, and back-up generator state (ON or OFF). A battery energy balance indicates the operating strategy of the PV/ Diesel system: charge (energy balance positive) or discharge (energy balance negative). If SOC (t) falls below SDM, the motor is started; and if SOC (t) exceeds SAR, it is stopped. So, the charge and discharge times of equations 3.104 and 3.105 must are calculated on the simulation time-step in order to compute the different energy flows in the system.

3.2.4.20. Optimal performance of the two energy configurations at the selected location.

3.2.4.20.1 Umuagwo – Imo state (South – East)

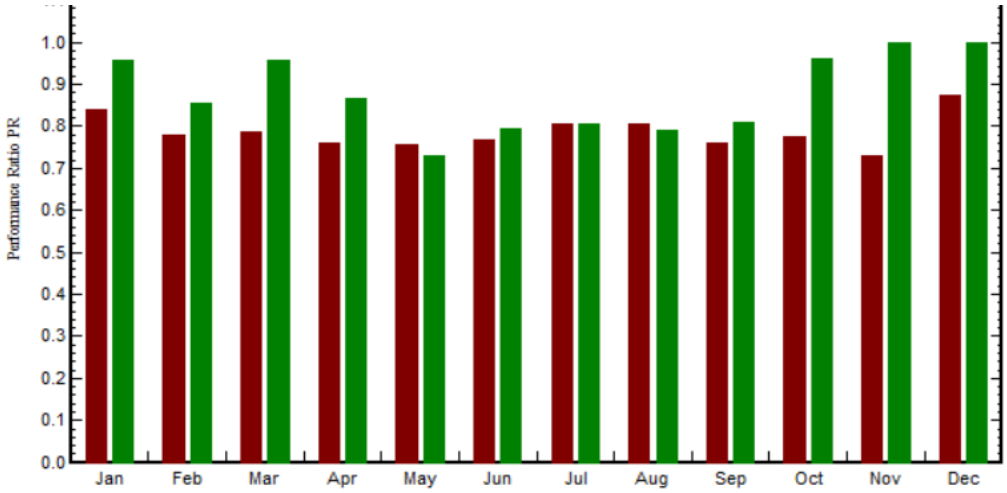

Figure 3.37: performance index of the two energy categories at Umuagwo.

Figure 3.37 shows the optimization performance ratio of the two energy systems as compared by HOMER model. The red bar is the performance index of the MFPV+DG+B configuration in terms of NPC, Land Usage and Pollutant emission while the green bar represents the performance index of the BFPV+B configuration based on the aforementioned criteria. It will be seen from the figure that the BFPV+B configuration gave the optimal performance index of the TBS energy solution

3.2.4.20.2 Chokocho – Rivers state (South – South)

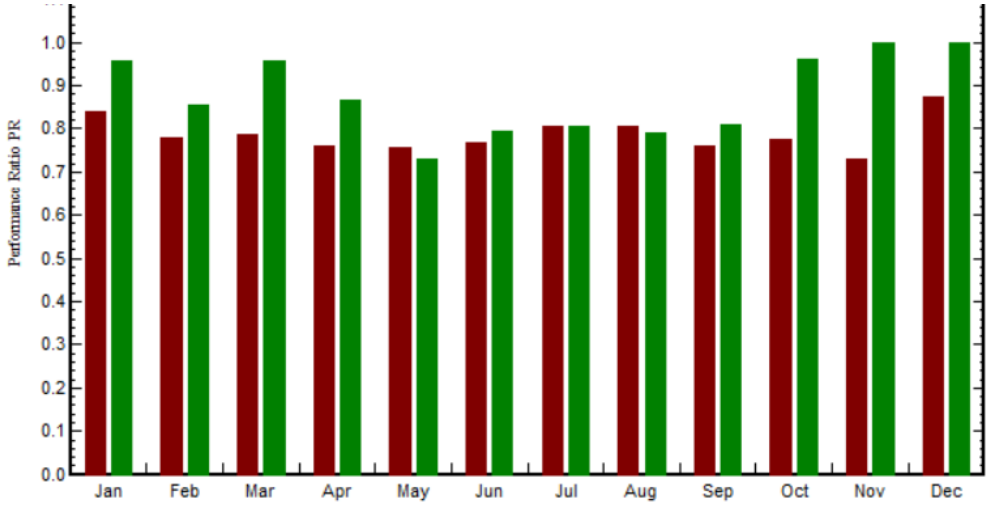

Figure 3.38: performance index of the two energy categories at Chokocho

Figure 3.38 represents the optimization performance ratio of the two energy systems as compared by HOMER model. The red bar is the performance index of the MFPV+DG+B configuration in

terms of NPC, Land Usage and Pollutant emission while the green bar represents the performance index of the BFPV+B configuration based on the aforementioned criteria. It will be seen from the figure that the BFPV+B configuration gave the optimal performance index of the TBS energy solution.

3.2.4.20.3 Kweme – Lagos state (South – West)

Similarly, the red bar is the performance index of the MFPV+DG+B configuration in terms of NPC, Land Usage and Pollutant emission while the green bar represents the performance index of the BFPV+B configuration based on the aforementioned criteria as compared by HOMER model. It will be seen from the figure 3.39 that the BFPV+B configuration gave the optimal performance index of the TBS energy solution. Note also that HOMER simulation at Umuagwo, Chokocho and Kweme gave the same optimal solution. The reason here is the cost of land to locate the TBS is kept constant at each location and pollutant emission from the diesel generator is the same in these areas. This is a clear conformation of the objective under this consideration.

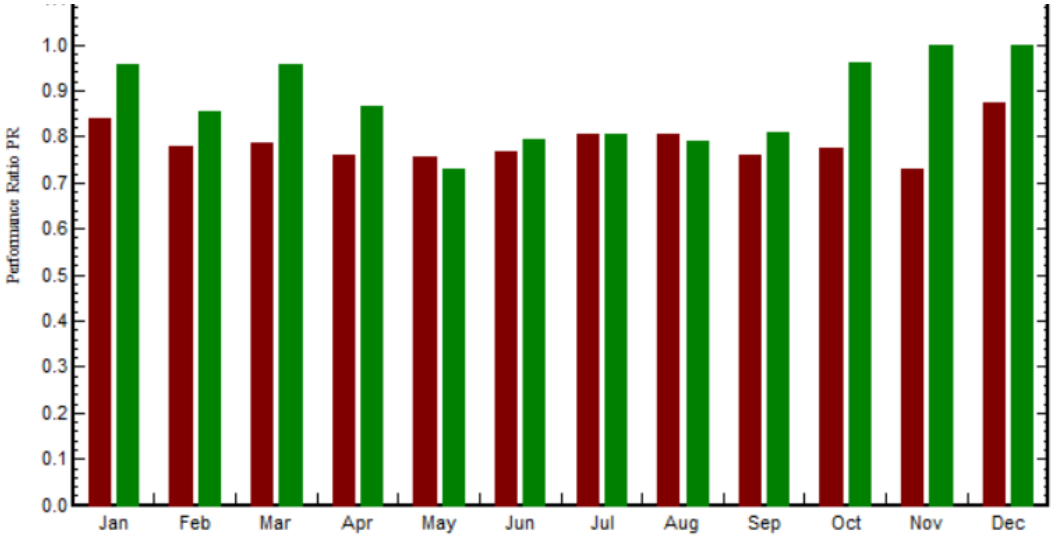

Figure 3.39: performance index of the two energy categories at Kweme

3.2.4.20.4 Kwara state (North – Central)

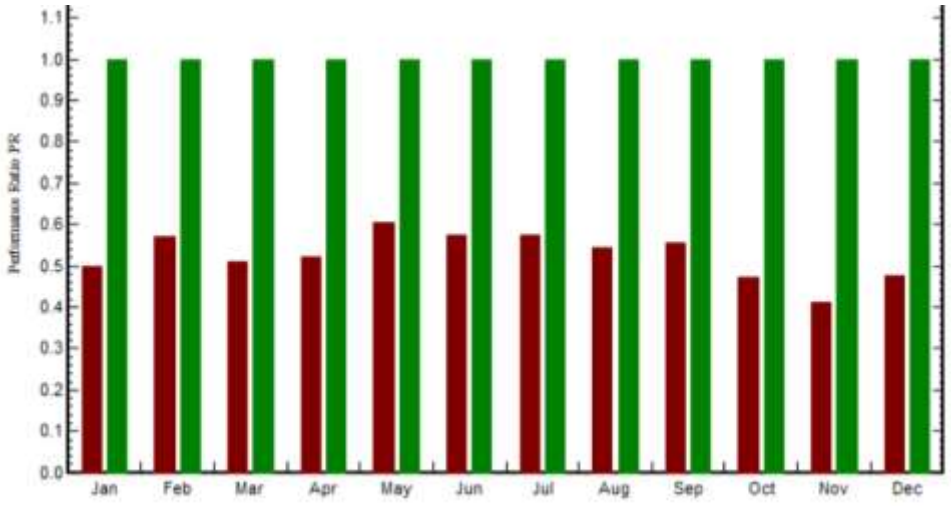

Figure 3.40: performance index of the two energy categories at Oje

Figure 3.40 represents the optimization performance ratio of the two energy systems as compared by HOMER model. The red bar is the performance index of the MFPV+DG+B configuration in terms of NPC, Land Usage and Pollutant emission while the green bar represents the performance index of the BFPV+B configuration based on the aforementioned criteria. Here, the BFPB+B configuration gave ratio (PR) as 100% in all the locations. It will be seen from the figure that the BFPV+B configuration gave the optimal performance index of the TBS energy solution.

3.2.4.20.5 Borno state (North – East)

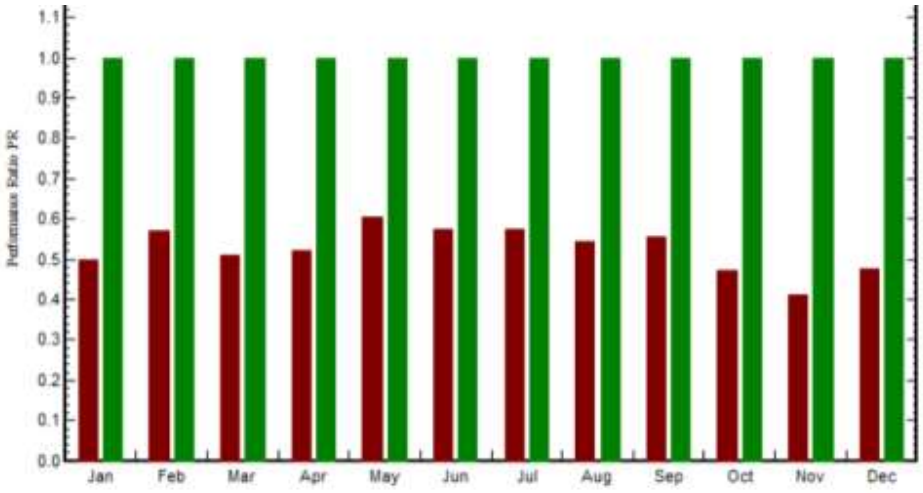

Figure 3.41: performance index of the two energy categories at Baje

In Baje, the red bar is the performance index of the MFPV+DG+B configuration in terms of NPC, Land Usage and Pollutant emission while the green bar represents the performance index of the BFPV+B configuration based on the aforementioned criteria as shown in figure 3.41. It will be seen from the figure that the BFPV+B configuration gave the optimal performance index of the TBS energy solution.

3.2.4.20.6 Sokoto state (North – West)

Figure 3.42: performance index of the two energy categories at Kiso

In figure 3.42, the red bar is the performance index of the MFPV+DG+B configuration in terms of NPC, Land Usage and Pollutant emission while the green bar represents the performance index of the BFPV+B configuration based on the aforementioned criteria. Here, the BFPB+B configuration gave ratio (PR) as 100% in all the locations. It will be seen from the figure that the BFPV+B configuration gave the optimal performance index of the TBS energy solution.

3.2.5 Cost-benefit analysis of the optimized systems using PVsyst and HOMER software

PVsyst and HOMER software were used for these processes. PVsyst used the internal rate of Return (IRR) and the cumulative cash flow to determine the energy configuration that gave the least cost at the optimal energy output. In the other hand, HOMER used the NPC and the pollutant emission to ascertain the energy configuration that will give the optimal solution in terms of cost. In each case, electrical parameters of the selected module were used. Results of the simulation are displayed in chapter four of this thesis.

CHAPTER FOUR

RESULTS AND DISCUSSION

4.1 RESULTS

This chapter presents the results of the PVsyst and HOMER simulations of each of the two energy system types of the six selected TBS location sites for the Optimization and Control of Solar-Powered Telecommunication Network Base Stations in Nigeria Using Standalone Bifacial Photovoltaic Module. Hourly and yearly irradiation Data were obtained from NASA based on the chosen sites on the selected geopolitical zone. In achieving the results, LG450W BFPV and MFPV solar panel was used to conduct the simulations based on the manufacturer's data sheet on the name plate of the selected Panel.

The chosen software performs three principal tasks namely; simulation, optimization, and energy analysis. The simulation process determines how a particular system configuration would behave in a given setting over a long period of time, and serves two purposes. First, it determines whether the system is feasible. A system is said to be feasible if it can adequately serve the electric and thermal loads as well as satisfy any other constraints imposed by the user. Secondly, it estimates the life-cycle cost of the system. The quantity used to represent the life-cycle cost of the system is the total net present cost (NPC), internal rate of return (IRR), and cost-benefit. The total net present cost of a system is the present value of all the costs that it incurs over its lifetime, minus the present value of all the revenue that it earns over its lifetime. These costs include capital costs, replacement costs, operation and maintenance costs, fuel costs, emissions penalties, and the costs of buying power from the grid. Revenues include salvage value and grid sales, but for this proposal, there are no sales to the grid. The optimization and energy management analysis depends on this simulation capability for a given set of constraints and sensitivity variables, which include, among other things, the electric energy (kWh) generated and the pollutant emissions (in tons of CO_2) produced by system type configuration under review. An energy system is considered as an optimal solution for any particular BTS site if it meets the required loads of the site at minimum total economic costs (NPC) and minimum adverse environmental impact. Thus, the simulation results are collated and classified according to these three major factors, namely: the total economic costs (NPC in $), the environmental impact

(pollutant emissions in tons of CO_2), and the electric energy (kWh) generated by each system configuration. More detailed analysis of these results highlights the following major findings:

i. the superiority of the standalone BFPV+Battery backup system over standalone MFPV+Diesel generator+Battery and MFPV+Battery configurations in meeting the objectives of the study;
ii. The more renewable energy components in a system, the higher the initial capital cost, but the lower the total net present cost (NPC) in the long run.

4.1.1 Simulation results.

In running the simulation and the optimization, we used project lifetime of 25 years, which represents the lifetime of the BS equipment and the MFPV and BFPV modules. Between all the components in a base station, BFPV module has been found to be the most expensive in terms of capital cost. Hence, solar cells have a lifetime of 25 years, which is the same as the project lifetime, so neither BS nor the solar cells require replacement during the 25-year period. In addition, the next-generation network, i.e. fifth generation (5G), is predicted to be implemented in the next 25years, based on historical evolution from the previous network cycle, e.g. 4G and 3G. The Nigerian annual real interest rate is 27.5% in 2024 (CBN, 2024) was also used in the simulation process. HOMER and PVsyst makes a decision in each time step to meet the power needs at the lowest cost, subject to the constraints of the dispatch strategy chosen in the simulation and a set point of 80%. The system must supply electricity to both the load (base station system) and the backup power system each hour. In the present research, the backup power needs 10% of the hourly load requirement to retain enough spare capacity to serve the load even under a sudden 10% decrease in the renewable energy output within an hour. Moreover, several sets of sizes will be considered in the simulation, taking into account the BFPV module, MFPV module, inverter and number of batteries needed to achieve cost-effective, reliable and efficient performance in the optimization process. The efficiency of the inverter is assumed to be roughly constant over the working range (e.g. 90 %,) and the battery efficiency is taken to be 90%. The DG configurations are based on (Dike, et al, 2023) where the DG cost is ₦800, 00.00/W.

4.1.1.1 Simulation Result of MFPV with MATLAB/SIMULINK

Using the mathematical model developed in section 3.2.1.1 of chapter three, we can determine the I-V and P-V curves of a MFPV. The initial input irradiance to the PV array model is 1000 W/m^2 and the operating temperatures are $25^0C, 45^0C, 65^0C$ and 85^0C. At steady-state (i.e. at t = 0.15 sec.), we get a PV voltage (V_{dc}_mean) of 600 V and the power extracted (P_{dc}_mean) from the array is 265 W. These values are far more below the expected values from the PV module of the manufacturer specifications due to non-tracking of the configuration. Figures 4.1 and 4.2 are the P-V and the I-V characteristics curve obtained from North-East, North-West, and North Central that receives the maximum amount of solar irradiation in the country.

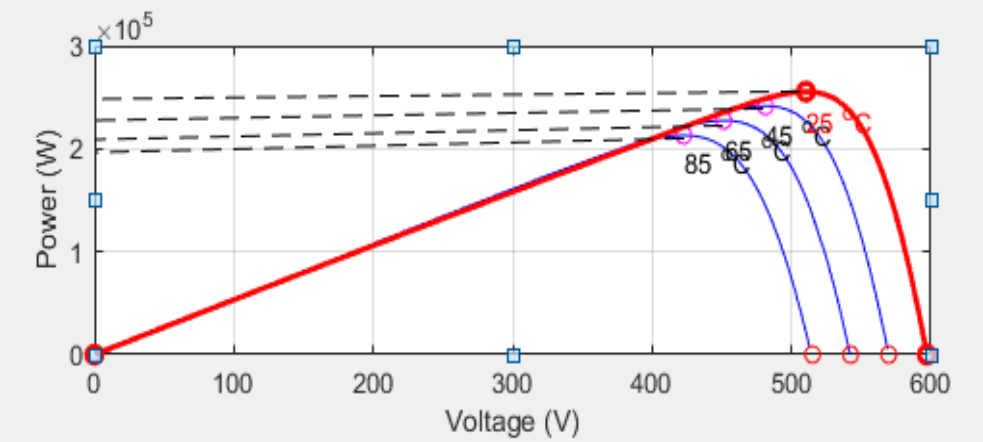

Figure 4.1: P-V characteristics curve of the solar module at constant irradiation

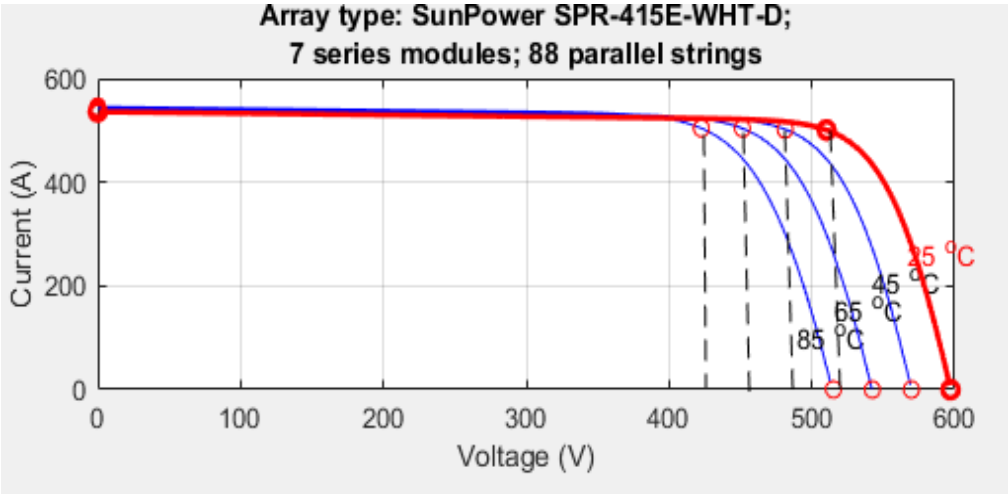

Figure 4.2: I-V characteristics curve of the solar module at constant irradiation

Table 4.1: Energy output from six geopolitical zones in Nigeria for MFPV module (Matlab/Simulink)

Region	**State/locality**	**Solar Radiation (W/m^2)**	**Energy Output**	**MFPV Energy Output per Location (kW)**
North-Central	Kwara/Oje	800.00	265.0	18.550
North-East	Borno/Baje	800.00	265.0	18.550
North-East	Sokoto/Kiso	800.00	265.0	18.550
South-South	Rivers/ Chokocho	650.00	180.0	12.600
South-East	Imo/Umuagwo	700.00	200.0	14.00
South-West	Lagos/Kwame	580.00	170.0	11.900

Table 4.1 shows the power output of each region based on monofacial panel simulation. The solar panel used in the simulation is LG-SUN-Power 450W monofacial. It is evident from the table that there are poor energy yield at the southern part of the country because of reduced illumination and lack of heliotropic tracking which is a major defect of the MFPV module optimization and control method. Module dimension is 2ft by 4ft (0.608m by 1.2136m) and 70 panels of 450W. The total area of land to be covered by the module is $(70 \times 0.608 \times 1.2136)\ 51.65m^2$. Hence, for the MFPV, total power output of the panel at each site is shown in the table. This is obtained by multiplying the location energy output with the number of panel i.e. for Oje in Kwara state (North-Central), the total kW is $(70 \times 265 = 18550\text{W} = 18.55\text{kW})$

4.1.1.2 Simulation Result of BFPV Using PVsyst 7.4.8 version software

In order to model a power system for any Base Station Site, we have to obtain some information about a particular remote location of the Base Station, such as the load profile that should be met by the system. Such information includes: solar radiation for PV generation (availability of solar resources), cost for each component (diesel, renewable energy generators, battery, converter, etc.), cost of diesel fuel (price of fuel), annual interest rate, project lifetime, etc. Outlined below are suggestions of systems that could determine the best option for a Base station site in Nigeria.

Table 4.2: Energy output from six geopolitical zones of BFPV module using PVsyst

Region	**State/locality**	**Front-side Solar Radiation (W/m^2)**	**Rear-side Solar Radiation (W/m^2)**	**Front Energy Output (W)**	**Rear-side Energy (W)**	**Total Energy Output (W)**	**BFPV Energy Output per Location (kW)**
North-Central	Kwara/Oje	1000	540	450.5	350.8	801.3	28.046
North-East	Borno/Baje	1000	540	450.5	350.8	801.3	28.046
North-East	Sokoto/Kiso	1000	540	450.5	350.8	801.3	28.046
South-South	Rivers/ Chokocho	1000	380	450.5	300.0	750.5	26.268
South-East	Imo/Umuagwo	1000	400	450.5	320.0	770.5	26.968
South-West	Lagos/Kwame	1000	320	450.5	280.0	730.5	25.568

Table 4.2 is the energy output of the simulated BFPV module the equivalent of the 70 MFPV panels which become 35 BFPV panel. The total area to be covered by the module is $(35 \times 0.608 \times 1.2136)\ 25.83m^2$ against the $51.65m^2$ area covered by using MFPV module. Therefore, by using BFPV, the gap of land constrain which is common with MFPV was covered by using BFPV. Hence, for the BFPV, total power output of the panel at each site is shown in the table. This is obtained by multiplying the location total energy output with the number of panel i.e. for Oje in Kwara state (North-Central), the total kW is $(35 \times 801.3 = 28046\text{W} = 28.046\text{kW})$. This conform the potency of the energy configuration. The rear side irradiation of the BFPV module was optimized using albedo of 0.2 and bifacial factor of 60%.

4.1.1.3 Optimal Performance of the two Energy configurations at the geopolitical zones

4.1.1.3.1 Umuagwo – Imo state (South – East) [Southern Region]

Figure 4.3: shows the optimization performance ratio of the two energy systems as compared by HOMER model. The red line is the performance index of the MFPV+DG+B configuration in terms of NPC, Land Usage and Pollutant emission while the green blue represents the performance index of the BFPV+B configuration based on the aforementioned criteria. The error bars are the respective monthly benefit/payoff of the BFPV module over the MFPV module (50%). It will be seen from the figure that the BFPV+B configuration gave the optimal performance index of the TBS energy solution. This scenario is applicable at Chokocho – Rivers state (South – South) and Kwame – Lagos state (South – West).

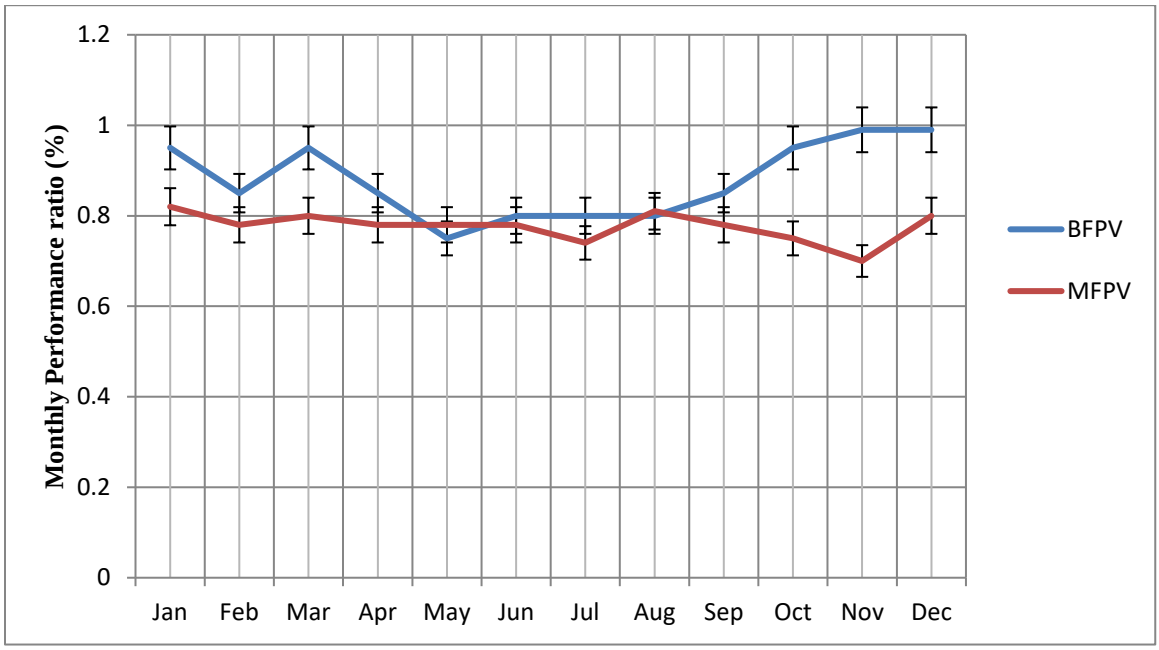

Figure 4.3: performance index of the two energy categories at Umuagwo.

4.1.1.3.2 Oje – Kwara state (North – Central) [Northern Region]

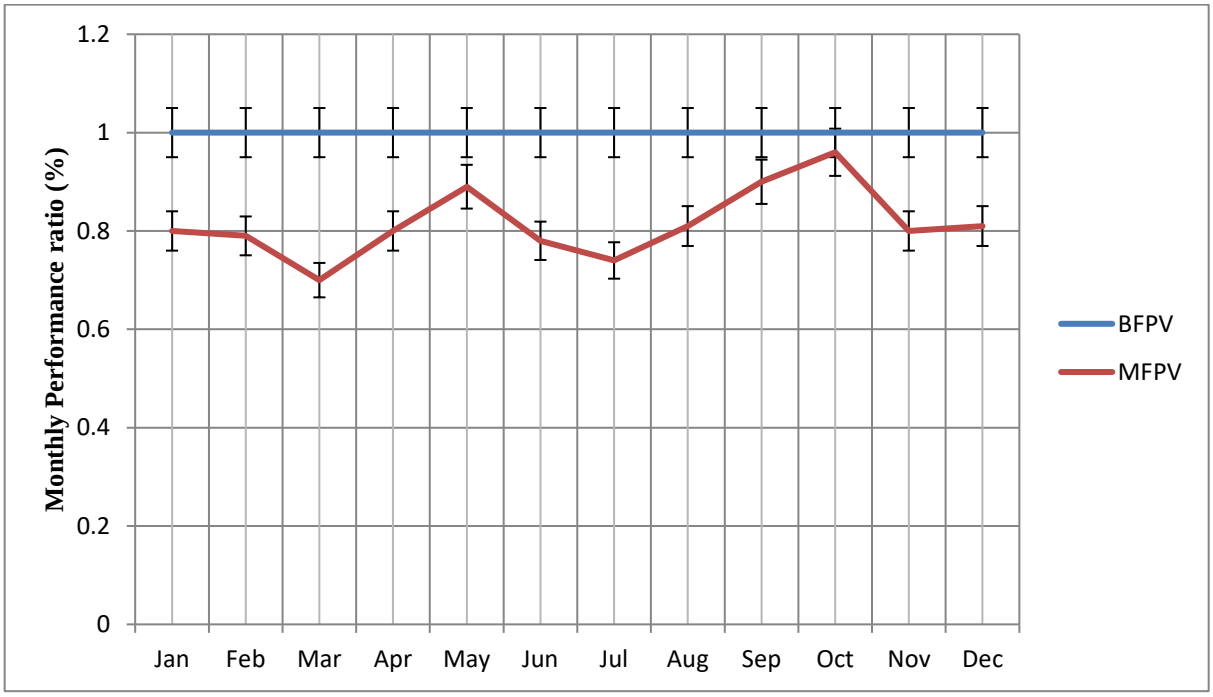

Figure 4.4: performance index of the two energy categories at Oje

Figure 4.4 represents the optimization performance ratio of the two energy systems as compared by HOMER model. The red line is the performance index of the MFPV+DG+B configuration in terms of NPC, Land Usage and Pollutant emission while the green blue represents the performance index of the BFPV+B configuration based on the aforementioned criteria. The error bars are the respective monthly benefit/payoff of the BFPV module over the MFPV module (60%). It will be seen from the figure that the BFPV+B configuration gave the optimal performance index (100%) of the TBS energy solution. This scenario is applicable at Baje – Borno state (North – East), and Kiso – Sokoto state (North – West)

4.1.1.4 Cost-benefit analysis of the optimized systems Configurations

4.1.1.4.1 PVsyst Cost-benefit Analysis of the two energy Configurations.

1. MFPV+DG+B

Figure 4.5 shows the economic output for the tested system. From the figure, it is evident that the installation cost of the module and the generator is ₦1, 288,000.00/Wp and the total yearly cost is ₦483, 200.00/Wp/Yr. The used energy cost is ₦4, 597,964,800.00/kWh. Therefore, the Levelized cost of energy (LCOE) is ₦4, 597,964,800.00/kWh. The net present value of the project is -₦7, 731,200.00 and the return on investment is -750.3%. Here, you will notice that this project is not profitable as highlighted by the simulation result. This is as a result of replacement cost, diesel cost, maintenance cost and lost due to diesel pilfering.

Figure 4.5: cumulative cash flow of the standalone with generator backup

2. BFPV+B

In figure 4.6 and 4.7, the Levelized cost of energy (LCOE) is ₦95,184.64.00/kWh. The net present value of the project is ₦266, 895,136 and the return on investment is 55191.3%. Here, you will notice that this project is profitable as highlighted by the simulation result. The project started giving returns from the first year to the 16th year when the IRO started falling due to panel degradation as flagged by the red bars.

Figure 4.6: cumulative cash flow of the standalone with battery backup only.

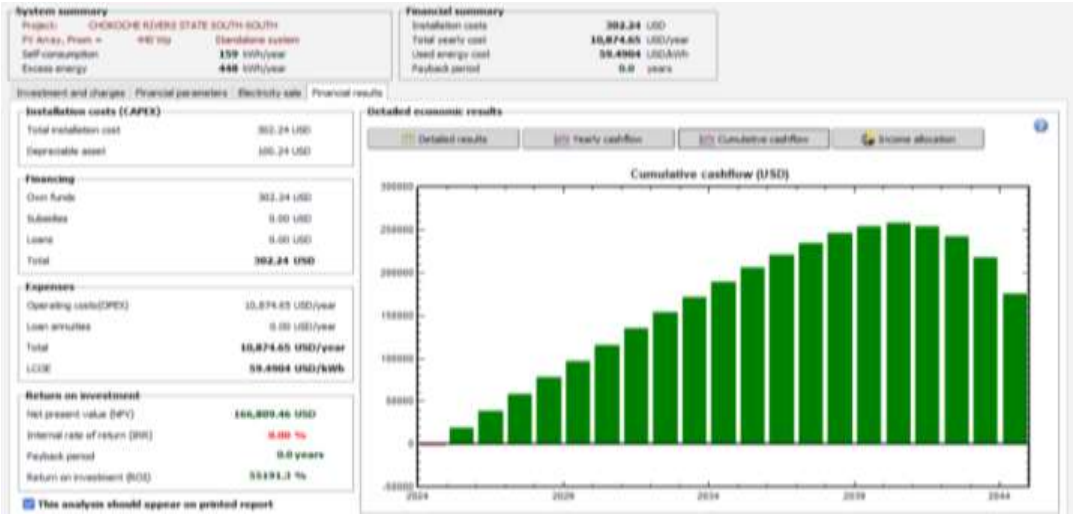

Figure 4.7: Economic cash flow of the standalone with battery backup only

4.1.1.4.2 HOMER Cost-benefit Analysis of the two energy systems

Tables 4.3 to 4.5 show the classification of the simulation results base on:

I. the total net present economic costs (NPC in ₦) as shown in table 4.1,

II. the environmental impact (pollutant emissions in kg of CO_2) shown in table 4.2, and

III. The electric energy (kWh) generated by each system type in table 4.3.

Table 4.3: Economic Costs (NPC) in ₦

S/N		Energy System 1	Energy System 2
	Site	MFPV+DG+B (₦)	BFPV/+ B (₦)
1	Umuagwo	528,000.00	128,000.00
2	Oje	352,000.00	96,000.00
3	Kiso	409,440.00	104,000.00
4	Chokocho	320,000.00	136,000.00
5	Kwame	240,000.00	144,000.00
6	Baje	400,400.00	96,000.00

The figures in table 4.3 are classified from the least cost (in blue) to the highest cost (in red) per energy type as well as per locations. For example, MPV+DG+B system type has the least NPC of ₦240,000.00 at Kwame Lagos state due to availability of grid electricity while BFPV+B has the least cost at Oje and Baje due to low cost of land area.

Table 4.4: Environmental Impact (pollutant emissions in tons of CO_2)

S/N		Energy System 1	Energy System 2
	Site	MFPV+DG+B	(BFPV/+ B)/100
1	Umuagwo	102.5	25
2	Oje	102.5	25
3	Kiso	102.5	25
4	Chokocho	102.5	25
5	Kwame	102.5	25
6	Baje	102.5	25

Table 4.4 are classified from the least environmental pollution in blue to the highest environmental pollution in red per system type as well as per location. It can be seen that energy system 2 is with the least particulate pollutant that energy system 1.

Table 4.5: Percentage of Energy Generated by the Renewable Energy Hybrid Systems Components.

S/N		Energy System 1	Energy System 2
	Site	MFPV+DG+B	BFPV/+ B
1	Umuagwo	8.8kW/20kW /8.5kW	22.8kW/12kW
2	Oje	8.9kW/20kW /9.4kW	25.2kW/12kW
3	Kiso	10.5kW/20kW/9.8kW	25.2kW/12kW
4	Chokocho	7.5kW/20kW /6.5kW	21.9kW/12kW
5	Kwame	6.8kW/20kW /6kW	18.2kW/12kW
6	Baje	9.6kW/20kW /8.5kW	25.2kW/12kW

Note: contributions made by each system components are demarcated by forward slashes

From the result of the simulation, the maximum power of the simulation of a monofacial panel is 265W. For the BFPV, it is 450.5W on the front side. On the rear side of the panel at 60% bifacial gain, the power output becomes $(0.6 \times 450.8 = 270.48\text{W})$. Therefore, the total power output of the BFPV module becomes 721.28W. When this is multiplied by 35, total power becomes 25,244.8W or 25.24kW which is above the calculated load of 10kW and the replaced generator capacity of 25kVA (20kW). This is a clear justification of the success of the BFPV module standalone system. Table 4.5 are arranged from the highest energy generated by energy configuration in blue to the least energy generated by the energy in red. These results are further illustrated with bar charts in figures 4.6 (NPC), 4.7 (environmental impact) and 4.8 (energy generated).

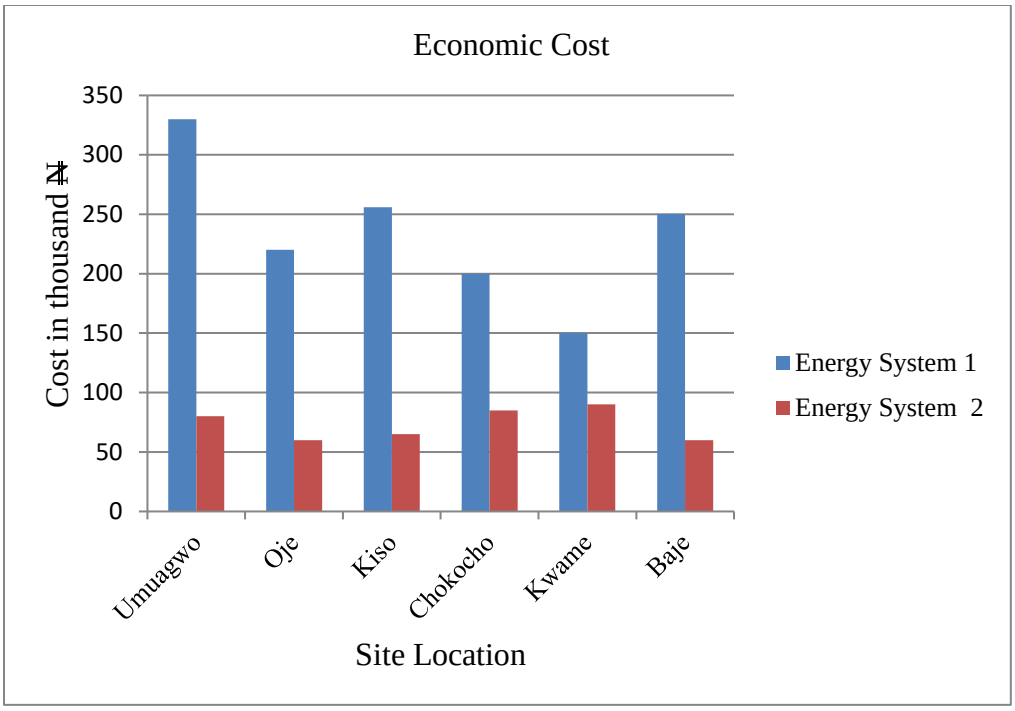

Figure 4.8: Economic Costs of Energy systems (NPC in ₦)

Figure 4.8 show that energy system 2 has the least economic cost in all the site location.

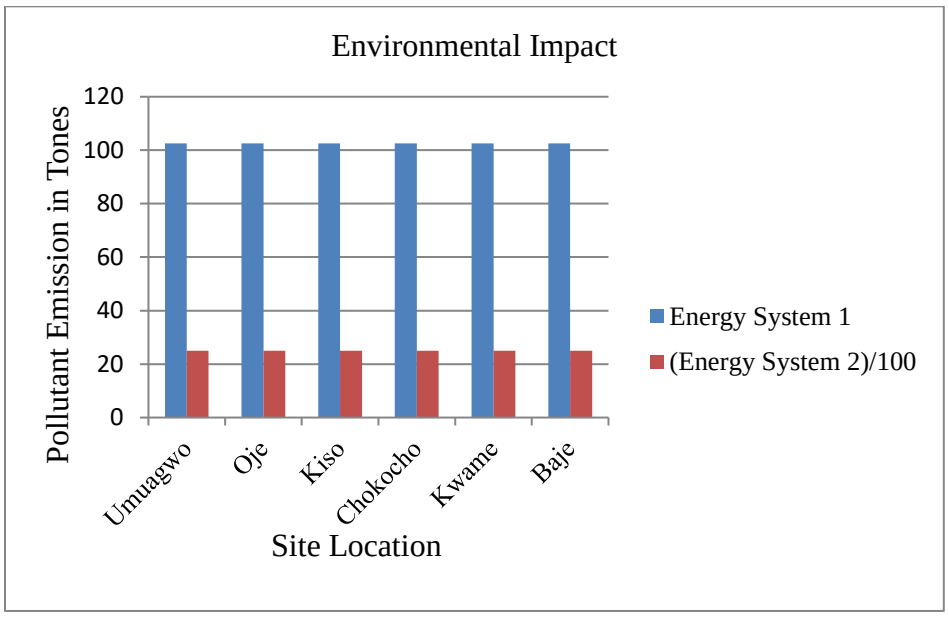

Figure 4.9: Environmental Impact (pollutant emissions in tons of CO_2)

Figure 4.9 show that energy system 2 which is standalone BFPV module has the least or no CO2 emission in all the site location.

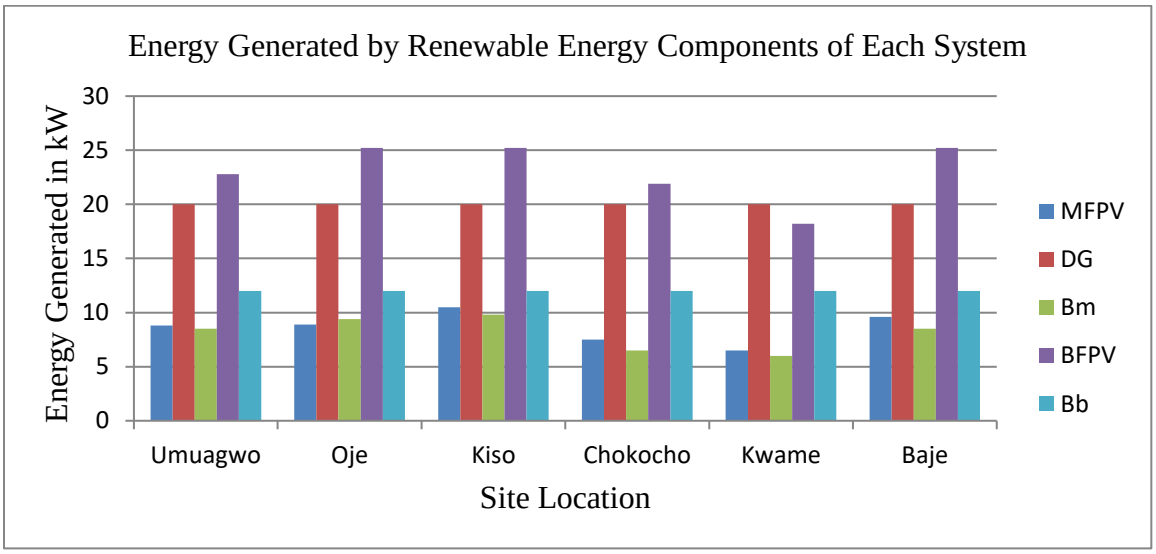

Figure 4.10: Energy Generated by Renewable Energy Components of Each energy System

Figure 4.10 show that energy system 2 which is standalone BFPV module has the ability to charge the batteries and at the same time produces the required system energy in all the locations.

4.1.2 Results Analysis

Different average daily solar radiation values of 5.1, 5.2, 5.3, 5.4, 5.4 and 5.6kWh/m^2 are used to simulate the application of solar energy across a wide range of the six geopolitical zones. The total power consumption by the TBS is 6695W (details given in Table 3.4). The energy output, the economic analysis of the systems and the related sensitivity analysis are provided in the following paragraphs

4.1.2.1 Optimization criteria

Table 4.7 shows a summary of the technical and economic criteria for the optimal design of the BFPV/MFPV/ DG system at different daily radiation values. The optimal size of the solar energy system is obviously the same for all solar radiation rates proposed (5.1 to 5.6 kWh/m^2/day) for the same capacity of the DG (1kW). However, the energy contribution differs, with the contribution of energy from the solar power system increasing with increasing radiation rate. This increase will decrease the energy contribution of the DG, lowering its operating period and providing the

benefits of reducing both the operating costs and pollution rate. The system costs consist of the following: (i) the initial capital cost paid at the beginning of the project and decreases with decreasing size of the elements of the project, with the largest proportion of these costs going towards BFPV module because of their high cost (approximately $4/W). Table 4 shows that the initial capital cost is fixed because the optimal system size is the same for all average daily solar radiation values studied. (ii)The operating cost is paid annually, and most of this cost goes towards operating and maintaining the DG. Table 4 indicates that the operating cost decreases with increasing solar radiation at the same optimal size of the system due to the increase in the energy contribution from the solar power system and the decrease in the energy contribution of the DG, which reduces the operating period of the DG. The NPC represents all costs that occur within the project lifetime, including initial setup costs, component replacements within the project lifetime and maintenance. More details will be provided in the next subsections.

4.1.2.2 Optimal Ranking of the System Types

An energy system may be considered as an optimal solution for any particular TBS site if it meets the required loads of the site at minimum total net present economic costs (NPC) and minimum adverse environmental impact. In one of the simulations, PVSyst and HOMER generated table 4.6 showing this statement; where the system types are ranked both:

Table 4.6 energy yields at site locations for the independent systems

SITE	MFPV(kW)	DG (kW)	BFPV(kW)	Bm (kW)	Bg (kW)	Bb (kW)
Umuagwo	8.8	20	22.8	8.5	12	12
Oje	8.9	20	25.2	9.4	12	12
Kiso	10.5	20	25.2	9.8	12	12
Chokocho	7.5	20	21.9	6.5	12	12
Kwame	6.8	20	18.2	6.0	12	12
Baje	9.6	20	25.2	8.5	12	12

Note: Bm is the battery power with MFPV combination, Bg is the battery power with generator combination and Bb is the battery power with BFPV combination. Therefore, the percentage energy yield for each system is shown in table 4.8.

Table 4.7: percentage energy contribution at various site locations with different system

SITE	MFPV (%)	DG (%)	BFPV (%)	Bm (%)	Bg (%)	Bb (%)
Umuagwo	58.7	133.3	152.0	56.6	70.0	80.0
Oje	59.3	133.3	168.0	62.6	70.0	80.0
Kiso	70.0	133.3	168.0	65.3	70.0	80.0
Chokocho	50.0	133.3	146.0	43.3	70.0	80.0
Kwame	45.3	133.3	121.3	40.0	70.0	80.0
Baje	64.0	133.3	168.0	56.6	70.0	80.0

Table 4.8: Optimal Ranking of the System Types as Generated by HOMER

S/N	HOMER Optimization Ranking	HOMER Ranking in %
1	BFPV + B	95.0
2	MFPV + DG + B	75.0
3	DG + B	60.0

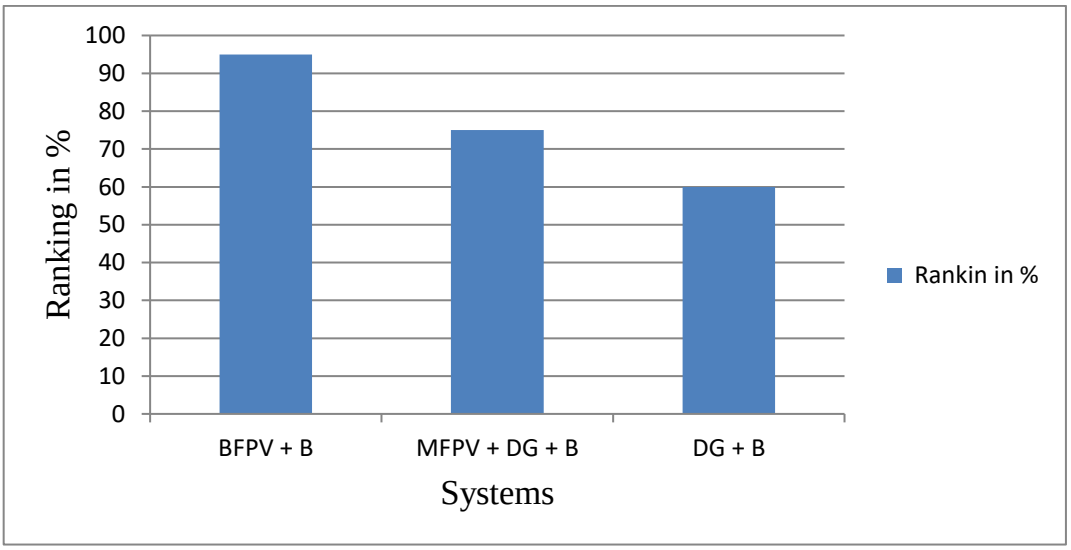

Figure 4.11: HOMER System ranking for optimal energy solution

Figure 4.11 is the HOMER ranking for the best optimization of energy system for TBS application. It is obvious from the figure that BFPV + B combination gave the highest energy optimization. Hence, this combination is applicable for this proposal.

HOMER result of table 4.8 shows the superiority of the BFPV + B system over the other two configurations in meeting the objectives of this research. Consequently, the BFPV+B energy

system type could be considered as the best Optimal renewable energy solution option for powering any base station at each of the six TBS location sites studied. This option is followed by MFPV+G+B energy system. The choice of the second options is against the objective of this research since this research work proposed zero CO_2 emission system.

4.1.2.3 Energy Rating of the Systems and Components

A renewable energy system is said to be feasible if it can adequately serve the electric and thermal loads as well as satisfy any other constraints imposed by the user. This makes energy the first criterion in the above optimal ranking of the configuration system types, and thereby imposes certain constraints not only on the choice and sizing of the individual components (MFPV, BFPV, DG and battery), but also on their configurations (number and combinations) for a given load demand at a TBS site. As illustrated in table 4.5, the percentage energy generated by the two configuration of renewable energy components (MFPV and BFPV) of each the system type depends on the number and combination of these components; the more the number the higher the percentage. Additionally, the percentage energy generated by certain combinations of the renewables (MFPV or BFPV) varies with the locations of the TBS sites.

4.1.2.4 Economic Rating of the System Types and Components

The second most important criterion for assessing an optimal solution for any particular TBS site is the economic cost of the system. The cost ratings here are discussed in terms of two major cost components: the initial capital cost (ICC), and the total net present cost (NPC). The initial capital ICC is completely exclusive, i.e., ICC excludes other costs, while the NPC is inclusive (i.e. includes the present value of all the costs that it incurs over its lifetime.

4.1.2.5 Initial Capital Costs (ICC)

The initial capital cost of a component is the total installed cost of that component at the beginning of the project. The results illustrated in figure 4.12 shows that the more the renewable energy components in a system, the higher the initial capital cost [ICC], and this cost has no significant variation with the TBS sites. The ICC is lower using BFPV module.

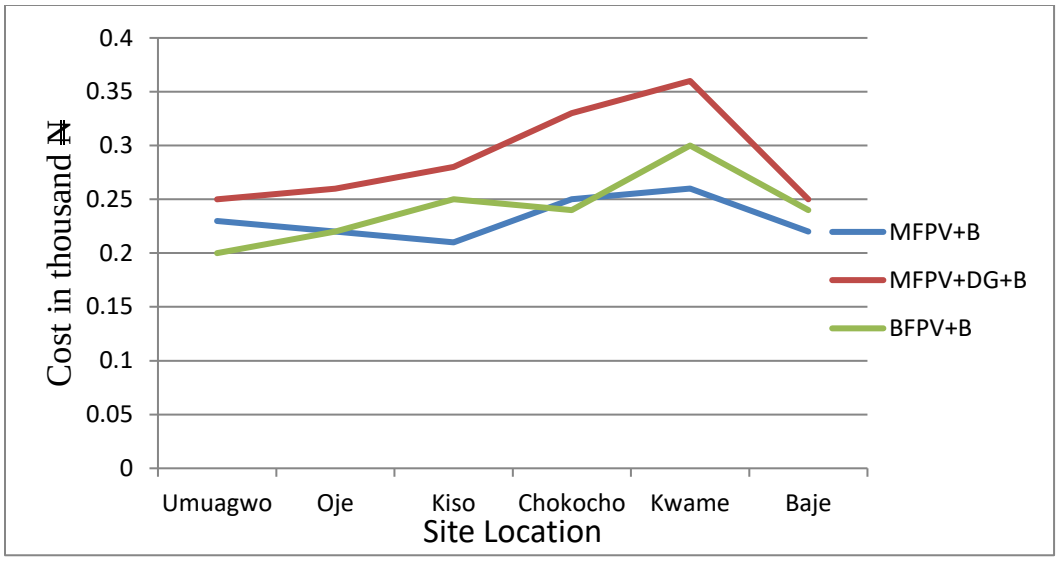

Figure 4.12: Initial capital Cost

4.1.2.5 The Total Net Present Cost (NPC)

The total net present cost (NPC) of a system has been described as the present value of all the costs that it incurs over its lifetime, minus the present value of all the revenue that it earns over its lifetime. Costs include capital costs, replacement costs, operation and maintenance costs, fuel costs, emissions penalties, and the costs of buying power from the grid. Revenues include salvage value and grid sales revenue. However, the analysis presented here considers neither the costs of buying power from the grid nor grid sales revenue, since the focus of this research is on Standalone TBS with or without grid connections. The highest percentage of energy generated by type 2 (BFPV+B) system is by far higher (95%) than that (75%) by type 1(MFPB+DG+B) system as shown in figure 4.9. This means more operational hours (5,286 hrs. vs. 0 hrs.) and more fuel consumption (20,000 vs. 0) by the diesel generator (DG), and consequently higher NPC, in type 1 (MFPV+DG+B) than in type 2 (BFPV+B) systems, respectively.

To appreciate the significance of the life cycle cost (NPC) in the choice of optimal combination of renewable energy components and the ranking of optimized renewable energy systems (as illustrated in figure 4.10) for a typical rural TBS site, further simulation runs were conducted. To determine the economic feasibility of the proposed standalone BFPV module, two test sites were used.

Generally, the optimal size of the solar array decreases with increasing solar radiation, the Initial capital cost (ICC) of the proposed solar power system per module, which is paid at the beginning of the project and depends on the components included in the solar power system. The O & M costs are the annually costs to operate and maintain the system components. The following discussion is based on the average daily solar radiation from the six geopolitical zones of 5.25 kWh m^2 as a case study. However, the analysis can be extended to include other cases of solar radiation with slight differences in daily peak sun hours per case. Referring to equation 3.70 of chapter three, the annual output energy of the solar power system is;

$$E_{PV} = 12\text{kW} \times 5.25 \times 0.9 \times 365 = 13,797\,\text{kW/Yr.}$$

This conforms to the inverter capacity of 15kW. The difference (15-13.25) is the loss factor. The total annual output energy of the solar power system is 21390 kWh, while the base station requires 6695kWh: AC load (air conditioner 1.49kW+lamps 100W (operation from 6p.m. to 6a.m.) + the DC load (base station 917W + microwave link 100W) multiplied by (24 h, 365 days/year).

4.2 DISCUSSION

MFPV Solar energy system is the most developed renewable energy systems (RES), and it has found wide and popular applications in various fields. The popularity of the MFPV energy systems is recent and it include: inexhaustible and readily available natural resources, predominantly present in most parts of Africa, relatively environmentally friendly, very scalable, and from single-panel to BFPV (solar) systems, and long lifetime (20-50 years) and very low maintenance cost.

Unfortunately, despite these attractions and the abundance of solar resources, neither the individual renewables nor their hybrid configuration has found considerable applications in Nigeria. The telecommunications sector of the economy is a case in point. This research has demonstrated that the telecommunications industry is one of the areas BFPV renewable energy systems could be deployed to maximum national economic and environmental benefits, as obtains in many developed and developing countries, including a number of countries in Africa. More specifically, this work has shown that telecom base Stations in rural areas of the country could adequately be powered by BFPV renewable energy system at minimum economic and environmental costs than the use of conventional MFPV and diesel generators, as it is the case now. Although

this statement has been substantiated in many instances presented in the result analysis, the highlights are summarized below.

4.2.1 Justification for energy category Power Options

When one considers the geographical location of Nigeria, the favourable climatic conditions across the country, its endowment with abundant solar radiation, and current developments in renewable energy technology, whereby the cost of renewable energy components continues to fall every day, the continued powering of TBS sites in any part of Nigeria solely with diesel generators is no longer justifiable. This is the case this research is addressing; more so, when the same telecommunication operators in world are deploying the same renewable technology in many parts of the world, including a number of countries in Asia and Africa (Mancuso et al., 2011) (Milosevic, 2011) less endowed with these renewable energy resources than Nigeria. If hitherto there was an excuse of no availability of reliable information to justify an investment in this area, such information could now be found in the result of this research and related works reviewed in the literature of this thesis. One such vital information for judicious investment is components sizing. As stated earlier in literature review of this thesis, in order to efficiently and economically utilize the renewable energy resources, an optimum sizing of the renewable energy components is paramount. The optimum sizing can help guarantee the lowest investment with full use of the system components, so that the system can work at the optimum conditions in terms of investment and system power reliability requirement. Therefore, this research presented a comprehensive review of current optimum sizing methods, such as simulation tools, numerical algorithm, probabilistic model, multi-objective planning technique, etc. Not only that, using PVsyst and HOMER to find the optimum configuration and sizing of components, this research was able to evaluate the performances of two different combination of solar module (MFPV and BPV) system at each of six different TBS sites located in six different geographical zones across the country. More specifically, the simulation results analyzed above shows the ability to optimize configurations of energy systems in order to maximize performance while minimizing both economic and environmental costs. For instance, among the two configurations investigated, the BFPV -Battery system was found to be the optimum combination to power each of the six TBS sites investigated because of its 95% performance against the 75% of the MFPV module. This research also confirmed the significance of facilities' locations in the choice of energy

configuration options.

Much ground was also covered in the literature review on economic costs not only as important determining factors for the choice of renewable power options, but as a very relevant information for making critical decisions on systems design and economic investment. Many assertions in the review were either confirmed numerically or illustrated graphically by the simulation results presented herein. These include:

1). That the more the renewable energy components in a system, the higher the ICC, and this cost have no significant variation with the TBS sites. On the other hand, diesel only system has lower ICC, but higher total net present cost NPC.

2). that the total NPC increases with the decrease of system components but decreases as the lifetime of the systems increases, and these differences vary significantly from one energy system configuration to another, but not with the TBS sites.

This work has also addressed the issue of pollution reduction as a major justification for alternative energy applications of BFPV module, as adequately reviewed in the literature and quantitatively demonstrated by the simulation results (in table 4.4). Given that the major source of pollution in any application, such as the MFPV+DG+B or DG+B systems, is CO_2 emitted by the diesel generator component of the application, this work confirmed the observations by many works in the literature that the more the number of the renewable energy components (in combination with a DG) in any renewable energy system, the lower the CO_2 generated by the generator and hence the minimum is the pollution of the environment by the system. Though this research limited its investigation on the energy systems of MFPV and BFPV module, in other words, by increasing the renewable energy penetration in any alternative energy system, the power drawn from the diesel component of the system is minimized, thereby reducing the amount of CO_2 emitted by the system. Laidi et al., (2012) in their paper confirmed this observation with the comparison of pollutant emissions of CO_2 with renewable energy and without renewable energy.

Concerning the PVsyst, simulations were conducted within the six geopolitical zones to ascertain the performance of the selected bifacial panel. LG panels were used throughout the entire simulation process. In each of the six geopolitical zones, NASA irradiation data obtained from the geographical sites were used and results shows that Nigeria, irrespective of the geopolitical zones receives good amount of solar radiation for the performance of the BFPV module all the year

round. The solar radiation maps are shown in chapter three of this thesis. A total number of 70 MFPV modules and 35 BFPV modules were used to achieve the set objectives. The LG 450W 2W BF panel was used as the base module. From the result of the simulation, the maximum power of the simulation of a front panel is 450.5W. On the rear side of the panel at 60% bifacial gain, the power output becomes $(0.6 \times 450.8 = 270.48\text{W})$. Therefore, the total power output of the BFPV module becomes 721.28W. When this is multiplied by 35, total power becomes 25,244.8W or 25.24kW which is conforms to the calculation obtained in chapter three of this thesis. This is a clear indication of the sustainability and reliability of the proposed standalone BFPV module renewable energy configuration.

CHAPTER FIVE

CONCLUSION AND RECOMMENDATIONS

5.1 CONCLUSION

The aim of this thesis is Optimization and Control of Solar-Powered Telecommunication Network Base Stations in Nigeria using Standalone Bifacial Photovoltaic Module based on PVsyst and HOMER simulations, in the perspective of technical and economic analysis. In conducting this research, two configurations were considered and the potential of each of them was simulated for six hypothetical TBS sites at six different locations selected as case study areas in Nigeria. Climatic data in the form of solar irradiance and wind speed were collected from each of these areas, which were used to study the effects of different climatic data on the optimization and the sizing of the energy system selected. The optimization was run on each of the case of data set and results were generated. These results (the load power level, MFPV power level, BFPV, and state of charge of a battery bank), were used as inputs to the controller, which was developed to control the amount of energy supplied to the load, and to ensure that the load was met as much as possible. The controller used here is the east-west tracking mechanism of the sunflower heliotropism. The controller also makes sure that the state of charge of the batteries stays between 30% capacity to 90% capacity, the minimum and maximum bounds of the batteries, respectively. Running the controller, the system enters different points. The controller shows the breakdown of energy generated and supplied for each hour over the year as well as the mode of control used in each hour.

The simulation results show the economic analysis of adopting each system configuration over a period of 25 years and compare it with using only a diesel generator. It has been shown that using any of the two component systems reduces the energy cost in all the test TBS sites but the elimination of CO_2 cannot be assured. By using MFPV/DG/B system for example, the network operators can save as high as N16 billion over a 25-year period and can supply at least 65% of the energy demand while with the system combination of BFPV/B system the network operators can save as high as $30 million over a 25-year period and can supply at least 95% of the energy demand. In terms of reducing the carbon dioxide emission, the BFPV/B system has the least CO_2 emission (between 0.1 and 0.25 tons) while the MFPV/DG/B has an CO2 emission of over 250 tons

Therefore, the BFPV Energy system can be more cost-effective and environmentally friendly in providing energy to TBS sites than the MFPV + DG + B system. The proposed scheme is highly preferable for rural and remote areas where there are no grid connections. However, it is important to note that there is no general least-cost option for powering GSM base station sites at different locations. It all depends on climatic conditions and available renewable energy resources. It is demonstrated that it is possible to develop an optimized energy map for appropriate locations of GSM Base Station sites in Nigeria, both as a design guide for network operators and for the formulation of energy use policies by the national telecommunications regulatory authority (the NCC). One of such policies could be the requirement that any network operator intending to site a base station in any location should first produce an optimized energy feasibility study of the location before an approval would be granted.

5.2 RECOMMENDATIONS

Due to cost, we couldn't build the prototype of the BFPV system proposed in this research. Therefore, we recommend that the system (data) proposed here in this thesis should be tested in a real life at TBS as a continuation of this research work. We also recommend that the application of this research in agrovolnics; the diffused beam could be used for plant photosynthesis instead of being wasteful to enhance food security and animal husbandry especially in the northern part of the country to limit herdsmen migration toward the southern Nigeria in search of greener pasture for their herds which often lead to clashes among the rural dwellers and herdsmen as a result of damages caused by cattle on agricultural farmlands of their community.

Additionally, one of the major factors that inhibit the reflection of sun beam at the rear-side of the panel is mismatch due to shading from the mounting frame of the module. Consequently, the researchers proposed the use of reflecting rectangular glass prism on the mounting structure. By using this, the researcher is of the hope that total internal reflection of the prism will further refracts the incident light back on the surface of the module instead of shading it.

5.3 CONTRIBUTIONS TO KNOWLEDGE

Space Constrain: In this research, 70 panels of MFPV are required to achieve the same result of the 35 BFPV modules. Each of the panel is measuring 4ft x 2ft (0.6068m x 1.3126m). Therefore, the area to be occupied by the MFPV is $[(0.6068\text{m} \times 1.3126\text{m} \times 70)] = 55.6m^2$. The BFPV

module area will be $[(0.6068\text{m} \times 1.3126\text{m} \times 35)] = 25.8m^2$ difference of approximately 30m^2 which represents about 54% reduction in land area. This will reduce the initial capital cost of the mobile operators.

Novel application: Nigeria has vast desert region where sun's irradiation is above 1000W/m^2. Therefore, installing BFPV module in this region can serve two purposes: for electricity generation and agrovolnics. In agrovolnics, it can serve as a shade thereby reducing excessive evaporation which will lead to growth of weeds. The diffused rays at the reversed side of the panel will be used by these weeds for photosynthesis. Hence, the weed can be used for animal husbandry in the northern region. This will reduce North-South herdsmen migration in search of greener pasture for their herds which most cases lead to clashes and loss of life.

Optimization and Control Strategy: This research developed and evaluates the current optimization and control strategies of the heliotropic process of the sunflower for maximizing energy yield. MFPV relies its tracking on MPPT, Perturbation and Observation (P & O) algorithms basically and assumes constant irradiation of 1000W/m^2 and temperature of 25^{0}C. Practically, this is not true because sun's irradiation and temperature of different geographical locations varies even at the same time. Therefore, the heliscope of the PVsyst track the sun and temperature on the instant geographical condition of the place and use if for control and maximizing energy output. This strategy can be applied to other solar-powered systems to enhance their efficiency and effectiveness.

REFERENCES

Agbo E.P. & Ekpo C.M., (2021): 'Trend analysis of the variations of ambient temperature using Mann-Kendall test and Sen's estimate in Calabar, southern Nigeria*, J. Phys.: Conf. Ser. 1734 (1) 012016.*

Abba, L. B., and Chee, W. T. (2019): "A review on stand-alone photovoltaic-wind energy system with fuel cell: System optimization and energy management strategy". J. Clean. Prod. 221, 73–88. doi:10.1016/j.jclepro.2019.02.228

Abdolvahhab, F., and Ehsan, K. (2015): "Size optimization for hybrid photovoltaic–wind energy system using ant colony optimization for continuous domains based integer programming". Appl. Soft Comput. 31, 196–209. Doi: 10.1016/ j.asoc.2015.02.047

Abdul, H., Babatunde, O., Benyoh, E., Kigha, N., Jong, W. R., Dongjun, S., and Jeung, S, (2019). '*Sustainable Energy Technologies and Assessments'; journal homepage: www.elsevier.com/locate/seta*

Abedi, S., Riahy, G. H., Hosseinian, S. H., and Alimardani, A. (2011): "Risk Constrained unit commitment of power system incorporating PV and wind farms". Isrn Renew. Energy 2011 (1)–8. doi:10.5402/2011/309496

Adeniji, N.O., Akinpelu, J.A., Adeola S.O., and Adeniji J.O., (2019): 'Estimation of global solar radiation, sunshine hour distribution and clearness index in Enugu, Nigeria', *J. Appl. Sci. Environ.Manag. 23 (2) 345–349.*

Agbo E.P. (2021). 'The role of statistical methods and tools for weather forecasting and modelling: *Weather Forecasting, Intech Open, Mar 22.*

Agbo E.P., Ettah E.B., & Eno E.E., (2020): 'The impacts of meteorological parameters on the seasonal, monthly and annual variation of radio refractivity', *Indian J. Phys.*

Agbo, E.P., Ekpo C.M., and Edet, C.O. (2021): 'Analysis of the effects of meteorological parameters on radio refractivity, equivalent potential temperature and field strength via the Mann-Kendall test'.*Theor. Appl. Climatol., 143 (3) pp. 1437-1456.*

Ahmad, R. J. (2021). Economic dispatch in grid-connected and heat network connected CHP microgrids with storage systems and responsive loads considering reliability and uncertainties. Sustain. Cities Soc. 73, 103101. doi:10.1016/j.scs.2021. 103101

Ai, B., Yang, H., Shen, H., and Liao, X., (2003): "Computer-Aided Design of PV/Wind Hybrid System," Renewable Energy, Vol. 28, No. 10, pp. 1491-1512,

Ajayi O.O., Ohijeagban O.D., Nwadialo C.E., &Olasope O., (2014): 'New model to estimate daily global radiation over Nigeria', Sustain. *Energy Technol. Assessments p.528–3*

Akbar, M., and Alireza, A. (2014). Artificial bee swarm optimization for optimum sizing of a stand-alone PV/WT/FC hybrid system considering LPSP concept. Sol. Energy 107, 227–235. doi:10.1016/j.solener.2014.05.016

Alexopoulos S., and Hoffschmidt, B. (2013): 'Concentrating receiver systems (solar power tower)'; Solar Energy, 10, *Springer, New York, pp. 978-981.*

Algora C. (2004): 'Chapter 6 in Next Generation Photovoltaics', edited by A. Marti and A. Luque, *Institute of Physics Publishing, Bristol and Philadelphia.*

Alsharif M.H, and Kim J., (2016): 'Optimal solar power system for remote telecommunication base stations: a case study based on the characteristics of South Korea's solar radiation exposure'; Sustainability, *p. 942. Google Scholar*

Alsharif, M.H., (2017): "Comparative Analysis of Solar-Powered Base Stations for Green Mobile Networks" *Energies* 10, no.8:1208. https://doi.org/10.3390/en10081208

Alvarado, D., Moreira, A., Moreno, R., and Strbac, G. (2019). Transmission network investment with distributed energy resources and distributionally robust security. IEEE Trans. Power Syst. 34 (6), 5157–5168. doi:10.1109/tpwrs.2018. 2867226

Amirhossein, D., Behnam, M., Mehdi, A., and Sajjad, T. (2017). Optimal stochastic design of wind integrated energy hub[J]. IEEE Trans. Industrial Inf. 13 (5), 2379–2388. doi:10.1109/TII.2017.2664101

Anayochukwu, A. V. and Nnene, E. A., (2013): "Simulation and Optimization of Photovoltaic/Diesel Hybrid Power Generation Systems for Health Service Facilities in Rural Environments," Electronic Journal of Energy & Environment, Vol. 1, No. 1, pp. 57 70,.

Andrychowicz, M., and Olek, B. (2016). "Optimal structure of the RES in distribution systems," in International Conference on the European Energy Market, EEM 13th International Conference on the European Energy Market, Portugal, June 6-9, 2016 (IEEE). doi:10.1109/EEM.2016.752133

Antonanzas, J., Jimenez, E., Blanco, J., and Antonanzas-Torres, F. (2014). Potential solar thermal integration in Spanish combined cycle gas turbines. Renew. Sustain. Energy Rev. 37, 36–46. doi:10.1016/j.rser.2014.05.006

Appelbaum, J.J.R.E (2016): 'Bifacial photovoltaic panels field' Renewable Energy

Arabli, S., Ghofrani, M., Etezadi-Amoli, M., Fadali, S., and Baghzouz, Y. (2013): Genetic-algorithm-based optimization approach for energy management. *IEEE Trans. Power Deliv. 28, 162–170. doi:10.1109/TPWRD.2012.2219598*

ArchimedesM, (2011): accessedDec72011, http://www.math.nyu.edu/~crorres/Archimedes/Mirrors/Tzetzes.html

Arnette, A., and Zobel, C. W. (2012). An optimization model for regional renewable energy development. Renew. Sustain. Energy Rev. 16 (7), 4606–4615. doi:10.1016/j.rser.2012.04.014

Asgharzadeh, A., Marion, B., Deline, C., Hansen, C., Stein, J.S., Toor, F.(2018): A sensitivity study of the impact of installation parameters and system configuration on the performance of bifacial PV arrays. *IEEE J. Photovoltaics 8(3), 798–805 (2018). https://doi.org/10.1109/JPHOTOV. 2018.2819676*

Askarzadeh, A. (2013). A discrete chaotic harmony search-based simulated annealing algorithm for optimum design of PV/wind hybrid system. Sol. Energy 97, 93–101. doi:10.1016/j.solener.2013.08.014

Auer, G.; Giannini, V.; Desset, C.; Godor, I.; Skillermark, P.; Olsson, M. (2011): How much energy is needed to run a wireless network? *IEEE Wirel. Commun., 18, 40–49.*

Augustine C., & Nnabuchi M.N (2009): 'Relationship between global solar radiation and sunshine hours for Calabar, Port Harcourt and Enugu, Nigeria, Int. *J. Phys. Sci. 4 (4) 182–188.*

Augusto, B., Marco, P., and Cesare, S. (2013). Solar steam reforming of natural gas integrated with a gas turbine power plant. Sol. energy 96, 46–55. doi:10.1016/j. solener.2013.06.030

Aydan, G. & Shanza N. H., (2024): "Electrical and thermal performance of bifacial photovoltaics under varying albedo conditions at temperate climate (UK)" research article

Backus C. E. (2003): "A Historical Perspective on Concentrator Photovoltaics", Proceedings of the International Solar Concentrator Conference for the Generation of Electricity or Hydrogen, Alice Springs, Australia

Baghernejad, A., and Yaghoubi, M. (2010). Exergy analysis of an integrated solar combined cycle system. Renew. Energy 35 (10), 2157–2164. doi:10.1016/j.renene. 2010.02.021

Baghernejad, A., and Yaghoubi, M. (2011). Exergoeconomic analysis and optimization of an integrated solar combined cycle system (ISCCS) using genetic algorithm. Energy Convers. Manag. 52 (5), 2193–2203. doi:10.1016/j. enconman.2010.12.019

Bagul, A. D., Z. M. Salameh, and B. Borowy. (2023): "Sizing of a stand-alone hybrid wind-photovoltaic system using a three-event probability density approximation." *Solar Energy* 56.4 323-335.

Baliozian, P., Tepner, S., Fischer, M., Trube, J., Herritsch, S., Gensowski, K., Clement, F., Nold, S., & Preu, R (2020); The International Technology Roadmap for Photovoltaics and the Significance of its Decade-Long Projections (ITRP), 37th European Photovoltaic Solar Energy Conference and Exhibition Institute for Solar Energy Systems ISE, 2, 79110 Freiburg, Germany

Bana, S., & Saini, R. P. (2016) : A mathematical modeling framework to evaluate the performance of single diode and double diode based SPV systems, Energy Reports, ISSN 2352-4847, Elsevier, Amsterdam, Vol. 2, pp. 171-187, https://doi.org/10.1016/j.egyr.2016.06.004

Banjo Ayoade A, Thomas O, Adnan M. A (2017): 'Solar PV Powered Mobile Cellular Base Station: Models and Use Cases in South Africa'*Conference Paper · https://www.researchgate.net/publication*

Barbato, M., Barbato, A., Meneghini, M., Tavernaro, G., Rossetto, M., Meneghesso, G. (2017): Potential induced degradation of N-type bifacial silicon solar cells: An investigation based on electrical and optical measurements. *Sol.Energy Mater. Sol. Cells 168, 51–61 (2017). https://doi.org/ 10.1016/j.solmat.04.007*

Barley Dennis, C., and C. Byron Winn. (2022): "Optimal dispatch strategy in remote hybrid power systems." *Solar Energy* 58.4 165-179.

Barun, K. D., and Mahmudul, H. (2021). Optimal sizing of a stand-alone hybrid system for electric and thermal loads using excess energy and waste heat. Energy 214, 119036. doi:10.1016/j.energy.2020.119036

Batzelis, E.I., Kampitsis, G.E., Papathanassiou, S.A., et al.: 'Direct MPPcalculation in terms of the single-diode PV model parameters', IEEE Trans.EnergyConvers.,2015,30,(1),pp.226–236

Baumann, T.; Nussbaumer, H.; Klenk, M.; Dreisiebner, A.; Carigiet, F.; and Baumgartner, F. (2019): 'Photovoltaic systems with vertically mounted bifacial PV modules in combination with green roofs'. Sol. Energy, 190, 139–146.

Bayod, R., and Angel, A (2019): "Solar Photovoltaics (PV)." Solar Hydrogen Production: Processes, Systems, and Technologies, 2019, pp. 237-295.

Benda, V., &Cerná, L. (2020): PV cells and modules—State of the art, limits and trends. Heliyon 6(12), e05666. https://doi.org/10.1016/j.heliyon. 2020.e05666

Bernal-Agustín, José L., and Rodolfo Dufo-López. (2009): "Simulation and optimization of stand-alone hybrid renewable energy systems." *Renewable and Sustainable Energy Reviews* 13.8 2111-2118

Bernal-Agustín, José L., Rodolfo Dufo-López, and David M. Rivas-Ascaso. (2006): "Design of isolated hybrid systems minimizing costs and pollutant emissions."*Renewable Energy* 31.14 2227-2244.

Bhandari, B., Lee, K.-T., Cho, Y.-M., Lee, C. S., Song, C.-K., et al., (2013): "Hybridization of Multiple Renewable Power Sources for Remote Village Electrification," Proc. of the International Symposium on Green Manufacturing and Applications,.

Bhandari, B., Lee, K.-T., Lee, C. S., Song, C.-K., Maskey, R. K., et al., (2014): "A Novel Off-Grid Hybrid Power System Comprised of Solar Photovoltaic, Wind, and Hydro Energy Sources," Applied Energy, Vol. 133, pp. 236-242,.

Bhandari, R. and Stadler, I., (2011): "Electrification using Solar Photovoltaic Systems in Nepal," Applied Energy, Vol. 88, No. 2, pp. 458-465,

Bhandari, R. and Stadler, I., (2011): "Electrification using Solar Photovoltaic Systems in Nepal," Applied Energy, Vol. 88, No. 2, pp. 458-465,.

Bhuiyan, M. and Ali, A. M., (2003): "Sizing of a Stand-Alone Photovoltaic Power System at Dhaka," Renewable Energy, Vol. 28, No. 6, pp. 929-938,

Binayak Bhandari; Kyung-Tae Lee; Gil-Yong Lee, Young-Man Cho;, and Sung-Hoon Ahn, (2015): "Optimization of Hybrid Renewable Energy Power Systems: A Review" *international journal of precision engineering and manufacturing-green technology vol. 2, no. 1, pp. 99-112 10.1007/s40684-015-0013-z*

Bingle, Z., and Xiao, W. (2022). Integrated capacity configuration and control optimization of off-grid multiple energy system for transient performance improvement. Appl. Energy 311, 118638. doi:10.1016/j.apenergy.2022.118638

Blaud, P. C., Haurant, P., Claveau, F., Lacarrière, B., Chevrel, P., and Mouraud, A. (2020). Modelling and control of multi-energy systems through multi-prosumer node and economic model predictive control. Int. J. Electr. Power & Energy Syst. 118, 105778. doi:10.1016/j.ijepes.2019.105778

Boonbumroong, U., Pratinthong, N., Thepa, S., Jivacate, C., and Pridasawas, W., (2011): “Particle Swarm Optimization for AC-Coupling Stand Alone Hybrid Power Systems,” Solar Energy, Vol. 85, No. 3, pp. 560-569,.

Bouchakour, S.; Caballero, D.V.; Luna, A.; Medina, E.R.; El Amin, K.B.; and Cortes, P.R.(2020): ‘Monitoring, modelling, and simulation of bifacial PV modules over normal and high albedos. *In Proceedings of the 9th International Conference on Renewable Energy Research and Application (ICRERA), pp. 252–256.*

Bradley, A., Thornes, J., &Chapman, L, (2022): “Modelling spatial andtemporal road thermal cli matology in rural and urban areas using a GIS”. Climate Research: 41–55 150.

Braslavsky, J. H., Wall, J. R., and Reedman, L. J. (2015). Optimal distributed energy resources and the cost of reduced greenhouse gas emissions in a large retail shopping centre. Appl. Energy 155, 120–130. doi:10.1016/j.apenergy.2015.05.085

Buchana, P. &Ustun T. S. (2015): “The Role of Microgrids & Renewable Energy in Addressingsub-SaharanAfrica’sCurrentandFutureEnergyNeeds,”IEEERenew. Energy Congress, pp. 1–6,.

Caishan, G., Fengji, L., Zexiang, C., Zhao, Y. D., and Rui, Z. (2021). Integrated planning of internet data centers and battery energy storage systems in smart grids. Appl. Energy 281, 116093. doi:10.1016/j.apenergy.2020.116093

Calderón, M., Calderón, A. J., Ramiro, A., Gonzalez, J. F., and Gonzalez, I. (2011). Evaluation of a hybrid photovoltaic-wind system with hydrogen storage

Campana P.E., Stridh B., Amaducci S., and Colauzzi M., (2021): “Optimisation of vertically mounted agrivoltaic systems”, J. Clean. Prod. 325, 129091.

Carolus, J., Tsanakas, J.A., van der Heide, A., Voroshazi, E., De Ceuninck, W., Daenen, M. (2019): Physics of potential-induced degradation in bifacial p PERC solar cells. Sol.Energy Mater. Sol. Cells 200, 109950. https://doi.org/10.1016/j.solmat.

Castillo-Aguilella J. E. and Hauser, P. S. (2016): "Multi-Variable Bifacial Photovoltaic Module Test Results and Best-Fit Annual Bifacial Energy Yield Model," in IEEE Access, vol. 4, pp. 498-506, 2016, doi: 10.1109/ACCESS.2016.2518399.

CBN, (2024): http: tradingeconomics.com, Nigeria Interest RateNigeria Interest Rate

Chapman A., Shigetomi Y., Ohno H., McLellan B., & Shinozaki A., (2021): Evaluating the global impact of low-carbon energy transitions on social equity, Environ. Innov. Soc. Transit. 40 332–347.

Charles, A., &Meisen, P. (2014): 'How is 100% Renewable Energy Possible in Nigeria?', Global Energy Network Institute.

Chedid, R., Karaki, S., and Rifai, A., (2005): "A Multi-Objective Design Methodology for Hybrid Renewable Energy Systems," Proc. of the IEEE on Power Tech, pp. 1-6,.

Chedid, Riad, and Saifur Rahman. (2020): "Unit sizing and control of hybrid wind-solar power systems." *Energy Conversion, IEEE Transactions on* 12.1 79-85.

Chinnu, P.R, &Athulya P. P, (2014): "Different methods of modelling PV panels, an overview.

Clifford W. Hansen, Joshua S. Stein, Chris Deline, Sara MacAlpine, Bill Marion, Amir Asgharzadeh, Fatima Toor . (2016) "Analysis of irradiance models for bifacial PV modules," 2016 IEEE 43rd Photovoltaic Specialists Conference (PVSC), Portland, OR, USA, 2016, pp. 0138-0143, doi: 10.1109/PVSC.2016.7749564.

Coello, Carlos A. Coello, Gary B. Lamont, and David A. (2007).Van Veldhuisen.*Evolutionary algorithms for solving multi-objective problems*. Springer,

Collette, Yann, and Patrick Siarry. (2003): "*Multi-objective optimization": principles and case studies*. Springer,

Dada B.M., & Okogbue E.C., (2017) 'Estimating daily solar radiation from monthly values over selected Nigeria stations for solar energy utilization', J. Fund. Renew. Energy Appl. 7 (6) 1–3.

De Groot, K.M., & Van Aken, B.B. (2017): Near-field partial shading on rear side of bifacial modules. Energy Procedia 124, 532–539. https://doi. org/10.1016/j.egypro.2017.09.254

Deepak, Lal Kumar, Bibhuti Bhusan Dash, and A. K. Akella. (2011): "Optimization of PV/Wind/Micro-Hydro/Diesel Hybrid Power System in HOMER for the Study Area." *International Journal on Electrical Engineering and Informatics* 3.3 307-325.

Deline C., MacAlpine S., Marion B., Toor F., Asgharzadeh A & Stein J., (2014): "Assessment of Bifacial Photovoltaic Module Power Rating Methodologies – Inside and Out", IEEE Journal of Photovoltaics, in press.

Deline, C., Macalpine, S., Marion, B., Toor, F., Asgharzadeh, A., Stein, J.S. (2018): Evaluation and field assessment of bifacial photovoltaic module power rating methodologies. In: 2016

IEEE 43th Photovoltaic Specialists Conference, PVSC 2016, Portland, Oregon, USA, 5-10 June 2016 pp. 1–6. https://www.nrel.gov/docs/fy16osti/66496.pdf

Deline, C., Macalpine, S., Marion, B., Toor, F., Asgharzadeh, A., Stein, J.S. (2017): Assessment of bifacial photovoltaic module power rating methodologies—*Inside and out. IEEE J. Photovoltaics 7(2), 575–580 (2017).https://doi.org/10.1109/PVSC.2017.8366887.*

Deline, C.P., Marion, S.A., Sekulic, B., Woodhouse, B., &Stien M, J. (2019): 'Bifacial PV System Performance: Separating Fact from Fiction'. In Proceedings of the IEEE 46th Photovoltaic Specialist Conference (PVSC), Chicago, IL, USA,

Deruyck M., Tanghe E., Joseph W., & Martens L., (2011): "Modelling and optimization of power consumption in wireless access networks,: "*Computer Communications, vol. 34, no. 17, pp. 2036-2046,.*

Deruyck, M.; Joseph, W.; Martens, L. (2014): Power consumption model for macro cell and microcell base stations. Trans. Emerg. Telecomm. Technol., 25, 320–333.

Dipti, D. (2018): A Review on Unit Sizing, Optimization and Energy Management of HRES. Int. J. Trend Sci. Res. Dev., 2, 419–426.

Du, J., Zhou, H., & Jacinthe, P. A., (2023): "Retrieval of lake water surface albedo from Sentinel-2 remote sensing imagery". Journal of Hydrology, 617: 128904 121.

Dufo-López, Rodolfo, and José L. Bernal-Agustín. (2005): "Design and control strategies of PV-Diesel systems using genetic algorithms." *Solar energy* 79.1 33-46.

Dufo-Lopez, Rodolfo, and Jose L. Bernal-Agustin. (2008): "Multi-objective design of PV– wind–diesel–hydrogen–battery systems." *Renewable energy* 33.12 2559-2572

Elhadidy, M. A., and S. M. Shaahid. "(2004): Role of hybrid (wind+ diesel) power systems in meeting commercial loads." *Renewable energy* 29.1 109-118

Elhadidy, M. A., and S. M. Shaahid. (2000): "Parametric study of hybrid (wind+ solar+ diesel) power generating systems." *Renewable Energy* 21.2 129-139.

Elhadidy, M. A., and S. M. Shaahid. (2023): "Optimal sizing of battery storage for hybrid (wind+ diesel) power systems." *Renewable Energy* 18.1 77-86

El-Khadimi, A., Bchir, L., and Zeroual, A., (2004): "Dimensionnement et Optimisation Technico-Economique D'un Système D'Energie Hybride Photovoltaïque-Eolien Avec Système de Stockage," Revue des Énergies Renouvelables, Vol. 7, pp. 73-83,.

El-Shimy, M., &Abdo, T. (2014): Photovoltaic technologies: History, advances, and characterization. In: Encyclopaedia of Energy Engineering and Technology. 2nd ed. pp. 1397–1424. CRC Press, Boca Raton, FL https://doi.org/10.1081/e-eee2-120051572

Emmanuel, P. A, Collins, .O. E, Thomas, .O. M, Armstrong. N, Chris. M. E and Hitler L.(2021): 'Solar energy': A panacea for the electricity generation crisis in Nigeria

Energy Commission of Nigeria (ECN), (2014):. http://www.reegle.info/countries/nigeria-energy profile/NG,

Ericsson Press Release (June 2008): "Energy-saving solutions helping mobile operators meet commercial and sustainability goals worldwide*"* *http://www.ericsson.com/res/thecompany/docs/corpinfo/energy_efficiency.pdf*

Ernst M., Liu X., Asselineau C.A., Chen D., Huang C., & Lennon A., (2024): "Accurate modelling of the bifacial gain potential of rooftop solar photovoltaic systems", Energy Convers. Manag. 300

Ersagun, T., and Mahir, K., (2022): Analysis of albedo effect in a 30-kW bifacial PV system with different ground surfaces using PVSYST software. Journal of Energy Systems 2022, 6 (4) 2602-2052 DOI: 10.30521/jes.1105348

Faturrochman, G.J.; de Jong, M.M.; Santbergen, R.; Folkerts, W.; Zeman, M.; and Smets, A.H.M (2020): 'Maximizing annual yield of bifacial photovoltaic noise barriers'. Sol. Energy 2018, 162, 300–305.

Fthenakis V. (2012): " Third Generation Photovoltaics, p. 232, intech.

G. S. f. M. A. (GSMA), "Total Power Africa, September (2014)," in "Total Power: Energy Challenges and Opportunities for the Mobile industries in Africa", Available:

Ganjei, N.; Zishan, F.; Alayi, R.; Samadi, H.; Jahangiri, M.; Kumar, R.; Mohammadian, A. (2022): Designing and Sensitivity Analysis of an Off-Grid Hybrid Wind-Solar Power Plant with Diesel Generator and Battery Backup for the Rural Area in Iran. J. Eng. 2022, , 4966761.

Garrod A., and Ghosh A., (2023): A review of bifacial solar photovoltaic applications, Front. Energy 17 (6) 704–726.

Garrod A., and Ghosh A., (2024): Solar photovoltaic applications, Front. Energy 17 (6) 704–726.

Gavanidous, E. S., and A. G. Bakirtzis. (2019): "Design of a standa lone system with renewable energy sources using trade off methods." *Energy Conversion, IEEE Transactions on* 7.1 42-48.

Ge, X.; Cheng, H.; Guizani, M.; Han, T. (2014): 5G wireless backhaul networks: Challenges and research advances. IEEE Netw., 28, 6–11.

George, J, (2009). “Plugging into the Sun”

Ghosh A., (2023): “A comprehensive review of water based PV: flotavoltaics, under water, offshore and canal top”, Ocean Eng. 281.

Goshwe, N. Y., Kureve, T. D., and Okeleke, A. (2015): “Performance Evaluation of Power in GSM BTS in Nigeria Using PV Solar System”, Journal of Energy Technologies and Policy ISSN 2224-3232 (Paper) ISSN 2225-0573 (Online) Vol.5, No.8.

Grätzel, M. (2004): "Conversion of sunlight to electric power by nanocrystalline dye-sensitized solar cells, J. Photochem. Photobiol", Vol.3, P. 164, p 68

GSM Mobile (2020): “Alternative and Sustainable Power for Nigerian GSM/Mobile Base Stations

GSMA Report (2015): ‘Digital Inclusion and the Role of Mobile in Nigeria,.

Gu W., Ma T., Ahmed S., Zhang Y., Peng J., (2020): A comprehensive review and outlook of bifacial photovoltaic (BPV) technology, Energy Convers. Management. 223, 113283.

Guerrero-Lemus, R., Vega, R., Kim, T., Kimm, A., Shephard, L.E. (2016): Bifacial solar photovoltaics—A technology review. Renewable Sustainable Energy Rev. 60, 1533–1549. https://doi.org/10.1016/j.rser.2016. 03.041

Gul M.S., and Puxty D., (2023): “Bifacial photovoltaics power plants in UK”,

Gul M.S., and Puxty D., (2024): “photovoltaics power plants”,

Hakimi, S. and Moghaddas-Tafreshi, S., (2009): “Optimal Sizing of a Stand Alone Hybrid Power System via Particle Swarm Optimization for Kahnouj Area in South-East of Iran,” Renewable Energy, Vol. 34, No. 7, pp. 1855-1862,.

Han,C.,Harrold,T.,Armour,S.,Krikidis,I.,Videv,S.,Grant,P.M.,&Le,T.A.(2011).Greenradio:Radio techniques to enable energy-efficient wireless networks. IEEE Communications Magazine, 49(6), 46–54. doi:10.1109/MCOM.2011.5783984

Han,T.,&Ansari,N.(2013).Ongreeningcellularnetworksviamulticellcooperation.IEEEWireless Communications, 20(1), 82–89. doi:10.1109/MWC.2013.6472203

Hassan H. A. H, Nuaymi , and Pelov A.,(2013): "Renewable energy in cellular networks: A survey," in Online Conference on Green Communications (GreenCom), IEEE, 2013, pp. 1-7: IEEE.

Herguth, A., Derricks, C., &Sperber, D. (2018): A detailed study on light-induced degradation of Cz-Si PERC-type solar cells: Evidence of rear surface related degradation. IEEE J. Photovoltaics 8(5), 1190–1201. https://doi.org/10.1109/JPHOTOV.2018.2850521

Hernández-Callejo, L., Gallardo-Saavedra, S., Alonso-Gómez, V. (2019): A review of photovoltaic systems: Design, operation and maintenance. Sol. Energy 188, 426–440. https://doi.org/10.1016/j.solener.2019.06. 017

Hidalgo-Leon, R.; Siguenza, D.; Sanchez, C.; Leon, J.; Jacome-Ruiz, P.; Wu, J.; Ortiz, D. (2017): A survey of battery energy storage system (BESS), applications and environmental impacts in power systems. *In Proceedings of the 2017 IEEE Second Ecuador Technical Chapters Meeting (ETCM), Salinas, Ecuador, 16–20 October; pp. 1–6.*

Hintz, A., Prasanna, U. R. and Rajashekara, K. (2016): "Comparative Study of the Three-Phase Grid-Connected Inverter Sharing Unbalanced Three-Phase and/or Single-Phase systems," in *IEEE Transactions on Industry Applications*, vol. 52, no. 6, pp. 5156-5164, doi: 10.1109/TIA.2016.2593680.

Hiroshi, M. (1966): Radiation energy transducing device. U.S patent, No. 3, 278, 811,

HOGA (Hybrid Optimization by Genetic Algorithms). Available from: http://www.unizar.es/rdufo/hoga-eng.htm

HOMER (2016): (Hybrid Optimization Model for Electric Renewables). Available from: http://homerenergy.com/

Hrayshat, E. S., (2009): "Techno-Economic Analysis of Autonomous Hybrid Photovoltaic-Diesel-Battery System," Energy for Sustainable Development, Vol. 13, No. 3, pp. 143-150,

Hrayshat, E. S., (2009): "Techno-Economic Analysis of Autonomous Hybrid Photovoltaic-Diesel-Battery System," Energy for Sustainable Development, Vol. 13, No. 3, pp. 143-150,

http://www.ericsson.com/res/thecompany/docs/corpinfo/energy_efficiency.pdf

http://www.gsma.com/mobilefordevelopment/programmes/green-power-for- mobile/tracker

Hwang S., Kang Y., Seok L. H., (2023): "Performance and energy loss mechanism of bifacial photovoltaic modules at a solar carport system", Energy Sci. Eng. 11 (8) 2866–2884.

IEA (2019): IEA PVPS Snapshot of Global PV Markets. https://resources. solarbusinesshub.com/images/reports/216.pdf. Accessed 4 Aug 2024

IEC, (2024): Technical Specification 60904-1-2: Photovoltaic devices- Part 1-2: Measurement of current-voltage characteristics of bifacial photovoltaic (PV) devices. https://webstore.iec.ch/en/publication/34357.

Infinite Focus (2020): “Alternative and Sustainable Power for Nigerian GSM/Mobile Base Stations” -. Globacom White Paper

Infinite Focus (2020):. Globacom White Paper Source: http://www.infinitefocus-group.com/services/energy_telecoms Airtel goes green with e-Site

Infinite Focus Group, (2014): White paper on ―Alternative and Sustainable Power for Nigerian GSM/Mobile Base Stations.

International Technology Roadmap for Photovoltaic (ITRPV) (2019):. In Results 2019 Including Maturity Report; VDMA: Frankfurt, Germany.

Iqbal M (1983): ‘An Introduction to Solar Radiation’. Toronto: Academic Press Canada. http://www.infinitefocus-group.com (2012): ‘Alternative and Sustainable Power for Nigerian GSM/Mobile Base Stations’ (Accessed on 12/01/2012) - Infinite Focus. Globacom White Paper

IRENA Technologies (2020): Renewable Capacity Statistics.

ITRPV, (2024):VDMA: InternationalTechnologyRoadmapForPhotovoltaic (ITRPV), Results 2023, 15 Edition. https://itrpv.vdma.org/en/ueber-uns. Accessed 16 June 2024

ITRPV-VDMA (2022): International Technology Roadmap for Photovoltaic (ITRPV) 2021 https://etip-pv.eu/news/other-news/international.technology-roadmap-for-photovoltaic-itrpv-r-d-findings-from-the 13th-edition/ Accessed 4 Aug 2024

Jaeckel, B., Volberg, G., Monokroussos, C., Muelhofer, G., & Roth, A. (2018): Type approval andsafety considerations for bifacial PV modules: Requirements for IEC 61215 and IEC 61730. In: 35th European PV Solar Energy Conference and Exhibition, pp. 1689–1699

Jhunjhunwala A. (2012): “Powering Cellular Base Stations: A Quantitative Analysis of Energy Options”, Technical Report, Indian Institute of Technology, Madras.

Jiang Q., Song, Z., Yan, Y. and Zhu, K., (2023): "Highly Efficient Bifacial Single Junction Perovskite Solar Cells," 2023 IEEE 50th Photovoltaic Specialists Conference (PVSC), San Juan, PR, USA, 2023, pp. 1-3, doi: 10.1109/PVSC48320.2023.10359603.

John, P. (2013): Let It Shine: The 6000 Year Story of Solar Energy; Revised Edition; New World Library: Novato, CA, USA,; Chapter 23.

John, S., Lee, K., Bhandari, B., Lee, G., Lee, C., et al., (2011): “Formation Strategy of Renewable Energy Sources for High Mountain Off-Grid System Considering Sustainability,” J. Korean Soc. Precis. Eng., Vol. 29, No. 9, pp. 958-963,

Josip, L., and Ivana B.,(2013): "Renewable Energy Sources for Power Supply of Base Station Sites," International Journal of Business Data Communications and Networking (IJBDCN), vol. 9, no. 3, pp. 53-74,

Kafle, B., Goraya, B.S., Mack, S., Feldmann, F., Nold, S., Rentsch, J. (2021):TOPCon—Technology options for cost efficient industrial manufactur-ing. Sol. Energy Mater.Sol. Cells 227, 111100.https://doi.org/10.1016/j.solmat.2021.111100

Kaldellis, J. K., E. Kondili, and A. Filios. (2006): "Sizing a hybrid wind-diesel stand-alone system on the basis of minimum long-term electricity production cost." *Applied Energy* 83.12 1384-1403.

Karaki, S. H., R. B. Chedid, and R. Ramadan. (2021): "Probabilistic performance assessment of autonomous solar-wind energy conversion systems." *IEEE Transactions Energy Conversion, on* 14.3 766-772.

Kashefi, K. A., Riahy, G., and Kouhsari, S., (2009): “Optimal Design of a Reliable Hydrogen-Based Stand-Alone Wind/PV Generating System, Considering Component Outages,” Renewable Energy, Vol. 34, No. 11, pp. 2380-2390,

Katagiri .H, Saitoh .K, Washio .T, Shinohara .H, Kurumadani .T and Miyajima S (2001): Solution Energy. Mat. Sol. C. 65 141.

Kellogg, W. D., M. H. Nehrir, G. Venkataramanan, and V. Gerez (2023): "Generation unit sizing and cost analysis for stand-alone wind, photovoltaic, and hybrid wind/PV systems." *Energy conversion, ieee transactions on* 13.1 70-75

Kenny, O.P., Lopez-Garcia, J., Menendez, E.G., Haile, B., Shaw, D. (2018): Characterizing bifacial modules in variable operating conditions. In: 2018 IEEE 7th World Conference on Photovoltaic Energy Conversion. https://doi.org/ 10.1109/PVSC.2018.8547853

Kenny, P.; Lopez-Garcia, J.; Menendez, E.G.; Haile, B.; and Shaw, D. (2014): ‘Characterizing Bifacial Modules in Variable Operating Conditions. In Proceedings of the WCPEC, Waikoloa Village, HI, USA, pp. 1210–1214.

Khan, M.R.; Hanna, A.; Sun, X.; and Alam, M.A.(2017): ‘Vertical bifacial solar farms Physics, design, and global optimization’. Appl. Energy 2017, 206, 240–248.

Khan,M.R.,Patel, M.T., Asadpour, R., Imran, H., Butt, N.Z., & Alam, M.A. (2021): A review of next generation bifacial solar farms: Predictive modeling of energy yield, economics, and reliability. J. Phys. D. Appl. Phys. 54(32), 323001. https://doi.org/10.1088/1361-6463/abfce5

Kharrich, M.; Kamel, S.; Abdeen, M.; Mohammed, O.H.; Akherraz, M.; Khurshaid, T.; Rhee, S.-B (2021): " Developed Approach Based on Equilibrium Optimizer for Optimal Design of Hybrid PV/Wind/Diesel/Battery Microgrid in Dakhla, Morocco". IEEE Access, 9, 13655–13670

Khatib, T., Mohamed, A., and Sopian, K., (2012): "Optimization of a PV/ Wind Micro-Grid for Rural Housing Electrification using a Hybrid Iterative/Genetic Algorithm: Case Study of Kuala Terengganu, Malaysia," Energy and Buildings, Vol. 47, pp. 321-331,

Kipp and Zonen, B.V (2015): Instruction Manuel: CMP Series Pyranometer; Kipp and Zonen B.V: Delft, The Netherlands

Kopecek, R. (2015): Bifaciality: One small step for technology, one giant leap for kWh cost reduction. Photovoltaics Int. 26, 1–11 https://www.pv-tech.org/publication-issues/photovoltaics-international-volume-26/24.

Kopecek, R., & Libal, J. (2021): Bifacial photovoltaics 2021: Status, opportunities and challenges. Energies 14(8), 2076. https://doi.org/10.3390/en1408207629. Hiroshi, M.: Radiation energy

Kopecek, R., (2019): 'Bifaciality: One Small Step for Technology, One Giant Leap for kWh Cost Reduction. Photovoltaic

Koutroulis, E., Kolokotsa, D., Potirakis, A., and Kalaitzakis, K., (2006): "Methodology for Optimal Sizing of Stand-Alone Photovoltaic/ Wind-Generator Systems using Genetic Algorithms," Solar Energy, Vol. 80, No. 9, pp. 1072-1088,.

Koutroulis, Eftichios, Dionissia Kolokotsa, Antonis Potirakis, and Kostas Kalaitzakis. (2006): "Methodology for optimal sizing of stand-alone photovoltaic/wind-generator systems using genetic algorithms." *Solar energy*80.9 1072-1088.

Kreinin, L., Bordin, N., Karsenty, A., Drori, A., Grobgeld, D., Eisenberg, N. (2010): PV module power gain due to bifacial design. Preliminary experi mental and simulation data. In: 35th IEEE Photovoltaic Specialists Conference, Honolulu, HI, USA pp. 2171–2175. https://doi.org/ 10.1109/PVSC.2010.5615874

Kreinin, L.; Karsenty, A.; Grobgeld, D.; Eisenberg, N. (2016): 'PV systems based on bifacial modules: Performance simulation vs. design factors. In Proceedings of the IEEE PVSC, Portland, OR, USA; pp. 2688–2691.

Kusakana, K. and Vermaak, H. J., (2013): "Hybrid Renewable Power Systems for Mobile Telephony Base Stations in Developing Countries," Renewable Energy, Vol. 51, pp. 419-425,

La, T. G., Salvina, G., and Tina, G., (2006): "Optimal Sizing Procedure for Hybrid Solar Wind Power Systems by Fuzzy Logic," Proc. of the IEEE on Electrotechnical Conference, pp. 865-868,

Laidi, Maamar, Salah Hanini, Brahim Abbad, Nachida Kasbadji Merzouk, and Mohamed Abbas (2012): "Study of a Solar PV-Wind-Battery Hybrid Power System for a Remotely Located Region in the Southern Algerian Sahara: Case of Refrigeration." *Journal of Technology* 1.1 30-38.

Lal, D. K., Dash, B. B., and Akella, A., (2011): "Optimization of PV/Wind/ Micro-Hydro/Diesel Hybrid Power System in Homer for the Study Area," International Journal on Electrical Engineering and Informatics, Vol. 3, No. 3, pp. 307-325,.

Lal, Sandeep, and Atul Raturi. (2012): "Techno-economic analysis of a hybrid mini-grid system for Fiji islands." *International Journal of Energy and Environmental Engineering* 3.1 1-10.

Lamers M.W.P.E., Ozkalay, E., Gali, R.S.R., Janssen, G.J.M., Weeber, A.W., Romijn, I.G., Van Aken, B.B., (2018): "Temperature effects of bifacial modules: hotter or cooler" Sol. Energy Mater. Sol. Cell. 185 192–197.

Laudani, A., Riganti, F.F., andSalvini, A.(2018): "One diodecircuital model of light soagphenom ena in DYE-sensitized solar cells.

Lawin A.E., Niyongendako C., and Manirakiza C., (2019): 'Solar irradiance and temperature variability and projected trends analysis in Burundi, Climate 7 (2019) 83.

Leadership News, (THE COLUMNIST) (2023): Time To Switch Nigerian Telecoms Sector To Clean, Sustainable Energy. Available at https://leadership.ng, August, 8.

Leonardi, M., Corso R., Milazzo R.G., Connelli C., Foti M., Gerardi C., Bizzarri F., Privitera S.M.S., and Lombardo S.A., (2022): "The effects of module temperature on the energy yield of bifacial photovoltaics": data and model, Energies 15 (1).

Lewis N. (2006): http://www7.nationalacademies.org/bpa/SSSC_Presentations_Oct,05_Lewis.pdf, August

Li, J., Wei, W., and Xiang, J., (2012): "A Simple Sizing Algorithm for Stand-Alone PV/Wind/Battery Hybrid Microgrids," Energies, Vol. 5, No. 12, pp. 5307-5323,

Li, J., Wei, W., and Xiang, J., (2012): "A Simple Sizing Algorithm for Stand-Alone PV/Wind/Battery Hybrid Microgrids," Energies, Vol. 5, No. 12, pp. 5307-5323,.

Li, S., Wunsch, D. C., O'Hair, E., and Giesselmann, M. G., (2001): "Comparative Analysis of Regression and Artificial Neural Network Models for Wind Turbine Power Curve Estimation," Journal of Solar Energy Engineering, Vol. 123, No. 4, pp. 327-332,.

Li, S., Wunsch, D. C., O'Hair, E., and Giesselmann, M. G., (2001): "Comparative Analysis of Regression and Artificial Neural Network Models for Wind Turbine Power Curve Estimation," Journal of Solar Energy Engineering, Vol. 123, No. 4, pp. 327-332,.

Licht S. (2003): "Solar Water Splitting to Generate Hydrogen. Fuel: Photothermal Electrochemical Analysis," J. Phys. Chem. 107 107 4253 4260.

Liliana, E. P. Yoewono and Intan R., (2016): "Transparency modelling for mesh object using ray tracing," 2016 International Electronics Symposium (IES), Denpasar, pp. 385-388.

Liu H., Khan I., Zakari A., Alharthi M., (2022): Roles of trilemma in the world energy sector and transition towards sustainable energy: a study of economic growth and the environment, Energy Pol. 170 113238.

Liu, B. Y. and Jordan, R. C., (1963): "The Long-Term Average Performance of Flat-Plate Solar-Energy Collectors: With Design Data for the Us, Its Outlying Possessions and Canada," Solar Energy, Vol. 7, No. 2, pp. 53-74,.

Lopez-Garcia J., Casado A., and Sample T., (2019): "Electrical performance of bifacial silicon PV modules under different indoor mounting configurations affecting the rear reflected irradiance", Sol. Energy 177, 471–482.

Lorenzo, E. (2021).: On the historical origins of bifacial PV modelling. Sol. Energy 218, 587–595 https://doi.org/10.1016/j.solener.2021.03. 006

Luceño, S., and José, A., (2019): "Materials for Photovoltaics: State of Art and Recent Developments." International Journal of Molecular Sciences, vol. 20, no. 4, 2019, pp. 976.

Luther J.M. and Law M (2008):' Structural, Optical, and Electrical Properties of Self-Assembled Films of PbSe Nanocrystals Treated with 1,2-Ethanedithiol'. ACS Nano.

Ma, T., Yang, H., and Lu, L., (2014): “Development of a model to simulate the performance characteristics of crystalline silicon photovoltaic modules/strings/arrays. Sol. Energy 100 (February), 31–41.

Mahalik M.K., Mallick H., Padhan H., (2021): Do educational levels influence the environmental quality”?: The role of renewable and non-renewable energy demand in selected BRICS countries with a new policy perspective, Renew Energy 164 419–432.

Mahdi, R., Lei, C., and Caisheng, W., (2021): Modeling, Configuration, and Grid Integration Analysis of Bifacial PV Arrays, IEEE TRANSACTIONS ON SUSTAINABLE ENERGY, VOL.12, NO.2, APRIL2021

Mahmud, M.S.; Rahman, M.W.; Lipu, M.S.H.; and Mamun, A.A. (2018): ‘Solar Highway in Bangladesh Using Bifacial PV. In Proceedings of the ICSCA, Pondicherry, India, 6–7; pp. 1–7. 5.

Mancuso, Vincenzo, and Sara Alouf. (2011): "Reducing costs and pollution in cellular networks." *Communications Magazine, IEEE* 49.8 63-71.

Mandys F., ChitnisM.,.and Silva S.R.P, (2023); “Levelized cost estimates of solar photovoltaic electricity in the United Kingdom until 2035”, Patterns 4 (5), 100735.

Markvart, T., Fragaki, A., and Ross, J., (2006): “PV System Sizing using Observed Time Series of Solar Radiation,” Solar Energy, Vol. 80, No. 1, pp. 46-50,

Markvart, T., Fragaki, A., and Ross, J., (2006): “PV System Sizing using Observed Time Series of Solar Radiation,” Solar Energy, Vol. 80, No. 1, pp. 46-50,

Marsan M.A., Bucalo G., di Caro A., Meo M., and Zhang Y. (2013): ‘Towards zero grid electricity networking: powering BSs with renewable energy sources’; Proceedings of the 2013 IEEE International Conference on Communications, ICC), Budapest, Hungary pp. 596-601.

Mas’ud, A.A., Wirba A.V., Muhammed-Sukki, F., Mas’ud I.A., Munir A.B. and Yunus N.M. (2015): ‘An assessment of renewable energy readiness in Africa; case study of Nigeria and Cameroon’ Renew. Sustain. Energy Rev., pp. 775-785.

Mattsson, Niclas, and Clas-Otto Wene (2023):. "Assessing new energy technologies using an energy system model with endogenized experience curves." *International journal of energy research* 21.4 385-393.

Mc Connell R (a), Kurtz S, and Symko-Davies M. (2005): “Concentrating PV Technologies:

Review and Market Prospects", ReFOCUS, Elsevier Ltd, 35 July/August.

Mc Connell R (b), Lasich J. B. and Elam C. (2005): "A Hybrid Solar Concentrator PV System for the Electrolytic Production of Hydrogen", Proceedings of the 20th European Photovoltaic Solar Energy Conference and Exhibition, Barcelona, Spain,.

Mc Connell R. (2008): Chapter 4 in 'Solar Hydrogen Generation,' edited by K. Rajeshwar, R. McConnell and S. Licht, Springer Science Business Media, LLC, New York, New York.

Mertens K. (2018): Photovoltaics: fundamentals, technology, and practice

Mesquita, D.d.B., Lucas de S Silva, J., Moreira, H.S., Kitayama, M., Villalva, M.G. (2019): A review and analysis of technologies applied in PV modules. In: 2019 IEEE PES Innovative Smart Grid Technologies Conference- Latin America (ISGT Latin America), Gramado, Brazil pp. 1–6 https://doi.org/10.1109/ISGT-LA.2019.8895369

Meyer, C. (2019): 'Agro PV-Next2Sun's vertical installations'. In Proceedings of the Bifacial PV Workshop, Amsterdam, Netherlands

Milosevic, F. (2011): "*.ICT Carbon Credit Programme (ICCP) for Telecom Operators"*, presentation at Innovation Africa Digital Summit, Mombasa, 22-24 March

Mohammad H. K. (2005). Robust Multi-criteria Optimization of Surface Location Error and Material Removal Rate in High-Speed Milling under uncertainty. A Dissertation presented to the Graduate School of the University of Florida in Partial Fulfillment of the Requirement for the Degree of Doctor of Philosophy, University of Florida.

Mohammadi, M., Hosseinian, S., and Gharehpetian, G., (2012): "Ga-Based Optimal Sizing of Microgrid and DG Units under Pool and Hybrid Electricity Markets," International Journal of Electrical Power & Energy Systems, Vol. 35, No. 1, pp. 83-92,.

Mohammadi, M., Hosseinian, S., and Gharehpetian, G., (2012): "Optimization of Hybrid Solar Energy Sources/Wind Turbine Systems Integrated to Utility Grids as Microgrid (MG) under Pool/ Bilateral/Hybrid Electricity Market using PSO," Solar Energy, Vol. 86, No. 1, pp. 112-125,.

Mohammed H.A and Jeong Kim (2016): Optimal Solar Power System for Remote Telecommunication Base Stations: A Case Study based on the Characteristics of South Korea's Solar Radiation Exposure.

Mohammed, A., Elgendy, B. Z., and David, J. A. (2012) "Assessment of Perturb and Observe MPPT Algorithm Implementation Techniques for PV Pumping Applications.

Mohammed, H.A (2017): Comparative Analysis of Solar-Powered Base Stations for Green Mobile Networks ID

Moreno-Buesa SM, Muñoz-Cerón E, NofuentesGarrido G, Gulkowski S, de la Casa Higueras J, Aguilera Tejero J. (2024): Characterization of bifacial technology Pv systems. Proceedings of the Institution of Mechanical Engineers, Part A: Journal of Power and Energy. 2024; 238(6):1084-1098. doi:10.1177/09576509241250128

Mostafa, A., Bahgaat, N., El sayed, M. E., & Othman, E.-S.A. (2017). Voltage Stability for a Photovoltaic SystemConnectedtoGridbyUsingGeneticAlgorithmTechnique.InternationalJournalofGridand Distributed Computing, 10(4), 33–42. doi:10.14257/ijgdc.2017.10.4.04

Motorola Reach (2017): Alternative Power for Mobile Telephony Base Stations. Solution Paper. http://content.motorolasolutions.com/web/Business/Solutions/Technologies/WiMax/ Access%20Services%20Network/_Documents/_Static%20Files/6682_MotDoc.pdf.

Motorola White Paper, (2007): Alternatives for Powering Telecommunications Base Stations.

MTN Nigeria wants tough laws to safeguard telecommunications industry. IT News Africa Article. Available at: http://www.itnewsafrica.com/2023/mtn-nigeria-wants- tough-laws-to-safeguard-telecoms-industry/.

Muselli, M., G. Notton, P. Poggi, and A. Louche. (2000): "PV-hybrid power systems sizing incorporating battery storage: an analysis via simulation calculations." *Renewable Energy* 20.1 1-7.

Muriele Bester de Souza, Édwin Augusto Tonolo, Renata Lautert Yang and Gerson Máximo Tiepolo (2019) “ Determination of Diffused Irradiation from Horizontal Global Irradiation - Study for the City of Curitiba”: *Brazilian Archives of Biology and Technology*, https://orcid.org/0000-0002-0409-4484 Jair Urbanetz Junior2 https://orcid.org/0000-0001-9355-1730

Naseem, M., Husain, M.A., Minai, A.F., Khan, A.N., Amir, M., Dinesh, Kumar, J., Iqbal, A. (2021): ‘Assessment of meta-heuristic and classical methods for GMPPT of PV system’.Tran Electr Electron Mater. 2021; 22(3):234. Article Google Scholar

National Bureau of statistics, (NBS), 2023

Nema, P.; Nema, R.K.; Rangnekar, S. (2008): A Current and Future State of Art Development of Hybrid Energy System Using Wind and PV-Solar: A Review. Renew. Sustain. Energy Rev.,

13, 2096–2103.

Nfah, E., Ngundam, J., Vandenbergh, M., and Schmid, J., (2008): “Simulation of Off-Grid Generation Options for Remote Villages in Cameroon,” Renewable Energy, Vol. 33, No. 5, pp. 1064-1072,.

Nikola, O., Čedomir, Z., and Predrag, M.,(2021): Simulating the Power Output of Large Bifacial Photovoltaic Plants. International Journal of Electrical Engineering and Computing Vol. 5, No. 1

Njok A.O. , Iloke J.I. , Panjwani M.K., and Panjwani S.K (2020): ‘The impact of coloured filters on the performance of polycrystalline photovoltaic panel in an uncontrolled environment’ Int. J. Electr. Comput. Eng., 10 (4) pp. 3927-3935.

Novas, N., Garcia, R.M., Camacho, J.M., andAlcayde, A. (2021): ‘Advances in solar energy towards efficient and sustainable energy. Sustainability (Switzerland). 2021;13(11):6295.

Nussbaumer, H., Klenk, M., Morf, M., Keller, N. (2019): ‘Energy yield prediction of a bifacial PV system with a miniaturized test array’. Sol. Energy, 179, 316–325.

Ogbulezie J.C., Njok A.O., Panjwani M.K., and Panjwani S.K (2020): ‘The impact of high temperature and irradiance source on the efficiency of polycrystalline photovoltaic (PV) panels in a controlled environment’; Int. J. Electrical. Computer. Eng., 10 (4) , pp. 3942-3947.

Ohtsuka, H. (2000): ‘Bifacial silicon solar cells with 21· 3% front efficiency and 19· 8% rear efficiency’ Prog Photovoltaics Res Appl

Ohunakin O.S., Adaramola M.S., . Oyewola O.M, and Fagbenle R.O. , (2014): ‘Solar energy applications and development in Nigeria: drivers and barriers, Renew. Sustain. Energy Rev., 32, pp. 294-301

Okundamiya M. S., Emagbetere J. O., and. Ogujor E. A, (2015):"Techno Economic Analysis of a Grid-Connected Hybrid Energy System for 1173 Developing Regions," Iranica Journal of Energy & Environment, vol. 6, no. 4, pp. 243-254,

Okundamiya M.S., Emagbetere J.O., & Ogujor E.A., (2016): ‘Evaluation of various global solar radiation models for Nigeria’, Int. J. Green Energy 13 (5) p.505–512.

Olabi, A.G., Abdelkareem, M.A., Semeraro, C., Al Radi, M., Rezk, H., Muhaisen, O., Al-Isawi, O.A., & Sayed, E.T.(2022): ‘Artificial neural networks applications in partially shaded PV systems.

Olatomiwa L, Mekhilef S, Huda ASN, and Sanusi K (2015): ‘Technoeconomic analysis of hybrid PV–diesel–battery and PV–wind–diesel–battery power systems for mobile BTS: the way forward for rural development’; Energy SciEng 3(4):271–285. https://doi.org/

Olwal T. O, Djouani K, and Kurien A. M (2016): "A Survey of Resource Management toward 5G Radio Access Networks," IEEE Communications Survey and Tutorials, vol 18, no 3 pp. 1656-1686,

Omar,H.A., Hamza, A., Rebhi, A., Damseh, A.H., AL-Zubi, S. O., and Shbool, B. (2023): Evaluating the real-world performance of vertically installed bifacial photovoltaic panels in residential settings: empirical findings and implications

Oodo O. S, Liu Y. Z, and Wei, S. H (2012): ‘Impact Of PV Generation For Small Autonomous Electricity Generation In Nigeria’. Transnational Journal of Science and Technology August 2012 edition vol. 2, No.7 81

Osama, A., G. M. Tina, G. Mannino, A. Vincenzo Cucuzza and F. Bizzarri, (2024): "Experimental and Numerical Performance Assessment of East-West Bifacial Photovoltaic Floating System in Freshwater Basins," in IEEE Access, vol. 12, pp. 141425-141447, ,doi: 10.1109/ACCESS.2024.3468228.

Osinowo A.A., Okogbue, E.C, Ogungbenro S.B, Fashanu, O. (2015): ‘Analysis of global solar irradiance over climatic zones in Nigeria for solar energy applications; J. Solar Energy (2015). Article ID 819307.

Osueke C.O. , . Ezugwu, C.A.K (2011): ‘Study of Nigeria’s energy resources and its composition’ Int. J. Sci. Res. Eng., 2 (12) (2011). Google Scholar.

Pandiarajan, N., and Muthu, R., (2011): “Development of Power Electronic Module with Simulink”, in Proceedings of the International Conference on Electrical Energy Systems(ICEES’11).

Parhizi,S.,Lotfi,H., Khodaei,A., andBahramirad,S. (2015): “Stateoftheartinresearchon microgrids: A review,” IEEE Access, vol. 3, pp. 890–925,

Pattantyus-Abraham A.G., Kramer I.J., Barkhouse A.R., Wang X., Konstantatos G., Debnath R., Levina L., Raabe I., Nazeeruddin M.K., Gratzel M., and Sargent E.H: (2020) ‘Depleted-Heterojunction Colloidal Quantum Dot Solar Cells’. ACSNano 4 (6) 3374–3380.

Pelaez, S.A. (2019): ‘Bifacial Solar Panels System Design, Modeling, and Performance’;The University of Arizona: Tucson, AZ, USA.

Pelet, Xavier, Daniel Favrat, and Geoff Leyland. "(2005): Multiobjective optimisation of integrated energy systems for remote communities considering economics and CO_2 emissions." *International Journal of Thermal Sciences*44.12 1180-1189.

Pendem, S.R., Mikkili, S., Bonthagorla, P.K. (2020): 'PV distributed-MPP tracking: total-cross-tied configuration of string-integrated-converters to extract the maximum power under various PSCs', IEEE Syst.J.,14,(1),pp.1046–1057

Perez R., Ineichen P., Seals R. and Michalsky, J (1990): "Modelling daylight availability and irradiance components from direct and global irradiances", Solar Energy 44: 271-289,

Posadillo, R. and López Luque, R., (2008): "Approaches for Developing a Sizing Method for Stand-Alone PV Systems with Variable Demand," Renewable Energy, Vol. 33, No. 5, pp. 1037-1048,.

Pourbehzadi, M.; Niknam, T.; Aghaei, J.; Mokryani, G.; Shafie-Khah, M.; Catalão, J.P. (2019): Optimal operation of hybrid AC/DC microgrids under uncertainty of renewable energy resources: A comprehensive review. Int. J. Electr. Power Energy Syst., 109, 139–159.

Qazi, S. (2017): "Standalone Photovoltaic (PV) Systems for Disaster Relief and Remote Areas." Elsevier,

Radionov, V., Bryazgin, N., andnAlexandrov. E.,(1997): "The snow covers of arctic basin". US Technical Report APL-UW TR, 9701.

Rahimat, O., Lena, David D.M., and Muyiwa, S. A., (2022): Improving solar photovoltaic installation energy yield using bifacial modules and tracking systems: An analytical approach Vol. 14(12) 1–12 DOI: 10.1177/1687813222113971

Rahman, FA., Aziz. MMA.,Saidur, R., Bakar, W., Hainin, M.R., Putrajaya, R and Hassan, N.A (2017): 'Pollution to the solution: capture and sequestration of carbon dioxide (CO2)', 71, 112–126. https:// doi.org/10.1016/j.rser.2017.01.011.

Raina G., and Sinha S., (2019): "A comprehensive assessment of electrical performance and mismatch losses in bifacial PV module under different front and rear side shading scenarios", Energy Convers. Manag.261, 115668.

Raina G., and Sinha S., (2022): "A comprehensive assessment of electrical performance and mismatch losses in bifacial PV module under different front and rear side shading scenarios", Energy Convers. Manag. 261, 115668.

Rajesh, R., & Mabel, M.C. 248 (2015): A comprehensive review of photovoltaic sys tems. Renewable Sustainable Energy Rev. 51, 231https:// doi.org/10.1016/j.rser.2015.06.006

Rao R.V. and Davin J. P. (2008). A decision-making framework model for material selection using a combined multiple attributes decision-making method. International Journal of advance Manufacturing Technology; vol. 35; pg. 751-60.

Ratheesh,R.,&Vetrivelan,P.(2016).Poweroptimizationtechniquesfornextgenerationwirelessnetworks.IACSITInternationalJournalofEngineeringandTechnology,8(1), 247–256.

Ratnakar,B.B.› Suresh,M,,Praveen,K. B., (2020): CriticalReviewonPVMPPTTechniques: Classical, Intelligent and Optimisation. ReviewArticle, IETRenewablePowerGeneration

Razak, Juhari Ab, Kamaruzzaman Sopian, Yusoff Ali, Mohammad Ahmed Alghoul, Azami Zaharim, and Ibrahim Ahmad (2009):. "Optimization of PV-wind-hydro-diesel hybrid system by minimizing excess capacity." *European Journal of Scientific Research* 25.4 663-671

Razak, Juhari Ab, Kamaruzzaman Sopian, Yusoff Ali, Mohammad Ahmed Alghoul, Azami Zaharim, and Ibrahim Ahmad. (2009) "Optimization of PV-wind-hydro-diesel hybrid system by minimizing excess capacity." *European Journal of Scientific Research* 25.4: 663-671

Razongles, G., Sicot, L., Joanny, M., Gerritsen, E., Lefillastre, P., Schroder, S. and Lay, P., (2016): Bifacial Photovoltaic Modules: Measurement Challenges. Energy Procedia, 92, pp.188-198.

Roest, S., Nawara, W., Van Aken, B.B., &Goma, E.G. (2018): Towards developing a standard for testing bifacial PV modules: Single-side versus double-side illumination method I-V measurements under different irradiance and temperature. In: IEEE 44th Photovoltaic Specialist Conference (PVSC), pp. 3462–3467. https://doi.org/10.1109/ pvsc.2017.8366734

Roy, P.; He, J.; Zhao, T.; Singh, Y.V. (2022): Recent Advances of Wind-Solar Hybrid Renewable Energy Systems for Power Generation: A Review. IEEE Open J. Ind. Electron. Soc., 3, 81–104.

Saga, T. (2010): Advances in crystalline silicon solar cell technology for industrial massproduction. NPGAsiaMater.2, 96–102. https://doi.org/10. 1038/asiamat.82

Said, A, Shahzada, P. A, Nicolas, B, and Amir, A (2019): Coupled Multi-Physics Model for Simulating Thermal Behavior, Electrical Yield and Structural Reliability of Monofacial and Bifacial Photovoltaic Modules Under Desert Environment. 36th European Photovoltaic Solar Energy Conference and Exhibition, Marseille, France, DOI: 10.4229/EUPVSEC20192019-4AV.1.41

Saloux, E., Teyssedou, A., &Sorin, M., (2011): Explicit model of photovoltaic panels to determine voltages and currents at the maximum power point. Sol. Energy 85 (5), 713–722.

Sambo A.S, (2005): 'Renewable energy for rural development: the Nigerian perspective'; ISESCO Sci. Technol. Vision (2005), pp. 12-22

Schmid, A., Dülger, G., Baraah, G., Kräling, U., & Ise, F. (2017): IV measurement of bifacial modules: Bifacial vs. monofacial illumination. Presented at the 33rd European PV Solar Energy Conference and Exhibition, Amsterdam, the Netherland, 25–29 September

Schmid, Aloísio Leoni, and Carlos Augusto Amaral Hoffmann (2004): "Replacing diesel by solar in the Amazon: short-term economic feasibility of PV-diesel hybrid systems." *Energy Policy* 32.7 881-898.

Schmidt, K., and D. J. Patterson (2018): "Benefits of load management applied to an optimally dimensioned wind/photovoltaic/diesel/battery hybrid power system."*Proceedings of solar*..

Schmitt G., (2009): 'The green base station ': Proceedings of the 4th International Conference on Telecommunication-Energy Special Conference, TELESCON, Vienna, Austria, pp. 1; Google Scholar.

Shaahid, S. M., and M. A. Elhadidy. (2004): "Prospects of autonomous/stand-alone hybrid (photo-voltaic+ diesel+ battery) power systems in commercial applications in hot regions." *Renewable energy* 29.2 165-177.

Shoukry, I., Libal, J., Kopecek, R., Wefringhaus, E., and Werner, J. (2016): Modelling of bifacial gain for stand-alone and in-field installed bifacial PV modules. Energy Procedia 92, 600–608. https://doi.org/10.1016/j.egypro. 2016.07.025

Singh, G. (2013): 'Solar power generation by PV (photovoltaic) technology': A review. Energy, 53, pp.1-13

Singh, R.; Bansal, R.C. (2018): Review of HRESs based on storage options, system architecture and optimisation criteria and methodolo gies. IET Renew. Power Gener., 12, 747–760.

SiyuGuo, Jai Prakash Singh, Ian Marius Peters, Armin G. ABERLE, Timothy M. Walsh, (2013):A Quantitative Analysis of Photovoltaic Modules Using Halved Cells . International Journal of Photoenergy 2013, DOI: 10.1155/2013/739374

Smertnik H., (2014): 'Green Power for Mobile Bi-annual Report, GSM Association'

Smith, B.L., (2021): Woodhouse, M., Horowitz, K.A.W., Silverman, T.J., Zuboy, J., Margolis, R.M.: Photovoltaic (PV) Module Technologies: 2020 Bench mark Costs and Technology

Evolution Framework *Results. National Renewable Energy Laboratory, Golden, CO. https://www.nrel. gov/docs/fy22osti/78173.pdf*

Sng, G. K. E., Chua, S. W., Roy, S. and Lim, L. H. I. (2021): 'Solar Energy Simulation of Bifacial Panels for Performance Optimisation'. *In: 47th IEEE Photovoltaic Specialists Conference (PVSC 47), 15 Jun - 21 Aug 2020, ISBN 9781728161167*

SOLAR MAG,(2022): IBC solar cells: Definition, benefits, vs. similartechs. https://solarmagazine.com/solar-panels/ibc-solar-cells/.Accessed 25 Nov 2022

Song, Z., Li, C., Chen, L., & Yan, Y. (2021): Perovskite solar cells go bifacial Mutual benefits for efficiency and durability. Adv. Mater.https://doi.org/10.1002/adma.202106805

Sonntag, R. E, Claus B, G., John V. W, and Steve V. W. (2023): "*Fundamentals of thermodynamics"*. New York: Wiley,

Stein, J.S., Christian, R, Johanna B.C, Gabi, F, Giosuè, M, Elías, U, and Chile, S. R, (2021): Bifacial PV modules and systems: Experience and results from international research and pilot applications. Report IEA-PVPS T13-14. https://iea-pvps.org/wp-content/uploads/2021/04/IEA-PVPS-T13-14

Steven K. C. (2000). Development of a Fuzzy Multi-Criteria Decision Support System for Municipal Solid Waste Management. Unpublished Thesis Submitted to the Faculty of Graduate Studies and Research University of Regina, Saskatchewan.

SUDOKET, (2021): 'Mapping, Consolidation, and Dissemination of Key Enabling Technologies (KETs) for the Construction Sector in the SUDOE Space. Available online: http://en.sudoket.com

Supriya, C. S., and M. Siddarthan. (2024): "Optimization and sizing of a grid-connected hybrid PV-wind energy system." *International Journal of Engineering Science* 3

Supriya, C. S., and Siddarthan M. (2011): "Optimization and sizing of a grid-connected hybrid PV-wind energy system." International Journal of Engineering Science

Susan Adams (2019): "Quality assurance for biophysical Earth-Observation (EO) products of vegetation flux and structure Jennifer". A dissertation submitted in partial fulfilment of the requirements for the degree of Doctor of Philosophy of University College London. Department of Geography University College London February 24

Taghizadeh-Hesary F., Yoshino N., (2019): The way to induce private participation in green

finance and investment, Finance Res. Lett. 31 98–103.

Tamm, Oliver, Christian Herms Meyer, and Allen Rush M.. (2010): "Eco-sustainable system and network architectures for future transport networks." *Bell Labs Technical Journal* 14.4: 311-327.

Taraba, M. (2015): "Properties of the Thin Film Solar Panels under Adverse Weather Conditions." Transportation Research Procardia, vol. 40, pp. 535-540.,

Thompson J. R,. McConell R. D, and Mosleh M. (2005): 'Cost Analysis of a Concentrator Photovoltaic Hydrogen Production System,' International Conference of Solar Concentration for the Generation of Electricity or Hydrogen, 1 5 May, Scottsdale, Arizona (NREL/CD-520-38172)

Tina, G., Gagliano, S., and Raiti, S., (2006): "Hybrid Solar/Wind Power System Probabilistic Modelling for Long-Term Performance Assessment," Solar Energy, Vol. 80, No. 5, pp. 578-588,.

Tsai, H.L., Tu, C.S., Sui, Y.J., (2008): "Development of Generalized photovoltaic". International: WCECS2008, October 22-24, San Francisco, USA.

Tsuchida, S. , Tsuno, Y. , Sato, D., Oozeki, T., and Yamada N., (2023): "Albedo-Dependent Bifacial Gain Losses in Photovoltaic Modules With Rear-Side Support Structures," in IEEE Journal of Photovoltaic, vol. 13, no. 6, pp. 938-944, Nov. 2023, doi: 10.1109/JPHOTOV.2023.3317970.

Urrejola, E., Felipe Valencia, Edward Fuentealba, Chris Deline, Silvana Ayala Pelaez, Jenya Meydbray, Tori Clifford, Radovan Kopecek, and Joshua S. Stein6 (2020): https://www.nrel.gov/docs/fy21osti/77817.pdf (2020). Accessed 4 Aug 2024

Vanguard Newsaper http://www.vanguardngr.com/ (2011): airtelgoes--with-e-site/ visited on

Vanguard Newsp aper (2019): online " http://www.vanguardngr.com

Verma, D., Nema, S., Shandilya, A.M. (2016): 'Maximum power point tracking (MPPT) techniques: recapitulation in solar photovoltaic systems', Renew. Sustain. Energy Rev., 54, pp.1018–1034

Viola, F.; Romano, P.; Miceli, R.; Spataro, C.; Schettino, G.; Caruso, M.; Busacca, A.; Parisi, A.; Guarino, S.; and Cino, A. (2019): 'Comparison on the use of PV systems in the vertical walls'. In Proceedings of the International Conference on Renewable Energy Research and Applications (ICRERA), Palermo, Italy, pp. 1651–1653

Vishakha, V.; Vardwaj, V.; Jadoun, V.K.; Jayalaksmi, N.; Agarwal, A. (2020): Review of Optimization Techniques for Hybrid Wind PV-ESS System. In Proceedings of the 2020 International Conference on Power Electronics & IoT Applications in Renewable Energy and its Control (PARC), Mathura, India, 28–29 February; pp. 202–207.

Vodafone Germany (2007) first to launch Ericsson's power-saving feature to reduce energy consumption and cut CO_2 emissions www.ericsson.com/thecompany/press/releases//12/1175972.

Wang P., Klein C., Humphry-Baker R., Zakeeruddin S. M., and M. Grätzel (2005): "Stable efficient nanocrystalline dye-sensitized solar cell based on an electrolyte of low volatility", Appl. Phys. Lett., Vol. 86.

Wang P., Zakeeruddin S. M., Moser J. E., Nazeeruddin M. K., Sekiguchi T. and. Grätzel M, (2003): " A stable quasi-solid-state dye-sensitized solar cell with an amphiphilic ruthenium sensitizer and polymer gel electrolyte", Nat. Mater., Vol.2, P. 402.

Wang P. (2011): 'The value of module efficiency in lowering the levelized cost of energy of photovoltaic systems' Renew Sustain Energy.

Waqas, Sana (2011): "Development of an Optimisation Algorithm for Auto sizing Capacity of Renewable and Low Carbon Energy Systems." *Master of Science,, Department of Mechanical Engineering,, University of Strathclyde Engineering*..

Wei Luo., Yong, S. K, Jai, P. S, Johnson K. W, Yan, W, Armin, G. Aberle, S. R., (2018) "Investigation of Potential-Induced Degradation in n-PERT Bifacial Silicon Photovoltaic Modules with a Glass/Glass Structure," *in* IEEE Journal of Photovoltaics, *vol. 8, no. 1, pp. 16-22, Jan. 2018, doi: 10.1109/JPHOTOV.2017.2762587.*

Wong L.T. (2001): 'Solar radiation model' Apple Energy

Xu, D., Kang, L., Chang, L., and Cao, B., (2005): "Optimal Sizing of Standalone Hybrid Wind/PV Power Systems using Genetic Algorithms," Proc. of the IEEE on Electrical and Computer Engineering, pp. 1722-1725,.

Xu, D., Kang, L., Chang, L., and Cao, B., (2005): "Optimal Sizing of Standalone Hybrid Wind/PV Power Systems using Genetic Algorithms," Proc. of the IEEE on Electrical and Computer Engineering, pp. 1722-1725,.

Yahya, K., and Alomari, O. (2020): "A new maximum power point tracking algorithm based on power differentials method for thermoelectric generators," International Journal of Energy Research, vol. 16, no. 2, pp. 760–785.

Yang, H., Lu, L., and Burnett, J., (2003): "Weather Data and Probability Analysis of Hybrid Photovoltaic-Wind Power Generation Systems in Hong Kong," Renewable Energy, Vol. 28, No. 11, pp. 1813-1824,.

Yang, H., Lu, L., and Zhou, W., (2007): "A Novel Optimization Sizing Model for Hybrid Solar-Wind Power Generation System," Solar Energy, Vol. 81, No. 1, pp. 76-84,

Yang, H., Wei, Z., and Chengzhi, L., (2009): "Optimal Design and Techno Economic Analysis of a Hybrid Solar-Wind Power Generation System," Applied Energy, Vol. 86, No. 2, pp. 163-169,.

Yang, H., Zhou, W., Lu, L., and Fang, Z., (2008): "Optimal Sizing Method for Stand-Alone Hybrid Solar-Wind System with LPSP Technology by Using Genetic Algorithm," Solar Energy, Vol. 82, No. 4, pp. 354 367,.

Yang, Hongxing, Wei Zhou, Lin Lu, and Zhaohong Fang (2008): "Optimal sizing method for stand-alone hybrid solar–wind system with LPSP technology by using genetic algorithm." *Solar energy*82.4 354-367.

Yunus Khan T.M., Soudagar M., Elahi M., Kanchan M.A, Nagaraj, A., Banapurmath R., Akram N., Mane S.D., and Shahapurkar K., (2020): "Optimum location and influence of tilt angle on performance of solar PV panels, J. Therm. Anal. Calorim. 141 (1), 511–532.

Yusufoglu U.A, Pletzer T.M., Koduvelikulathu L.J., Comparotto C., Kopecek R., and Kurz H.,(2015): "Analysis of the annual performance of bifacial modules and optimization methods", IEEE J. Photovoltaics 5 (1) 320–328.

ZekâiSen, (2009): "Solar irradiation fundamentals", solar energy conversion and photo-energy system, vol. 2, p67

Zhang, Y., Gao, Q., Yu, Y., and Liu, Z. (2018): Comparison of double-side and equivalent single-side illumination methods for measuring the I-V characteristics of bifacial photovoltaic devices. IEEE J. Photovoltaics 8(2), 397–403.

Zhu X.,Han X.Q.,Qin W.P, and Wang P., (2015):"Past, today and future development of micro-grids in China," Renew. Sustain. Energy Rev., vol. 42, pp. 1453–1463,